3129

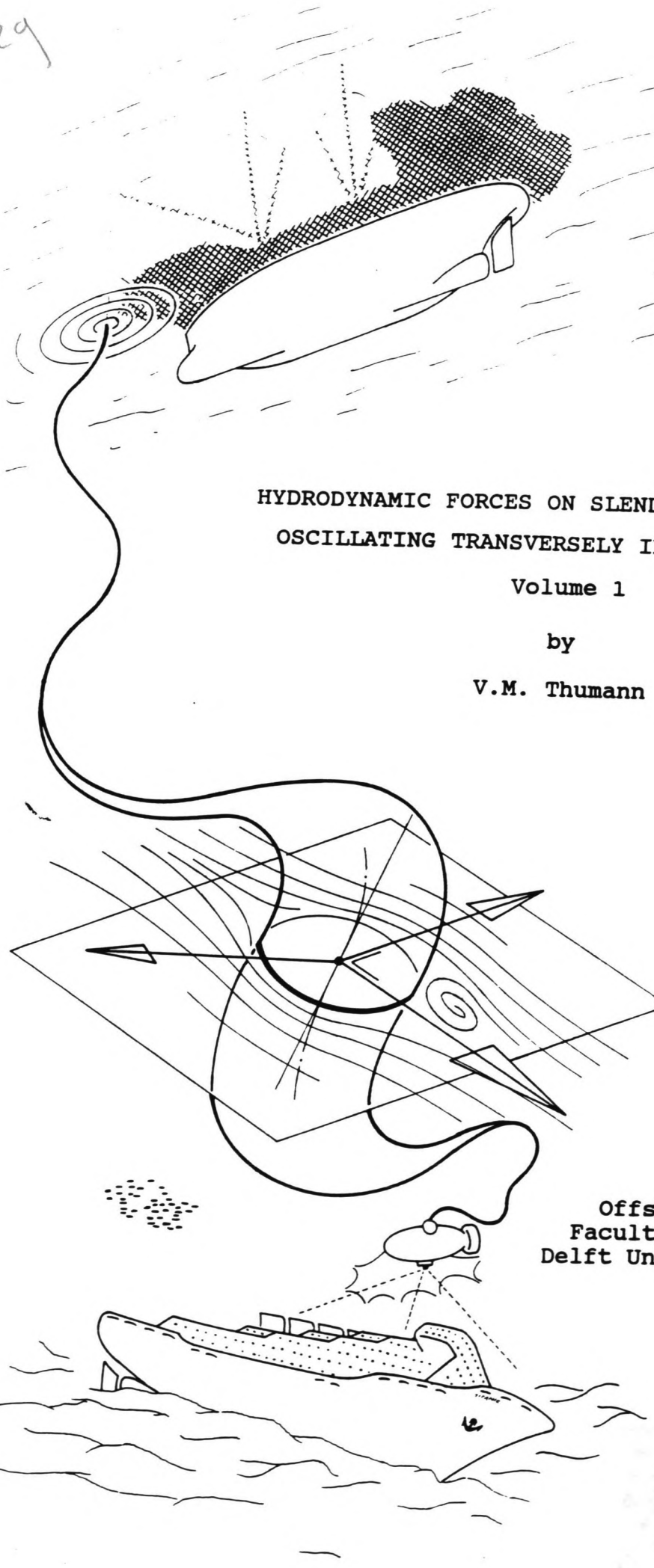

HYDRODYNAMIC FORCES ON SLENDER CYLINDERS OSCILLATING TRANSVERSELY IN A CURRENT

Volume 1

by

V.M. Thumann

Offshore Engineering Major
Faculty of Civil Engineering
Delft University of Technology

June, 1991

TU Delft
Delft University of Technology
Offshore Technology

HYDRODYNAMIC FORCES ON SLENDER CYLINDERS OSCILLATING TRANSVERSELY IN A CURRENT

by

V.M. Thumann

Offshore Engineering Major
Faculty of Civil Engineering
Delft University of Technology

June, 1991

PREFACE

The study "Hydrodynamic Forces on Slender Cylinders Oscillating Transversely in a Current" presented in this report has been the main part of the author's graduation program at the Faculty of Civil Engineering, University of Technology, Delft.
The author explicitly wishes to thank the following people for their assistance in the past fifteen months:
Mr. W.W. Massie, executive supervisor, who managed to keep the overall picture during all stages of the study and whose time spent discussing with the author has been appreciated very much;
the skilful staff members of the Ship Hydromechanics Laboratory, Delft;
my dear friend Herma and my family for their patience and support and all others who were willing to solve the author's (little) problems.

V.M. Thumann
Rotterdam, June 1991.

Graduation Committee:

Prof. dr. ir. J.A. Battjes (president)

ir. M.W.J.W. Dijkman
ir. J.M.J. Journée
W.W. Massie, MSc, P.E. (supervisor)
Prof. ir. J.G. Wolters

TABLE OF CONTENTS

ABSTRACT

The study of the hydrodynamic interaction of cables has become more important in recent years since umbilical cables of more than 3000 meters length have been used when photographing the wreck of the HMS Titanic or the Bismarck. Cable vibration can cause distorting of the digital signals being transmitted as well as premature fatigue failure of the cable conductors. The objective of the present study is to describe the hydrodynamic interaction of an element of such a rather vertical cable which is vibrating more or less crosswise in a constant current.

The hydrodynamic forces model has been built up based upon literature information using a drag force component and an inertia force component (both proved to be properly described by Morison's theory), and a lift force component that has been described including a time varying vortex shedding frequency (analogous to the model of Verley [1982]); this was found to be more suitable than a constant frequency.
The literature study has revealed that little seems to be known about the hydrodynamic interaction of cylinders (cable segments) vibrating with large amplitudes (over two cylinder diameters) in currents. Additional laboratory tests as part of this project have filled this information gap.
Measured forces on a vertically mounted test cylinder came from the experiments carried out in the towing tank of Ship Hydromechanics Laboratory, TU Delft, in December 1990. These tests were carried out using a variety of towing speeds (currents), and oscillation frequencies and amplitudes.
The model has been verified by the comparison of measured and computed (model) forces. An efficient procedure for determining the coefficients needed (Cd, Ca, Cl, St, initial phase phi) has been developed for the processing of the recorded force signals in the time domain.
Most of the Cd, Ca and St coefficient values found for the experiments were surprisingly close to those found by others, even though their flow conditions were different. The lift force was properly described by the model, although the Cl coefficient values found varied with all input parameters.

The description of the hydrodynamic interaction presented in this study could be used with a discrete element simulation of the cable (using the NOSDA software) in the time domain, to better understand and even predict its vibratory behaviour.

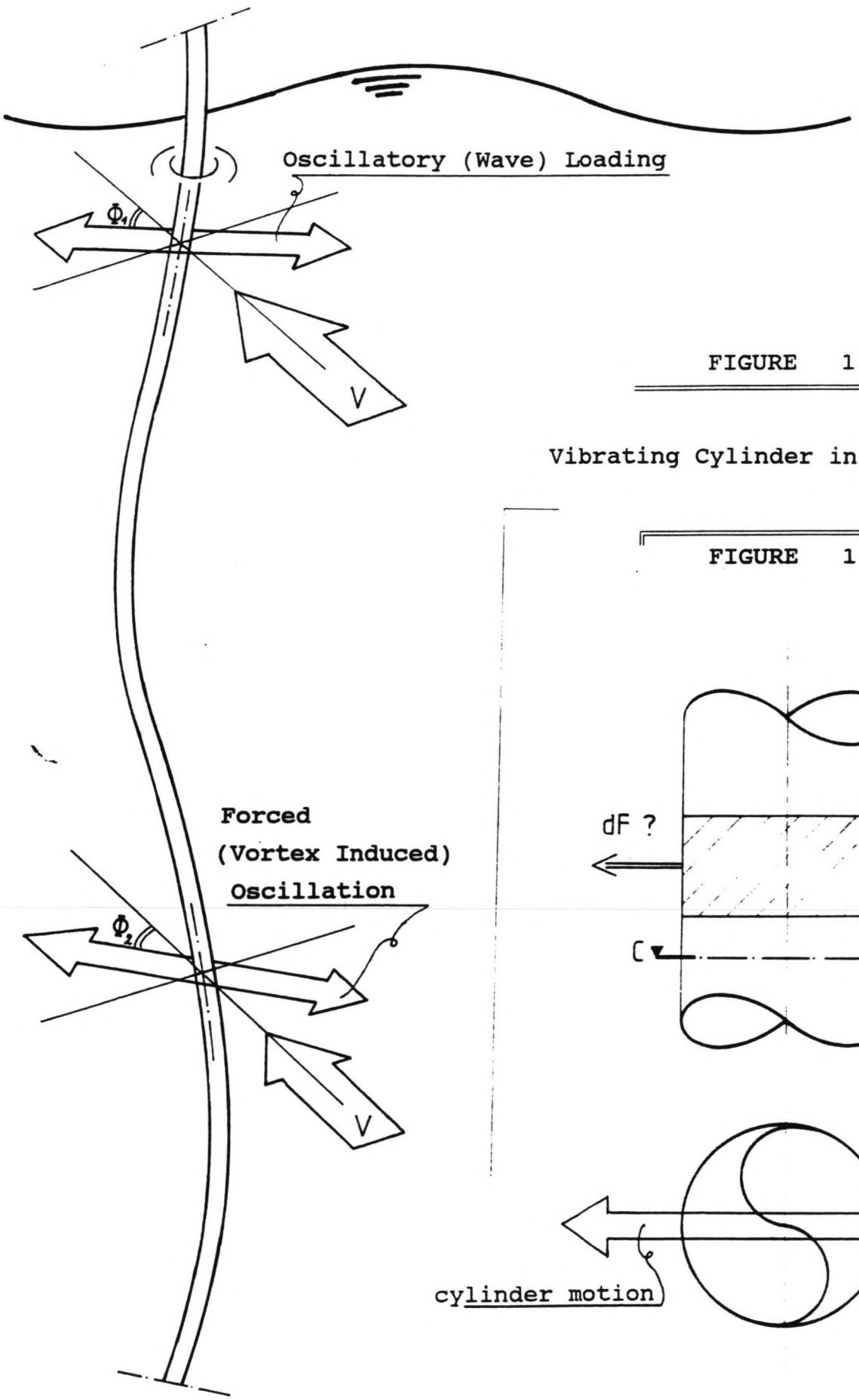

FIGURE 1.1

Vibrating Cylinder in a Current

FIGURE 1.2

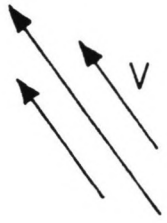

1 INTRODUCTION

One of the most common problems in Offshore Engineering involves the prediction of the hydrodynamic interaction between (moving) structures and the sea. This study is targeted on this interaction for a slender element - such as a cable - which is vibrating crosswise in a current. In such a case force components act simultaneously along two mutually perpendicular axes which are also perpendicular to the cylinder axis.

The study of the hydrodynamic interaction of cables has become more important in recent years since umbilical cables of more than 3000 meters length have been used when photographing the wreck of the HMS Titanic or the Bismarck. Near the water surface, these cables are loaded by (oscillatory) wave forces as well as constant currents. Deeper into the water, the cables are loaded by constant currents again, and they also experience the constrained motions coming from other parts of the cable (figure 1.1). Cable vibration can cause distorting of the digital signals being transmitted as well as premature fatigue failure of the cable conductors.

The objective of the present study is to describe the hydrodynamic interaction of an element of such a rather verticle cable which is vibrating more or less crosswise in a constant current (see figure 1.2). The resulting description of the hydrodynamic interaction can then be used with a discrete element simulation of the cable to better understand and even predict its vibratory behaviour.

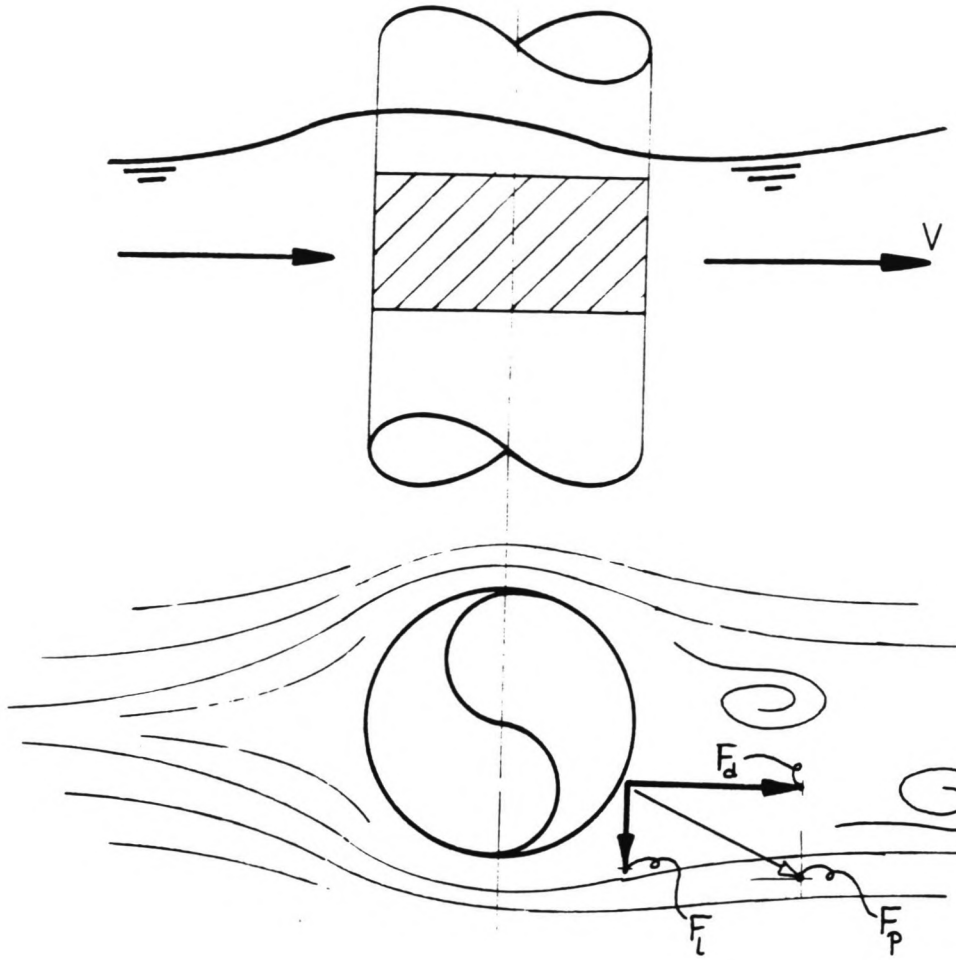

FIGURE 2.1

FIGURE 2.2

FIGURE 2.3

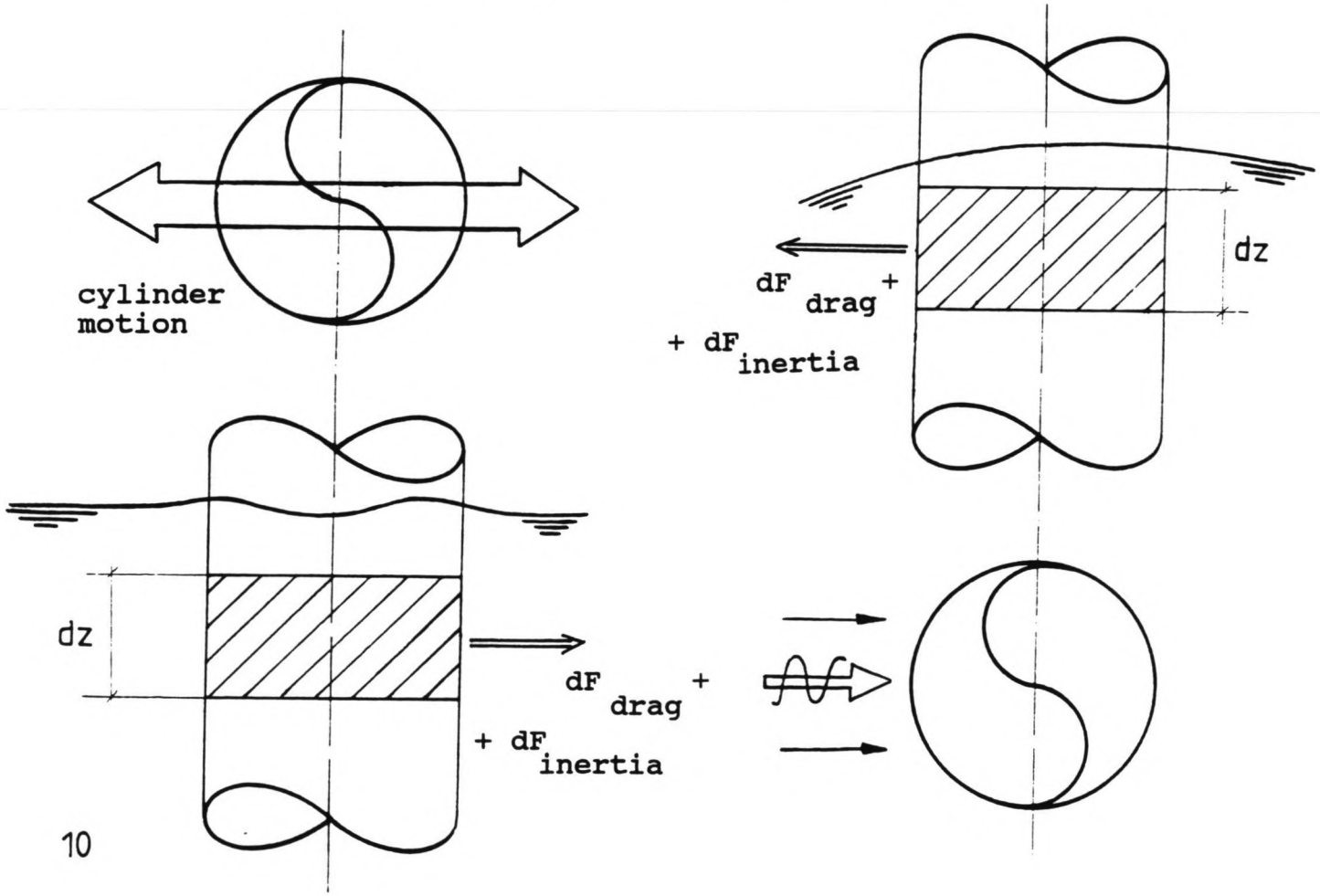

2 THE PROBLEM

2.1 Problems Description

A few specific situations concerning the hydrodynamic load on a cylinder in moving water have already been elaborated:

(a) - A turbulent flow of a current around a fixed cylinder, as in figure 2.1. Due to the vortex shedding, which depends on the value of the Reynolds Number, the line of action of the resulting pressure force moves along the cylinder wall. This force is usually split into two components: one parallel to the flow direction (the drag force), and one perpendicular to the flow (the lift force).

(b) - An oscillating cylinder in still water or a vertical cylinder under a wave attack, as in figures 2.2 and 2.3, with the water motion and the cylinder motion in the same direction. The forces acting on the cylinder can now be split into two components: one due to viscosity of the fluid, and one due to the inertia of the fluid. This situation can be described with Morison's formula (eq. 2.1 and 2.2).

$$dF = C_I \cdot A_I \cdot \frac{dV}{dt} \cdot ds + C_D \cdot A_D \cdot |V| \cdot V \cdot ds \quad (N) \qquad (2.1)$$

$$A_I = \frac{\pi}{4} \cdot \rho \cdot D^2 \; ; \; A_D = \frac{1}{2} \cdot \rho \cdot D \qquad (2.2)$$

A description of forces on an oscillating cylinder, located in a flow pattern which is NOT in the same direction as the movement of the cylinder, is still missing; the superposition of the situations as mentioned above in (a) and (b) is not possible; the forces are non linearly interdependent.

2.2 Problems Definition

A calculation method to determine the forces acting on a cylinder is available, if the cylinder axis and the flow velocity form a stationary plane as in figure 1.2.
In case the water motion and the cylinder movement are NOT in a fixed plane, such descriptions and methods are not (yet) available.

2.3 Objective

This study will move towards an acceptable, more universal description of the hydrodynamic forces working on a finite element of a moving cylinder.
A theoretical model for this time dependent interaction is to be developed. This will be done starting with a literature survey augmented by laboratory tests where necessary. This model is to be suited for inclusion in software for predicting the non linear dynamic motions of offshore structures in the time domain.

2.4 Limitations

Cylinder:

- its cross section will be circular;
- its properties in material and shape will be considered as given constant parameters;
- the orientation of its axis is arbitrary and will not be rotating;
- the cylinder has to be a slender structure.

Surrounding water:

- viscosity, density etc. will be considered as given parameters;
- if necessary, linear short-wave theories (for deep water) will be used;
- all flow parameters will be taken from a single point corresponding to the cylinder centerline.

Physical description:

- a model is needed to describe the force on a cylinder segment as a function of time.

3 LITERATURE SURVEY

3.1 Introduction

The literature study has been executed in order to find out what is known about the interaction between (moving) cylinders and (moving) water, and more specifically:

- applicability of Morison's Formula;
- results of investigations on drag-, lift- and inertia-forces for (moving) cylinders;
- phenomena that occur during the interaction between water and cylinder, such as vortex shedding, etc.;
- restrictions and hypotheses made in the items mentioned above.

About twenty from the more than one hundred articles or books found during the literature search (Thumann, (1990)), have been selected. These twenty have been studied carefully, and each one that seemed to have some significance for this study is presented in section 3.3. These selections have been made considering the following:

- the information given should concern (one of) the items mentioned above;
- the information given should not be valid for special conditions only;
- the information given should be of practical use for this study.

3.2 Scaling Factors

The possible scaling difference that exists between the real geometry of the examples described in chapter 1 (prototypes), and the geometry of the models described in the articles deserves some attention.
When the model diameter is equal to n times the prototype diameter, comparing the values for prototype and model of the following parameters gives the necessary insight in the scaling effects:

- Reynolds number; Reynolds scaling yields (eq. 3.1 to 3.3):

$$Re_{prototype} = \frac{V_p \cdot D_p}{\nu_p} = \frac{V_m \cdot D_m}{\nu_m} = Re_{model} \qquad (3.1)$$

$$D_p = \left(\frac{1}{n}\right) \cdot D_m \quad ; \quad \nu_p = \nu_m \tag{3.2}$$

$$\rightarrow \boxed{V_p = (n) \cdot V_m} \tag{3.3}$$

- Strouhal number; Strouhal scaling yields (eq. 3.4 to 3.6, see also section 3.3, eq. 3.14):

$$St_p = \frac{f_p \cdot D_p}{V_p} = \frac{f_m \cdot D_m}{V_m} = St_m \tag{3.4}$$

$$D_p = \left(\frac{1}{n}\right) \cdot D_m \quad ; \quad V_p = (n) \cdot V_m \tag{3.5}$$

$$\rightarrow \boxed{f_p = (n^2) \cdot f_m} \tag{3.6}$$

- maintainance of flow geometry; since the transverse velocity should be of the same scale as the scale of the towing velocity one obtains (eq. 3.7 to 3.10):

$$V = \frac{dy}{dt} = \frac{d(A \cdot \sin(f \cdot t))}{dt} = A \cdot f \cdot \cos(f \cdot t) \tag{3.7}$$

$$\rightarrow \quad V_m = A_m \cdot f_m = \left(\frac{1}{n}\right) \cdot A_p \cdot f_p = \left(\frac{1}{n}\right) \cdot V_p \tag{3.8}$$

$$f_p = (n^2) \cdot f_m \tag{3.9}$$

$$\rightarrow \boxed{A_p = \left(\frac{1}{n}\right) \cdot A_m} \tag{3.10}$$

For the present study, scaling according to the equations 3.3, 3.6 and 3.10 will be sufficient.

3.3 Information Gathered

Almost every article found uses the Morison et al. publication (1950) as a reference. The following (in sections 3.3.1 to 3.3.3), a part of Chakrabarti's work (1987), is thought to be a proper reproduction of that.

3.3.1 Morison Equation

(Wave) forces on structures are calculated in three different ways, using:

1 the Morison Equation which should be applied when the drag force is significant;

2 Froude-Krylov Theory which should be applied when only the inerta force is significant but the drag is relatively small;

3 the Diffraction Theory which should be applied when a large structure alters the wave/flow field in the vicinity of the structure causing diffraction; the flow is examined on a point to point basis.

Since only SLENDER structures were to be examined in this study (see section 2.4), the Diffraction Theory will therefore not be relevant.
The Morison equation can be written as follows (eq. 3.11 and 3.12):

$$dF = C_I \cdot A_I \cdot \frac{dV}{dt} \cdot ds + C_D \cdot A_D \cdot |V| \cdot V \cdot ds \quad (N) \qquad (3.11)$$

$$A_I = \frac{\pi}{4} \cdot \rho \cdot D^2 \; ; \; A_D = \frac{1}{2} \cdot \rho \cdot D \qquad (3.12)$$

Borgman (1958) has applied the Morison equation for an inclined cylinder, and takes into account only the components of velocity and acceleration NORMAL to the cylinders axis. This approach has been justified later by Chakrabarti et al. (1977) among others.
According to Chakrabarti it appears that the Morison Equation application to a complex time dependent flow can be questioned. The Morison Equation is in case of a cross current with an oscillation at least less satisfactory if not inadequate. He does not explain this further, however.

3.3.2 Oscillating Flow Vortex Shedding

In the KC (Keulegan Carpenter number: eq. 3.13) range of 8-20 the results from the current only flow cannot be combined with the results from the oscillatory flow.

$$KC = \frac{\hat{V} \cdot T}{D} \quad (-) \qquad (3.13)$$

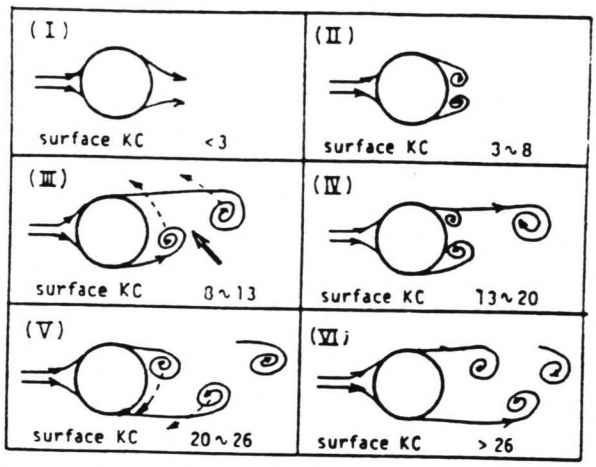

Vortex shedding patterns around a vertical cylinder in waves as functions of KC [Iwagaki, *et al.* (1983)]

FIGURE 3.1

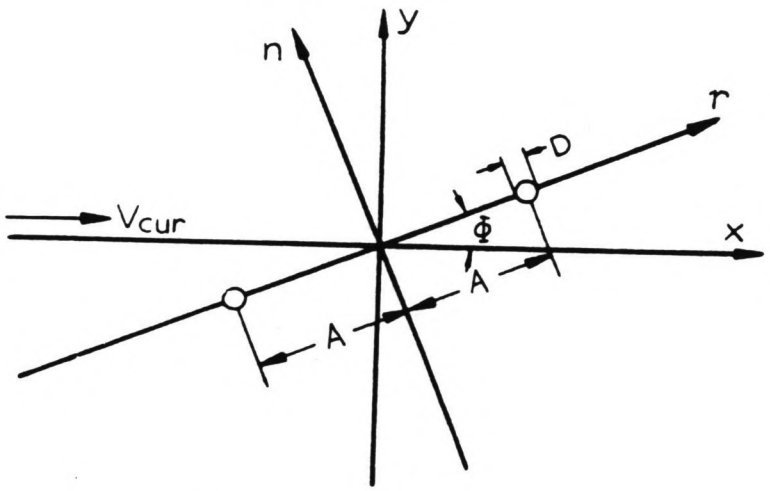

Direction of uniform current and cylinder's sinusoidal oscillation

FIGURE 3.2

FIGURE 3.3

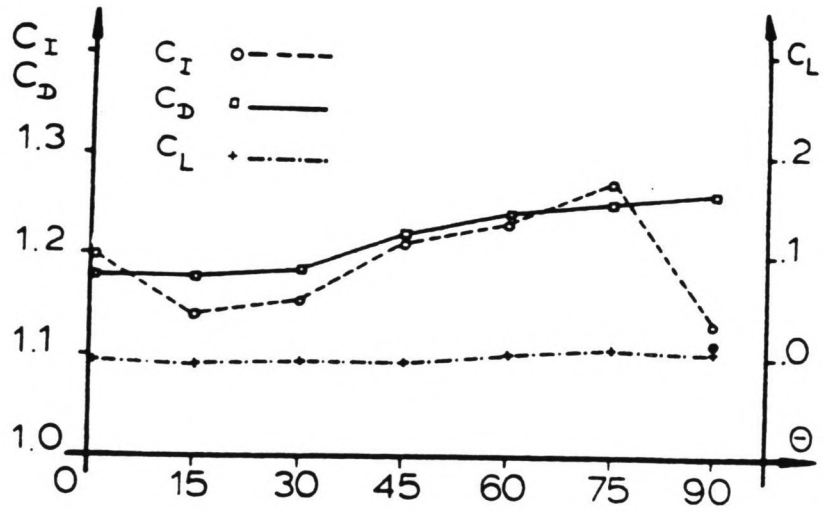

C_I , C_D , C_L , **versus Angle** Φ

The forces on and motion of the structure are dependent upon the water particle kinematics as well as the velocity and acceleration of the structure itself. The transverse forces are the result of the flow separation from the cylinder wall. When the KC number exceeds 5, vortices will shed from the cylinder wall asymmetrically, causing an alternating lift force transverse to the flow direction (fig. 3.1).

3.3.3 Vortex Shedding in Currents

In a constant current the frequency of the vortex shedding together with the flow velocity and the cylinder diameter can be written as a dimensionless parameter: the Strouhal number (eq. 3.14). At subcritical Reynolds numbers, the Strouhal number appears to be nearly constant (St=0.20), and the vortex shedding frequency then determined from equation 3.14 is often called the "Strouhal" frequency.

$$St = \frac{f_v \cdot D}{V} \quad (-) \qquad \textbf{(3.14)}$$

However, the shedding appears to be somewhat irregular, and with the presence of a flow field that influences the motion of the vortices shed (earlier) it gives a pressure distribution around the cylinder that can be considered as a random function of time. The description of this situation with a model has been the objective of many studies, including this one.

3.3.4 Further Results

Bernitsas (1979) has investigated the influence on the hydrodynamic coefficients for the non-stationary flow conditions occurring when a cylinder oscillates such that the plane of the oscillation direction and the cylinder axis make an angle, Φ, with the current (fig 3.2). The KC number was relatively small. The information about the angles could perhaps be used later on when modelling the situation for computational purposes, although no mathematical expressions are presented in this article. Some qualitative aspects are of interest (the coefficients are defined according to Morison's theory):

- the (time averaged) drag coefficient Cd increases with the angle, Φ, and reaches a higher value than for stationary conditions (fig. 3.3). This result is confirmed in detail by Every, King and Griffin (1982);
- the (time averaged) inertia coefficient appeared to be a strongly dependent on Φ (fig. 3.3);

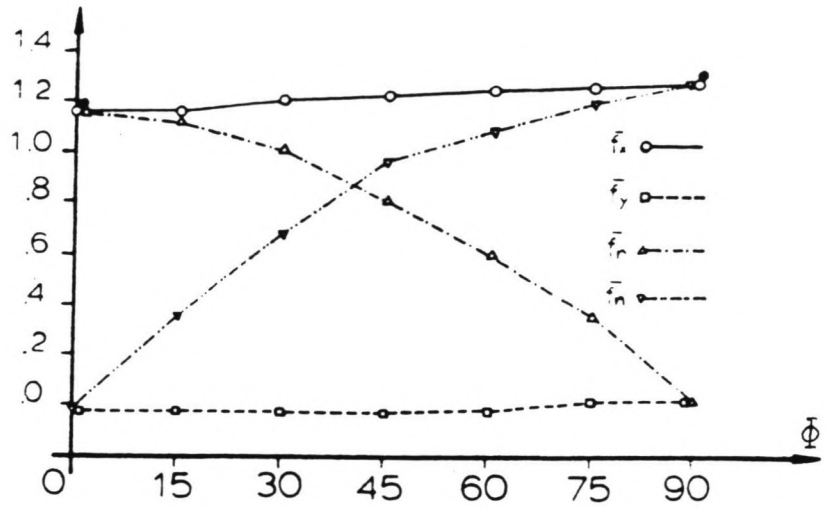

F_x, F_y, F_r, F_n, versus Angle Φ

FIGURE 3.4

FIGURE 3.5

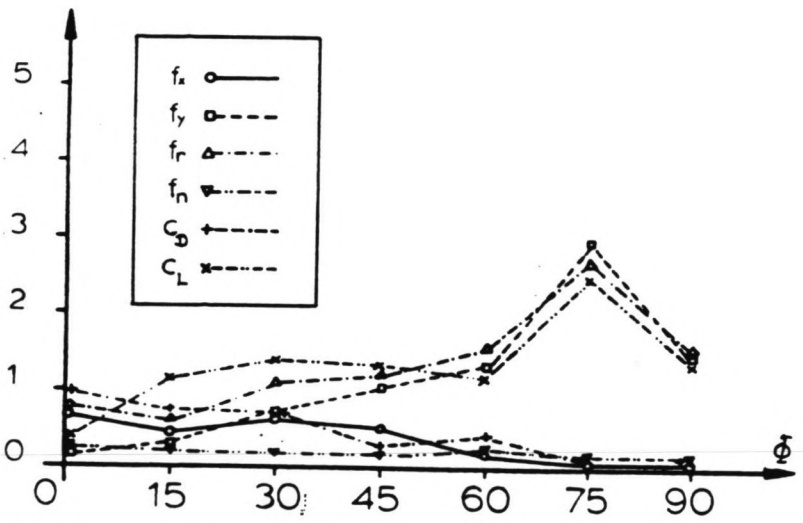

P.S.D.'s of f_x, f_y, f_n, f_r, C_D, C_L for f = 1 Hz, versus Angle Φ

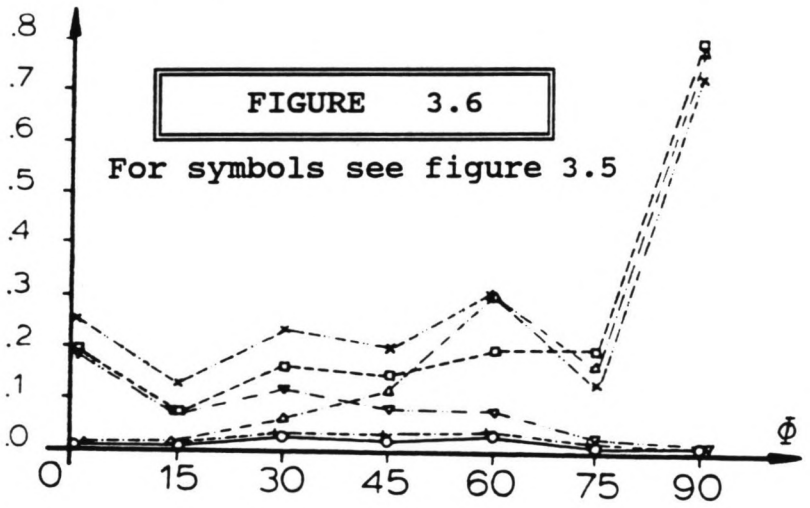

FIGURE 3.6

For symbols see figure 3.5

P.S.D.'s of f_x, f_y, f_n, f_r, C_D, C_L for f = 2 Hz, versus Angle Φ

- the average lift coefficient is close to zero (fig. 3.3). More interesting is the spectral analysis of the lift forces. At the frequency close to the Strouhal frequency a rather high density is found at Φ = 90 degrees, and less at other angles. At other frequencies, the density peaks occur at other angles as in fig. 3.4 to 3.10. No explanations are given, however.

Griffin (1980) gives a description of resonant vortex excited vibrations (the lock-in situation: the vortex shedding frequency is very close to the (natural) oscillating frequency of the cylinder) of flexibly mounted rigid tubes or flexible tubes in a fluid. He characterizes the hydrodynamic forces in a linear way as:

- an exciting force;
- a reaction (damping) force proportional to the structure velocity;
- an added mass force, proportional to the structure acceleration;
- a fluid inertia force.

The cylinder exciting coefficient (the lift force coefficient, perpendicular to the flow direction) reaches a maximum of 0.5 to 0.75 at a cross flow displacement of 0.6 to 1.0 cylinder diameters. This coefficient decreases to zero at a displacement of about 2 to 3 diameters. Of course, these values are influenced by the cylinder mounting and the mass-damping parameter (the Scruton number: eq. 3.15, see also Ruscheweyh (1986)), but indicate that there is a maximum oscillation amplitude for lock-in situations.

$$Sc = \frac{2 \cdot M \cdot \delta}{\rho \cdot D^2} \quad (-) \qquad (3.15)$$

Ericsson (1980) tried to explain the behaviour of the cylinder motion during a lock-in situation via the Magnus Effect: this effect is the development of a lift force due to the rotation of the cylinder around its axis. The following items are of practical interest:

- cross flow oscillations; these occur due to resonance with the vortex shedding near the Strouhal frequency and the ODD super- and sub-harmonics of the Strouhal frequency;
- in line oscillations; these occur at EVEN super- and sub-harmonics of the Strouhal frequency, but only at high subcritical Reynolds numbers and not at the Strouhal frequency itself.

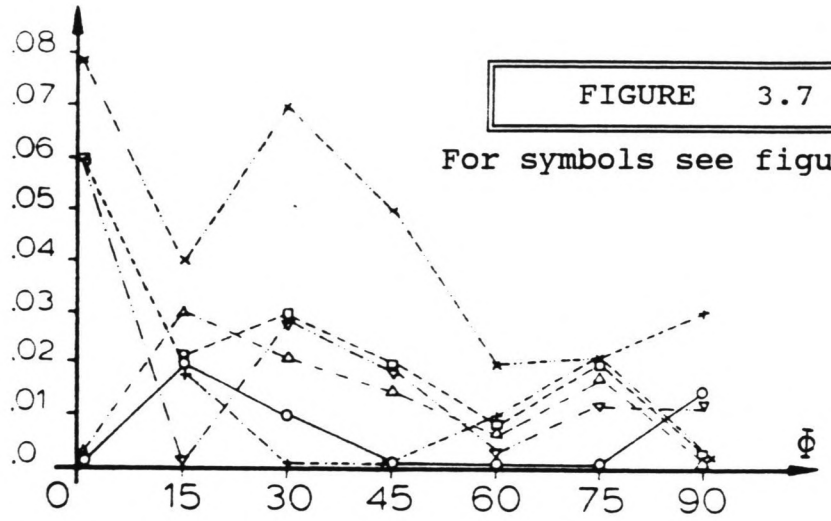

FIGURE 3.7

For symbols see figure 3.5

P.S.D.'s of f_x, f_y, f_n, f_r, C_D, C_L for f = 3 Hz, versus Angle Φ

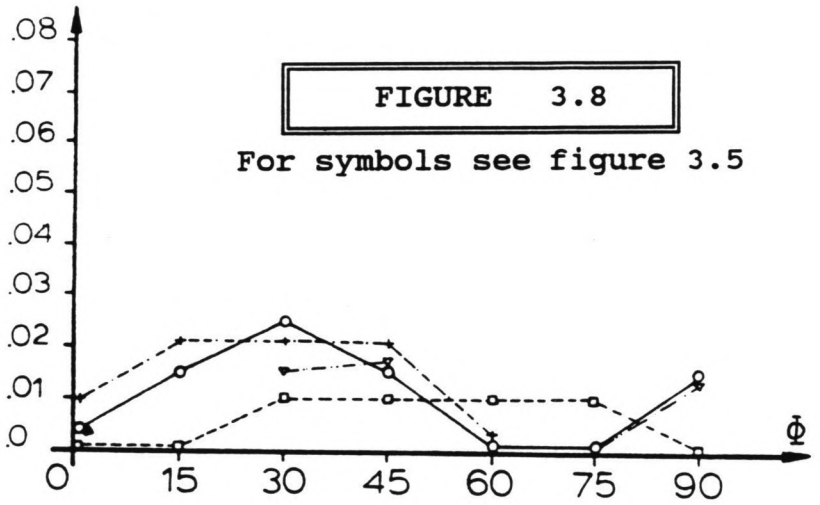

FIGURE 3.8

For symbols see figure 3.5

P.S.D.'s of f_x, f_y, f_n, f_r, C_D, C_L for f = 4 Hz, versus Angle Φ

FIGURE 3.9

For symbols see figure 3.5

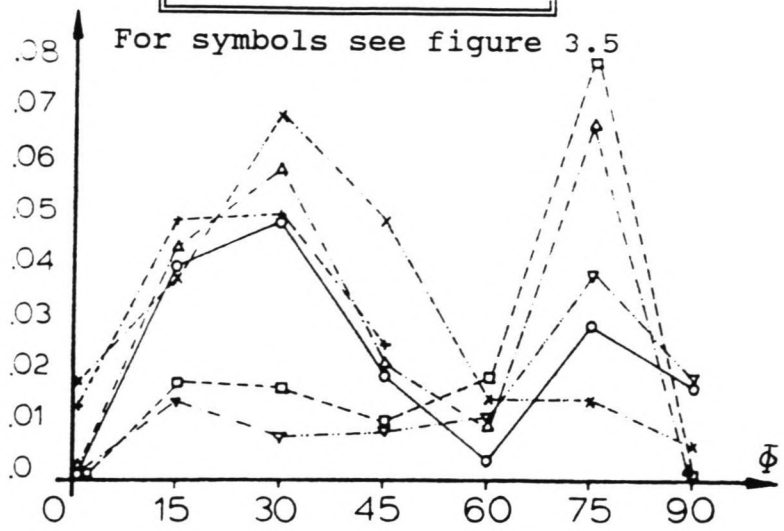

P.S.D.'s of f_x, f_y, f_n, f_r, C_D, C_L for f = 5 Hz, versus Angle Φ

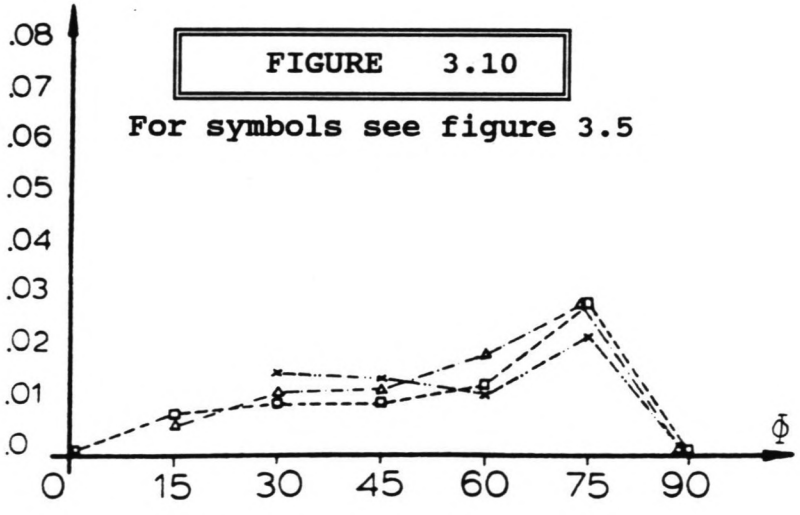

FIGURE 3.10

For symbols see figure 3.5

P.S.D.'s of f_x, f_y, f_n, f_r, C_D, C_L for f = 6 Hz, versus Angle Φ

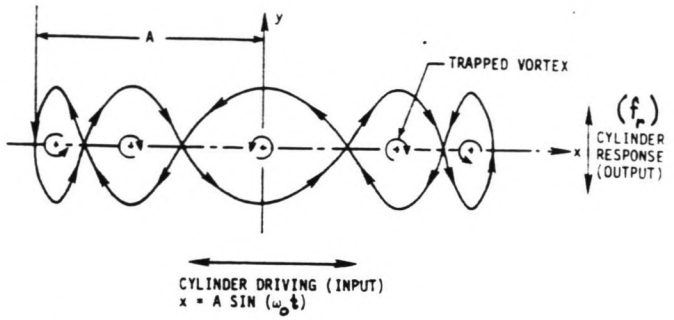

An example of Lissajous loop of cylinder motion when $f_r/f_o = 5$.

FIGURE 3.11

FIGURE 3.12

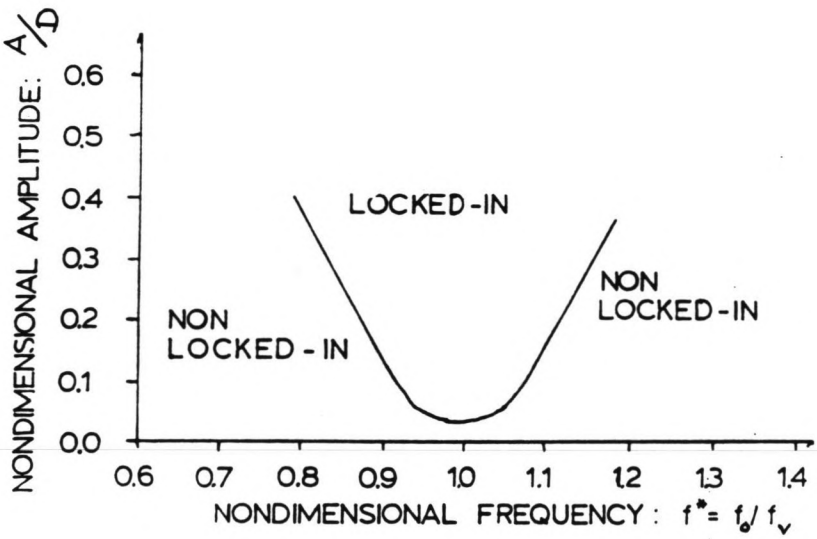

LOCK-IN BOUNDARIES IN $\frac{A}{D} - f^*$ SPACE
R_e = 19,300

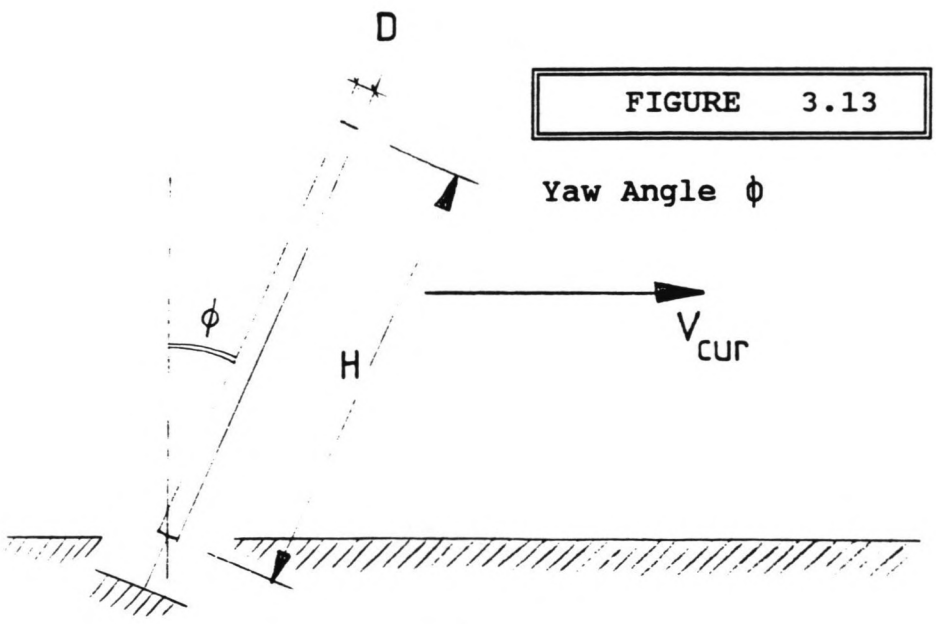

FIGURE 3.13

Yaw Angle ϕ

The (simple) model for the vortex induced forces developed by Verley (1982) is very practical for computer applications. Although this model is based upon an oscillating flow around a fixed cylinder, it seems rather easy to modify the model for the conditions of this study. The model uses instantaneous values of the velocity to determine the lift force on a finite cylinder element with length ds and its (Strouhal) frequency from eq. 3.16 to 3.18, as a function of time. Knowing the situation at time (t), the lift force at time (t+dt) can be calculated.

$$dF_L(t_2) = A_L \cdot C_L \cdot V(t_2)^2 \cdot \sin[\phi(t_1) + \psi(t_2)] \cdot ds \quad (N) \qquad (3.16)$$

$$A_L = \frac{1}{2} \cdot \rho \cdot D \;\; ; \;\; t_2 = t_1 + dt \qquad (3.17)$$

$$\psi(t_2) = 2 \cdot \pi \cdot f_v(t_2) \cdot dt = 2 \cdot \pi \cdot \frac{St \| V(t_2) \|}{D} \cdot dt \qquad (3.18)$$

Every, King and Griffin (1982) found that, compared with stationary conditions, the drag coefficient in Morison's formula is larger for the lock-in situation resulting in a 250 % larger drag force in the flow direction. A mathematical expression is presented for the value of this coefficient in equation 3.19, depending on the Strouhal frequency, the transverse oscillation amplitude and the reduced velocity:

$$C_D' = C_D \cdot [A_1 + B_1 \cdot [A_2 \cdot (1 + B_2 \cdot (1 - \cos(\frac{\pi \cdot x}{2})))]] \qquad (3.19)$$

$$A_1 = 1.00 \;\; ; \;\; B_1 = 1.16 \;\; ; \;\; St = 0.20 \qquad (3.20)$$

$$A_2 = \frac{1}{St \cdot V_{red}} = \frac{f_o}{f_v} \;\; ; \;\; B_2 = \frac{2 \cdot y_{max}}{D} \;\; ; \;\; V_{red} = \frac{V_{cur}}{f_o \cdot D} \qquad (3.21)$$

A similar expression could be used in the computational model (see chapter 7) when calculating the drag force on a moving cylinder as a function of time. The formula underestimates the drag coefficient at higher amplitudes and overestimates it at lower amplitudes, however.

McConnell and Park (1983) examined an oscillating flow field around an elastically mounted cylinder. They observed a cylinder motion that followed a Lissajous Loop (fig. 3.11, see for example Alonso and Finn (1983)), and related the lock-in conditions to a modified Strouhal number. These equations (3.22 and 3.23) suggest a linear relationship between the KC number and the ratio of the vortex shedding frequency and the oscillation frequency, but this appeared not to be true for lock-in conditions.

$$St = \frac{f_v \cdot D}{V_{max}} \quad ; \quad V_{max} = 2 \cdot \pi \cdot f_o \cdot A \qquad (3.22)$$

$$\Rightarrow \quad St = \frac{f_v}{f_o \cdot KC} \quad (-) \qquad (3.23)$$

However, this different definition of the Strouhal number justifies the use of another Strouhal number for other than stationary conditions.

Moeller and Leehey (1983) carried out experiments with an oscillating cylinder with amplitudes under 0.5 diameters in a cross flow. Their spectral analysis gave the following results:

- there is a dominant lift force frequency at the oscillation frequency and/or at the Strouhal frequency (the latter is defined for stationary conditions);
- when the oscillation frequency is not equal to the Strouhal frequency, it is possible that the lock-in situation occurs at this oscillation frequency for large amplitude oscillations, but does not occur for smaller oscillation amplitudes.

For amplitudes larger than 0.5 diameters figure 3.12 (derived from this article) gives no further information. This means that for larger amplitudes it is not sure at what frequency a lift force appears.

Bearman et al. (1984) further investigated the model developed by Verley (1982, described above), and made some corrections. They also executed laboratory experiments to investigate the validity of the model, which Verley did not. The experiments concerned oscillatory flows only, and the measurements of just one half cycle of flow oscillation were tried to be reproduced.
Their model appeared to be quite accurate at higher KC numbers (KC > 25) but showed rather poor results at lower KC values (KC < 15).
The use in this article of the viscous parameter bèta (equation 3.24) makes the comparison of Reynolds Number values for various (not only stationary) flow conditions possible (equation 3.25).

$$\beta = \frac{D^2}{\nu \cdot T} \quad (-) \qquad (3.24)$$

$$Re = \beta \cdot KC \; (= \beta \cdot 2 \cdot \pi \cdot \frac{A}{D}) \qquad (3.25)$$

The results from this investigation can be used when judging the validity of the theoretical model of the present study, when the oscillation-only experiments are analysed.

Ruscheweyh (1986) has investigated the influence of the yaw angle (fig. 3.13) and the Scruton number (eq. 3.15), of a cylinder in a cross flow on the appearance of cross flow vibrations (lock-in situation). According to Griffin (1980) the lock-in situation can occur for Scruton numbers $1.22 < Sc < 100$; according to Ruschewey the lock-in situation could occur at $Sc < 20$ without a significant influence of the yaw angle (which was varied from -50 degrees to +50 degrees), provided that the component of the velocity normal to the cylinder axis is used to determine the Strouhal frequency. For $Sc > 20$ the vibration amplitudes are getting too small and any yaw angle disturbs the vortex shedding in such a way that lock-in no longer occurs.

3.4 Summary and Conclusions

Information was needed about all possible flow conditions, in order to develop a universal mathematical model that describes the hydrodynamic interaction of a slender circular cylinder. In short, information has been found concerning (slender) circular cylinders in the following conditions:

- stationary flow conditions with the cylinder axis normal to the flow direction;

- stationary flow (cylinder axis normal to the flow direction) with additional fluid or cylinder oscillations;

  The following oscillation conditions have been reported:

  * inline with the flow direction ("inline": $\Phi = 0.0\,^\circ$);
  * perpendicular to the flow direction and normal to the cylinder axis ("crossflow": $\Phi = 90.0\,^\circ$);
  * making an angle Φ with the flow direction and normal to the cylinder axis ($0.0\,^\circ < \Phi < 90.0\,^\circ$).

  The origin of the cylinder oscillations in the literature examined was:

  * induced, caused by vortex shedding which implies that the frequency of oscillations is equal to the vortex shedding (Strouhal) frequency. Only crossflow oscillations and no oscillation amplitudes larger than 1.5 cylinder diameters were found here (Griffin [1980]);
  * forced, caused by other parts of the cylinder. Only oscillation amplitudes less than one cylinder diameter were investigated (Bernitsas [1979], Moeller and Leehey [1983]);

- oscillatory flow conditions.

    * Here, large amplitude oscillations have been investigated, but without the presence of a stationary flow field (McConnell and Park [1983]).

A mathematical description for the hydrodynamic forces according to the Morison theory is quite often questioned but always applied because no better alternative is available. The Morison equation (equations 3.11 and 3.12) describes the steady flow and oscillatory flow with reasonable accuracy where the drag- and inertia forces are concerned. However, the hydrodynamic coefficients Cd and Ci depend upon the Reynolds number or the Keulegan Carpenter number, and within some ranges of those parameters the error made will be large.
A (universal) description of the lift forces has not been found in the literature consulted. There is some information that can be used, however:

- In a stationary flow, vortex shedding introduces a lift force perpendicular to the flow direction.

- This lift force is often described as a harmonic oscillation with a frequency that can be related to the nature of the flow using Strouhal's relationship (equation 3.14).

- When the lift force frequency approaches either the natural frequency of the cylinder, or the frequency of oscillation of the cylinder, a resonant motion appears ("lock in").

- For oscillatory flow conditions two mathematical descriptions for the lift force frequency have been developed starting with the Strouhal relationship. One uses the maximum flow velocity to determine the vortex shedding frequency (McConnell and Park [1983]), the other uses the instantaneous flow velocity (Verley [1982]). The latter form seems to this author to be more appropriate for extension to more general flow and oscillation situations.

An information gap exists in the literature investigated for the following situation:

A stationary flow perpendicular to the cylinder axis combined with large amplitude, cylinder oscillations which are normal to the cylinder axis but not in the flow direction.

In other words, information is not available where non stationary flow conditions occur, or where the cylinder body motion is an important parameter.

4 MATHEMATICAL DESCRIPTION

In this chapter a theoretical model for the hydrodynamic forces on slender cylinders will be developed, partially based upon the information found in the literature survey (chapter 3). The model could be of practical use when the hydrodynamic forces on a finite cylindrical element have to be determined. In section 4.3 a simplified version of this model is presented, which will be considered as a "standard". The theoretical model I should be more accurate in predicting the hydrodynamic forces than this (standard) model II.

4.1 Theoretical Model for the Hydrodynamic Forces on Slender Cylinders (Model I)

A description of the hydrodynamic forces for all conditions (lock-in and non lock-in, small and large oscillations) is presented here. Its basic assumptions are:

- the forces (drag-, inertia- and lift-) are described as functions of time;
- the drag- and inertia force will be described using the Morison equation: the drag force is proportional to the $V \cdot \|V\|$ term (quadratic drag) and the inertia force is proportional to the dV/dt term. Their lines of action are the same as those of the velocity and acceleration;
- the forces are related to the instantaneous relative motion between the cylinder and the surrounding water (velocity V and acceleration dV/dt) and are thought to act in a plane perpendicular to the cylinder axis;
- the lift force is described as follows:
  * the lift force is orientated perpendicularly to the drag force;
  * the lift force has a harmonic character, with a frequency equal to the vortex shedding frequency;
  * the lift force frequency is determined using equation 4.1,

$$f_{lift} = f_v(t) = St \cdot \frac{\|\vec{V}(t)\|}{D} \quad (Hz) \qquad (4.1)$$

  with a constant Strouhal number (St = 0.20, meaning that this approach is valid for subcritical Reynolds numbers only), and the instantaneous value of the resulting flow velocity V(t);
  * with the items mentioned above the lift force can be determined as a function of time, analogous to the model of Verley (1982): equation 4.2 to 4.4.

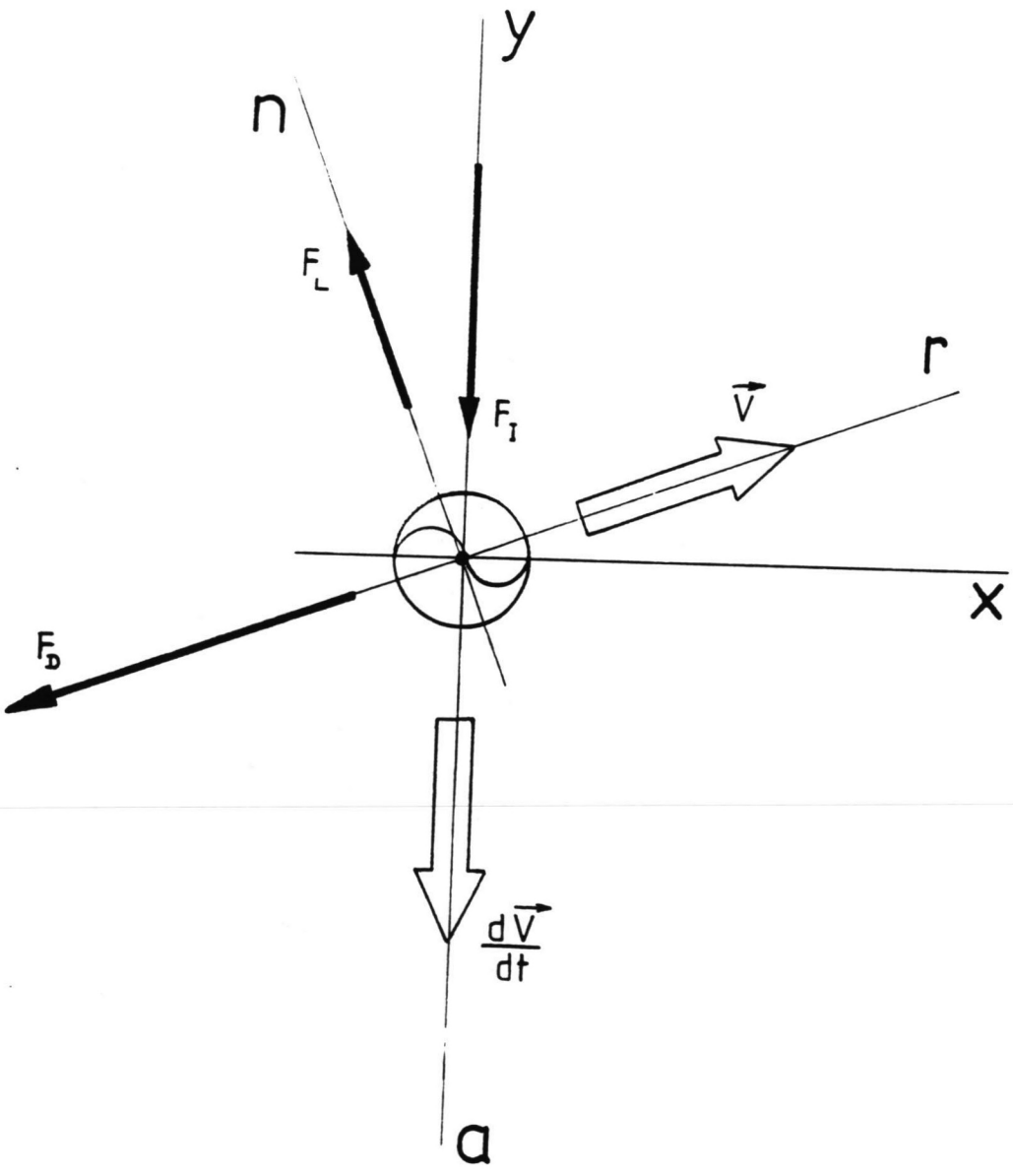

FIGURE 4.1

Hydrodynamic Forces Model

$$dF_L(t_2) = A_L \cdot C_L \cdot V(t_2)^2 \cdot \sin[\phi(t_1) + \psi(t_2)] \cdot ds \quad (N) \qquad (4.2)$$

$$A_L = \frac{1}{2} \cdot \rho \cdot D \;\; ; \;\; t_2 = t_1 + dt \qquad (4.3)$$

$$\psi(t_2) = 2 \cdot \pi \cdot f_v(t_2) \cdot dt \qquad (4.4)$$

The complete model I of the forces dF(t) on an element ds of a circular cylinder can be written as in equations 4.5 to 4.8, with t2 = t1 + dt (see also figure 4.1).

$$d\vec{F}_D(t_2) = A_D \cdot C_D \cdot V(t_2) \cdot \|V(t_2)\| \cdot ds \quad (N) \qquad (4.5)$$

$$d\vec{F}_I(t_2) = A_I \cdot C_I \cdot \frac{\partial V(t_2)}{\partial t} \cdot ds \quad (N) \qquad (4.6)$$

$$d\vec{F}_L(t_2) = A_L \cdot C_L \cdot V(t_2)^2 \cdot \sin[\phi(t_1) + \psi(t_2)] \cdot ds \qquad (4.7)$$

$$A_D = A_L = \frac{1}{2} \cdot \rho \cdot D \;\; ; \;\; A_I = \frac{\pi}{4} \cdot \rho \cdot D^2 \;\; ; \;\; \psi(t_2) = 2 \cdot \pi \cdot f_v(t_2) \cdot dt \qquad (4.8)$$

4.2 Lift Force Frequency Analysis

The lift force frequency of model I appears to include two special situations in case a vertical cylinder oscillates transverse to a stationary flow, as will be illustrated in this section.
When a cylinder is sinosoidally oscillating transverse to a steady current, the velocity V of the cylinder, relative to the surrounding flow, stays within the range of equation 4.9.

$$\|\vec{V}_{cur}\| \le \|\vec{V}\| \le \|\vec{V}_{cur} + \vec{V}_{o,max}\| \qquad (4.9)$$

Together with equation 4.1 this results in a range for the lift force frequency (or "Modified Strouhal Frequency") to appear, as in equation 4.10.

$$St \cdot \frac{\|\vec{V}_{cur}\|}{D} \le f_{lift} \le \frac{St}{D} \cdot \sqrt{\|\vec{V}_{cur}\|^2 + (2 \cdot \pi \cdot f_o \cdot A)^2} \qquad (4.10)$$

Two degenerate cases are included in equation 4.10: equation 4.11 represents the steady flow only case (with f_o = 0.0 or A = 0.0), and equation 4.12 the oscillation only case (with V = 0.0).

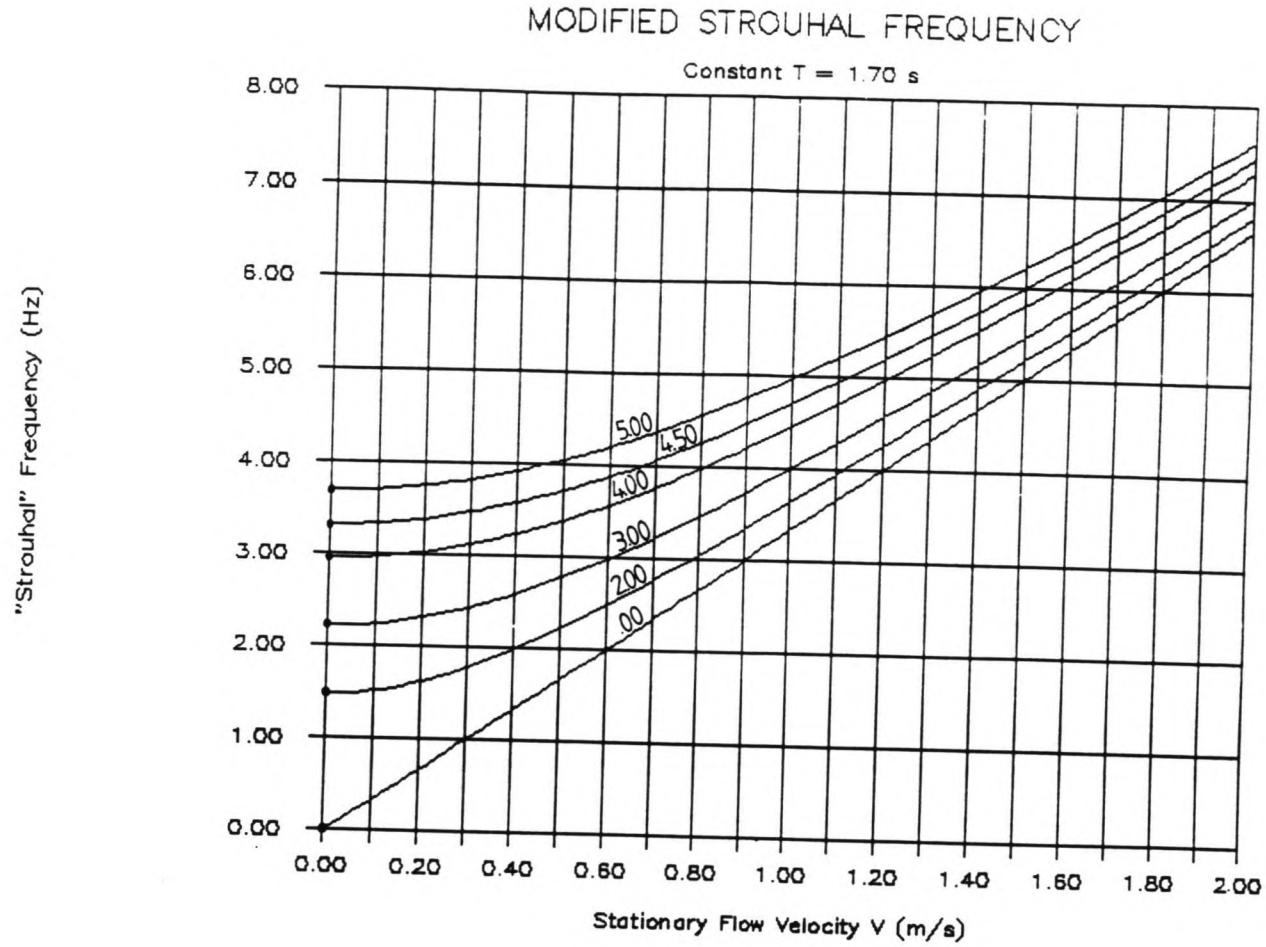

FIGURE 4.2 Lines of Constant A/D (-) **FIGURE 4.3**

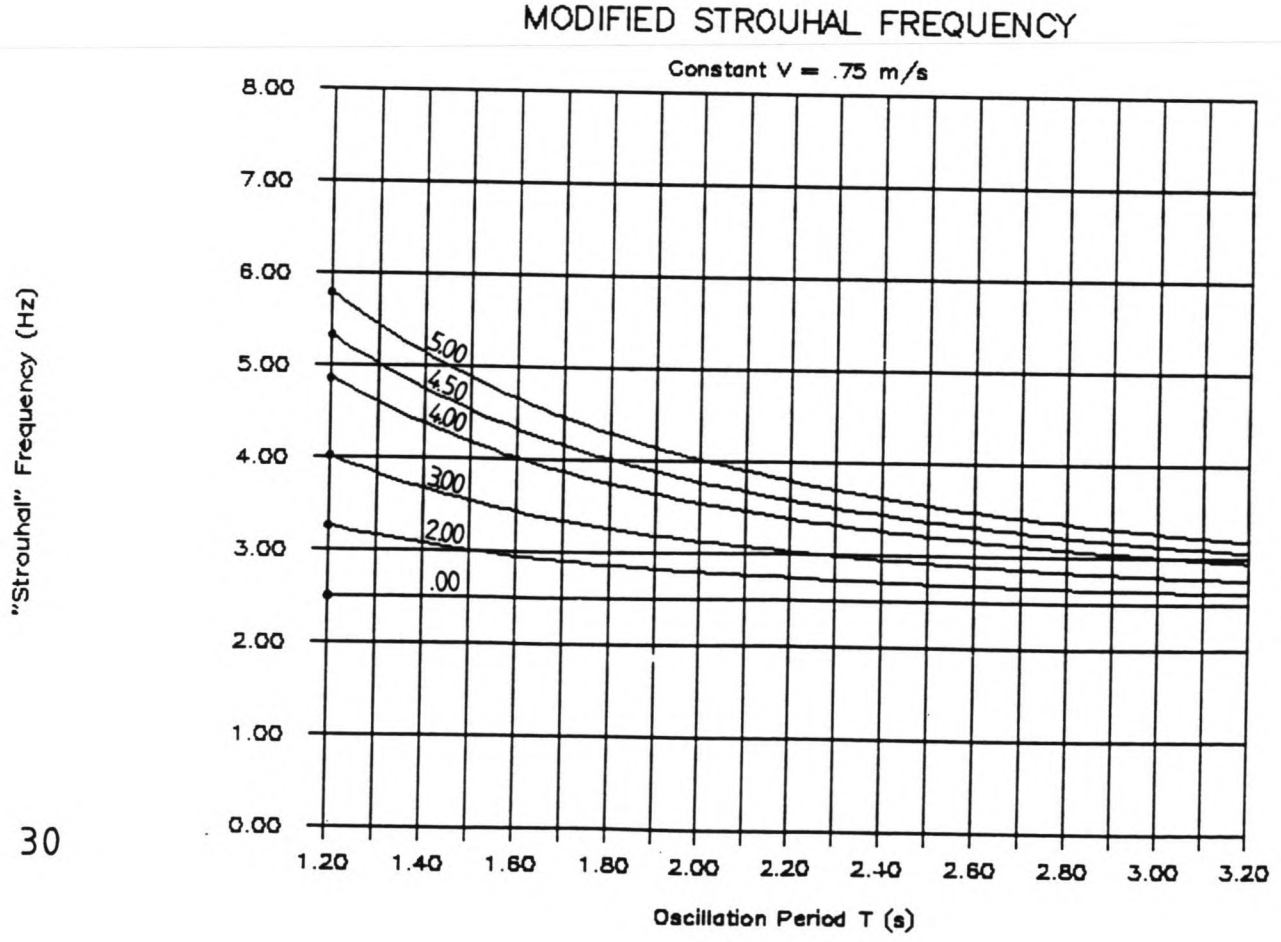

$$f_{lift} - f_v \tag{4.11}$$

$$0 \leq f_{lift} \leq St \cdot \frac{KC}{T_o} \tag{4.12}$$

The oscillation only case has been described by McConnell and Park (1983). They were able to describe this situation using the maximum value of the Modifies Strouhal Frequency from equation 4.12. This means that it would be possible to determine the Modified Strouhal Frequency for an oscillating cylinder in a cross flow from equation 4.13.

$$f_{lift} - \sqrt{f_v^2 + (St \cdot f_o \cdot KC)^2} \tag{4.13}$$

In figure 4.2 the Modified Strouhal Frequency from equation 4.13 is plotted for various velocity V and one constant period of oscillation T_o, and in figure 4.3 for various T_o and one constant V. A Strouhal Number value of 0.20 was used here.

4.3 Simplified Version (Model II)

The simplified version of the model differs from model I in only one way: the lift force frequency.
In model I the frequency of the lift force varies with the instantaneous resulting velocity V(t) (equation 4.1).
The simplified version considers the lift force frequency as a constant parameter. This means that the vortex shedding frequency is defined here by another (unknown) relationship than equation 4.1. When this relationship is known, the complete model II is also given by equations 4.5 to 4.8.
For the present study, just the basic assumption of a constant lift force frequency was enough to compare this with the model I (see chapter 9).

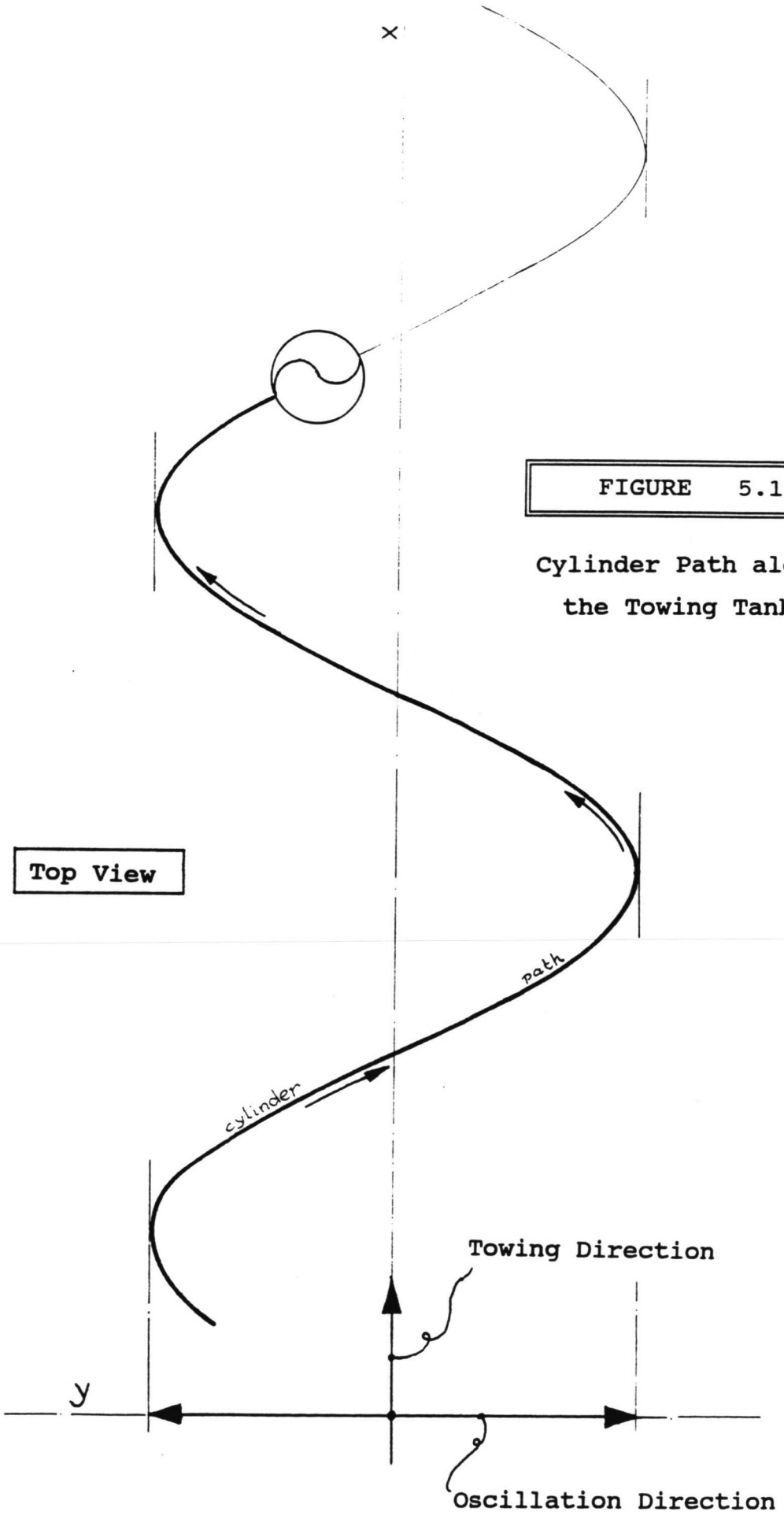

FIGURE 5.1

Cylinder Path along the Towing Tank

5 NEED FOR EXPERIMENTS

5.1 Missing Information

In general, the model of the equations 4.5 to 4.8 in section 4.1 can characterize the hydrodynamic forces that act on a finite cylinder element as a function of time, instantaneous acceleration and velocity.
To justify this model, a comparison should be made with already published theories and experimental results. Well known situations are described in section 3.3.
No investigations were found during the literature study for the forces on a cylinder undergoing large amplitude oscillations in a cross flow (see section 3.4). Only smaller amplitudes ($A/D < 1.5$) have been examined, at lock-in conditions. Bernitsas (1979) has paid some attention to non lock-in situations, but then only for one of the smaller amplitudes. A universal description for the hydrodynamic forces on a moving cylinder, including a proper lift force description, has not been found. Therefore a series of experiments should fill this information gap.

5.2 Laboratory Experiment Description

There has been the opportunity to execute the following experiments in the towing tank of Ship Hydromechanics Laboratory, TU Delft.
Each time, a vertically mounted cylinder has been towed with a constant speed V along the tank while being oscillated perpendicular to the towing direction with a constant amplitude A and constant oscillation frequency f_o ($= 1/T_o$).
The path of the cylinder is plotted in figure 5.1. By changing the three parameters V, A (or A/D) and f_o, the character of the flow experienced by the cylinder could be changed from a towing-only ($A/D = 0.0$) to an oscillation-only ($V = 0.0$ m/s) situation.
From these experiments information has been found about the hydrodynamic forces working on slender circular cylinders due to large amplitude forced oscillations in a cross current.

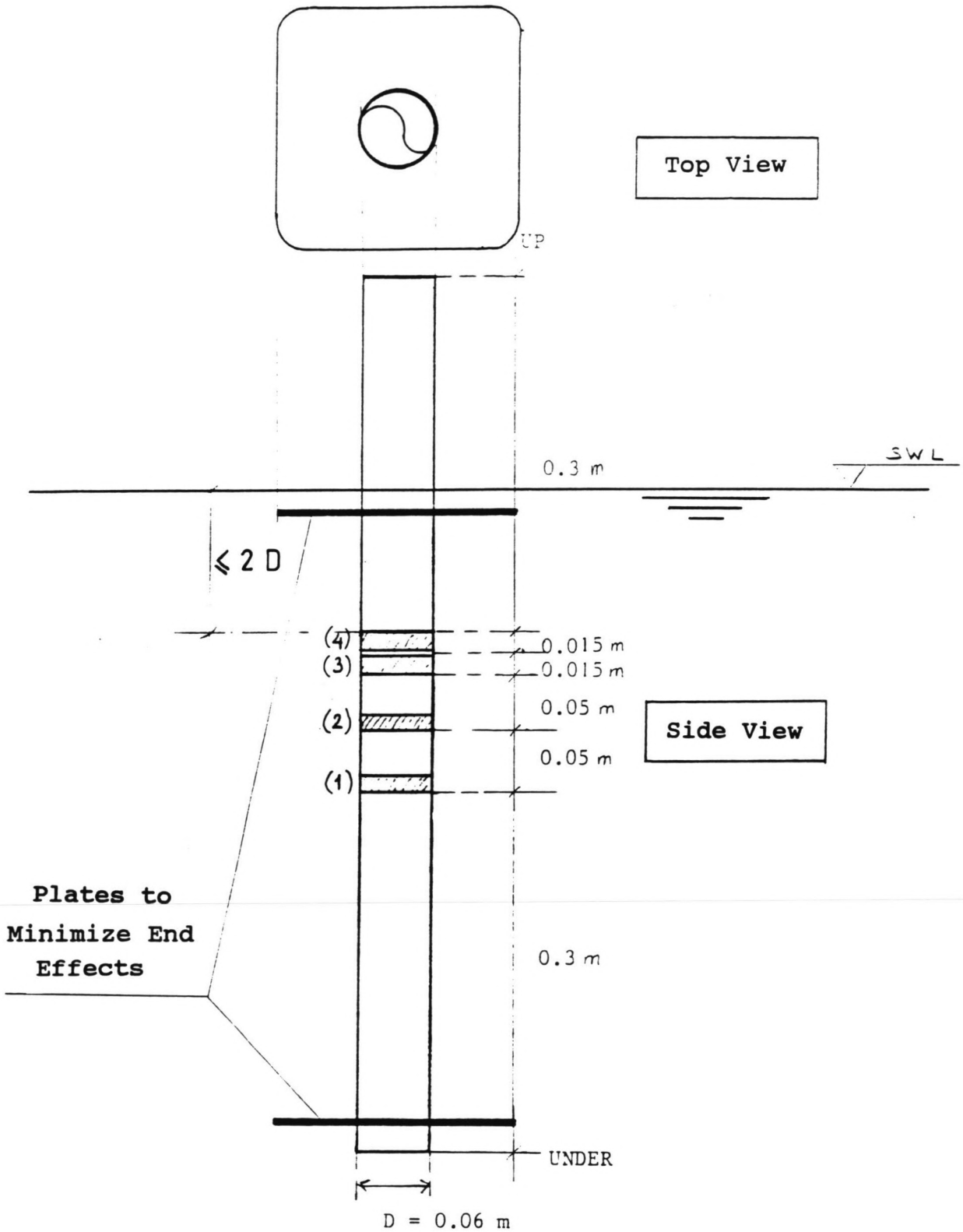

FIGURE 6.1

Marintek Test Cylinder

6 TEST CYLINDER CALIBRATION

6.1 General Aspects

The experiments (see section 5.2) have been executed using the test cylinder shown in figure 6.1, that has been manifactured by Marintek (Trondheim, Norway).
The force transducers were able to measure the hydrodynamic forces on each of the four rings, in two perpendicular directions.
Because of shallow submergence resulting from top-end cylinder mounting above the water surface the upper ring (no. 4) has not been used during the experiments; the influence of the disturbed water surface was considered to be too high. Therefore, this ring has not been examined during this calibration. Even so, if this ring was not going to be used, the distance between the water level and the top ring (no. 3) was small: two diameters or less.
The force transducers gave a signal by means of a series of strain-gages that are connected in a Bridge of Wheatstone.
Since the cylinder is not completely waterproof, water will enter the cylinder body. It is expected that water behind the ring inside the cylinder will have a significant influence on the (dynamic) forces measured, due to an added mass effect. A rubber skin could close the remaining (narrow) gaps between the ring and the cylinder wall. However, the presence of the rubber skin will certainly give another relationship between Volts and Newtons, and also the dynamic behaviour of the rings will probably be different.

N.B.: After the execution of the entire program of experiments, which took several days, it appeared that the use of the rubber skin probably saved the entire experiment (and the cylinder). Because of a potential difference that existed over the laboratory equipment (including the cylinder) and the water in the towing tank, the cylinder - made of aluminium - had corroded extremely fast. If no rubber skin had been used, the rings would probably have been stuck onto the cylinder wall. In that case, the measured forces would have been very, very low.

6.2 Calibration Program

The calibration program has investigated the following items:

- What is the relationship between the output signal (electrical: Volts) and the loading (forces: Newtons)?

  This relationship should be linear and should not show any hysteresis when the ring is loaded and unloaded.

- What is the influence of the rubber skin?

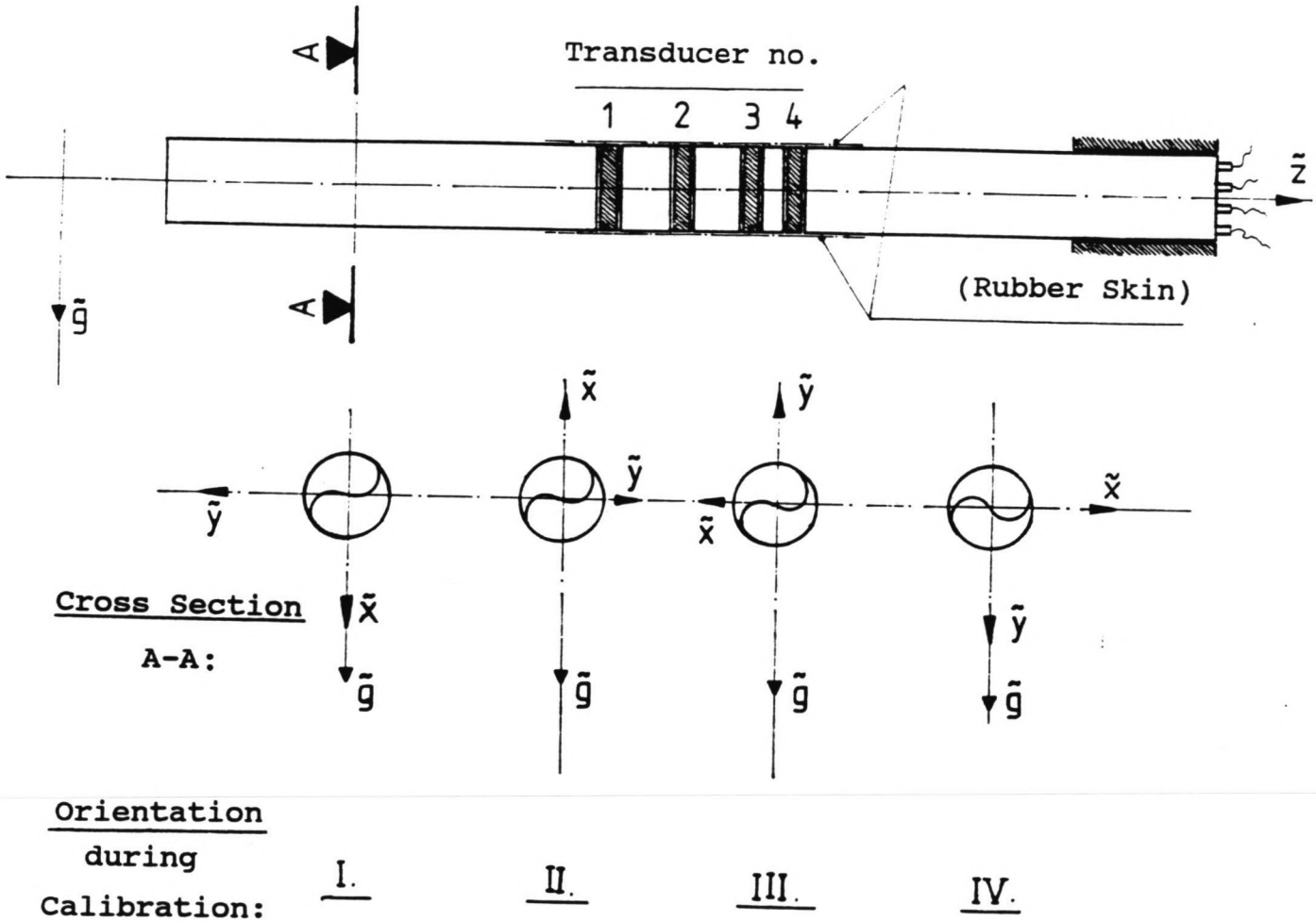

FIGURE 6.2

Test Cylinder Calibration Set Up

- What is the mass of the ring of each force transducer?

  When the cylinder is accelerated, the rings of the force transducers experience the same acceleration and will therefore cause a force signal that has got nothing to do with the hydrodynamic forces. When the ring mass is known, this force component can be eliminated.

- What is the behaviour of the instrument under dynamic loading conditions?

The calibration of the force transducers has been carried out in two phases: at first a static calibration, followed by a dynamic calibration.

6.3 Static Calibration Results

This calibration was carried out in October 1990 and had to give information about the calibration factors, mainly.
For each of the force transducers the relationship between the static loading and the output signal from the strain-gages has been investigated, with and without a rubber skin around the cylinder.
All (three) rings have been loaded in four different directions (I, II, III and IV). The set up of this calibration is shown in figure 6.2.
Weights associated with masses of 0.1 kg have been used, with a maximum load of 1.2 kg. At the time of this calibration it was not expected that the forces measured in the real experiments would stay under 2.0 N or would even stay close to the minimum of 0.05 N that can be measured (Marintek specification). This was caused by unexpected laboratory equipment limitations. Nevertheless, the assumption is made that the results found in this section are also valid for this range of small forces.
Because it is a static loading, an added mass effect will not be measured, so this calibration could take place in air as well as in water. For convenience the calibration has been done in air.
The cylinder has been marked in order to see in what directions forces components are registered.

6.3.1 Calibration Factors

The calibration factors for each direction of the transducers 1, 2 and 3, without a rubber skin are presented in table 6.1. The graphical presentation in figure 6.3 of the calibration should give two straight lines: one for an increasing load and one for a decreasing load. If the two lines are identical, no hysteresis occurs. The greater the distance between these lines, the greater the hysteresis effect.

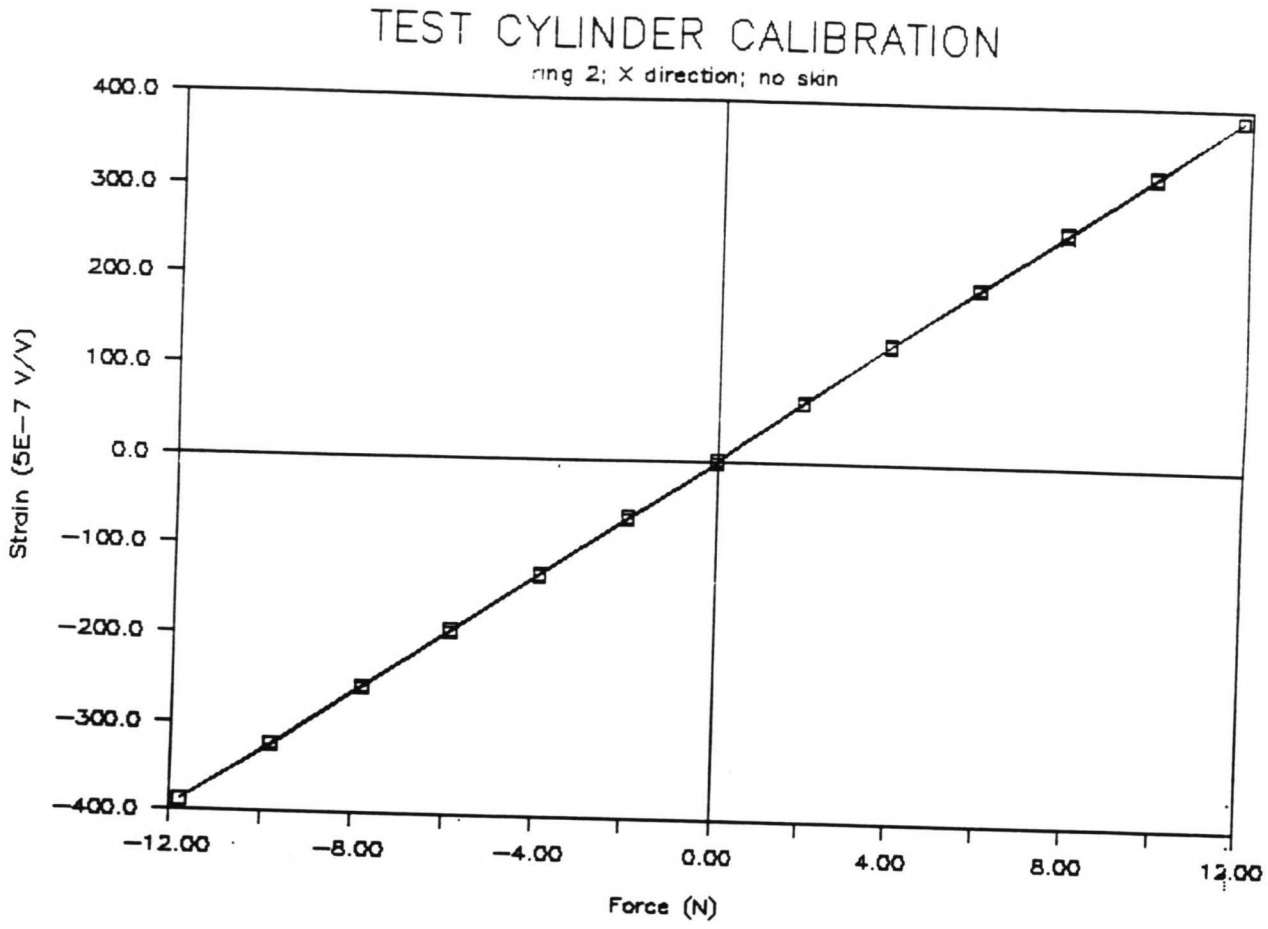

FIGURE 6.3

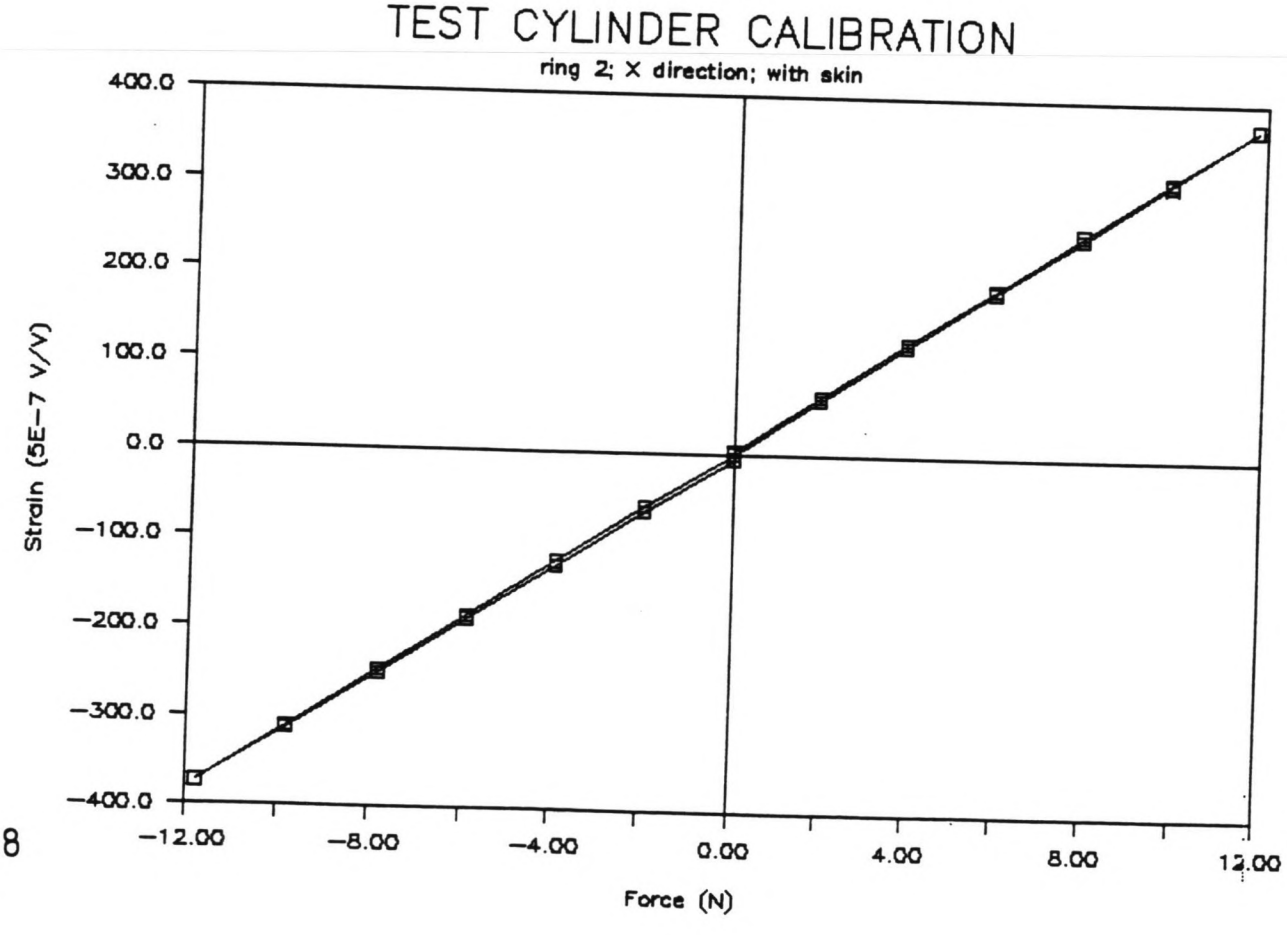

FIGURE 6.4

6.3.2 Rubber Skin Influence

The calibration factors for each direction of the transducers 1, 2 and 3, with a rubber skin are presented in table 6.2; the graphical result is shown in figure 6.4.
An additional hysteresis effect occured when using the rubber skin, but the figures in appendix C show that this is of minor importance (the regression constant still appeared to be close to 1.000 for all transducers).
The time dependency of the behaviour of the rubber skin is illustrated in table 6.3 (data figures in appendix C). Here the influence of time is presented for one of the loading directions (see section 6.1).
These data figures and those given in table 6.1 show that after one day the influence of the skin on the calibration factors has become less important. The difference is probably caused by relaxation of the rubber.

6.3.3 Axes Orientation

When comparing the measured force signals of different rings, one should know the rotation of the x and y axis of one transducer around the cylinder axis relative to the rotation of the x and y axis of the other transducers (see figure 6.5).
There appeared to be a (small) difference in orientation of the axes of each transducer relative to those of the other transducers (see tables 6.4 and 6.5, and appendix C), less than about 3 degrees (~ 0.05 rad). These relative rotations were found to be very small and varied for each orientation, probably because the x- and y- axis in each transducer are not exactly perpendicular.

6.4 Dynamic Calibration Results

The dynamic calibration was carried out in December 1990. An oscillation of the cylinder in air gave information about the ring masses. By loading the rings with a short pulse excitation, the dynamic response behaviour could be determined.

6.4.1 Ring Mass Determination

When oscillating the cylinder in air, the only forces working on the transducers that can be measured are those caused by the acceleration of the ring masses. Knowing the oscillation amplitude A and period T_o, the measured force in oscillation direction and the calibration factors of section 6.3.2, the ring mass can be determined from equations 6.1 and 6.2.

cylinder WITHOUT rubber skin (data figures in appendix C)			
transducer:	direction:	calibration factor: (1E-3 V/V/N)	
		Marintek calibration	Author's calibration
1	x	0.016919	0.016915
	y	0.016026	0.015532
2	x	0.015636	0.016438
	y	0.01503	0.015375
3	x	0.01438	0.014209
	y	0.01472	0.014795
(table 6.1)			

cylinder WITH rubber skin (data figures in appendix C)			
transducer:	direction:	calibration factor: (1E-3 V/V/N)	
		Author's calibration	
1	x	0.015966	
	y	0.014846	
2	x	0.015749	
	y	0.014292	
3	x	0.013766	
	y	0.013957	
(table 6.2)			

relaxation time: none	orientation: IV
transducer:	calibration factor: (1E-3 V/V/N) y- direction
1	0.014705
2	0.014261
3	0.013871
relaxation time: one day	orientation: IV
transducer:	calibration factor: (1E-3 V/V/N) y- direction
1	0.015230
2	0.014251
3	0.014037
(table 6.3)	

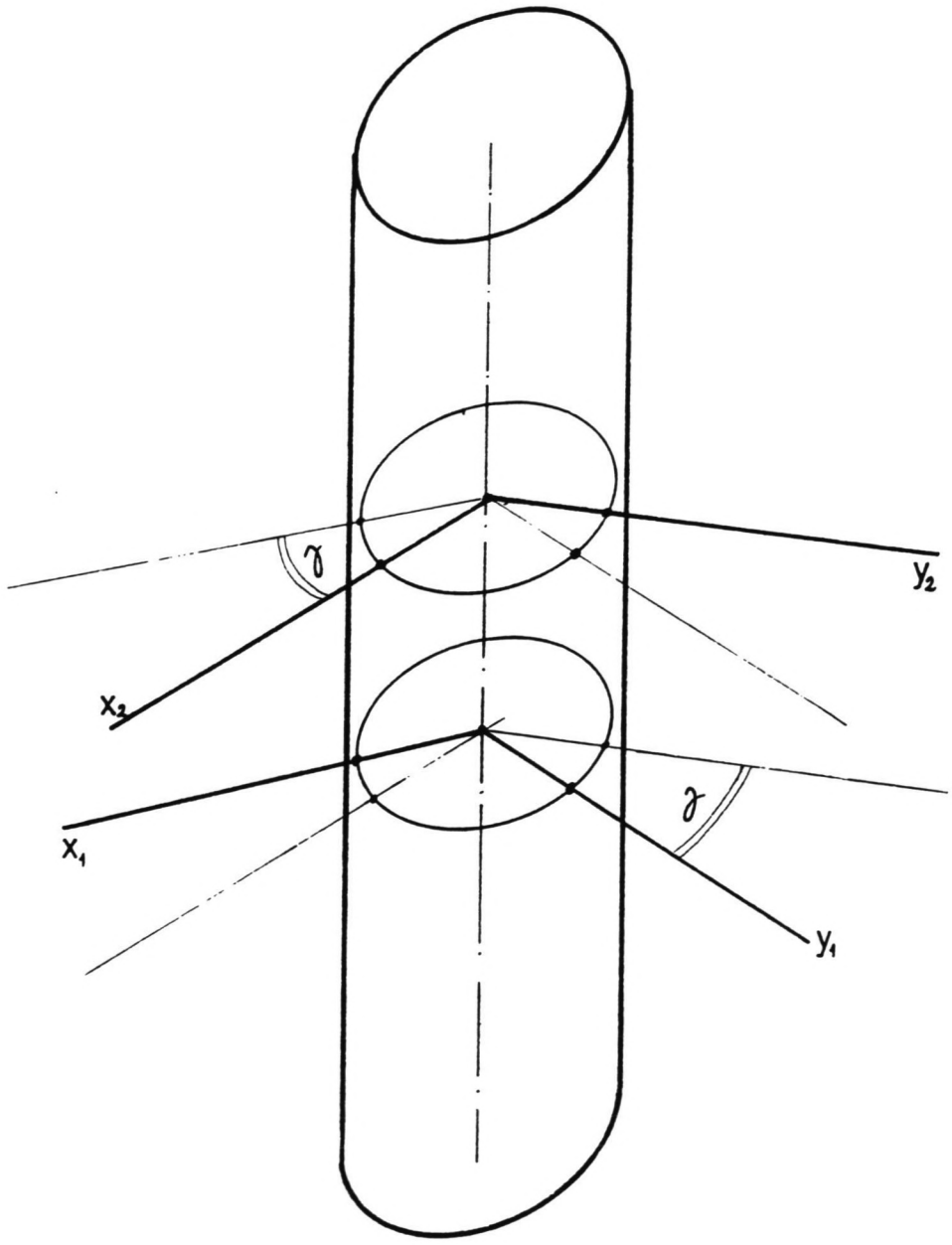

FIGURE 6.5

Relative Rotation between the Transducers

rotation: (rad)		
I	1	-0.0334
	2	-0.0199
	3	-0.0500
II	1	0.0112
	2	0.0097
	3	0.0328
III	1	0.0000
	2	-0.0388
	3	-0.0419
IV	1	0.0128
	2	0.0395
	3	0.0548

(table 6.4)

rotation: (rad)		
I	1	0.0000
	2	0.0000
	3	0.0000
II	1	0.0000
	2	-0.0068
	3	0.0338
III	1	0.0000
	2	-0.0415
	3	-0.0364
IV	1	-0.0181
	2	0.0000
	3	0.0253

(table 6.5)

ring masses from air oscillation	
ring no.	mass (kg)
1	0.0403
2	0.0407
3	0.0424

(table 6.6)

$$m_{ring} = \frac{F_{measured}}{a_{cylinder}} \qquad (6.1)$$

$$a_{cylinder} = -\left(\frac{2\cdot\pi}{T}\right)^2 \cdot A \cdot \sin\left(\frac{2\cdot\pi}{T}\cdot t\right) \qquad (6.2)$$

The ring masses determined are given in table 6.6. More detailed calculations are given in appendix C.

6.4.2 Dynamic Response Behaviour

6.4.2.1 Introduction

Each ring can be considered as a damped spring-mass system, as in figure 6.6.
In general, the response of this system to a harmonic excitation with frequency f_e is depending upon the stiffness of the spring and the damping ratio δ of the system. If the exciting force frequency is greater than a certain frequency f_k, the force transducer will indicate a force signal that is unrealistic, especially when the damping ratio is low and when fe is close to the natural frequency fn of the sytem (see figure 6.7).
Only for f_e < f_k the system can be considered as linear (i.e. the amplitude and phase of the registered force are equal to the exciting force: the relative response function = 1.0), which is needed to obtain proper measurements.

6.4.2.2 Determination of Natural Frequencies and Damping Ratio

The natural frequency fn and damping ratio δ can be determined from the theoretical force signal (figure 6.8) that is the result of a short pulse excitation.
This signal is, for the system of figure 6.6, described by equation 6.3. Here, the resonance frequency f_o of the spring in figure 6.6 is given by equation 6.4, where k is the calibration factor (see section 6.3) and m is the mass of the ring.

$$F(t) = A\cdot e^{-\frac{\delta}{\omega_o}\cdot t}\cdot\cos(2\cdot\pi\cdot f_n\cdot t+\phi_0) \qquad (6.3)$$

$$\omega_o = 2\cdot\pi\cdot f_o = \sqrt{\frac{1}{m\cdot k}} \qquad (6.4)$$

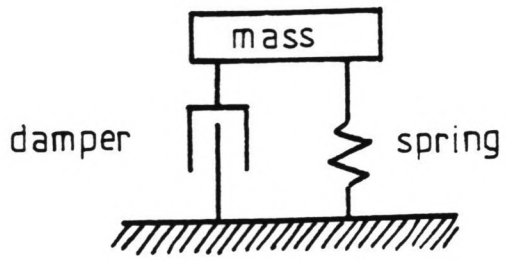

FIGURE 6.6

FIGURE 6.7

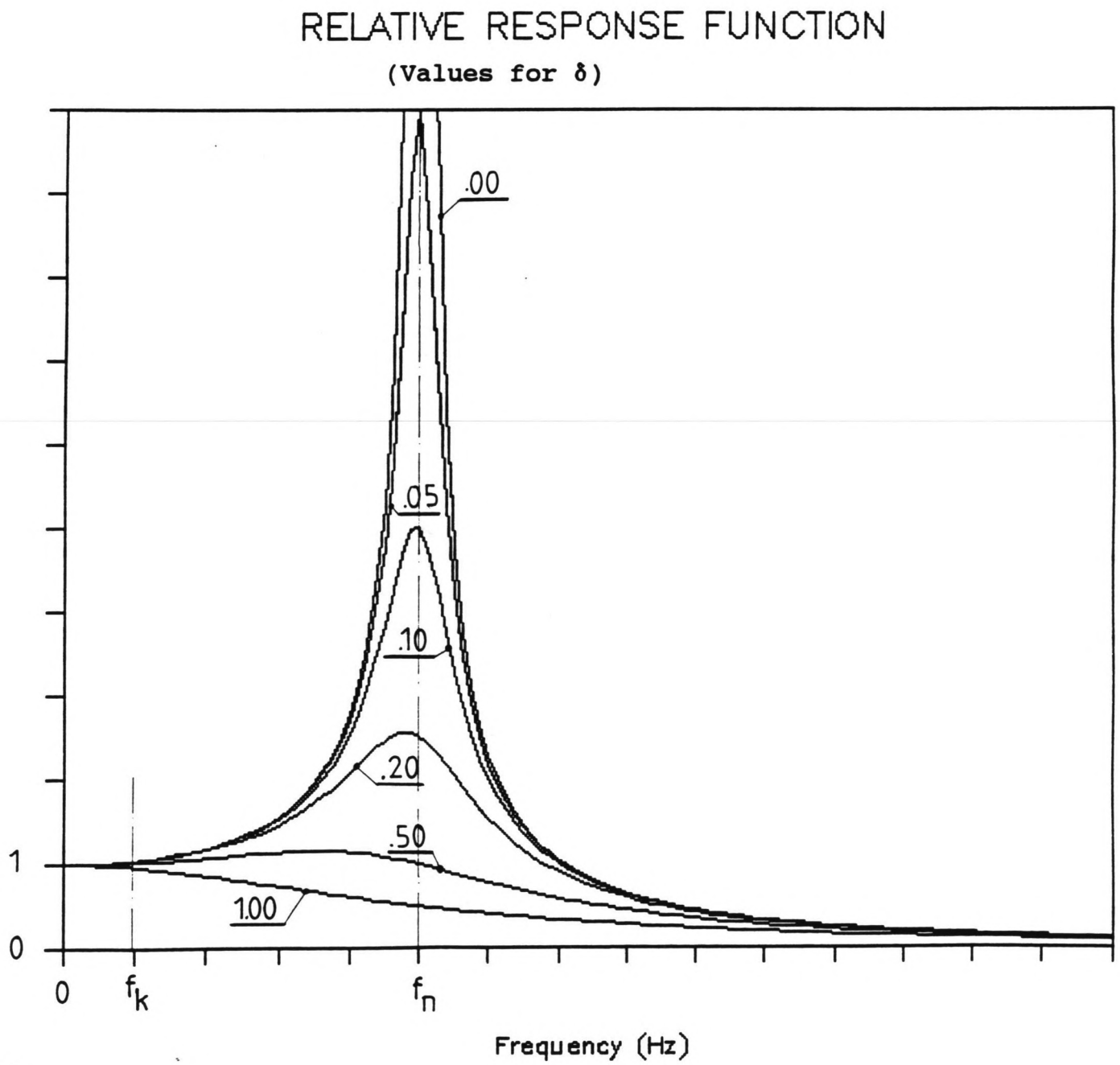

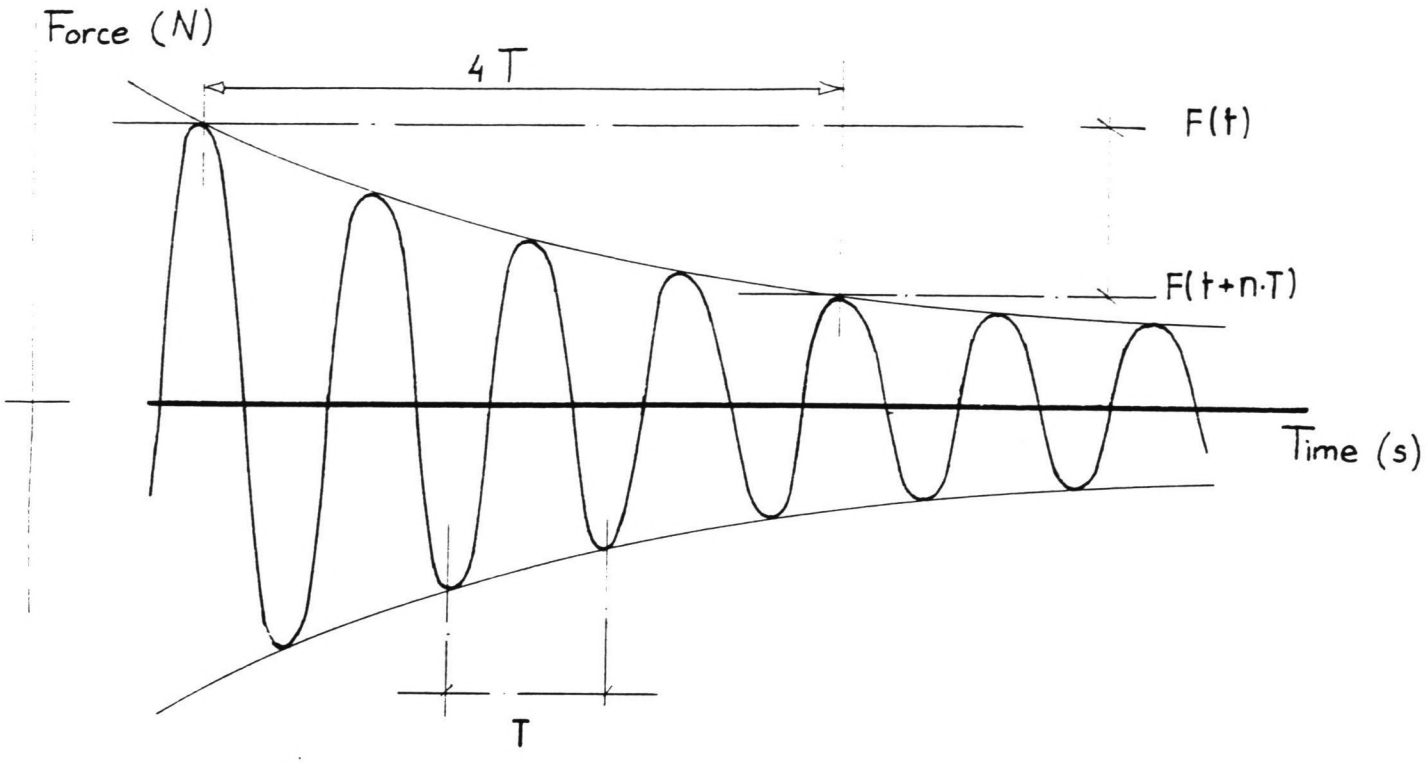

FIGURE 6.8

Cylinder Response to Pulse Excitation (Theoretical)

ring response to pulse excitation				
direction:	damping ratio (-)		natural frequency (Hz)	
	x	y	x	y
ring no.:				
1	?	0.0226	284.1	251.2
2	?	?	268.8	235.3
3	?	0.0273	279.3	243.3

(table 6.7)

direction:		calibration factor (1E-3 V/V/N)		natural frequency (Hz)	
		x	y	x	y
ring no.:	mass (kg)				
1	0.0403	0.015966	0.014846	198.5	205.9
2	0.0407	0.015749	0.014292	198.7	208.6
3	0.0424	0.013766	0.013957	208.3	206.9

(table 6.8)

In this case, the natural frequency follows from the measured period T between two upward zero crossings, and the damping ratio is given by equation 6.5, where the decrease of the oscillation amplitude over a number of cycli has to be inserted.

$$\delta = -\left(\frac{1}{n \cdot 2 \cdot \pi}\right) \cdot \ln\left(\frac{|F(t+n \cdot T_o)|}{|F(t)|}\right) \qquad (6.5)$$

The pulse excitation was achieved by hitting the ring with a stick which caused an oscillation of the ring at its natural frequency. These tests have been done in air only, with the rubber skin attached to the cylinder. The transducer signal has been recorded digitally, with a sample interval of 0.001 seconds.
It appeared that the recorded signals (see figures 6.9 to 6.11) were not like the expected from figure 6.8. This is probably caused by two effects:

- the pulse excitation has not been an ideal one;
- the sample interval was too long, causing (large) errors in the peak values.

Nevertheless, it has been tried to determine the natural frequencies and the damping ratios from these figures (table 6.7).
Another way to determine the natural frequency is presented below.
Using the calculated ring masses and calibration factors, the value for the natural frequencies of the system was determined from equation 6.4, assuming that the damping ratio is small. The results of this calculation are presented in table 6.8. Comparing the values of the frequencies determined in table 6.7 and 6.8, quite a divergence can be noticed. This is probably caused by the reasons mentioned earlier in this section. The (few) determined damping ratios were very small, which justifies the use of equation 6.4 for the (more reliable) calculation of the natural frequencies, instead of analysing the recorded force signals.

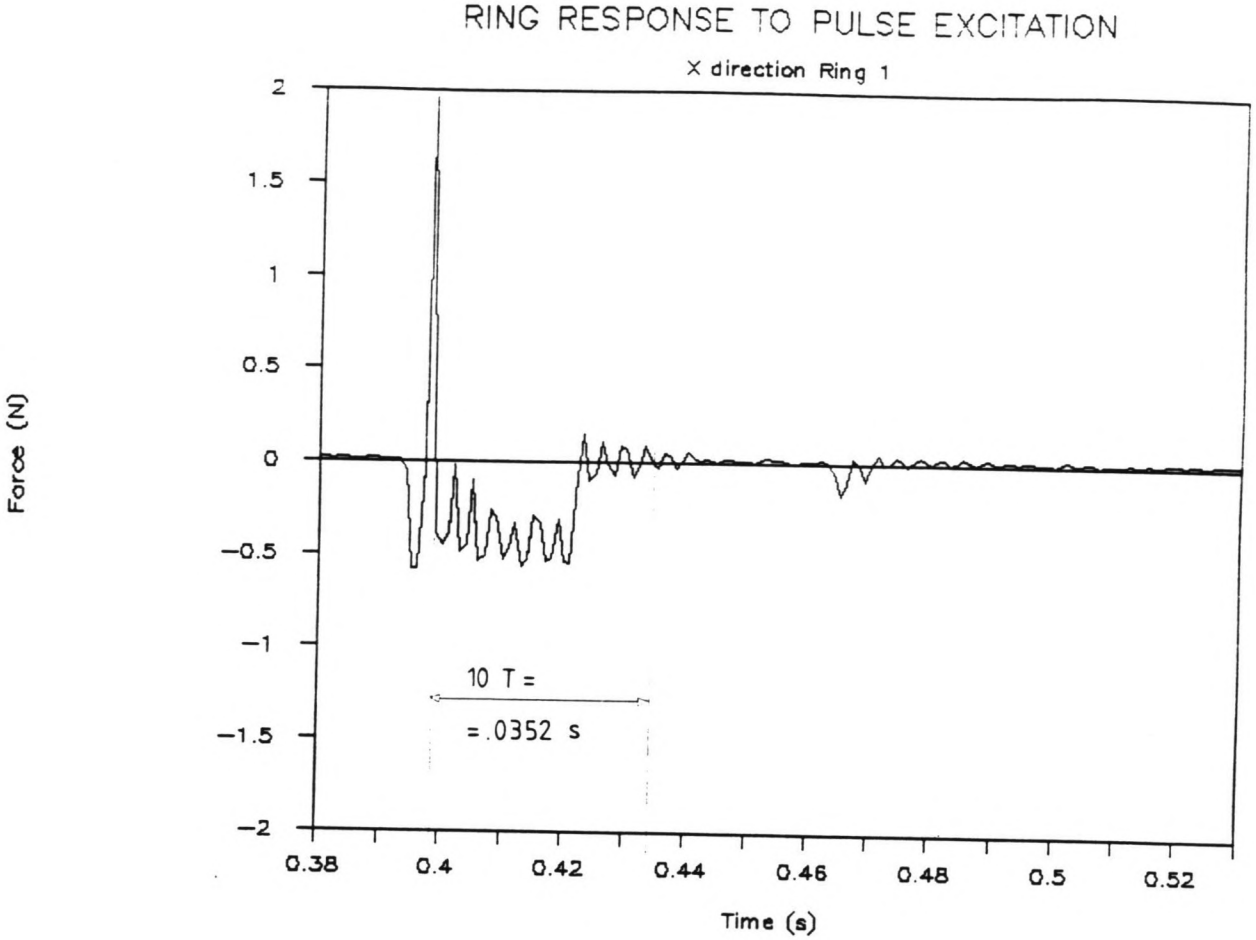

FIGURE 6.9.1

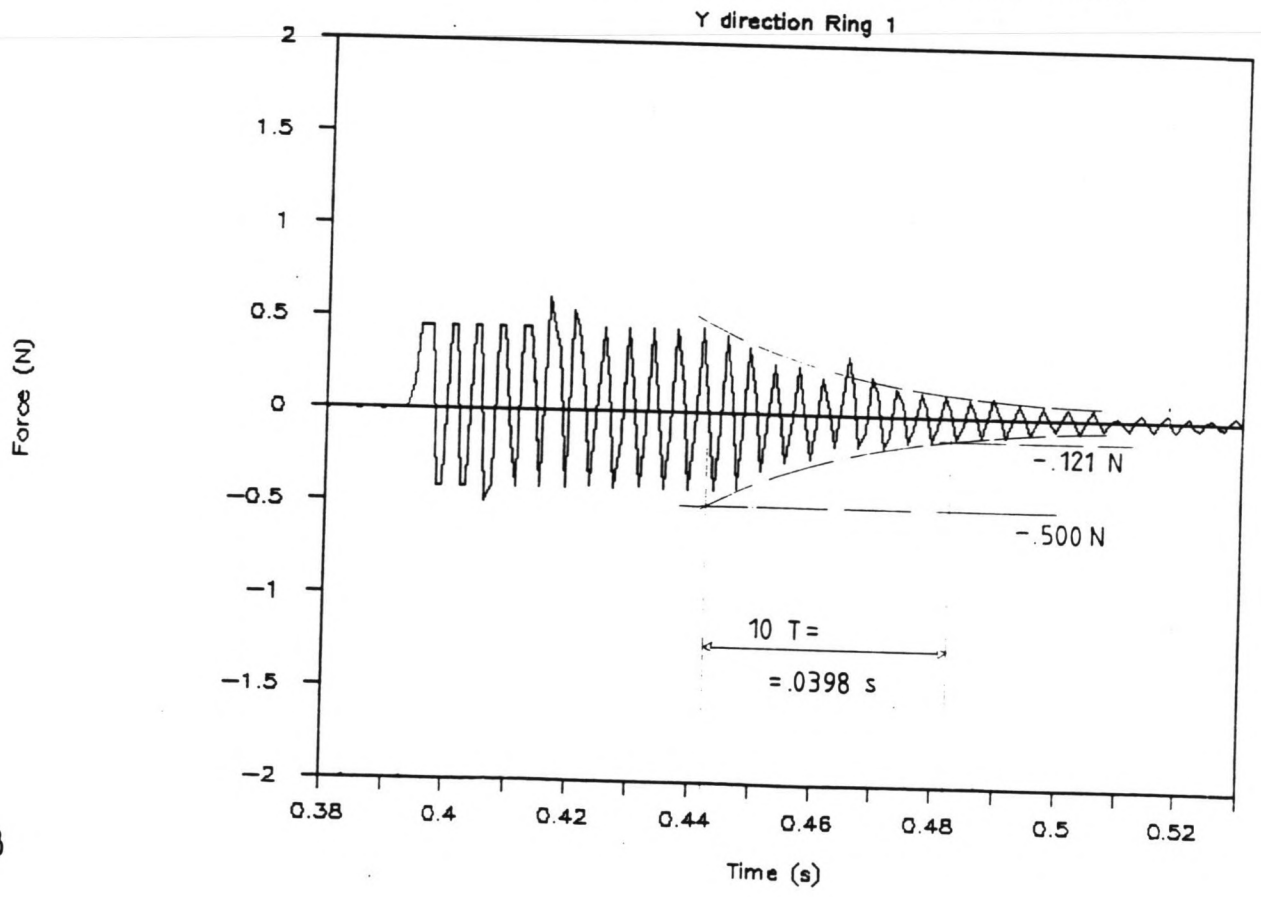

FIGURE 6.9.2

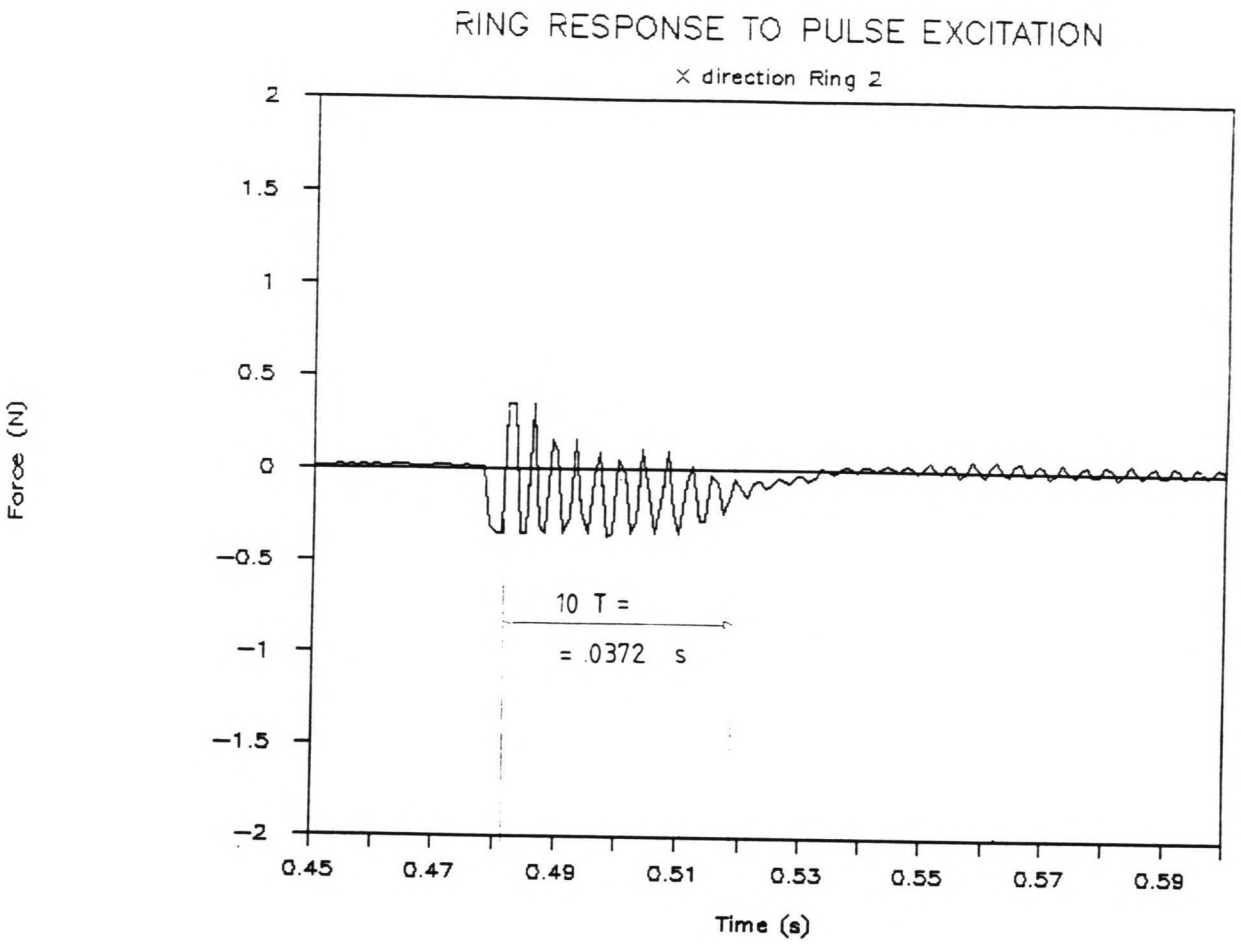

FIGURE 6.10.1

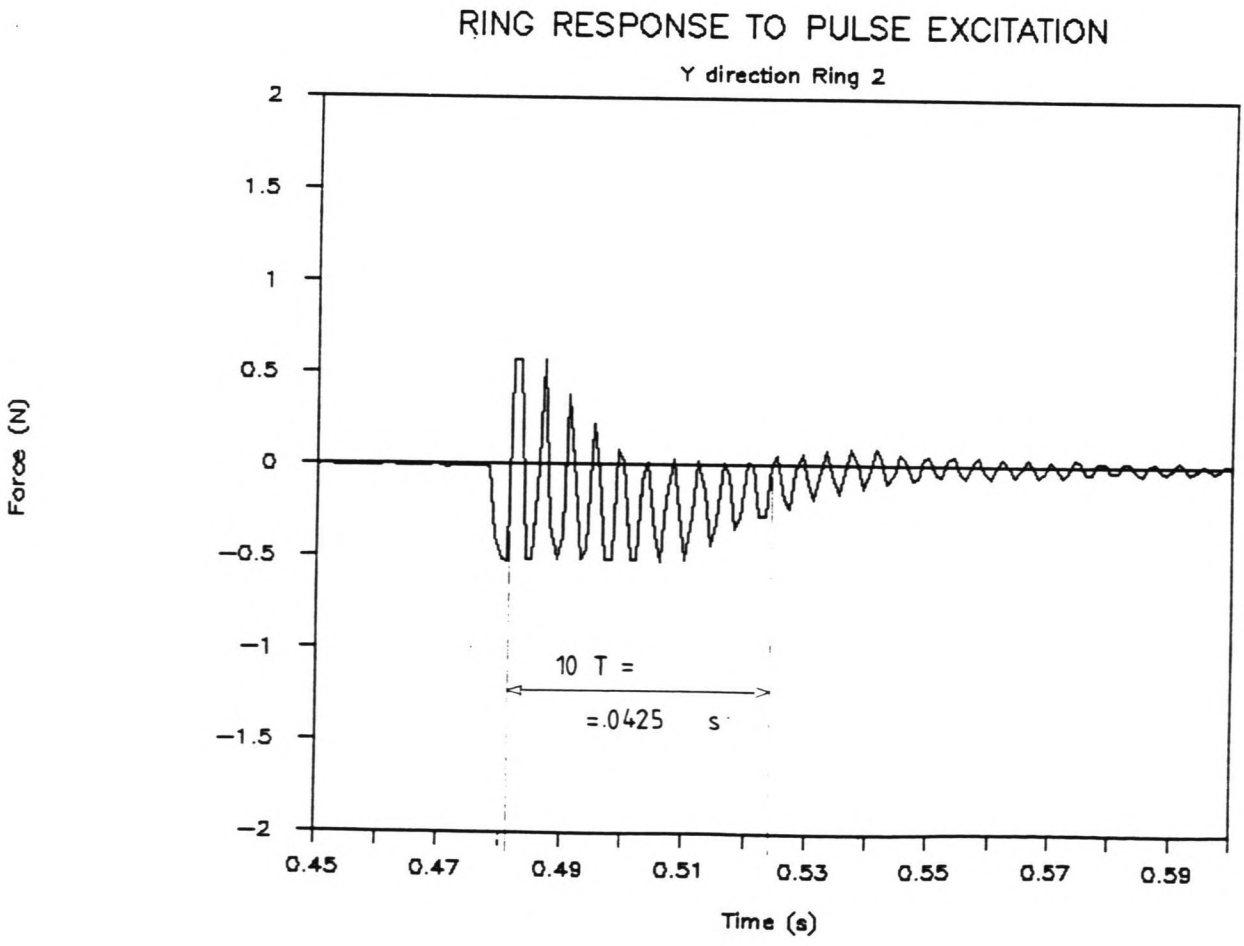

FIGURE 6.10.2

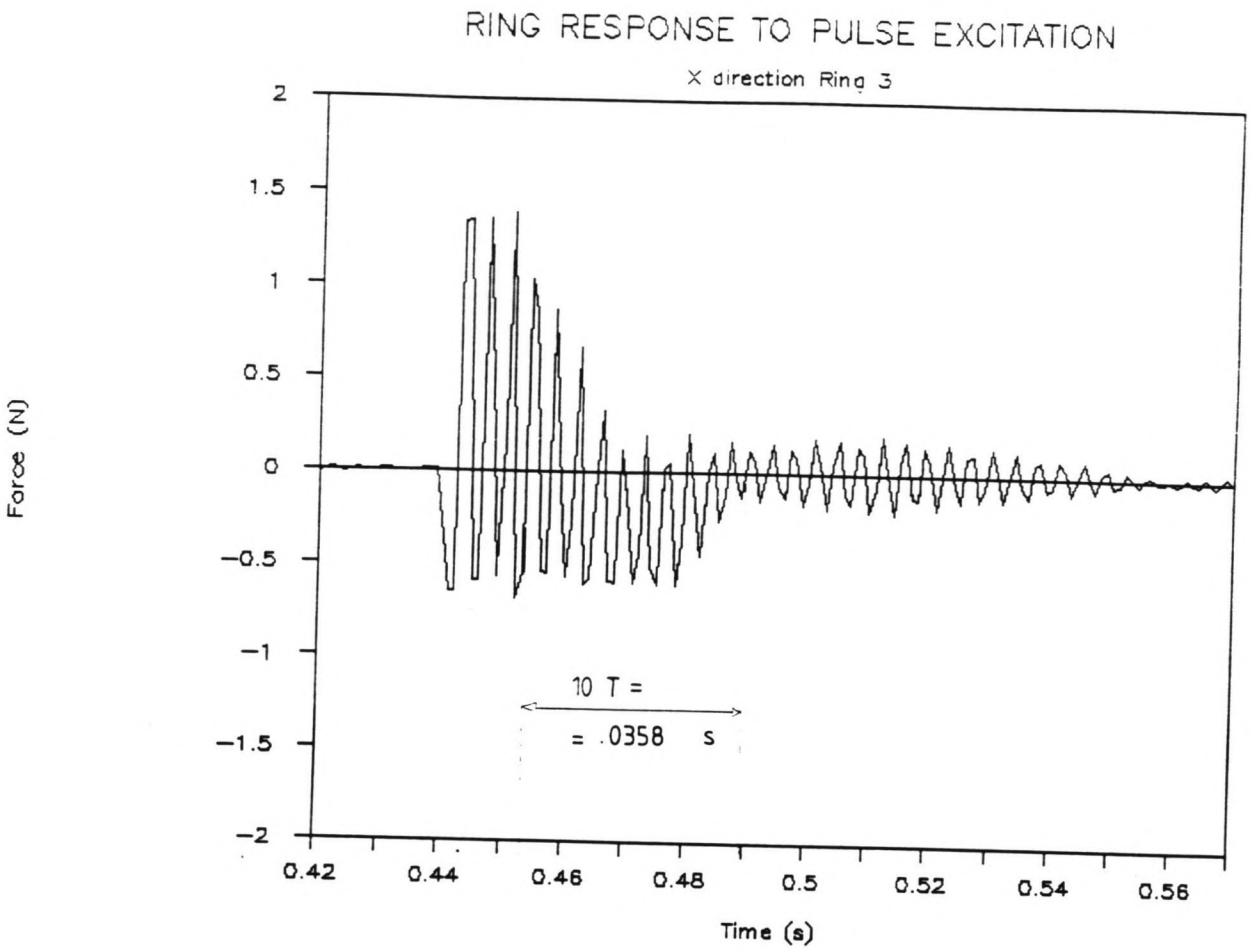

FIGURE 6.11.1

FIGURE 6.11.2

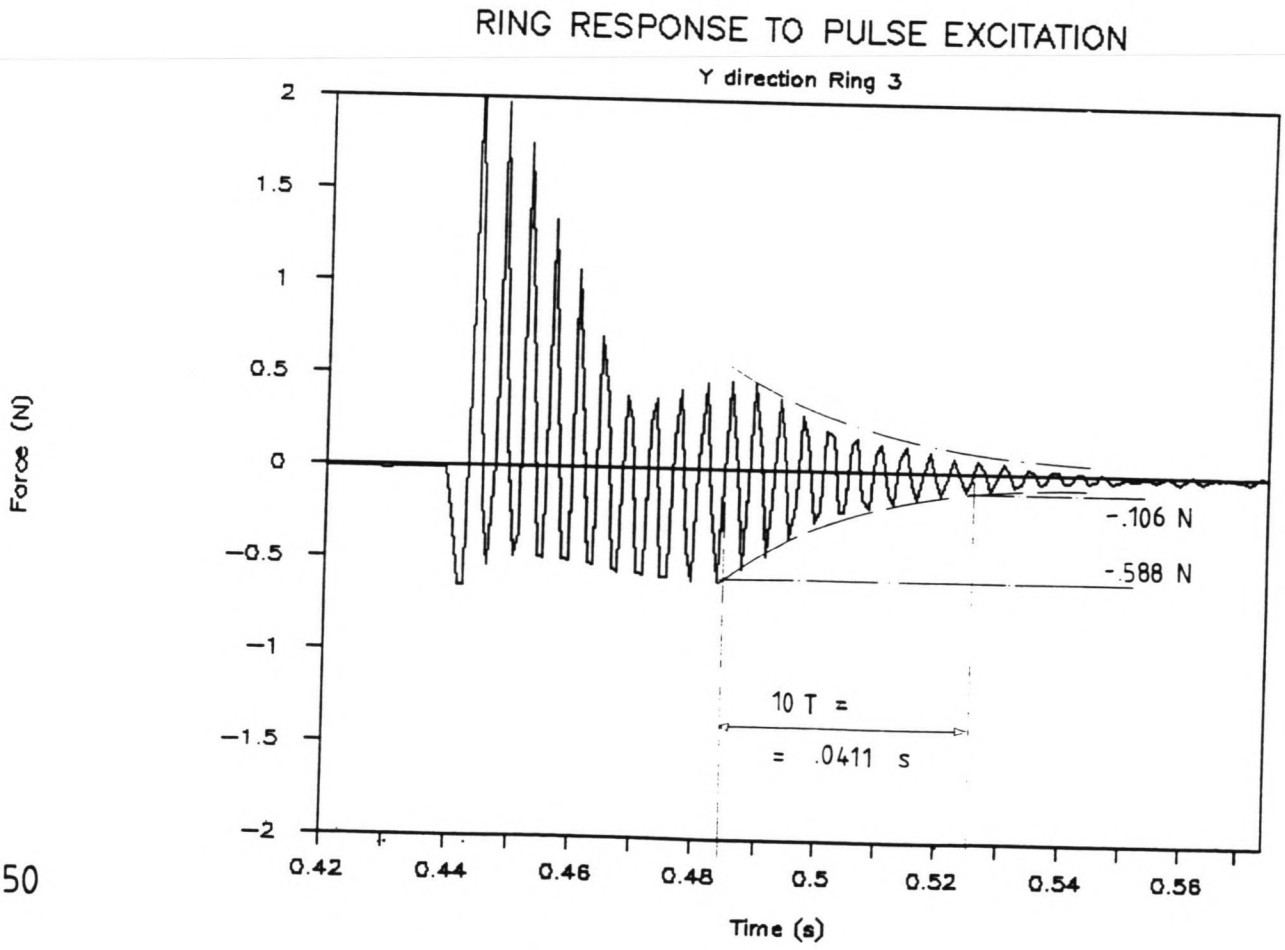

6.5 Conclusions

- Only three transducers have been examined in this calibration, since the fourth one was not going to be used (figure 6.1).

- The transducers appeared to behave properly: a (nearly) linear relationship exists between the input (force: Newtons) and the output (Volts). The calibration factors correspond within acceptable limits with those specified by Marintek (table 6.1).

- The use of a rubber skin, which should keep the water outside the inner of the cylinder during the experiments in order to eliminate an added mass effect, has some influence on the values of the calibration factors (tables 6.1 and 6.2).

- The use of a rubber skin introduces a time dependency of the calibration factors, probably caused by the relaxation of the rubber material. During the calibration test held in air, the rubber became weaker.
  This effect can be reduced by attaching the skin a period of time before the experiments will be held (table 6.3).

- The x- and y- axis of each transducer can be considered as being orientated perpendicular to each other. The rotation of one transducer relative to another is very close to zero (tables 6.4 and 6.5, and appendix C).

- The hysteresis that occurred when using the rubber skin can be neglected (figure 6.4).

- The ring mass of each transducer is about 0.040 kg (table 6.6).

- The natural frequency of the damped mass-spring system that characterizes the rings has been determined in two ways:

  * by analysing the force signals from a pulse excitation;
  * using the ring masses and the calibration factors.

  The frequencies calculated following the second option are expected to be the most accurate, and appeared to be located at around 200 Hz (table 6.8).
  The damping ratio's were very difficult to determine, but the few results show very low values. These low values are illustrated by the fact that after a large number of periods, the system is still oscillating (figures 6.9 to 6.11).

- The frequencies of the forces to be measured are expected to stay far under the determined natural frequencies, which means that these dynamic forces will be recorded correctly (figure 6.7).

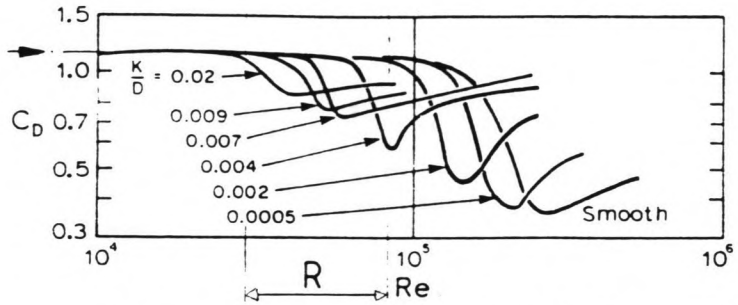

Drag coefficient versus Reynolds number for steady flow about a smooth and rough circular cylinder where K/D = roughness parameter [ref. ?]

$$\beta = \frac{D^2}{\nu T} \simeq 2120$$

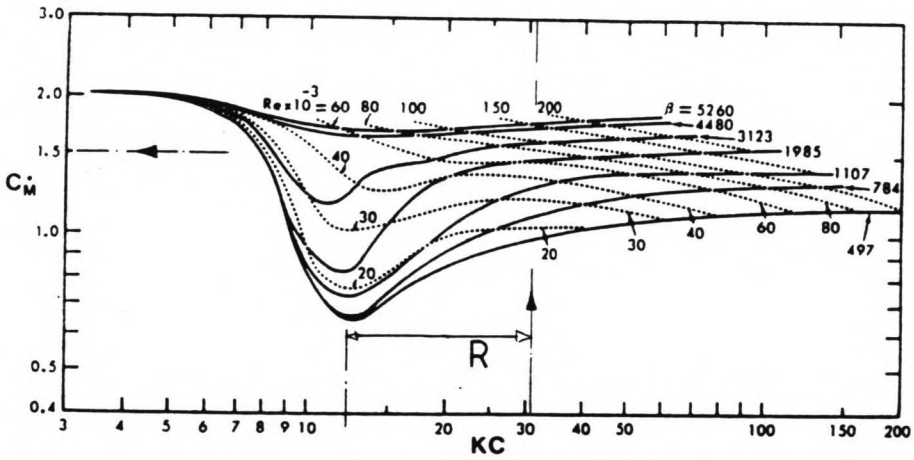

C_M vs. KC number for various values of Re (or $\beta = Re/KC$) for smooth circular cylinder [Sarpkaya (1976)]

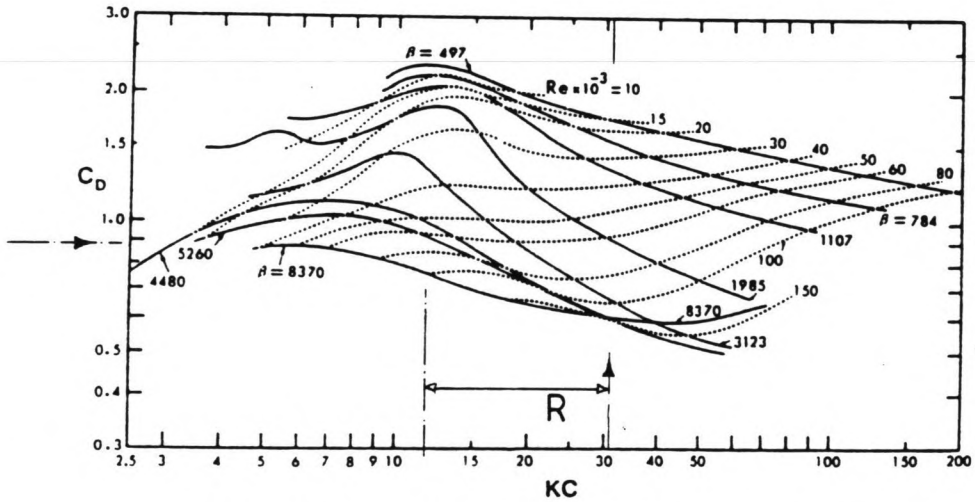

C_D vs. KC number for various values of Re (or $\beta = Re/KC$) for smooth circular cylinder [Sarpkaya (1976)]

FIGURE 7.1

R: range of experiments

Hydrodynamic Coefficients

7 EXPERIMENT DESIGN

7.1 Data Registration

The following (input) variables have been recorded, when executing the model tests in the towing tank (see also section 5.2):

- towing in x direction with speed (steady flow velocity) V (m/s);
- oscillation in y direction with period T (s) or frequency f (Hz);
- oscillation amplitude A (m) or A/D (-).

In addition the following output signals have been recorded:

- the forces F in x and y direction on each of the (three) transducers;
- a reference signal that relates all signals to the oscillatory motion of the cylinder.

Any combination of V, T and A chosen is called a RUN. It was possible to execute more than one run during each RIDE along the towing tank.

7.2 Range for Variable Values

The force transducers will only give proper information when the loading stays within acceptable limits: a too heavy loading could even damage the (sensitive) apparatus inside the cylinder. On the other hand, the values for the variables chosen should cause forces that are not too small to be measured.
Therefore, a rough estimate of the forces that could be expected is presented here, in order to determine the range in which the variables V, T and A were to be chosen.
First, in section 7.2.1, the maximum oscillation frequency allowed is calculated assuming that the maximum oscillation amplitude possible was installed, and that the forces should not exceed the Marintek specifications.
Second, in section 7.2.2, the (hydrodynamic) forces are determined that could be expected to occur during the experiments, depending on the limitations of the laboratory equipment and realistic choices of the variables.
With the information derived from these calculations a program for the experiments has been set up in section 7.3.
Carrying out the calculations, the classical Morison theory has been used when necessary. Hydrodynamic coefficients were taken from Sarpkaya (1976) (fig. 7.1).

7.2.1 Force Transducer Capacity

Each transducer should not be loaded above Marintek specifications: F < 10 N (incl. a safety allowance).
In the x (towing) direction the only force the cylinder will experience is the drag force.
In the y (oscillation) direction the cylinder will experience drag- as well as inertia forces. The maximum oscillation amplitude possible (A = 0.300 m, see also section 7.2.2) causes the highest forces and is therefore used here. The force in the y direction included the ring mass acceleration force, that cannot be neglected. The next upper limits for towing velocity and oscillation frequency were determined:

$$V < 4.30 \text{ m/s}$$

$$f_o < 2.15 \text{ Hz}$$

(calculations in appendix D)

7.2.2 Force Transducer Loading

The actual loading that occurred during the experiments depends upon the values used for the variables V, f_o and A. These values have been chosen considering the following:

(a) since the theoretical model of section 4.1 needs subcritical Reynolds conditions (asymmetrical shedding of vortices, related to a constant Strouhal number) the steady flow velocity V should stay in the range of:

$$5.0E+3 < Re < 2.0E+5, \text{ thus:}$$

$$0.083 < V < 3.33 \text{ m/s}$$

(b) the laboratory equipment could handle the following values for minimum oscillation period T (= $1/f_o$), maximum towing speed V and maximum oscillation amplitude A:

$$T \geq 1.50 \text{ s}$$

$$V < 7.50 \text{ m/s}$$

$$A \leq 0.300 \text{ m}$$

(c) comparing the experiments with realistic or needed circumstances, the following ranges for V, f_o and A appeared:

* $0.50 < V < 1.50$ m/s, which are common current velocities;
* A > 1.50 cylinder diameters (see section 3.4 and 5.1);
* the range for f_o should include the vortex shedding frequency.

(d) scaling effects as described in section 3.2 are of great importance when choosing values for variables in experiments.

(e) the forces on the transducers induced by the cylinder motion had to be large enough to be measured: according to Marintek specifications (static) forces as low as 0.05 N could be measured.

With respect to the cross sections the test cylinder with diameter D (= 0.060 m) is of about the same size as an umbilical cable. Therefore a scaling (d) 1:1 could be applied. This implied that the ranges for V and A mentioned under (c) could be chosen, although A remained under 5 cylinder diameters because of (b).
The limitations of the laboratory equipment had a major effect on the oscillation frequencies to be chosen. Using equation 7.1, with 0.50 < V < 1.50 m/s, St = 0.20 and D = 0.060 m, the vortex shedding frequencies were located in a range that unfortunately could not be reached at all: 1.67 < f_v < 5.00 Hz.

$$f_o = f_v = \frac{St \cdot V}{D} \quad (Hz) \qquad (7.1)$$

The total force on a transducer in the y direction as a function of T (=1/f_o) and A (calculated with appendix D, equations III to VI) is plotted in figure 7.2. From this figure it follows that the range where T could be chosen appears to be rather small, considering what is stated under (e). The dynamic loading however, which occurs in the experiments, will probably slightly increase the capacity and accuracy of the transducers in the smaller force range.

7.2.3 Ranges of Possible Values

Based upon the information given in section 7.2.1 and 7.2.2 the following variable values have been used in the experiments:

$$0.33 < f_o < 0.67 \text{ Hz, or } 3.00 > T_o > 1.50 \text{ s;}$$

$$2.00 < A/D < 5.00;$$

$$0.10 < V < 1.50 \text{ m/s.}$$

7.3 Execution Strategy

The choice of variables can be illustrated as in figure 7.3. First of all, two sets of calibration runs were done, representing the well known cases like flow-only and oscillation-only (note: the oscillation-only case has also been executed with a towing velocity of 0.10 m/s in order to eliminate the effect of waves reflected from the tank wall).

FIGURE 7.2

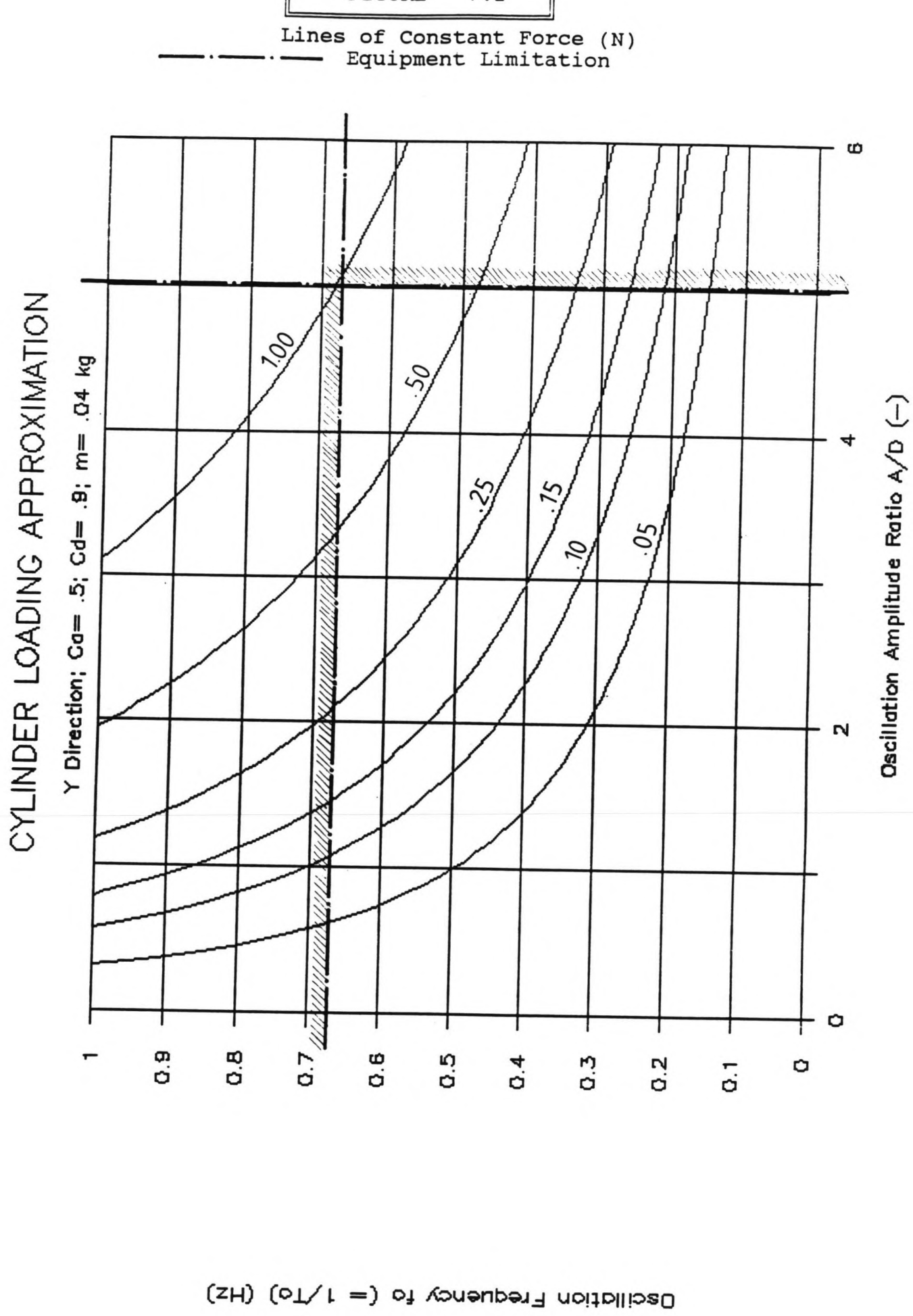
Lines of Constant Force (N)
Equipment Limitation
CYLINDER LOADING APPROXIMATION
Y Direction; Ca= .5; Cd= .9; m= .04 kg
100
50
25
15
10
05
Oscillation Amplitude Ratio A/D (–)
0
2
4
6
1
0.9
0.8
0.7
0.6
0.5
0.4
0.3
0.2
0.1
0
Oscillation Frequency fo (= 1/To) (Hz)

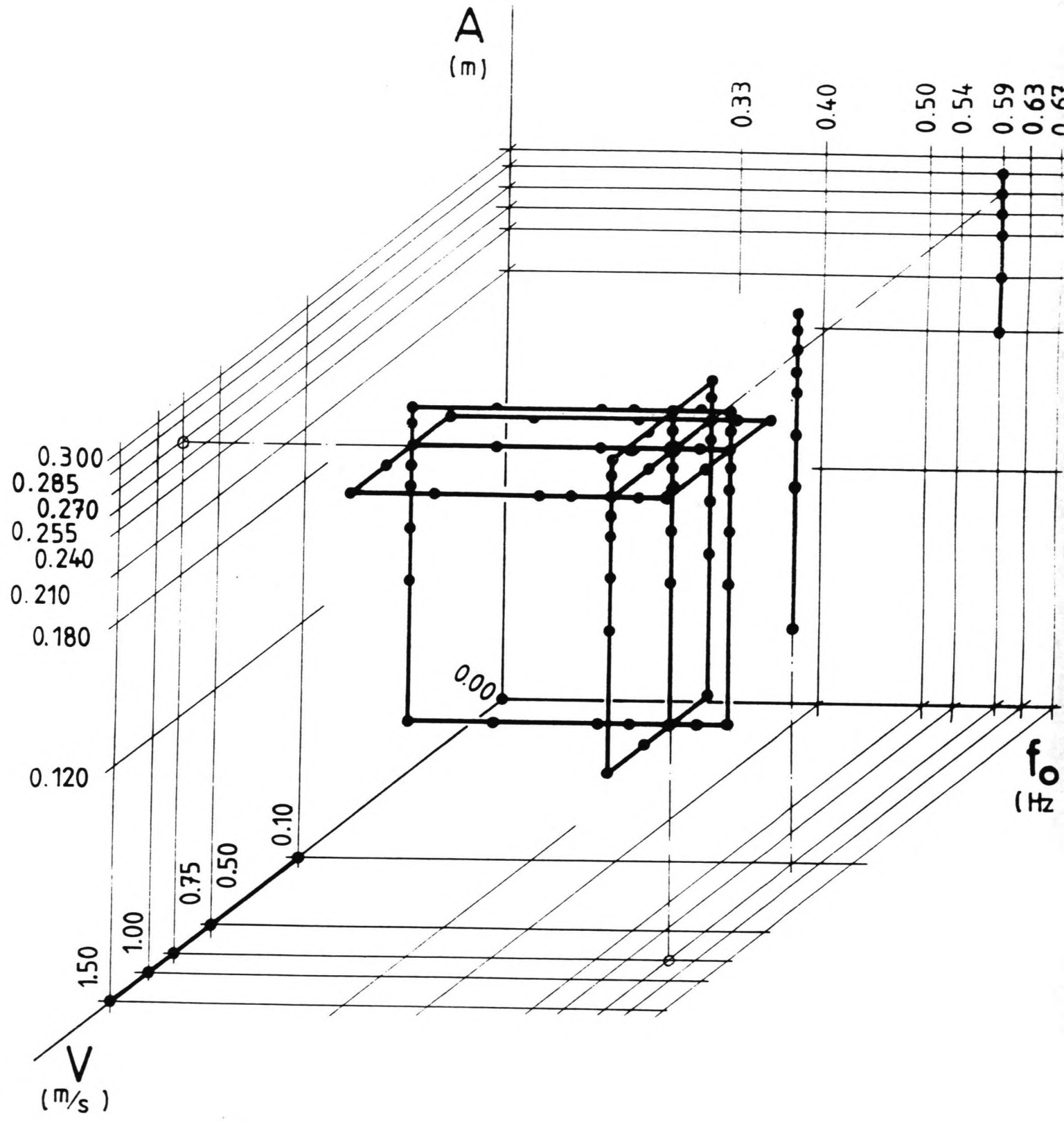

FIGURE 7.3

- Test Run Executed (Combinations of A, V, T_o (= $1/f_o$))

Next, from the central point in this figure that represents the standard run with V = 0.75 m/s, A/D = 4.50 and f_o = 0.59 Hz (T_o = 1.70 s), each one of the variables has been changed along its range (see paragraph 7.2.3) while the other two have been kept at their standard value (three series of runs). After this, the series of runs were done in which one variable had its standard value, another one had an extreme value (minimum or maximum) and the third variable has been changed along its range (twelve series of runs). Some of the runs were repeated. (see also section 7.4).

7.4 Test Runs Executed

In the first part of appendix E the chosen parameters A/D, V and T_o are given for each run number; this has been the following order of the execution of the experiments.
In the second part, the runs of one series, described in section 7.3, have been put together. From this table can also be determined which runs have been done more than once.

8 DATA CORRECTION

Before the analysis of the experiment data, the data had to be evaluated first because the signals possibly contained non relevant information, or had to be transformed to other coordinates.
The calibration factors derived from the static calibration (see section 6.3) were used in the experiments. In appendix E is described what data signals have been registered and what run numbers have been used.

8.1 Cylinder Installation Error

The cylinder was neither removed nor rotated during the days of the experiments, so errors made during the installation of the cylinder had the same effect on all signals.
Since it is rather difficult (if not impossible) to give the cylinder the exact orientation, all data had to be recalculated if a significant rotation error was introduced.
The mounting rotation error of the cylinder was calculated from the measured forces of the runs 34-37. A varying towing speed in x direction and no oscillation is used in these runs. The exact cylinder orientation is given in figure 8.1, the actual situation is given in figure 8.2. From the ratio of the average values of the forces in the y direction and the x direction follows for the rotation error that (eq. 8.1):

$$\epsilon = \arctan\left(\frac{F_{\bar{y},\,measured}}{F_{\bar{x},\,measured}}\right) \qquad (8.1)$$

The rotation errors are given in table 8.1.
A value for the rotation error cannot be given explicitly: the rotation error determined varies from -2.76 to +1.52 degrees, while the cylinder was not moved at all.
Since the rotation errors in table 8.1 cause errors in the measured forces that are less than, or of the same order of magnitude as, the accuracy of the measuring instrument (0.05 N, see section 6.3), the rotation error has been neglected further on in the analysis (see figure 8.2).

8.2 Ring Mass Force

A totally different effect is that of the mass of the ring of the force transducers. The acceleration of the cylinder introduced an extra force component in the data signals that had to be eliminated in order to obtain force signals that represent the hydrodynamic forces only.
This has been achieved via the runs 18-24, which had oscillations in air, at all frequencies used in the other runs. This was helpful in two different ways:

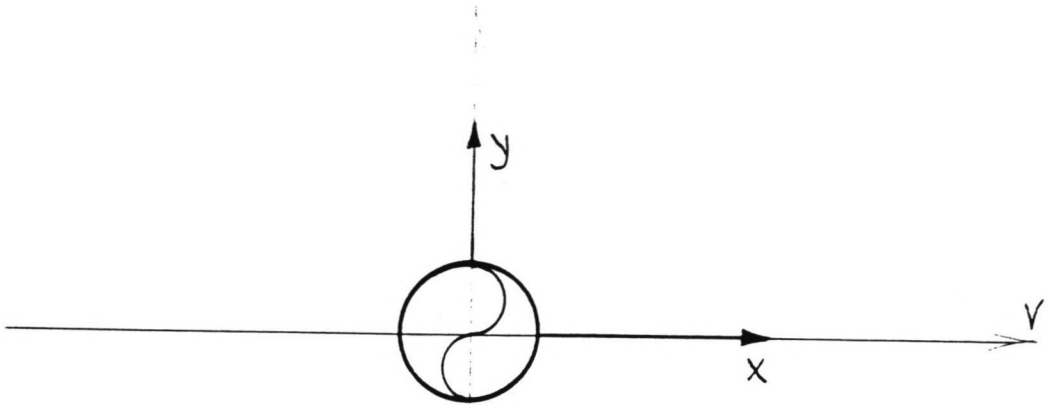

FIGURE 8.1

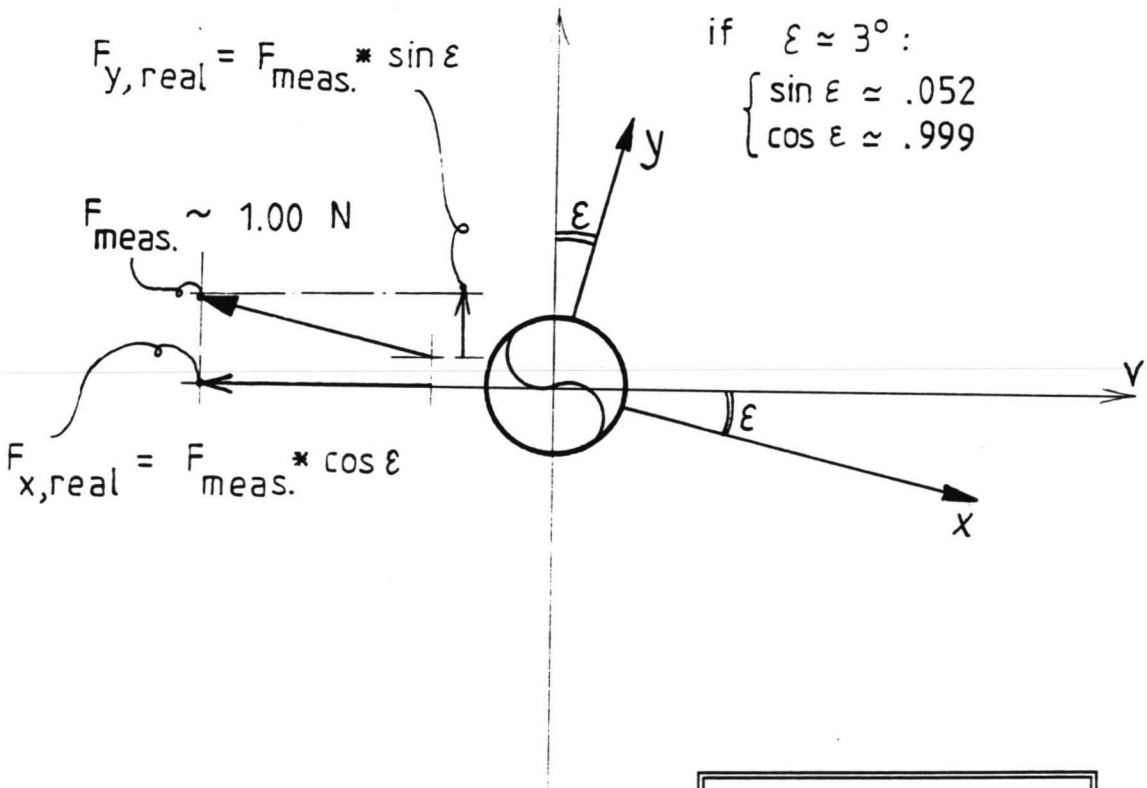

FIGURE 8.2

Test Cylinder Installation Error ε

and its Influence on the Measured Forces

- the mass of the ring has been determined from these runs (see section 6.4.1), and using the reference signal, it is rather easy to subtract the calculated mass force from the data signal measured (eq. 8.2 to 8.4);

$$F_{mass} = m_{ring} \cdot \bar{a}(t) \tag{8.2}$$

$$\bar{a}(t) = \frac{d^2\bar{y}(t)}{dt^2} = -A \cdot (2 \cdot \pi \cdot f_o)^2 \cdot Rfinf(t) \tag{8.3}$$

$$F_{hydrodyn.}(t) = F_{y,meas.}(t) - [-A \cdot (2 \cdot \pi \cdot f_o)^2 \cdot m_{ring} \cdot Rfinf(t)] \tag{8.4}$$

- the signal from one of the runs in air could be subtracted directly from the recorded signal of a run in water, provided that the frequencies are the same and the possible amplitude difference is taken into account.

A problem with the latter option was that the setting of the oscillation frequency could not be done accurately. Also it was rather difficult to synchronize both signals. Therefore, the first method has been applied.

8.3 End Effects

There possibly has been some influence of the presence of the water surface near the upper transducer (no. 3) and the end of the cylinder near the bottom transducer (no. 1) on the recorded data signals there. These so-called "end effects" were checked upon their significance by comparing the analysis results of all three transducers of a run (table 8.2).
It appeared that the parameter values found varied slightly along the cylinder length, which is probably not the result of an end effect, but more likely caused by the following:

The determination of the coefficients has been done according to the procedure of chapter 9. Here, the analysis was carried out using the reference signals of the oscillatory motion. This means that, when a phase difference occurred between the forces along the cylinder length during the experiments, not all recorded forces will fit in the model with the same accuracy and the same coefficients.

Since the analysis of the experiments concerned the measured forces on one of the rings (no. 2), no further attention has been paid to this effect.

run: no.	V: (m/s)	avg. force Y: (N)	avg. force X: (N)	rotation ring 2: (deg)
34	.50	-.0048	.0997	-2.76
35	1.00	.0055	.3790	.83
36	.75	-.0018	.2279	- .44
37	1.50	.0201	.7584	1.52

(table 8.1)

	ring:	Cd:	Ca:	*) Cl:	*) St:	CritfX:	CritfY:
Run 46:	1	1.042	.514	.494	.1737	.102E+0	.809E-1
	2	1.140	.574	.511	.1773	.695E-1	.628E-1
	3	1.190	.556	.450	.1785	.813E-1	.795E-1
Run 47:	1	1.180	.298	.917	.1326	.294E+0	.752E-1
	2	1.306	.370	.825	.1330	.293E+0	.641E-1
	3	1.340	.426	.752	.1335	.415E+0	.760E-1
Run 49:	1	.804	.760	.121	.1729	.174E-1	.860E-1
	2	.854	.744	.106	.1841	.102E-1	.402E-1
	3	.910	.722	.072	.1831	.989E-2	.523E-1

(Note: ring 1 is the nearest to the bottom end, ring 3 is the nearest to the water surface).

(table 8.2)

	time: (days)	Cd:	Ca:	*) Cl:	*) St:	CritfX:	CritfY:
Run 46 :	0	1.042	.514	.494	.1737	.102E+0	.809E-1
:	1	(not available)					
Run 150:	4	.946	.390	.293	.1742	.583E-1	.447E-1
(A/D = 4.50; V = .75 m/s; T = 1.70 s)							
Run 51 :	0	1.210	.772	.722	.1828	.603E-1	.493E-1
Run 140:	1	1.052	.640	.406	.1865	.717E-1	.580E-1
Run 153:	4	.966	.442	.179	.1781	.744E-1	.665E-1
(A/D = 4.50; V = .75 m/s; T = 1.50 s)							
Run 55 :	0	1.000	.636	.276	.1865	.251E-1	.733E-1
Run 139:	1	.948	.526	.277	.1835	.297E-1	.718E-1
Run 158:	4	.894	.550	.198	.1842	.239E-1	.406E-1
(A/D = 4.50; V = .75 m/s; T = 3.00 s)							

(table 8.3)

*) average values

8.4 Equipment Deterioration

The influence of equipment deterioration on the data measured has been examined, since the time interval between the first and the last run is about four days.
Comparing the results of the analysis of the runs shown in table 8.3, it is clearly visible that there is an important change in results, especially after the four days interval. The reason is probably the condition of the rubber skin during the days of the experiments. The rubber apparently became stiffer and changed the calibration factors of the transducers. As a result, (much) "lower" forces were measured. The fact that no systematic change appeared in the values for the Strouhal numbers and the data fitting criterium function values confirms this opinion.
The analysis program discussed in chapter 9 included only runs that were executed on the first and the second day. Although probably not small enough to be neglected, no special measures were taken to eliminate the one-day time influence on these analysis results.
The runs carried out on the fourth day all were copies of earlier executed runs.

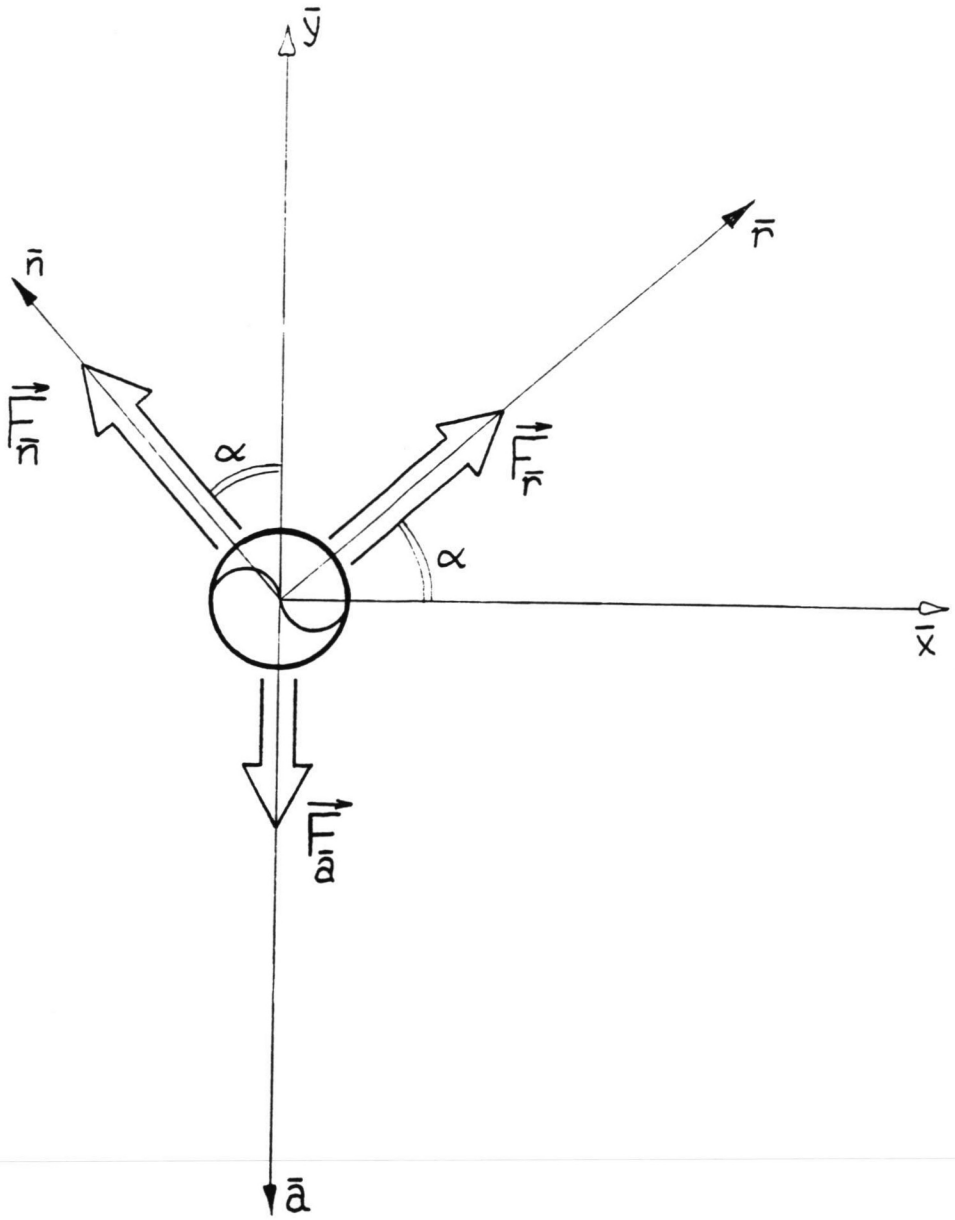

FIGURE 9.1

Model Coordinate System

9 SINGLE TEST DATA PROCESSING

9.1 Objective

In this chapter the data analysis procedure for all runs is described, and illustrated by following one single run (no. 46) during the consecutive stages of the analysis. As an additional check all data from degenerate runs (towing only or oscillation only) are presented in section 9.4.1.
The validity of the theoretical models as described in section 4.1 has been investigated in light of the following items:

- how well are the force signals from the experiments reproduced using the model I developed?
- is the r-n-a coordinate system (see figure 9.1) a proper one for describing the situation?
- is there any resemblance between the frequencies at which (lift) forces occurred in the experiments comparing these with the frequencies predicted by the model developed?

9.2 Analysis Procedure

9.2.1 Required Model Constants

Keeping model I in mind, the measured forces in the x- and y-direction, Fx and Fy, are assumed to be a function of the resulting velocity V (V itself depending upon the towing speed Vt, oscillation amplitude A and period T_o), the Strouhal number St and the hydrodynamic coefficients Ca, Cd and Cl. Since the recording of the signal was started arbitrarily, a initial phase phi representing the phase of the lift force component at t = t_0 had to be introduced, too.
Fx and Fy, Vt, A, and T_o are known within respectable limits, since they have been measured or set.
To reproduce the data, five missing parameters had to be determined: St, Cd, Ca, Cl and phi(t=t_0).
The model uses a coordinate system, that will be referred to as the r-n-a system, different from the x-y system, as in figure 9.1. The transformation of the determined model force components from the r-n-a to the x-y system (projection) goes according to equations 9.1 and 9.2.

$$F_{\bar{x}} = + F_{\bar{r}} \cdot \cos\alpha - F_{\bar{n}} \cdot \sin\alpha \qquad (9,1)$$

$$F_{\bar{y}} = + F_{\bar{r}} \cdot \sin(\alpha) + F_{\bar{n}} \cdot \sin(\alpha) - F_{\bar{a}} \qquad (9,2)$$

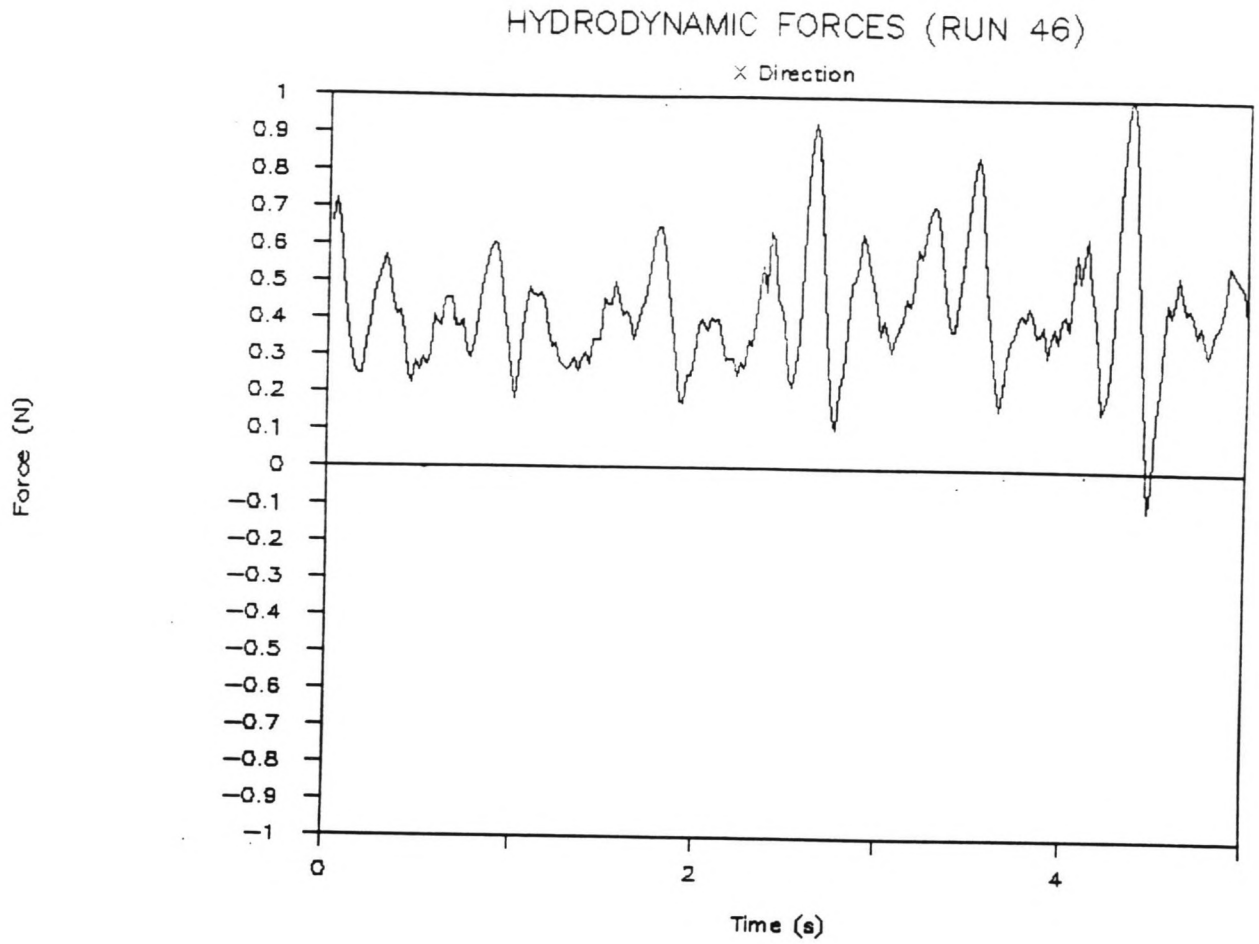

FIGURE 9.2.1

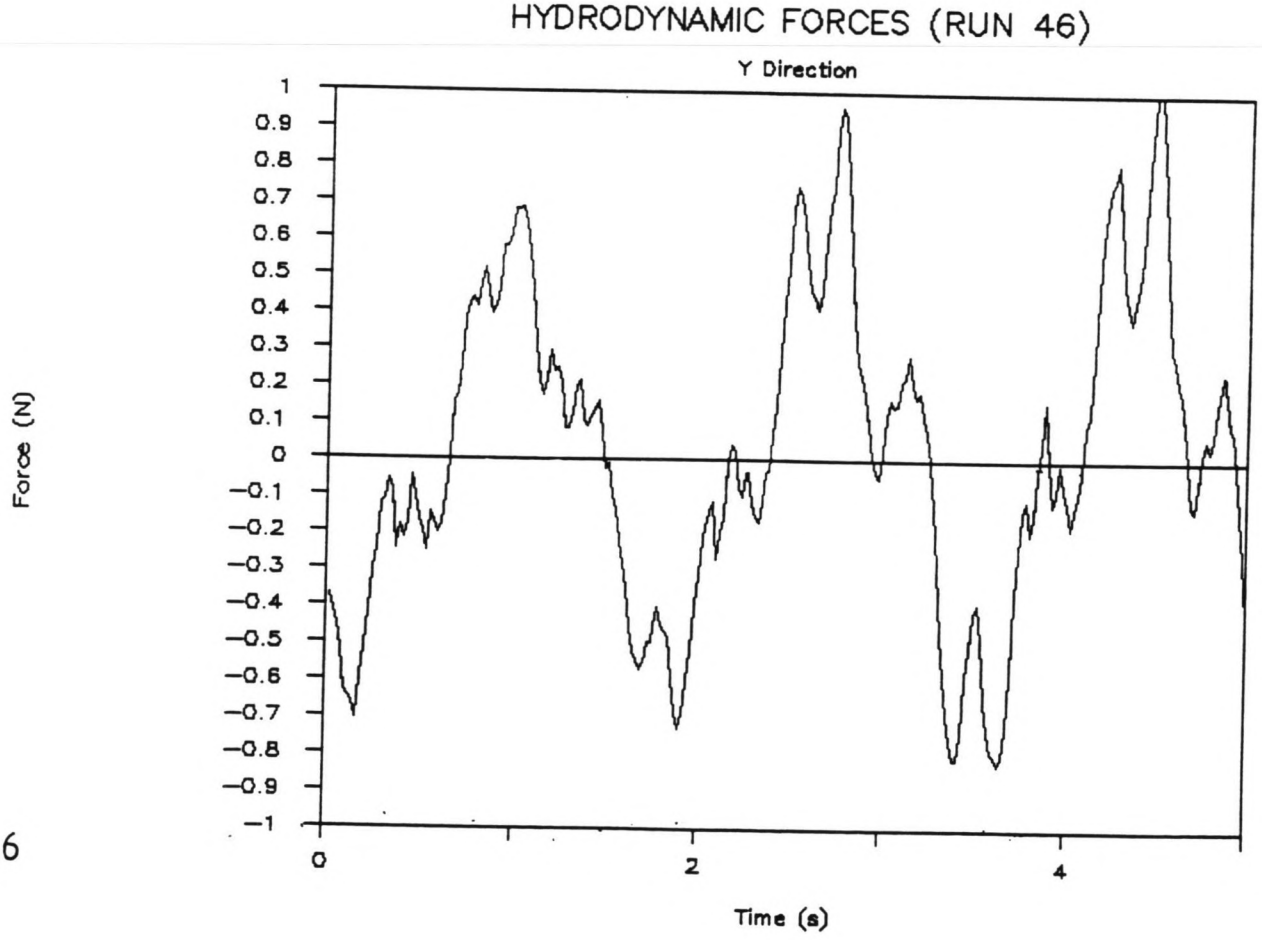

FIGURE 9.2.2

By comparing the Fx and Fy predicted by the model and measured in the experiments two equations are obtained: one for the x and one for the y direction.The problem that arises here is a shortage of 3 equations to determine all five unknown parameters, this without considering the inaccuracy of the recorded force signals.
A "best-fit" procedure has been applied to find all parameter values. Here, a predefined fit criterium function (see section 9.2.2) is minimized.
An efficient procedure for finding proper variable values is described in section 9.2.3.

9.2.2 Fit Criterium Function

The analysis has been carried out trying to find the required parameters for which the criterium function(s) of equation 9.3 reached a minimum value. This can be applied to the x, y or total force components.

$$Critf = \frac{\sum [F_{i,measured} - F_{i,model}]^2}{\sum [F_{i,model}]^2} \qquad (9,3)$$

The criterium function values for the x and the y forces were summed when determining the Cd and Ca values.
For the Cl, St and phi determination, only the criterium function of the direction in which the lift force was primarily thought to act was taken into account: for oscillation-only situations the x direction, for relatively large towing speeds the y direction.

9.2.3 Searching Strategy

When looking at the y force record of run 46 (figure 9.2), it is clear that the dominant force component is the result of a force which is characterized by the cylinders oscillatory motion. A spectral analysis confirms this, too: most of the energy is concentrated near the oscillation frequency of .59 Hz (figure 9.3). The forces working on the cylinder during the experiments are shown in figure 9.4 and can be written as in equations 9.4, 9.5 and 9.6.

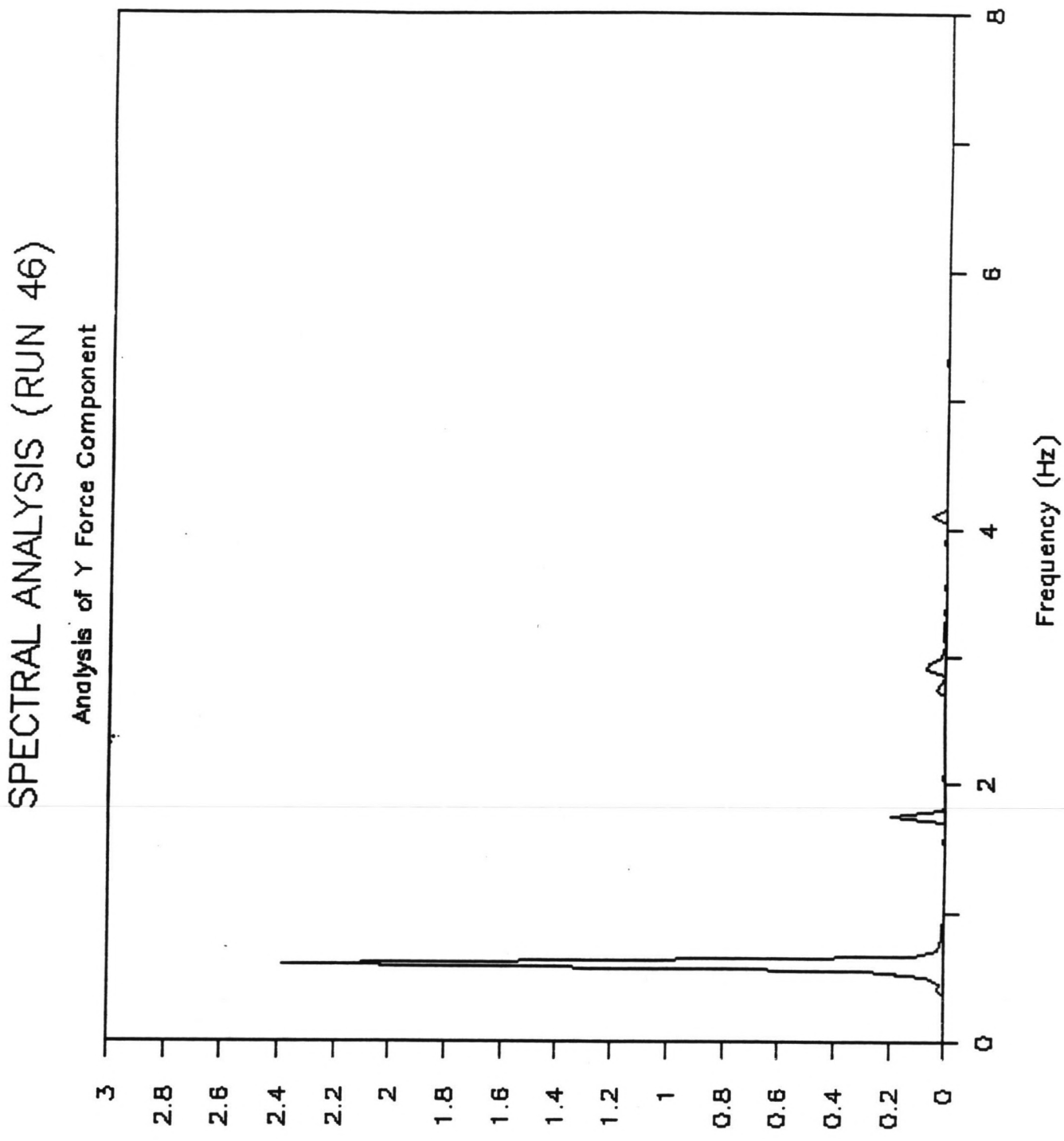
SPECTRAL ANALYSIS (RUN 46)
Analysis of Y Force Component
3
2.8
2.6
2.4
2.2
2
1.8
1.6
1.4
1.2
1
0.8
0.6
0.4
0.2
0
0
2
4
6
8
Frequency (Hz)

FIGURE 9.3

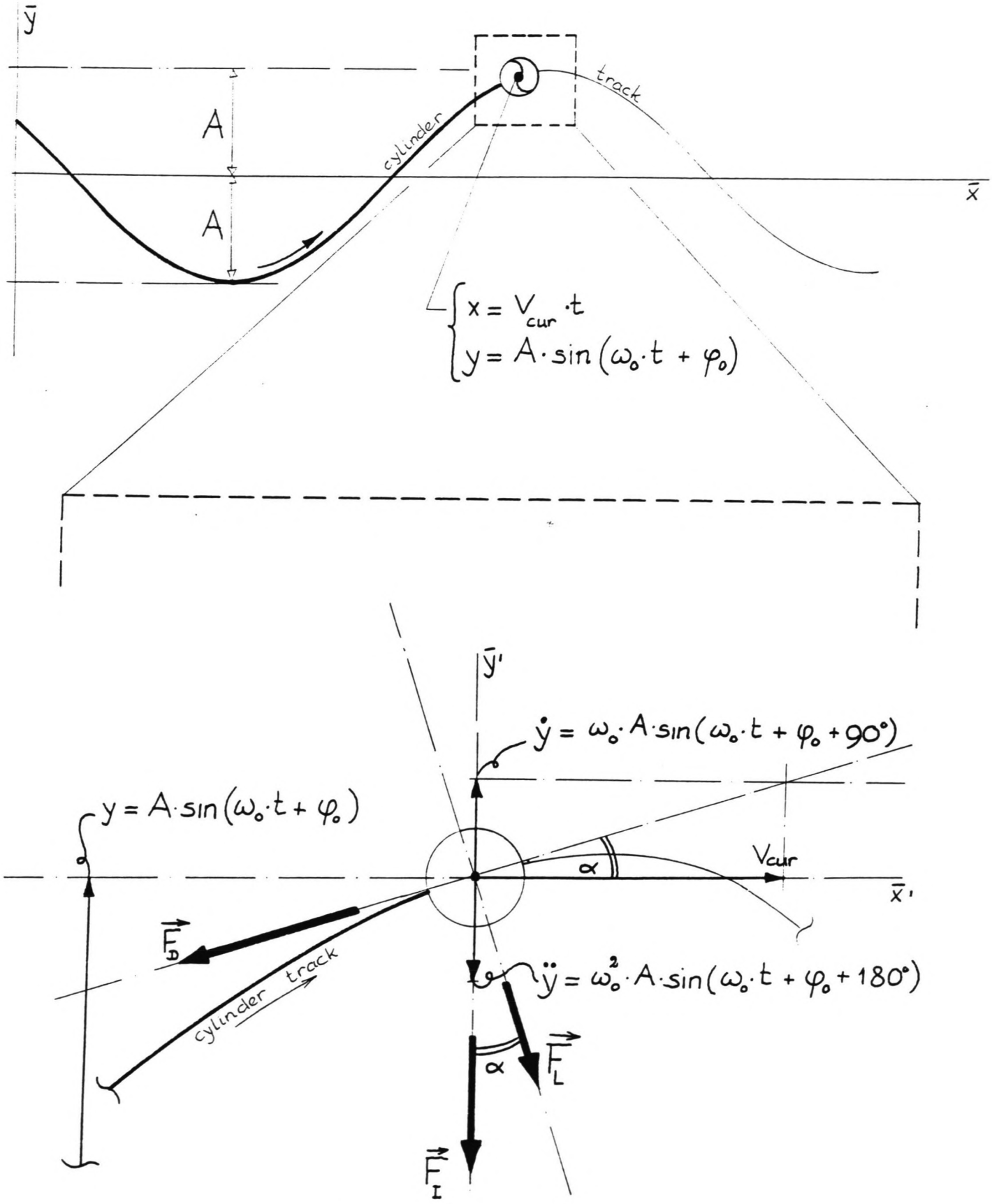

FIGURE 9.4

Forces Working on the Cylinder during the Experiments

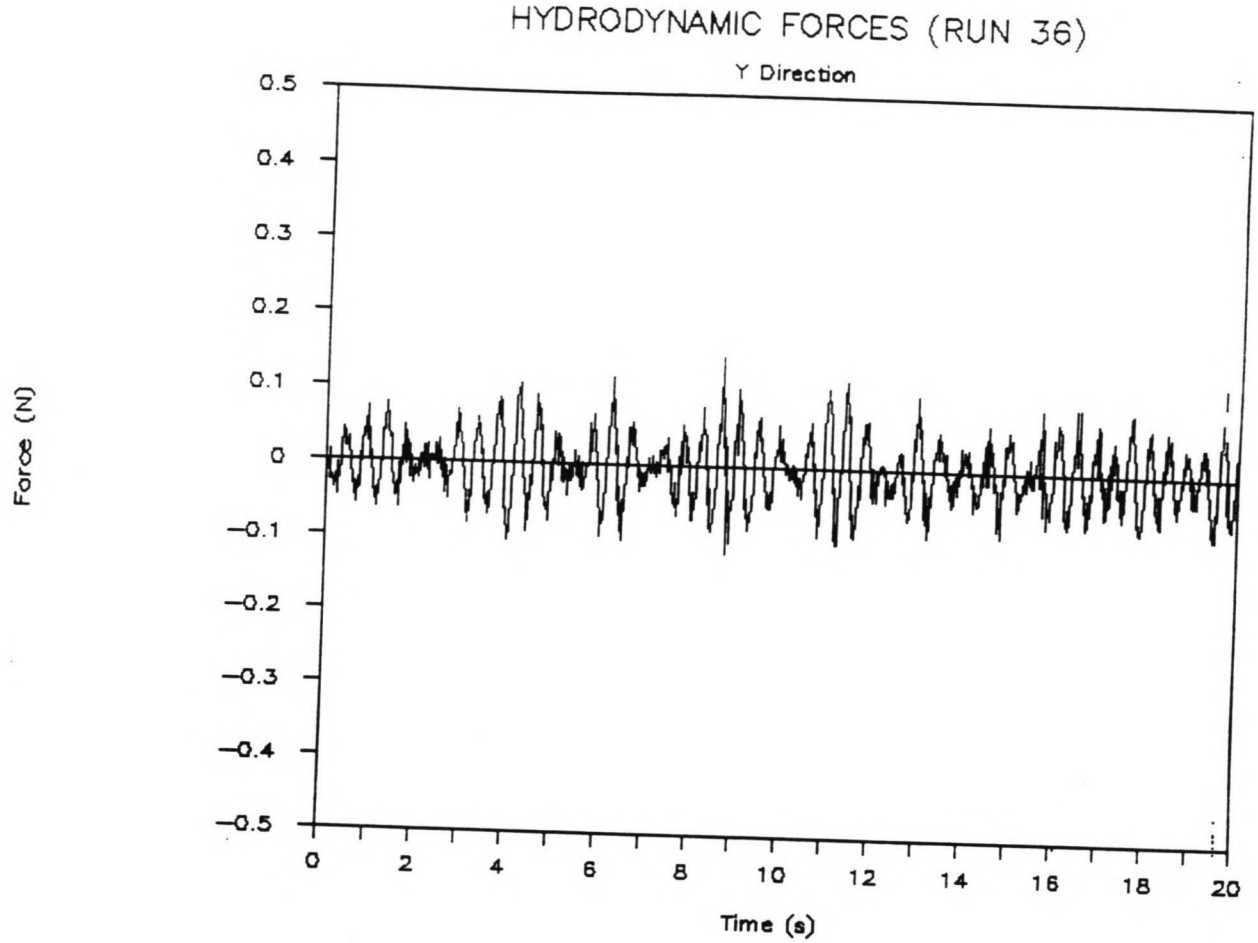

FIGURE 9.5

FIGURE 9.6

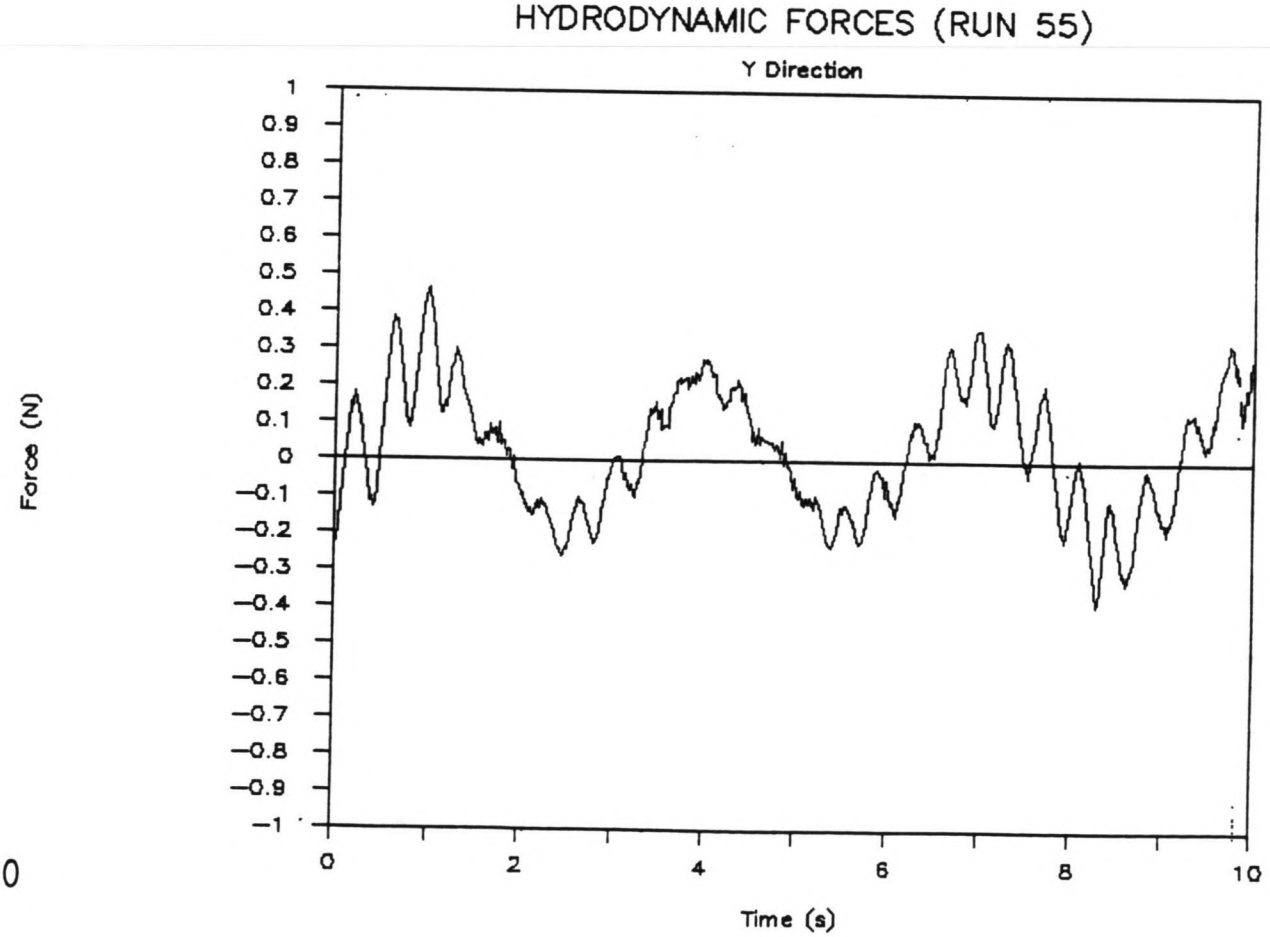

$$\alpha = \tan^{-1}\left(\frac{\omega \cdot A \cdot \sin(\omega \cdot t + \phi_0 + 90^\circ)}{V_{cur}}\right) \qquad (9,4)$$

$$F_{\bar{x}} = -F_D \cdot \cos(\alpha) + F_L \cdot \sin(\alpha) \qquad (9,5)$$

$$F_{\bar{y}} = -F_D \cdot \sin(\alpha) - F_L \cdot \cos(\alpha) - F_I \qquad (9,6)$$

Both the x and the y force contain components at the oscillation frequency: the inertia force Fi and/or the drag force Fd. Although regularly appearing, the high frequency (lift?) force signal added to the dominant force signal was primarily considered as "noise" when starting the analysis.
Comparing measured data and model values in the x and y directions (using the model drag and inertia force components only) a least square fit has been achieved for Ca and Cd simultaneously. After this, the model drag and inertia force (using the Ca and Cd values found) has been subtracted from the measured data signals and the analysis continued with the remaining (lift) force signal.
This signal is described by the theoretical models for given parameters Cl, St and phi(t=t_0). First, the coefficient Cl was estimated roughly, proportional to the maximum force that occured in this remaining signal.
Subsequently, for various chosen Strouhal numbers St, phi(t=0) was varied from $-\pi$ to $+\pi$ for each St value, looking for a least square fit comparing (for this particular run) the model y (lift) force and the measured y (lift) force only.
At last, the Cl value was optimized using the other (four) fixed parameter values found.

9.3 Data Reproduction Aspects

The reproduction of the measured force signals, with the theoretical models and the coefficients found after applying the procedure described in the previous section, gave the following problem: due to "beats" occurring in the lift force component a rather poor fit was sometimes found.
In the towing-alone runs (no oscillation), where a constant Strouhal number is commonly accepted and therefore should result in regular harmonic lift forces, these (unexpected) "beats" were also found (figure 9.5).
The "beats" occurring in some of the experiments with additional oscillation seem to be of the same origin (as an example run 55 in figure 9.6).
This effect means that the conclusion from the analysis procedure will be too pessimistic for some runs when the validity of the theoretical models is questioned.
Therefore, after having determined the Cd and Ca coefficients for the entire recorded force signals of one run, the recorded force signals have been cut into several (eight) pieces which were analysed separately. An average value for Cl and St could be determined now, and the reproduction of the recorded force

Analysis of Stationary Flow

run: no.	Cd: (-)	Ca: (-)	*) Cl: (-)	*) St: (-)	A: (m)	V: (m/s)	T: (s)	critfX: (-)	critfY: (-)
34	.886		.232	.1864		.50		.189E-1	.478E+0
36	.900		.185	.1874		.75		.706E-2	.487E+0
35	.842		.105	.1837		1.00		.504E-2	.845E+0
37	.748		.068	.1739		1.50		.469E-2	.671E+0

(table 9.1)

Analysis of Oscillatory Flow

run: no.	Cd: (-)	Ca: (-)	*) Cl: (-)	*) St: (-)	A: (m)	V: (m/s)	T: (s)	critfX: (-)	critfY: (-)
116	1.238	.052	.810	.1816	.180	.000	1.70	.120E+1	.152E+0
121	1.102	.052	.725	.2050	.210	.000	1.70	.103E+1	.143E+0
126	1.042	.052	.636	.1949	.240	.000	1.70	.102E+1	.142E+0
131	.946	.052	.660	.2129	.255	.000	1.70	.107E+1	.144E+0
136	.944	.052	.624	.2106	.270	.000	1.70	.890E+0	.132E+0
141	.886	.052	.517	.2171	.285	.000	1.70	.129E+1	.148E+0

(table 9.2.1)

run: no.	Cd: (-)	Ca: (-)	*) Cl: (-)	*) St: (-)	A: (m)	V: (m/s)	T: (s)	critfX: (-)	critfY: (-)
66	1.388	.306	.804	.2146	.180	.100	1.70	.166E+1	.124E+0
64	1.234	.190	.651	.1800	.210	.100	1.70	.168E+1	.151E+0
62	1.182	.104	.642	.1711	.240	.100	1.70	.101E+1	.138E+0
60	1.106	.052	.722	.1833	.255	.100	1.70	.822E+0	.147E+0
45	1.086	.052	.638	.1778	.270	.100	1.70	.106E+1	.137E+0
58	1.050	.146	.634	.1981	.285	.100	1.70	.157E+1	.138E+0

(table 9.2.2)

*) average values

signal gave a much better fit. An indication of the better fit gave also the average Cl value, that appeared to be (much) higher than the value found when analysing the record in one piece.
A few things have to be pointed out here:

- splitting the record into too many pieces will always give a good fit;
- the connection between two adjacent pieces will be discontinuous: a phase shift in the lift force always occurs.

9.4 Analysis and Reproduction (using Model I)

9.4.1 Analysis of Degenerate Cases

The degenerate cases of section 9.4.1.1 and 9.4.1.2, a stationary flow and an oscillatory flow respectively, have been analysed. The coefficients found in these analyses have been compared in section 9.4.1.3 with the values mentioned in the literature consulted.
This analysis can be seen as a calibration and gives an indication of the value of the data obtained. Data from all degenerate runs are reported here.

9.4.1.1 Stationary Flow

For a cylinder in a stationary flow have been found:

- the drag force coefficient Cd as function of the towing velocity V (Reynolds number);
- the value of the Strouhal number St;
- the value for the lift force coefficient Cl.

The results of the analysis are presented in table 9.1.

9.4.1.2 Oscillatory Flow

For a cylinder in an oscillatory flow have been found:

- the drag force coefficient Cd as function of the A/D ratio (Keulegan Carpenter number);
- the inertia force coefficient Ca as function of the A/D ratio (Keulegan Carpenter number);
- the value of the Strouhal number St;
- the value of the lift force coefficient Cl.

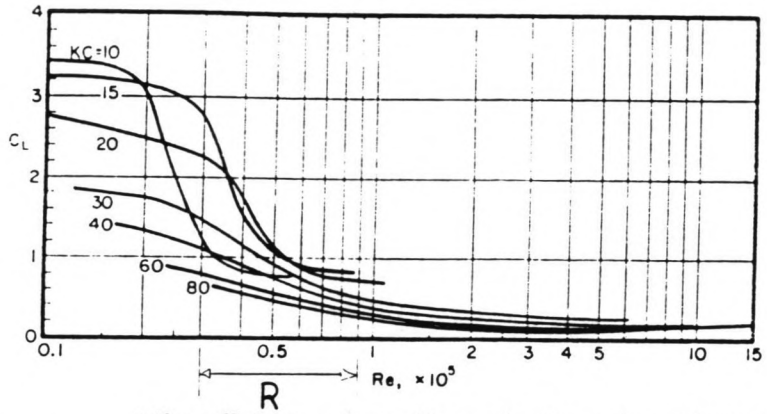

Lift coefficient vs. Reynolds number for various values of KC for smooth circular cylinder [Sarpkaya (1976)]

FIGURE 9.7 FIGURE 9.8

R: Range of Experiments

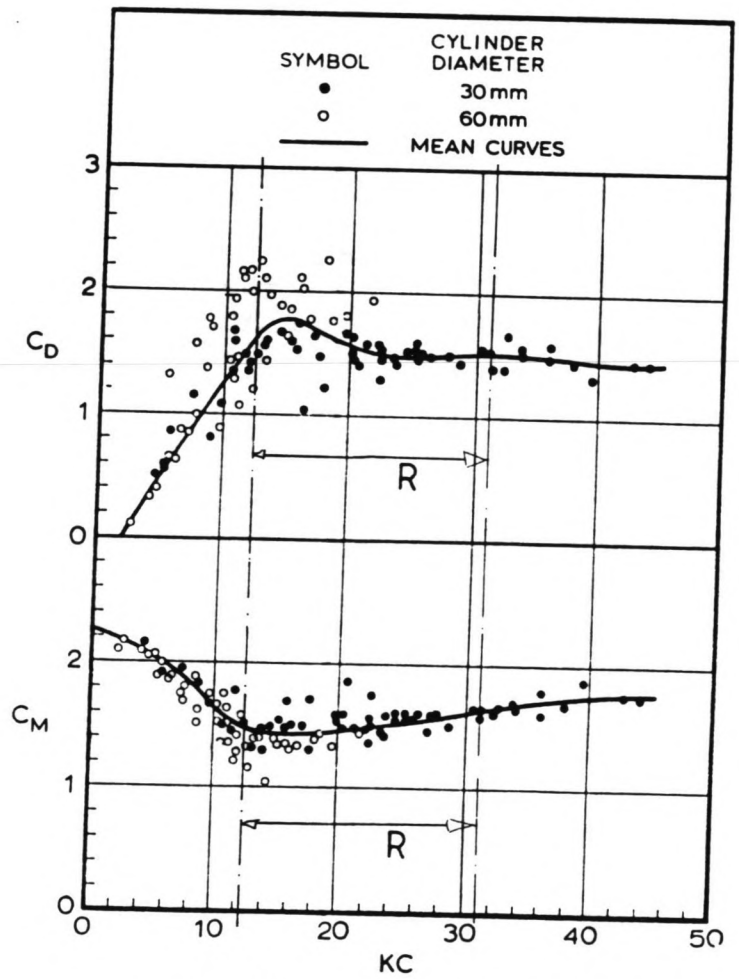

Inertia and drag coefficients for a fixed vertical cylinder in wave-adverse-current relative field [Iwagaki, *et al.* (1983)]

The results of the analysis are presented in table 9.2.1 and 9.2.2 (Note: the velocity Vt = 0.1 m/s in table 9.2.2 was installed in order to eliminate reflections from the tank wall; see also section 7.3).

9.4.1.3 Comparison with Literature

The Cd and Ca coefficients presented in section 9.4.1.1 and 9.4.1.2 will be compared here with the results from some investigations reported by Chakrabarti (1987). These results are shown in the figures 7.1 and 9.7 to 9.10. The ranges of KC number and Reynolds number of the laboratory experiments have been marked in the diagrams.
The Cd values found in the present study are in the vicinity of the already known values.
The value of Ca found in the present study appears to be rather low sometimes (Note: Cm = [1 + Ca]).
The value of the Strouhal number St for stationary flow conditions appears to be a bit lower than 0.20, which is the generally accepted value.

9.4.2 Analysis of Remaining Data

9.4.2.1 Reproduction of Force Signals

As an example, the analysis of run 46 (the standard run) is follwed here in detail, for both directions. The items mentioned in section 9.3 have to be considered here.
In figures 9.11 a part of the recorded signal is drawn. The figures 9.12 show, as the result of the first phase of the analysis, the fitted curves that represents the drag and inertia forces only. After the subtraction of these drag and inertia forces from the recorded signal, the remaining registration is shown in figures 9.13.
The second phase of the analysis is executed using (in this case) the y force component only. The result is shown in figure 9.14.2. Looking at the x force component in figure 9.14.1, it shows clearly that the curve drawn here, using the parameters found in the analysis of the y force component, fits quite well, even though the analysis has not paid any attention to this component.
The complete reproduction of the registration is shown in the figures 9.15.

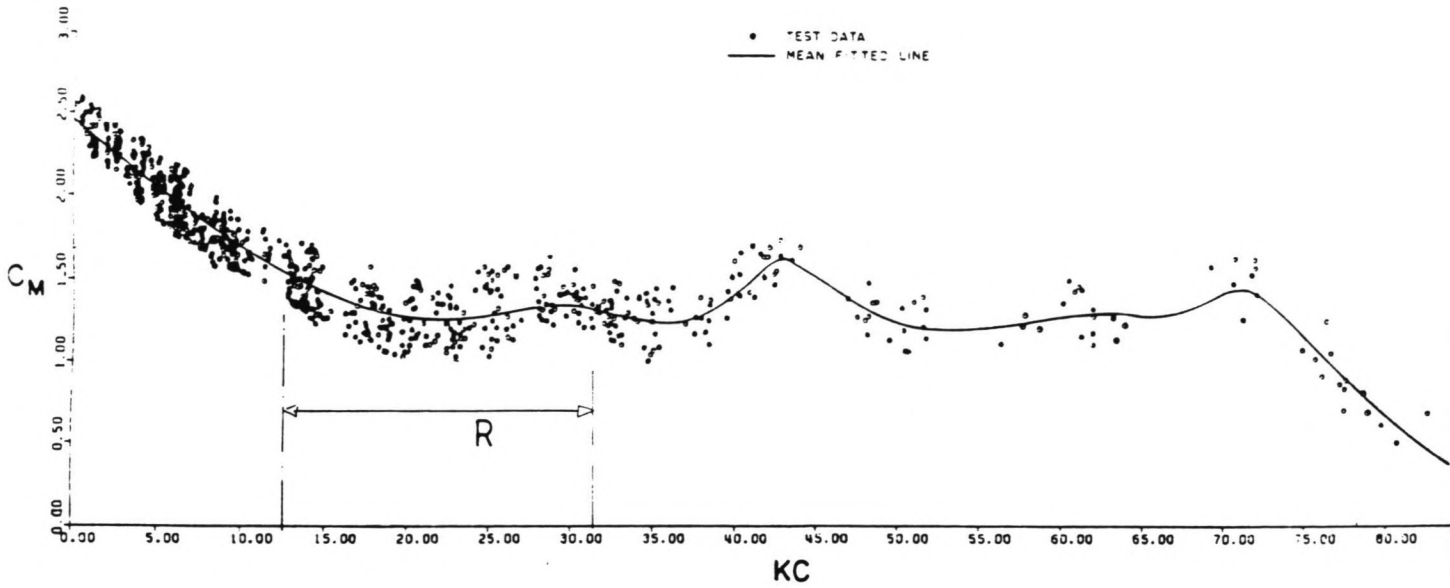

Inertia coefficient vs. KC for a smooth circular cylinder in waves

FIGURE 9.9 **[Chakrabarti (1980)]** **FIGURE 9.10**

R: Range of Experiments

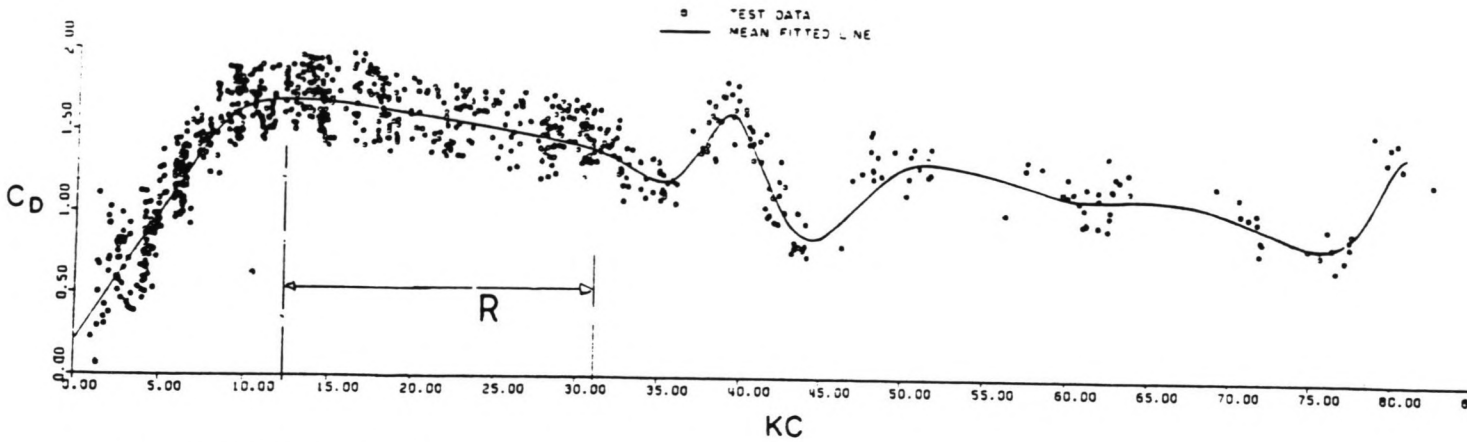

Drag coefficient vs. KC for a smooth circular cylinder in waves

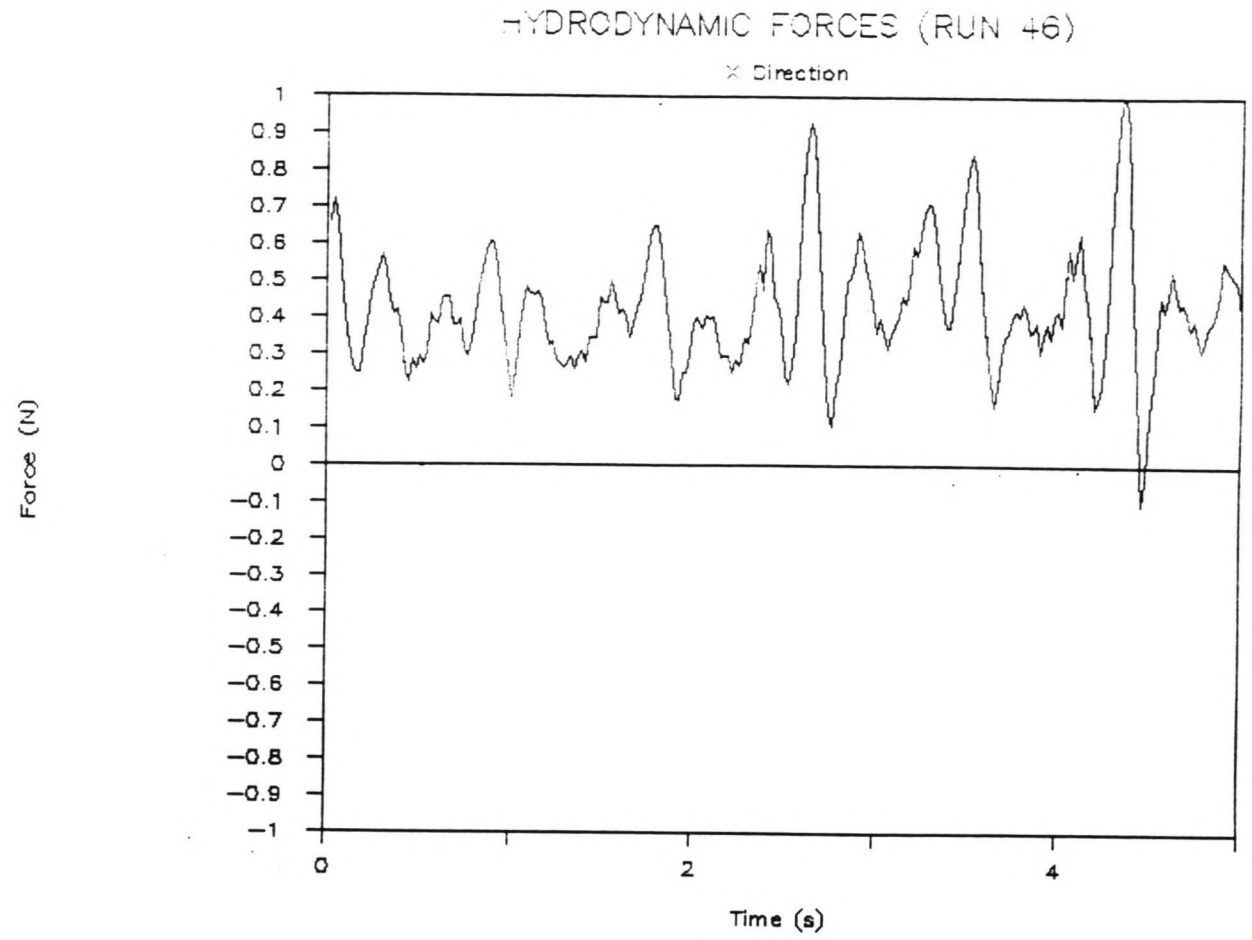

FIGURE 9.11.1

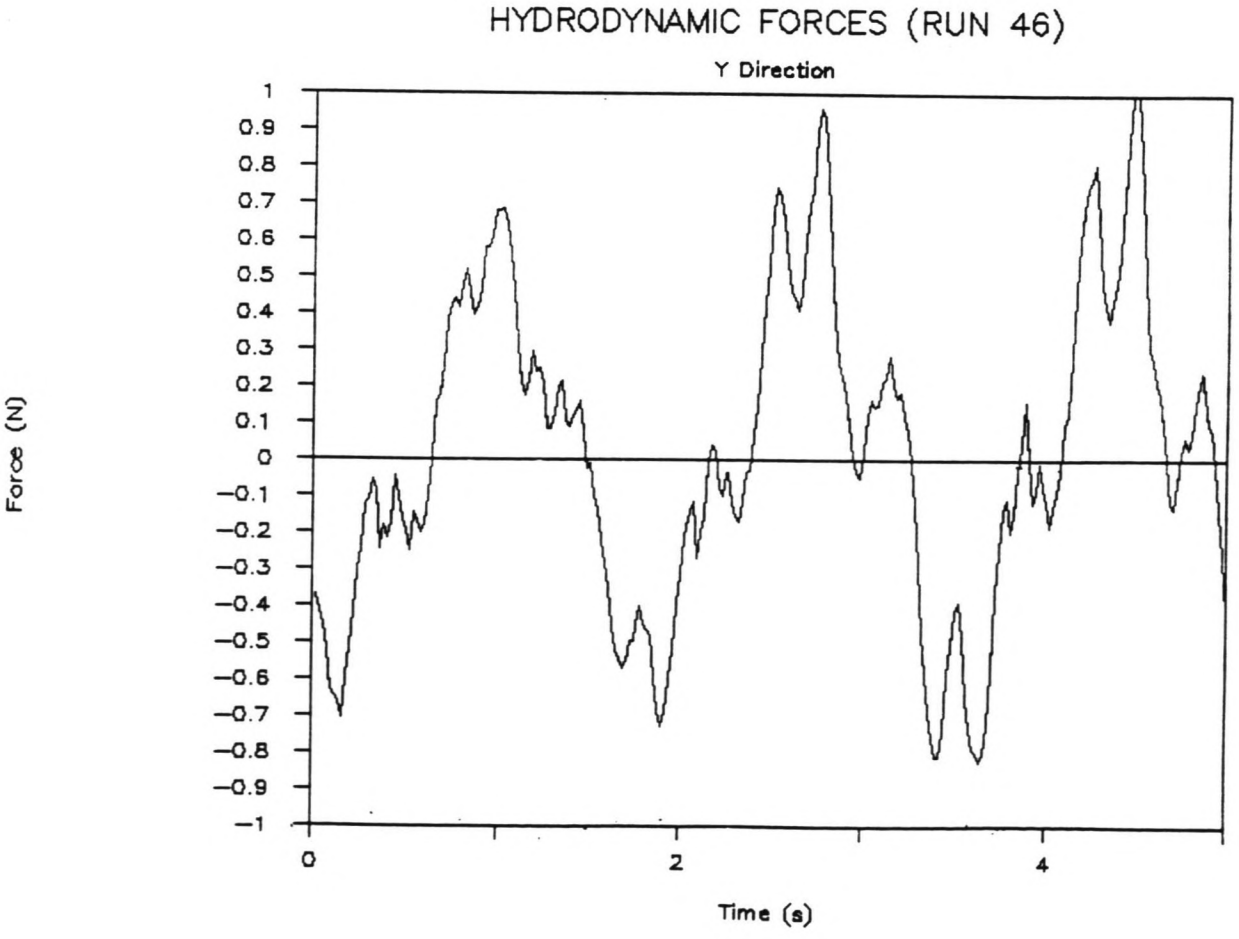

FIGURE 9.11.2

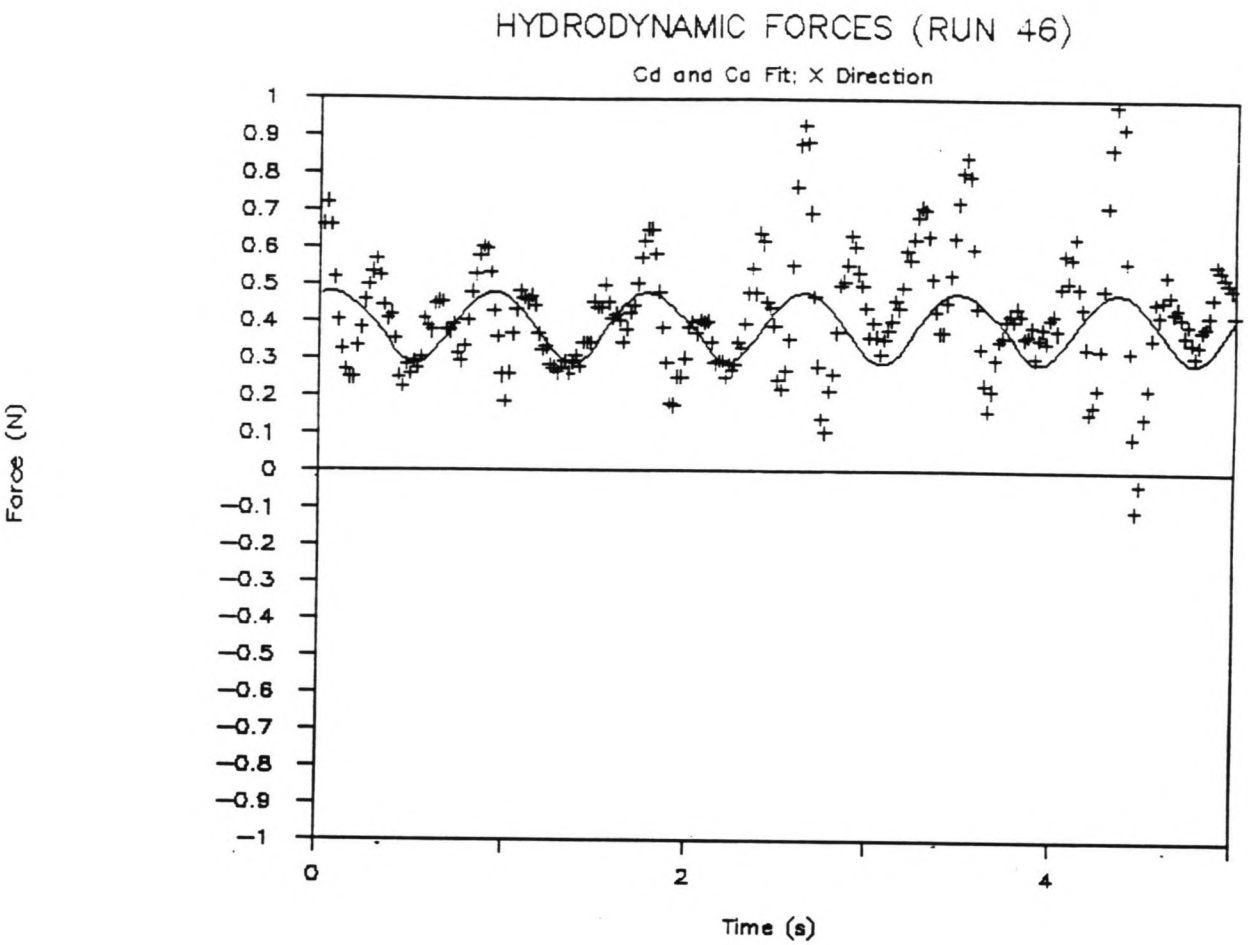

FIGURE 9.12.1

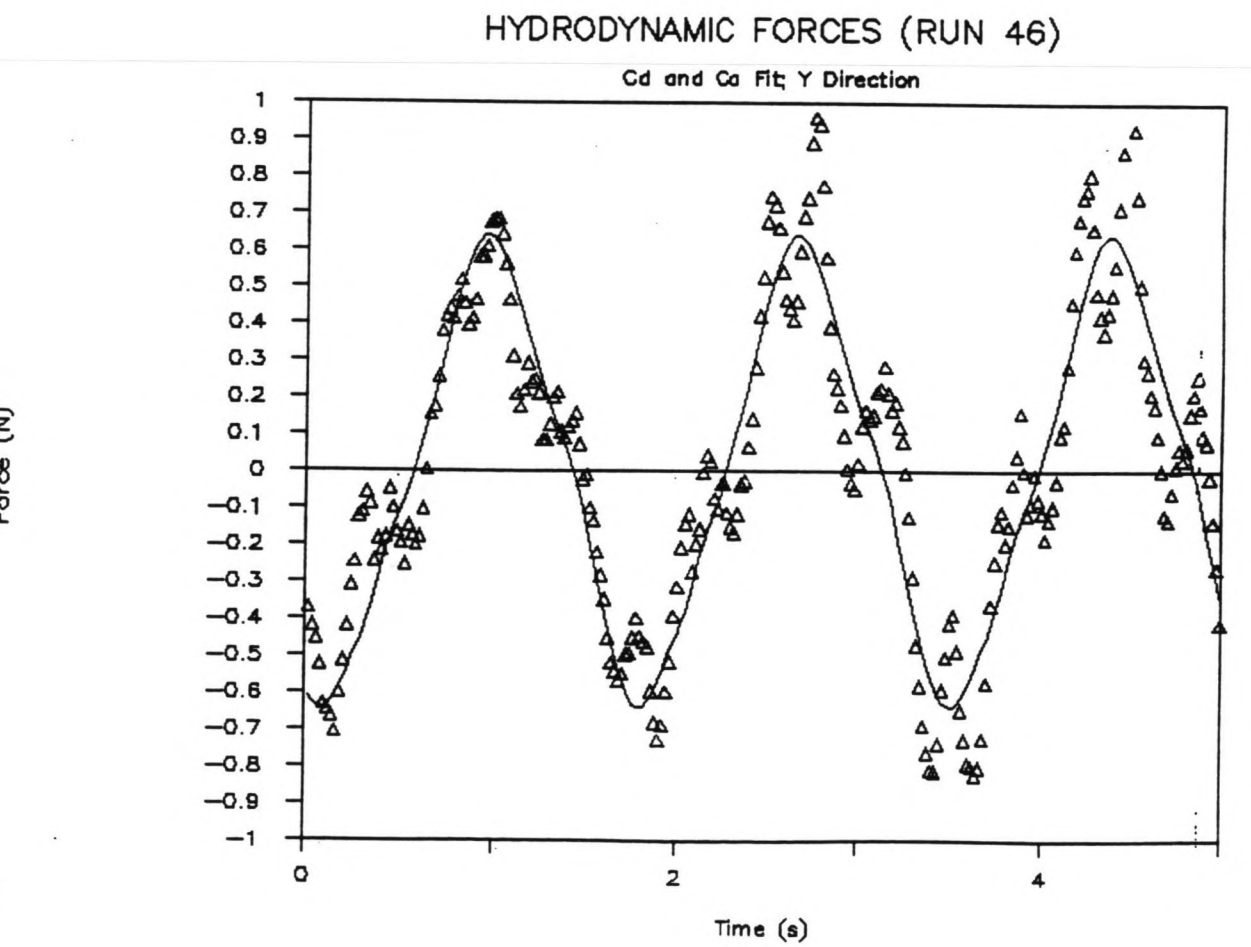

FIGURE 9.12.2

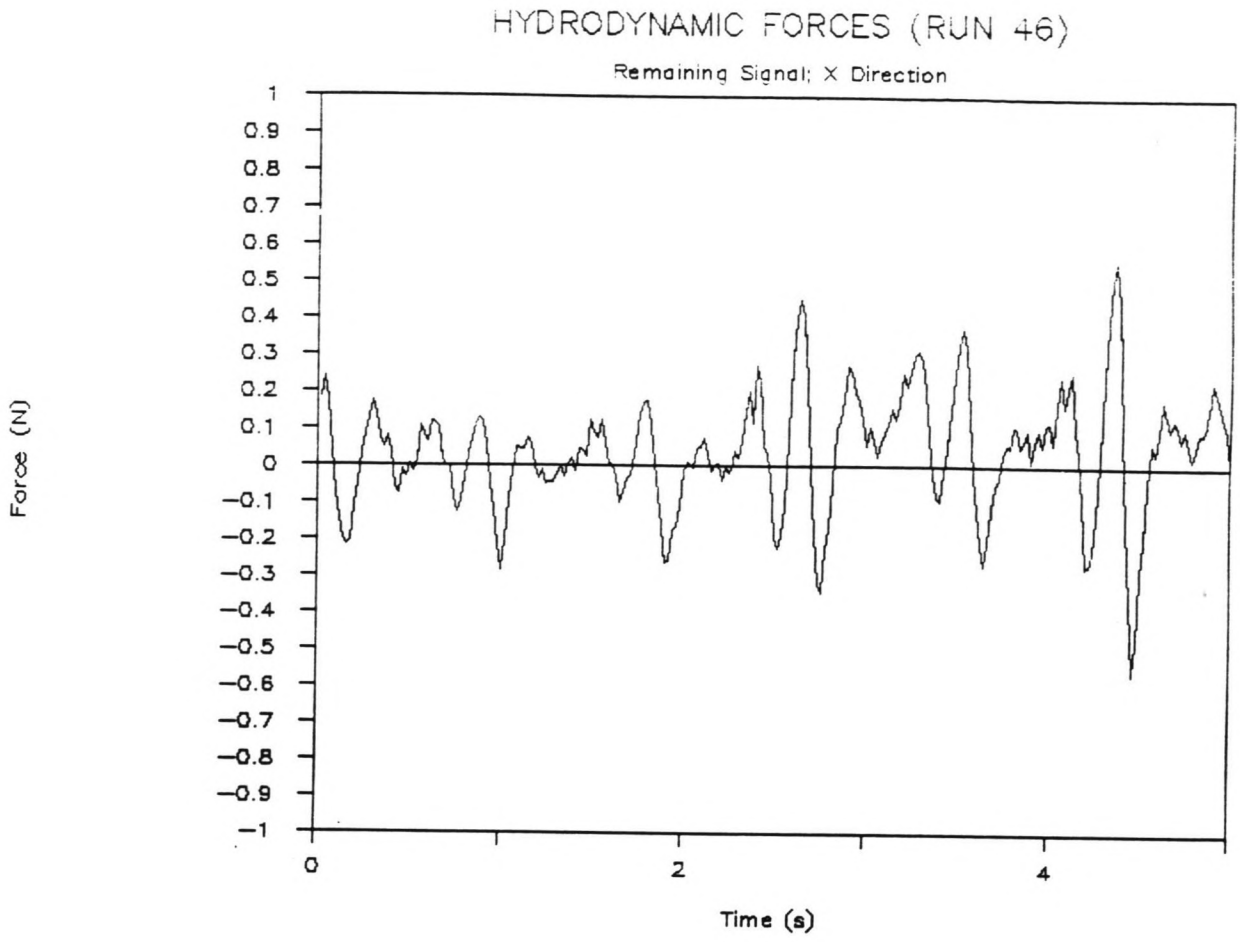

FIGURE 9.13.1

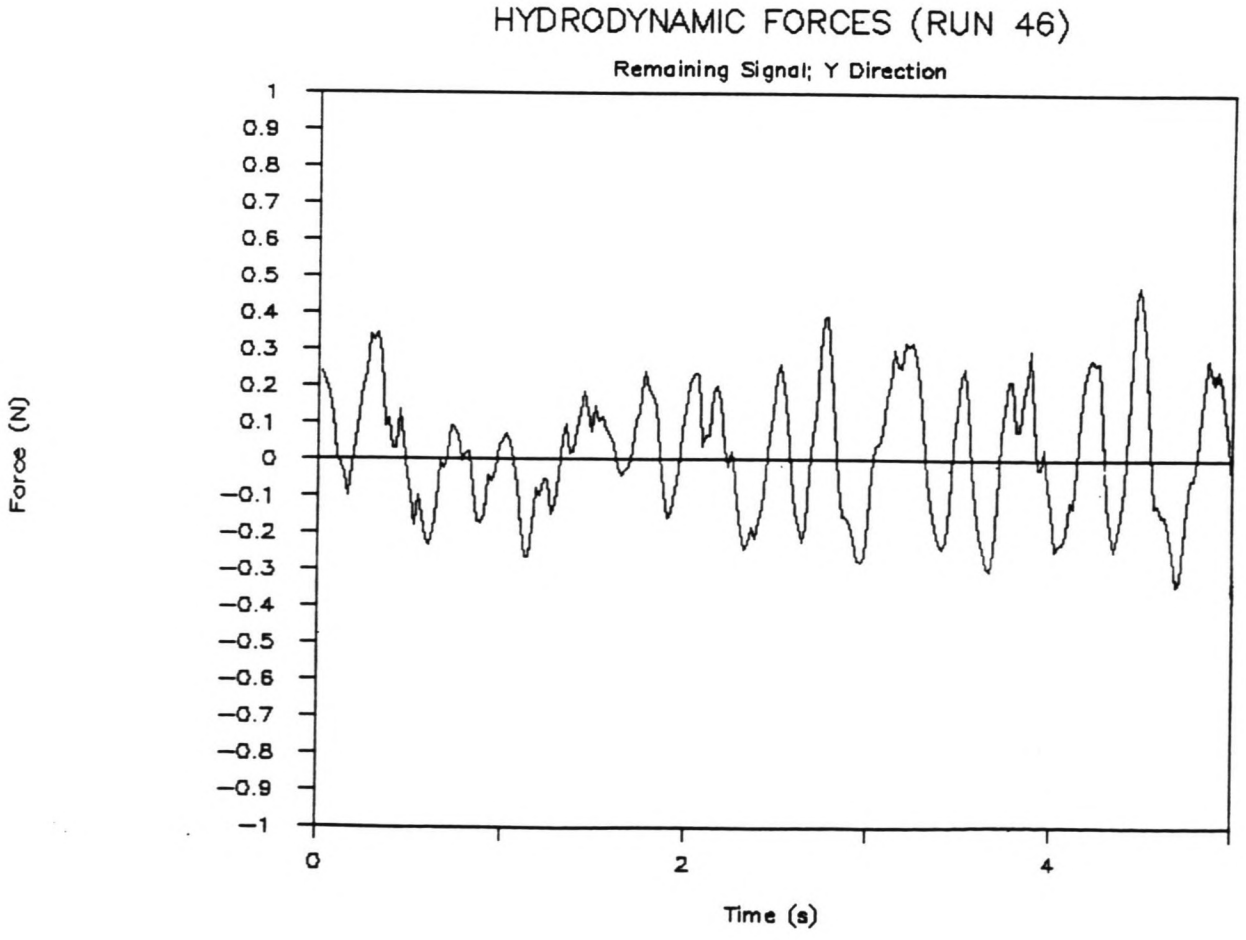

FIGURE 9.13.2

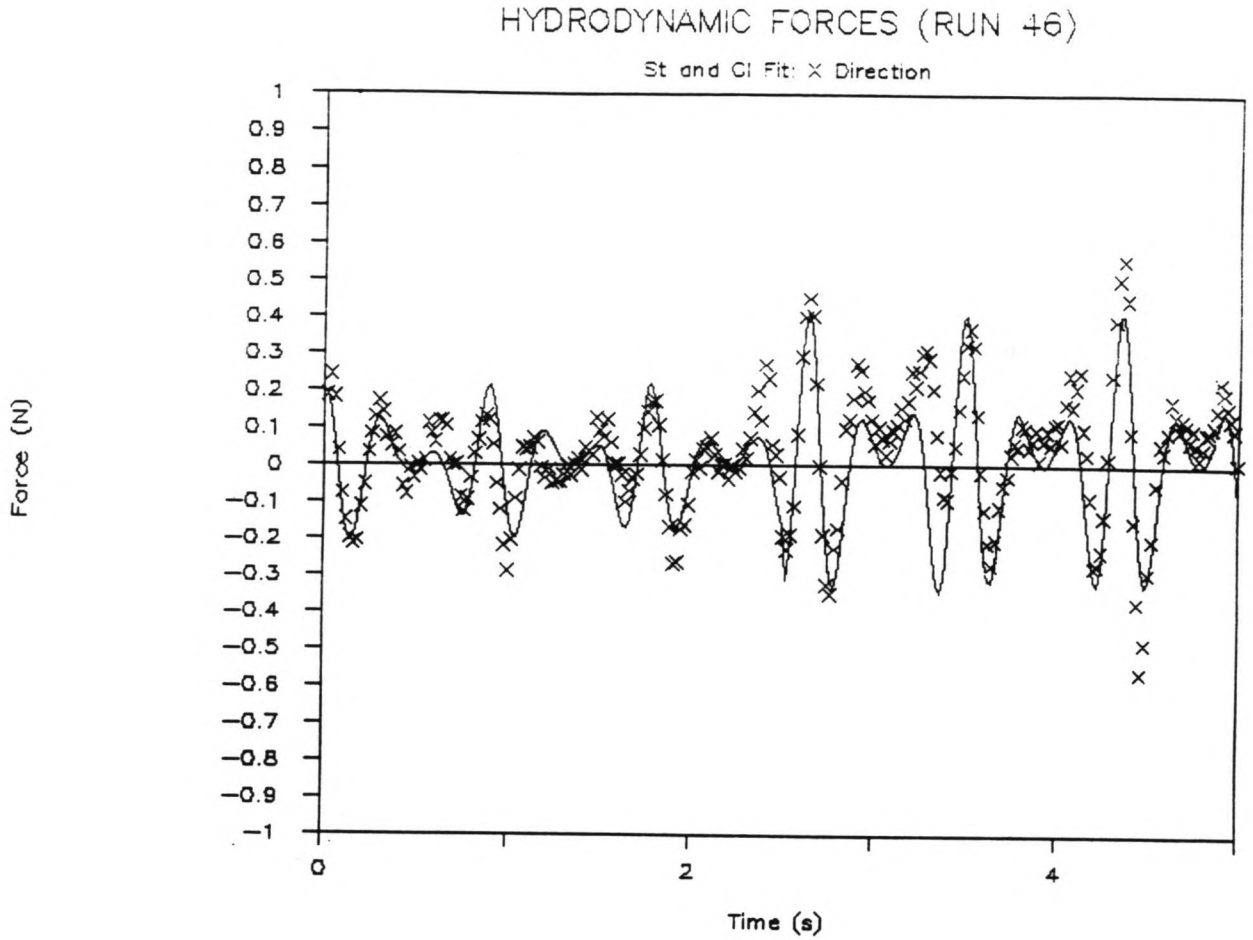

FIGURE 9.14.1

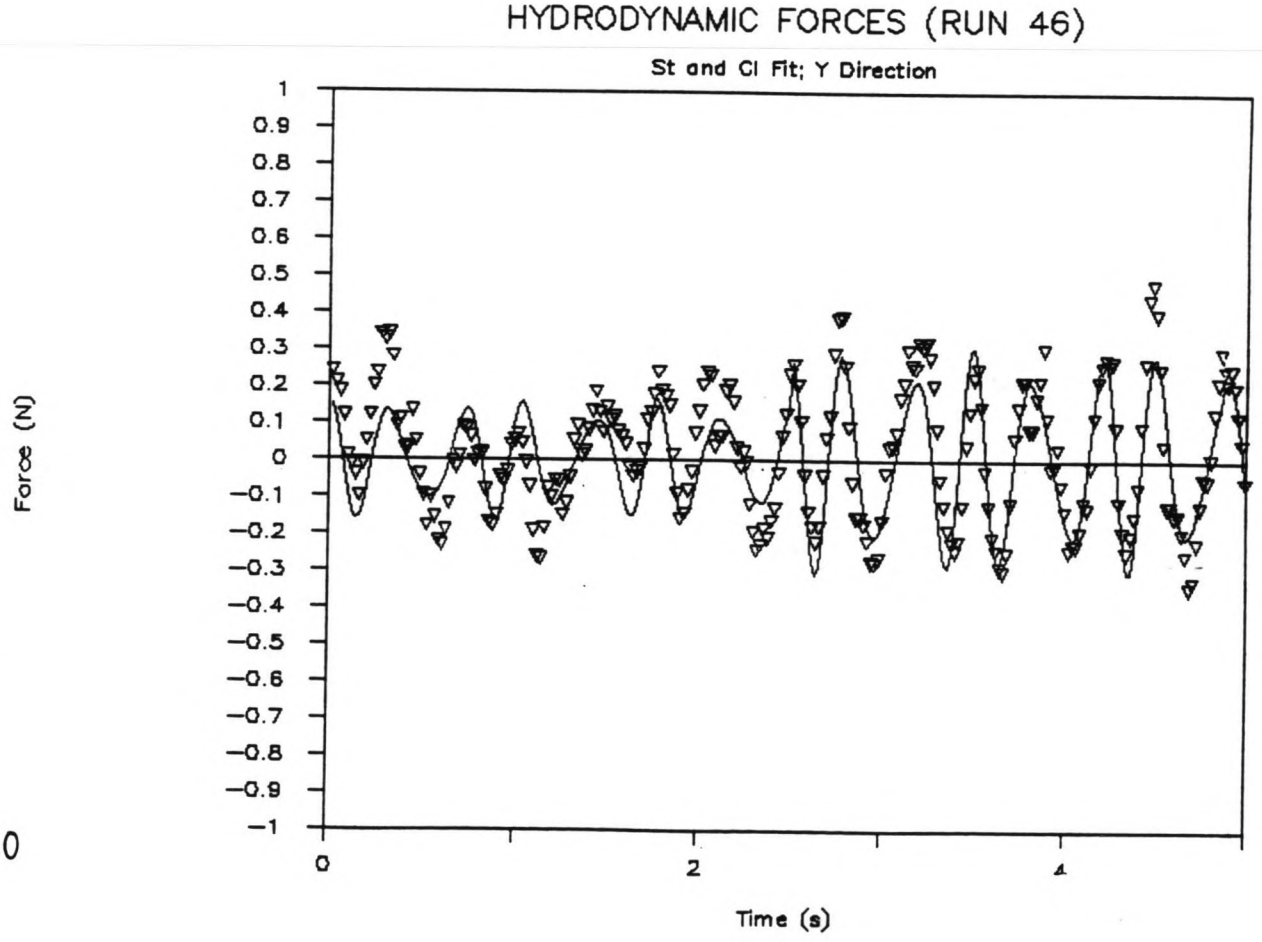

FIGURE 9.14.2

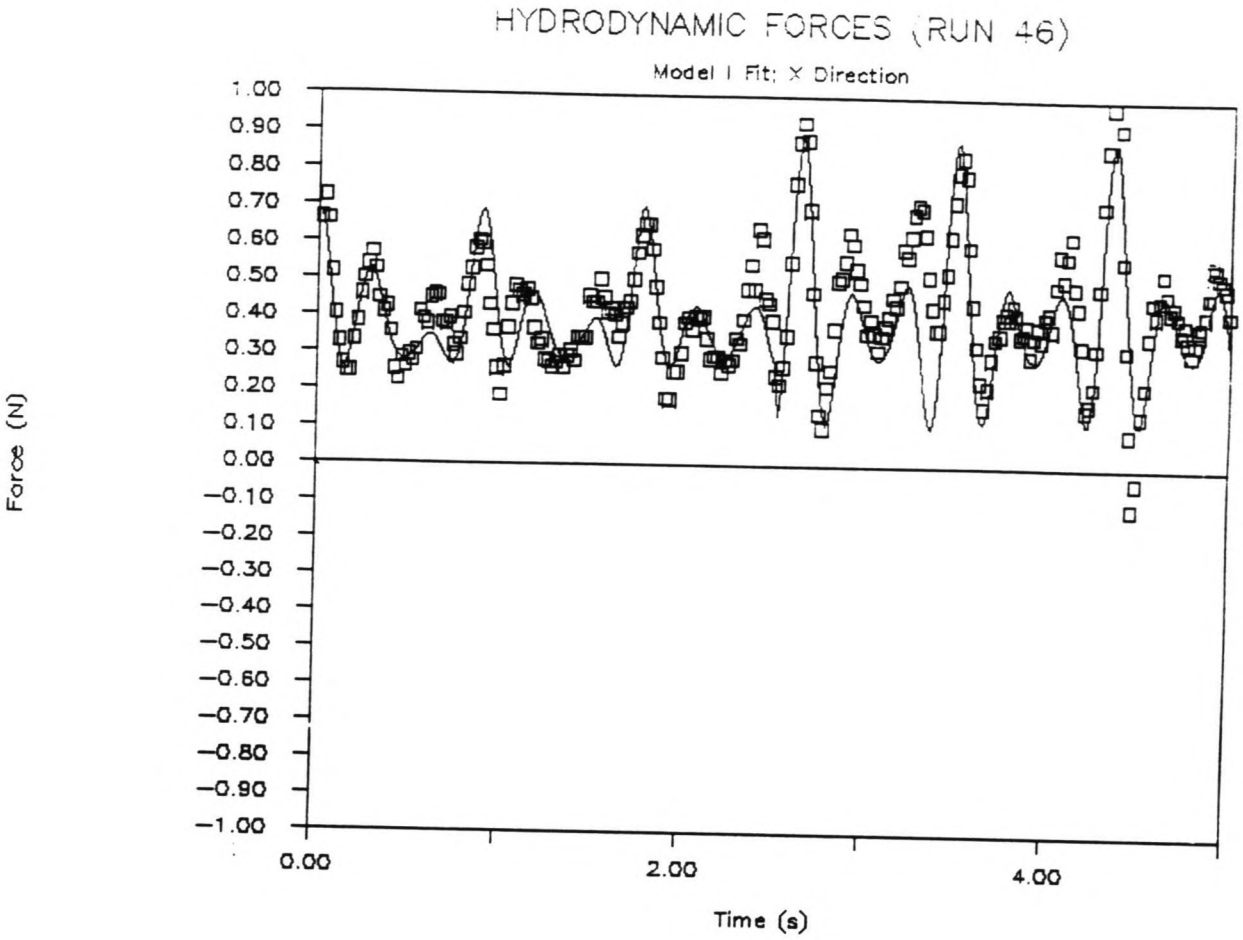

FIGURE 9.15.1

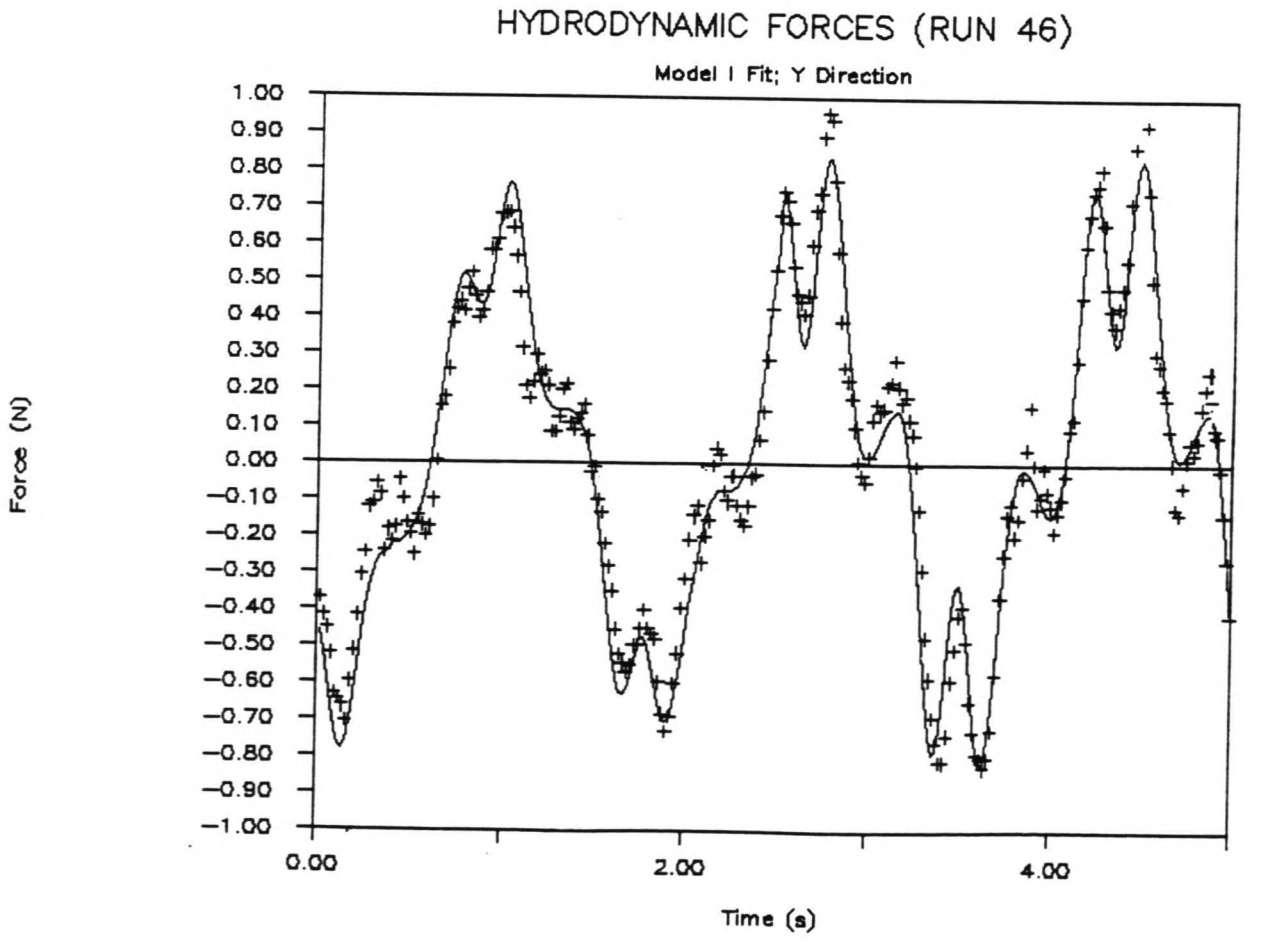

FIGURE 9.15.2

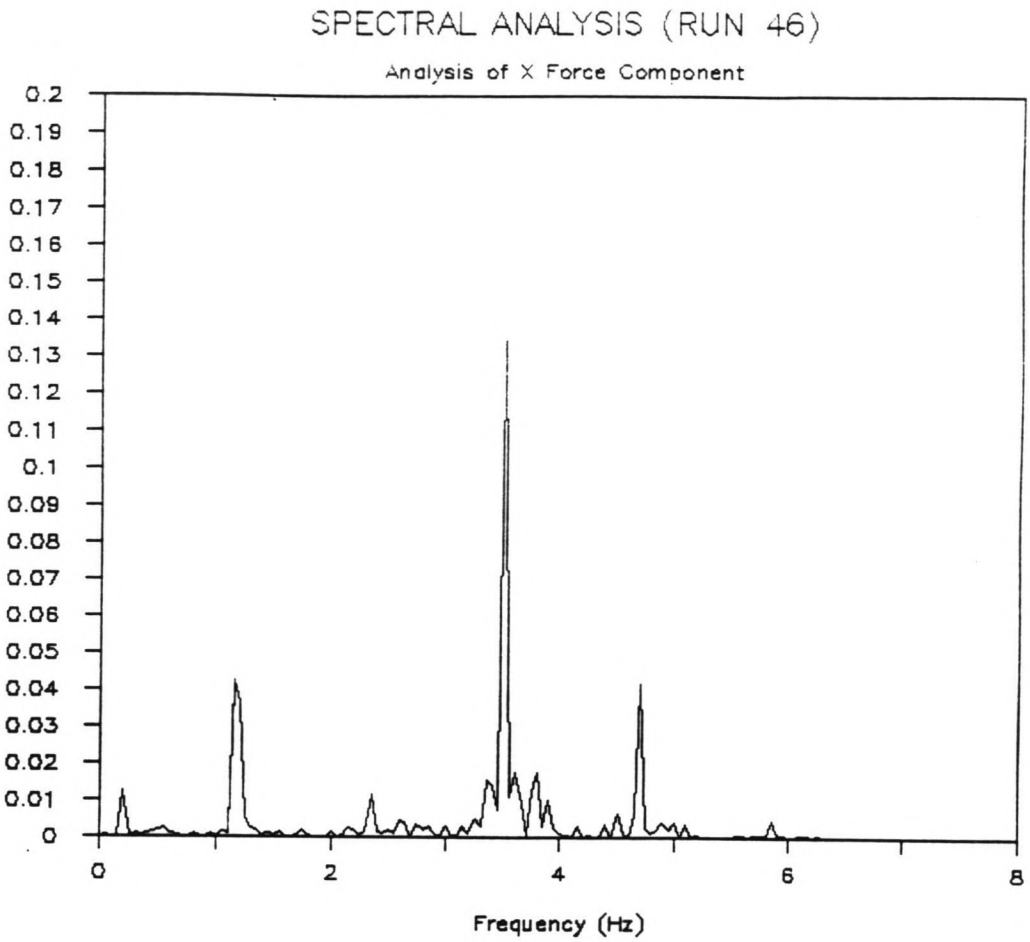

FIGURE 9.16.1

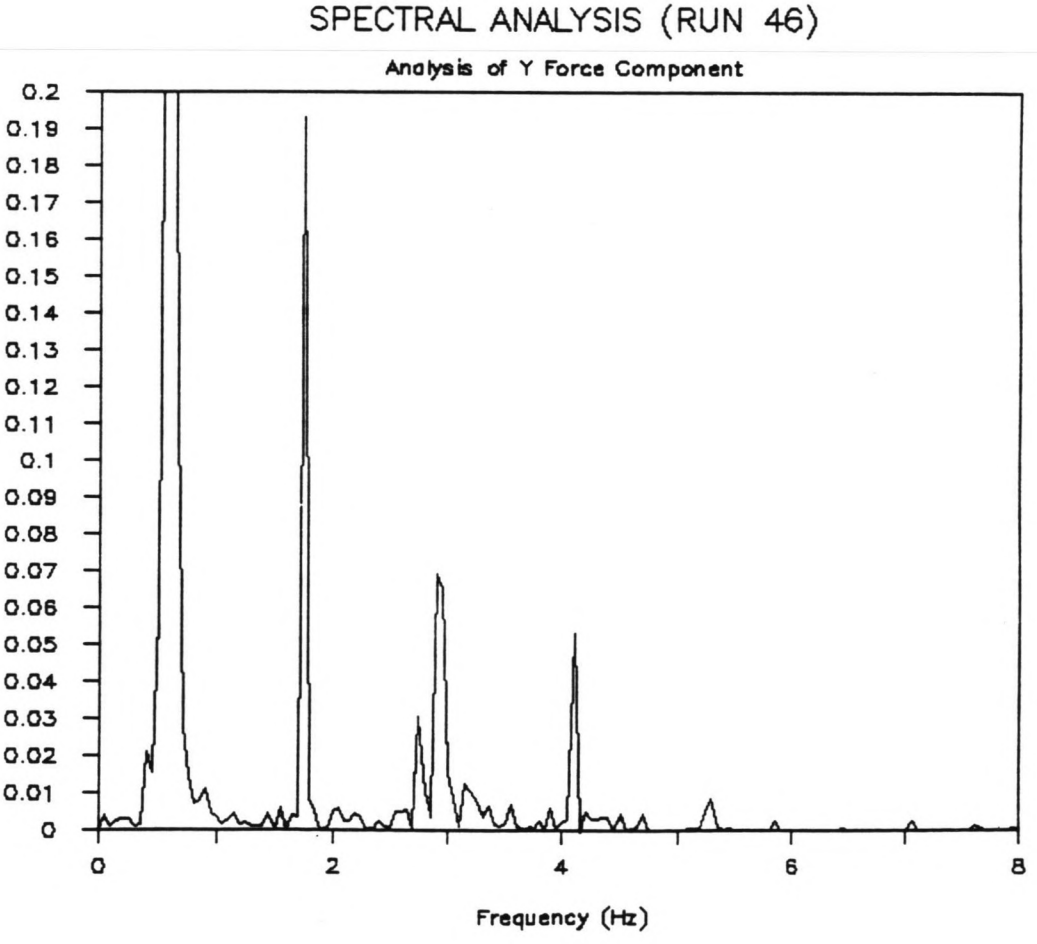

FIGURE 9.16.2

9.4.2.2 Spectral Analysis of Experiments and Model I

The spectra of the force signals of run 46 are shown in the figures 9.16.
The spectra of the model forces can be obtained as follows:

a - The spectral analysis could be applied to the reproduced forces from section 9.4.2.1 (figures 9.15). This means that the phase shifts between all pieces of the record are included and will affect the result.

b - The spectral analysis could be applied to a synthesized model registration of the entire record, using the averaged values from the analysis for Cd, Ca, St and Cl, and a single (starting) value of phi.

The possibility mentioned under b) has been applied here, because this represents the original model correctly.
The peak at the oscillation frequency is very high (see also figure 9.3), but has been reproduced by the first phase of the analysis, as shown in the figures 9.17 and figure 9.18.
The model spectra of the lift forces from the figures 9.13 are presented in the figures 9.19. The complete model spectra are shown in the figure 9.20.

9.5 Conclusions

- The analysis procedure presented gives averaged values for the five required model parameters (section 9.2.1), which are obtained by analysing segments of the recorded signal seperately.

- The analysis has been executed by fitting a curve through all measured data points, trying to find a minimum for the criterium functions (section 9.2.2). The criterium function values for the x and the y forces were summed when determining the Cd and Ca values. For the Cl, St and phi determination, only the criterium function of the direction in which the lift force was primarily thought to act was taken into account: for oscillation-only situations the x direction, for relatively large towing speeds the y direction.

- The analysis procedure presented gave proper information about the values for the experiment parameters. This can be concluded from the results from the analysis of the degenerated cases, which do not differ too much from literature information (section 9.4.1.3).

- For a stationary flow and an additional oscillation (run 46), the model (I) describes the forces very well (figure 9.15). Also, the spectra of the forces calculated with model I look like the spectra of the recorded forces (figure 9.20).

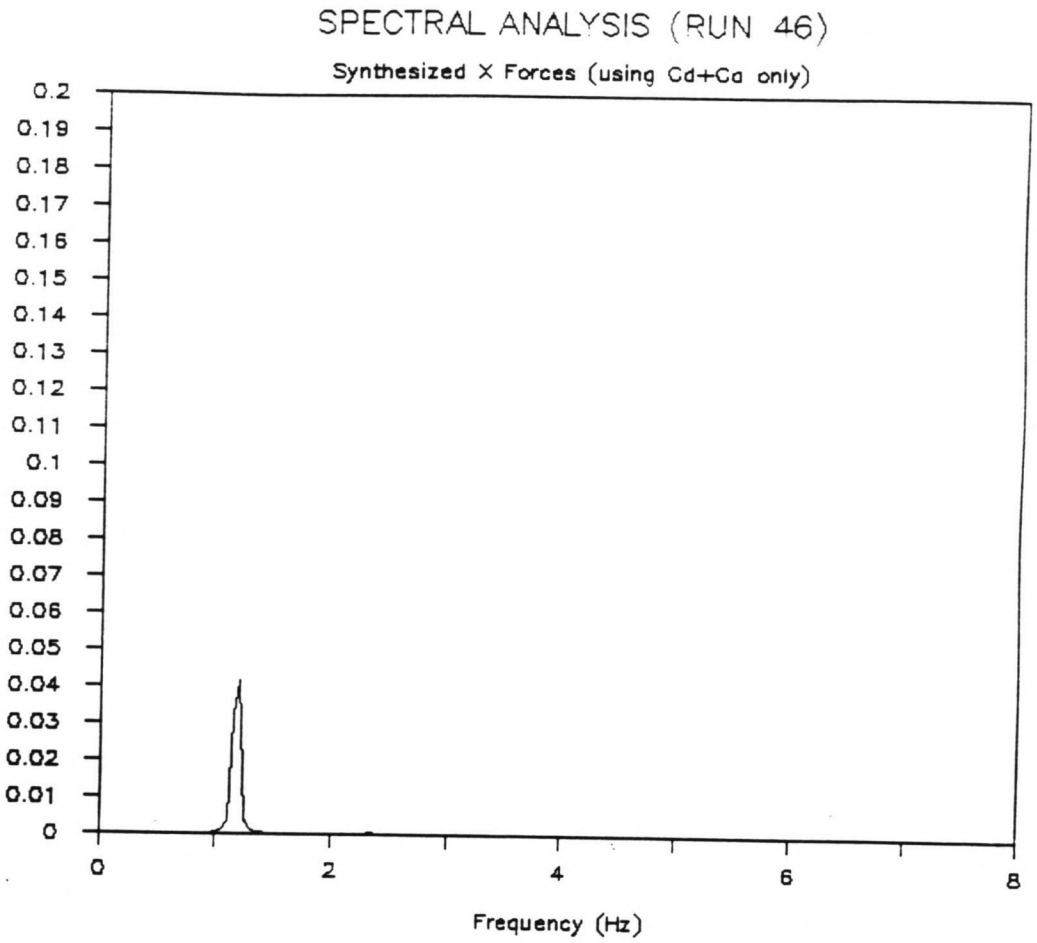

FIGURE 9.17.1

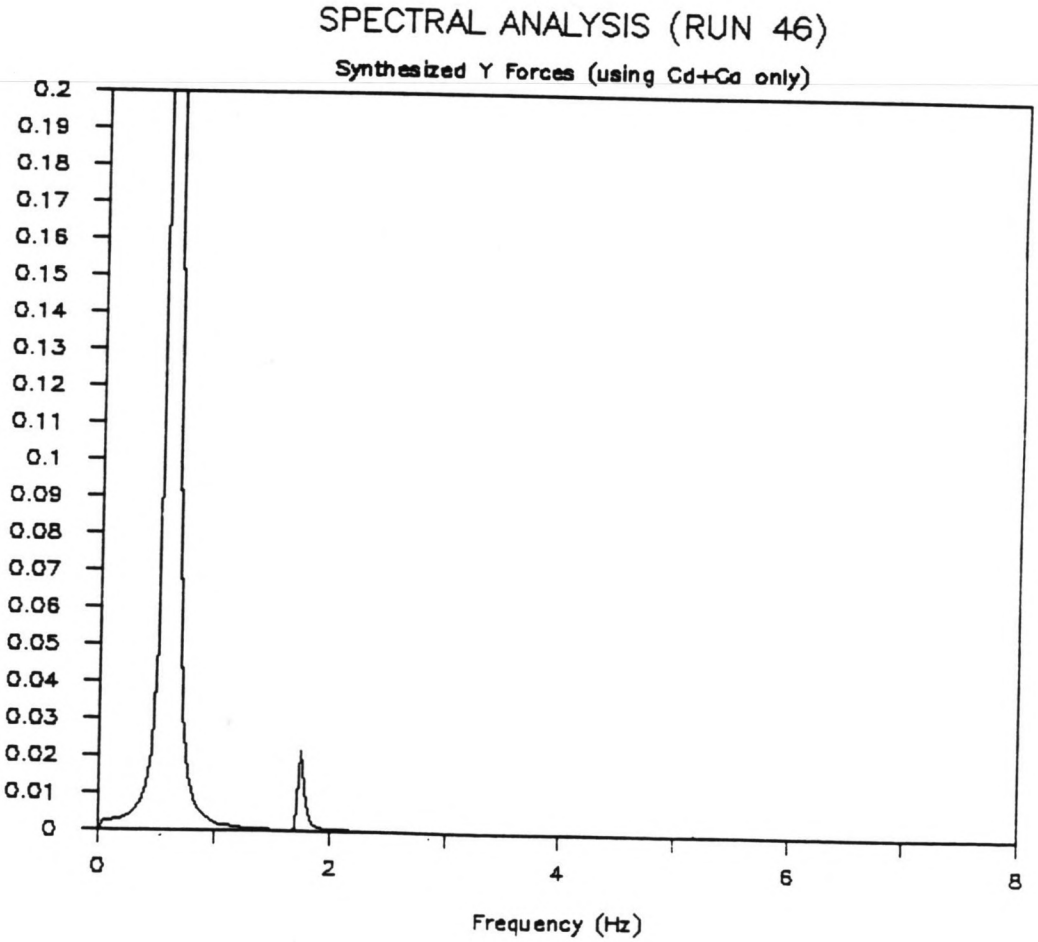

FIGURE 9.17.2

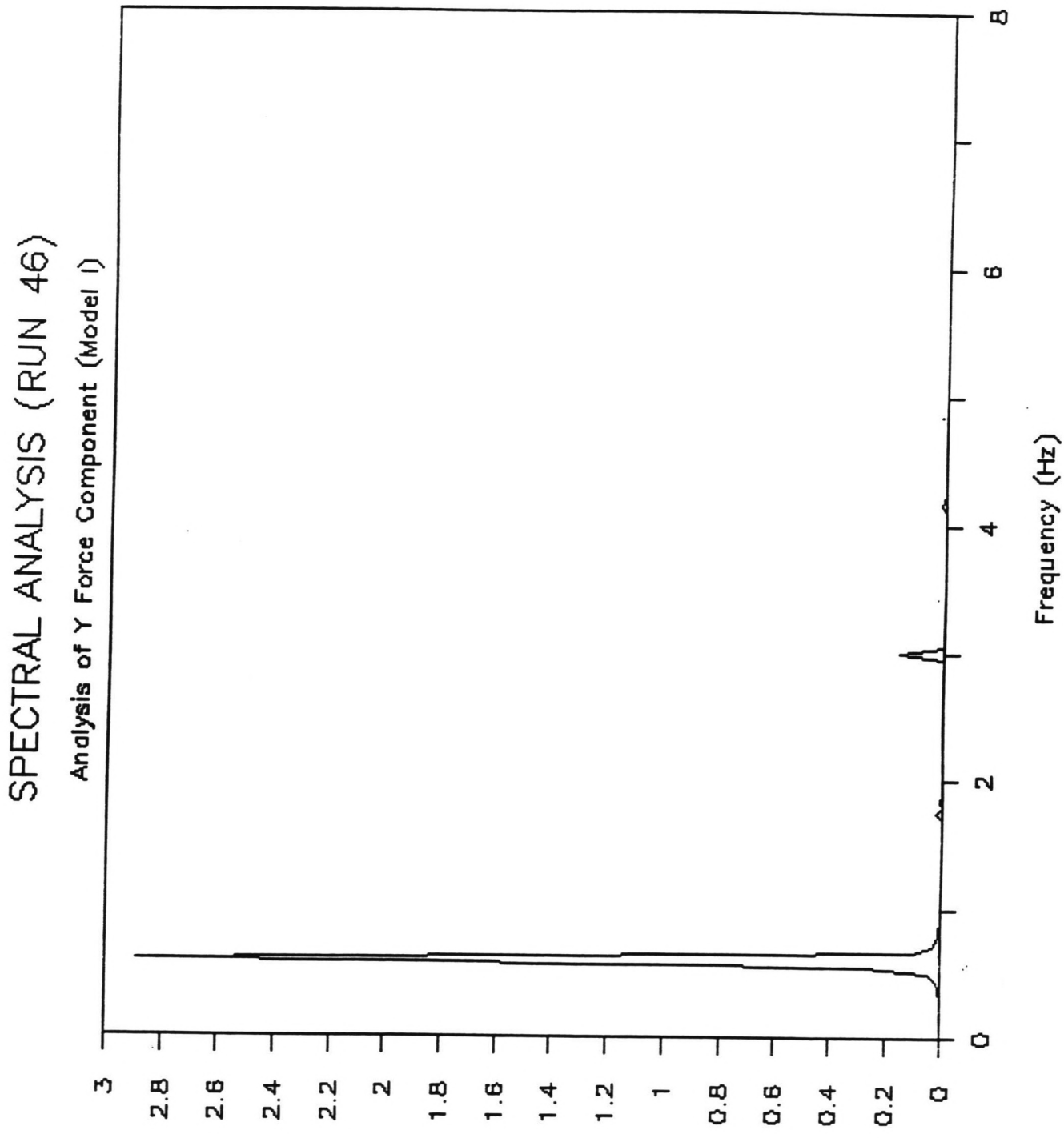
SPECTRAL ANALYSIS (RUN 46)
Analysis of Y Force Component (Model I)
3
2.8
2.6
2.4
2.2
2
1.8
1.6
1.4
1.2
1
0.8
0.6
0.4
0.2
0
0
2
4
6
8
Frequency (Hz)

FIGURE 9.18

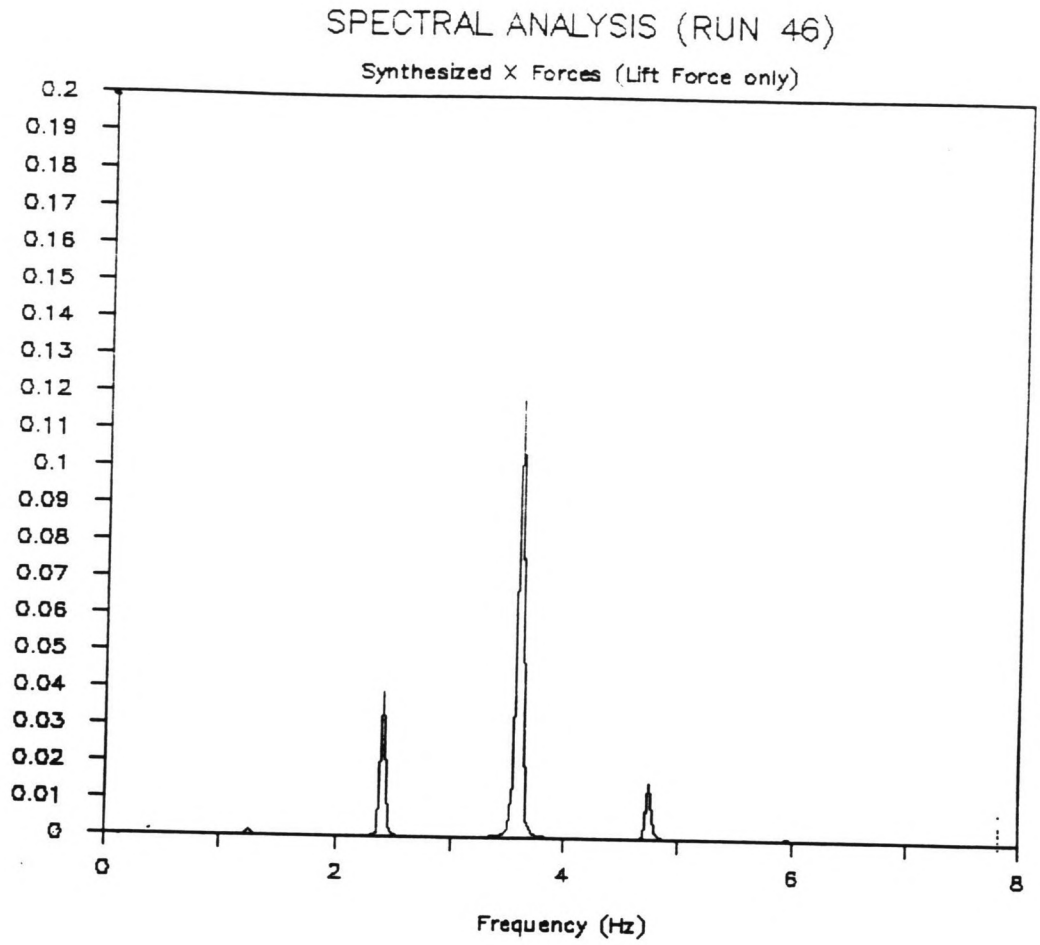

FIGURE 9.19.1

FIGURE 9.19.2

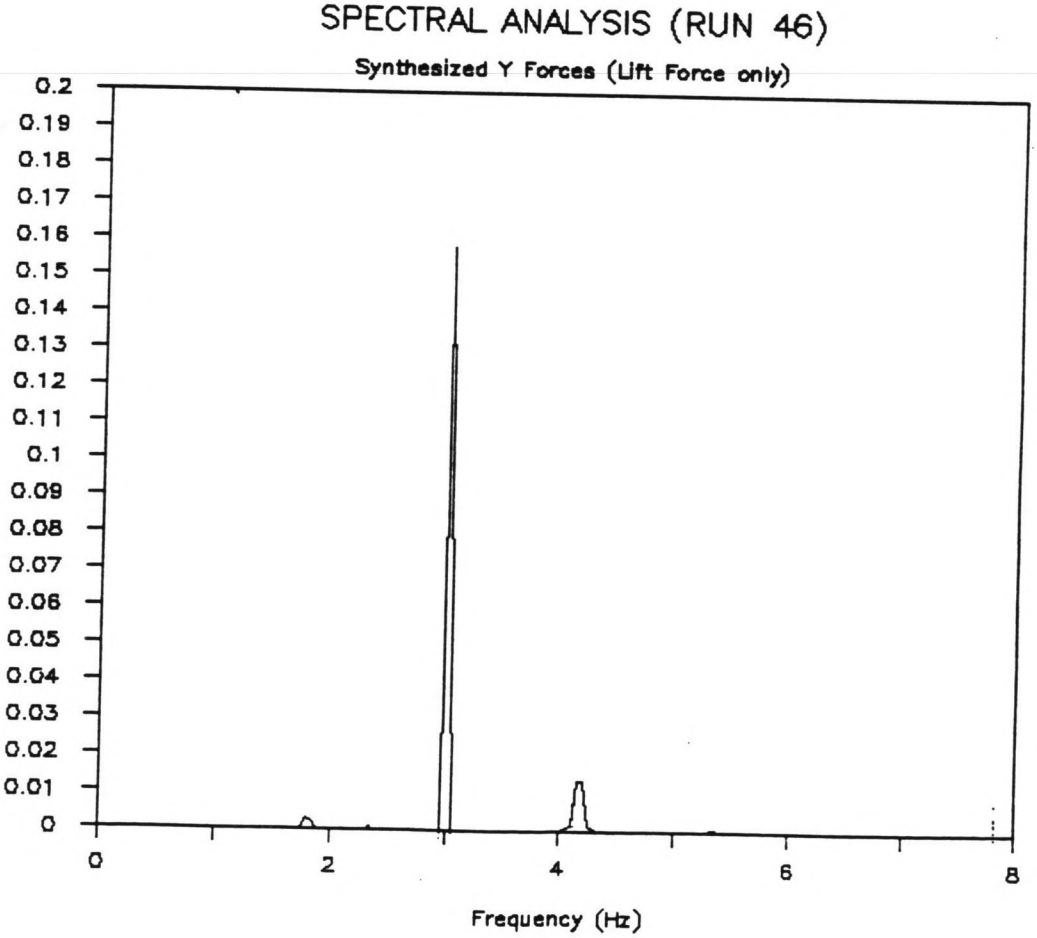

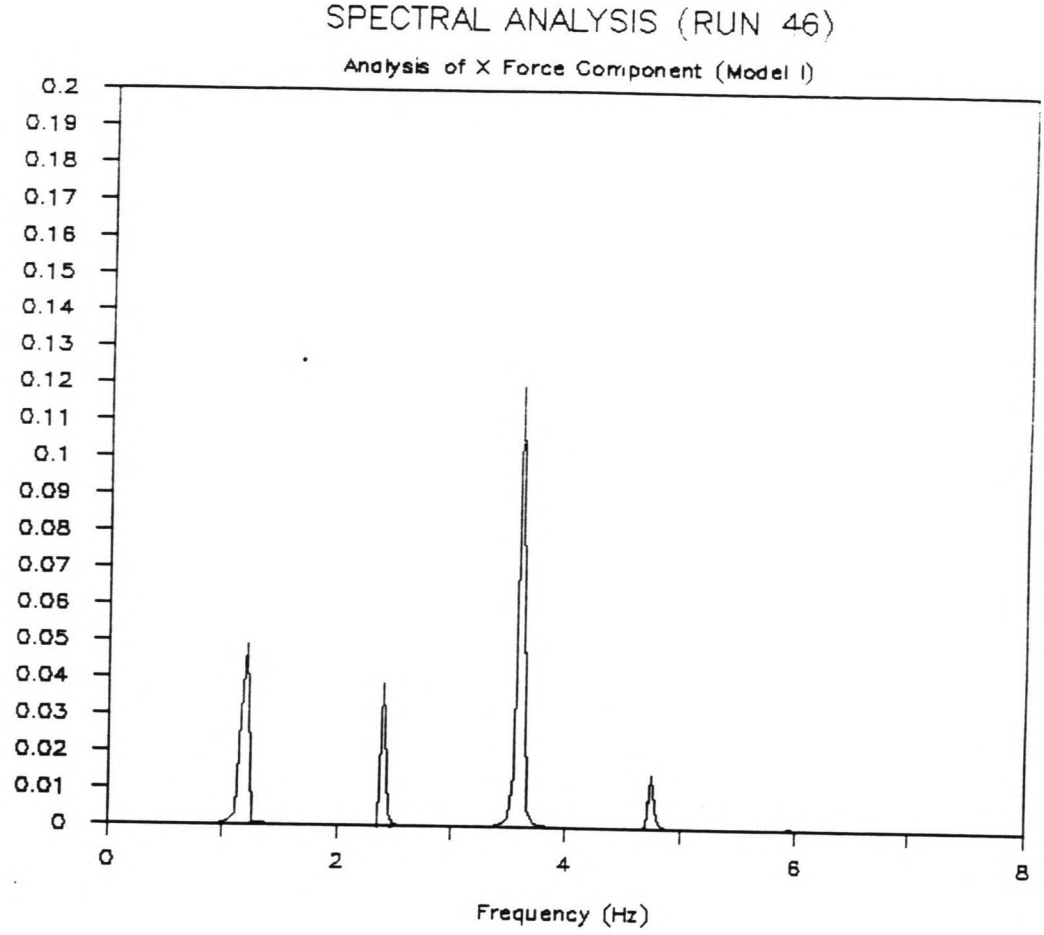

FIGURE 9.20.1

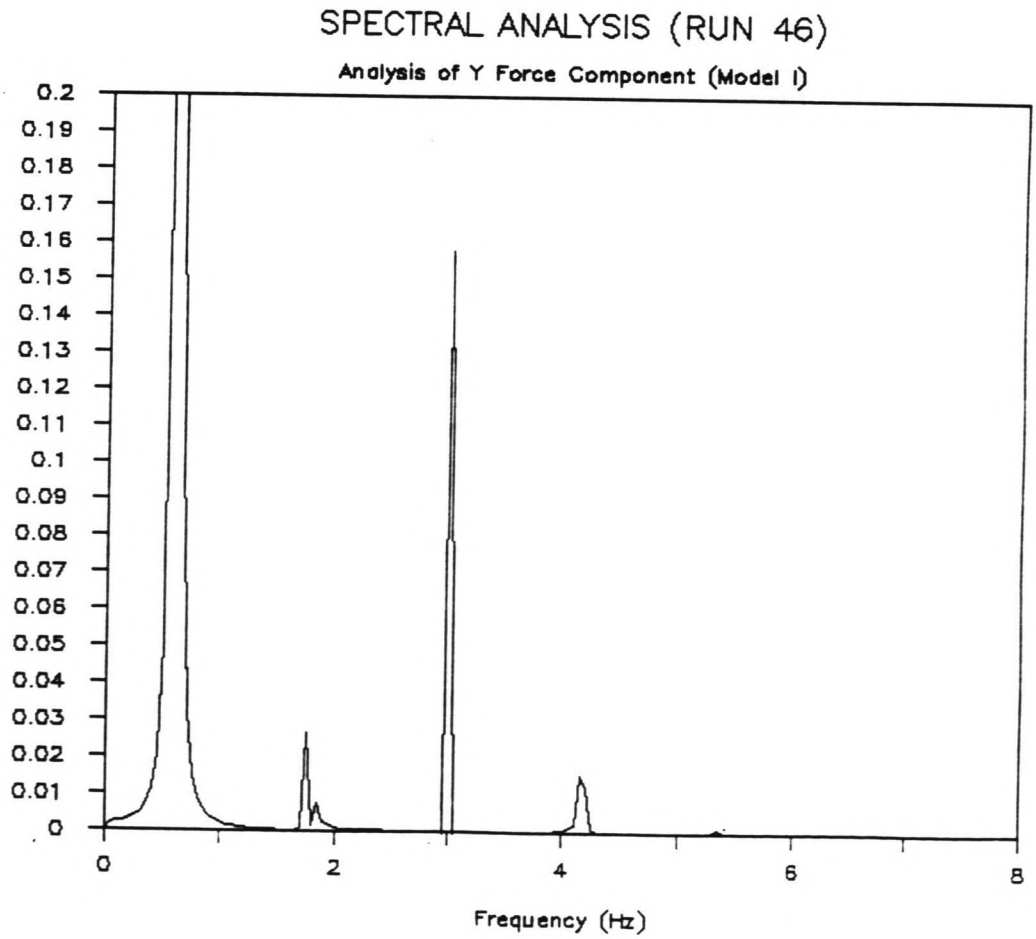

FIGURE 9.20.2

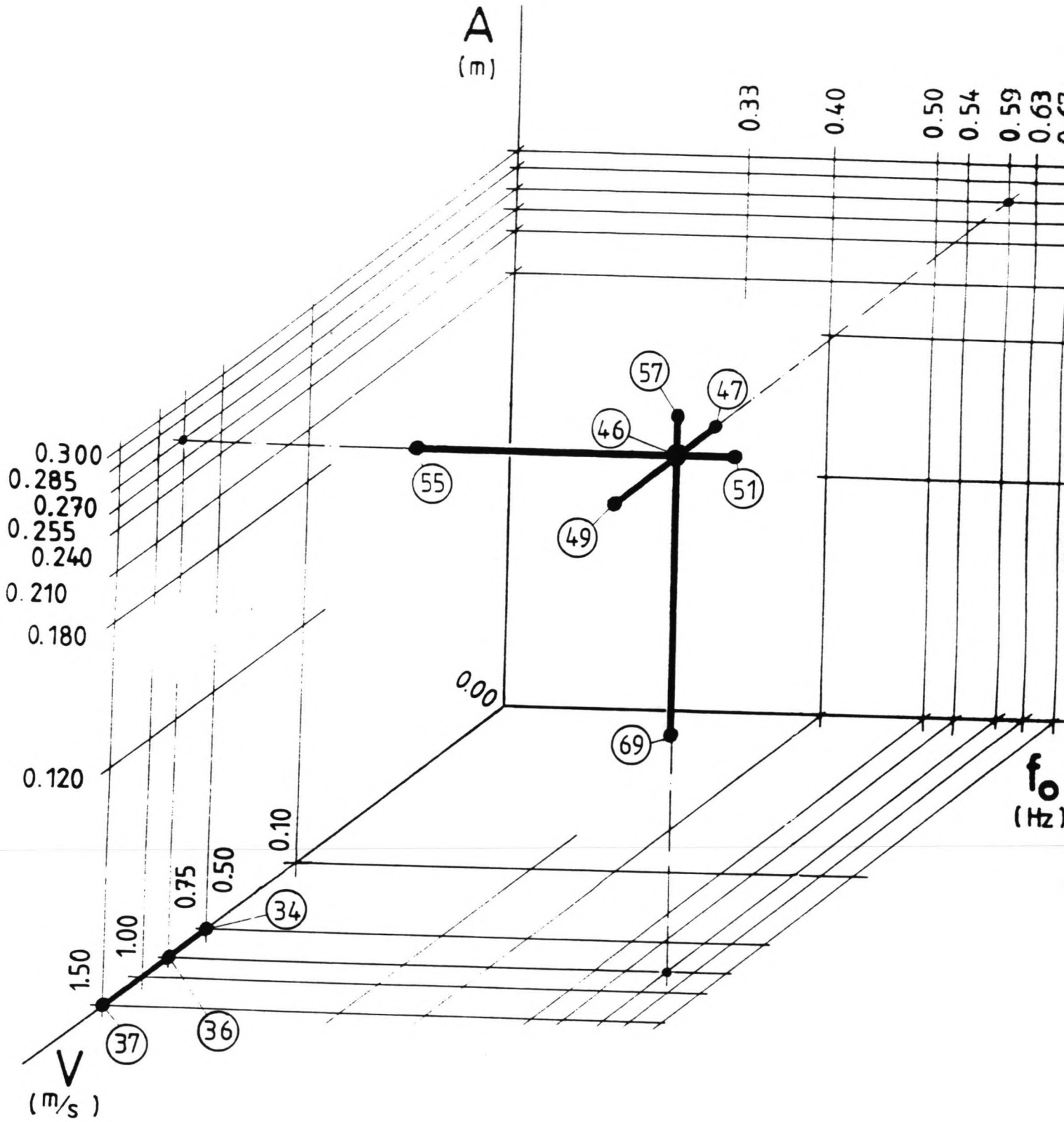

FIGURE 10.1

Runs Analysed Using Model I and II

10 COMPARISON OF MODELS AND INTERPRETATION OF RESULTS

10.1 Comparison of Model I and Model II

Ten runs (no. 34, 36, 37, 46, 47, 49, 51, 55, 57 and 69) have been analysed using both models (see figure 10.1 and figure 7.3), in order to find which model gives the best description of the hydrodynamic (lift) forces.

10.1.1 Determination of Model Constants

The model constants from the analyses are presented in the tables 10.1 and 10.2.
Comparing the values of the determined criterium functions of these runs, it appeared that for stationary flow conditions (runs 34, 36 and 37) it does not matter which model (I or II) is used. This is no surprise since the flow velocity does not change here and therefore the lift force frequency will be constant for model I. The lift force frequency of model II is by definition constant: the two models then will give essentially identical results.
In general, model I describes the forces better than model II. This can be seen in two ways:

- the criterium function values given (calculated using the complete model forces) are always (much) lower for model I;

- the lift coefficient values found with model I are always (much) higher than the values found with model II.

The second argument indicates that model I fits better. When a models description would be completely wrong, a least-square analysis procedure would eliminate the coefficients influence by inserting a zero value for it in this case. Thus, the higher the coefficient, the better the model.

10.1.2 Reproduction of Force Signals

The reproduction of the forces of run 46 according to model I and II are shown in the figures 10.2 and 10.3.
Model I gives a visually better fit. This is confirmed by the lower criterium function values found in the previous section. This comparison holds true for the other runs mentioned earlier in this section (except for no. 34, 36 and 37) as shown in appendix G.

Listing of Output Parameters (Model I + II)

MODEL I

Run: (no.)	Cd: (-)	Ca: (-)	*) Cl: (-)	*) St: (-)	A: (m)	V: (m/s)	T: (s)	CritfX: (-)	CritfY: (-)
46	1.140	.574	.511	.1773	.270	.750	1.700	.695E-01	.628E-01
47	1.306	.370	.825	.1330	.270	.500	1.700	.293E+00	.641E-01
49	.854	.744	.106	.1841	.270	1.500	1.700	.102E-01	.402E-01
51	1.210	.772	.722	.1828	.270	.750	1.500	.603E-01	.493E-01
55	1.000	.636	.276	.1865	.270	.750	3.000	.251E-01	.733E-01
57	1.126	.530	.497	.1636	.300	.750	1.700	.927E-01	.846E-01
69	.926	.696	.226	.1797	.120	.750	1.700	.154E-01	.714E-01
34	.886	.252	.232	.1864	.000	.500	1.700	.189E-01	.478E+00
36	.900	.300	.185	.1874	.000	.750	1.700	.706E-02	.487E+00
37	.748	.060	.068	.1739	.000	1.500	1.700	.469E-02	.671E+00

(table 10.1)

MODEL II

Run: (no.)	Cd: (-)	Ca: (-)	*) Cl: (-)	*) f: (Hz)	A: (m)	V: (m/s)	T: (s)	CritfX: (-)	CritfY: (-)
46	1.140	.574	.407	3.0082	.270	.750	1.700	.995E-01	.985E-01
47	1.306	.370	.695	2.5125	.270	.500	1.700	.378E+00	.838E-01
49	.854	.744	.039	3.3660	.270	1.500	1.700	.125E-01	.713E-01
51	1.210	.772	.671	3.3368	.270	.750	1.500	.110E+00	.645E-01
55	1.000	.636	.263	2.5527	.270	.750	3.000	.264E-01	.871E-01
57	1.126	.530	.379	3.3338	.300	.750	1.700	.147E+00	.117E+00
69	.926	.696	.223	2.4340	.120	.750	1.700	.155E-01	.752E-01
34	.886	.252	.232	1.5523	.000	.500	1.700	.189E-01	.478E+00
36	.900	.300	.185	2.3430	.000	.750	1.700	.706E-02	.487E+00
37	.748	.060	.068	4.3320	.000	1.500	1.700	.469E-02	.681E+00

(table 10.2)

*) average values

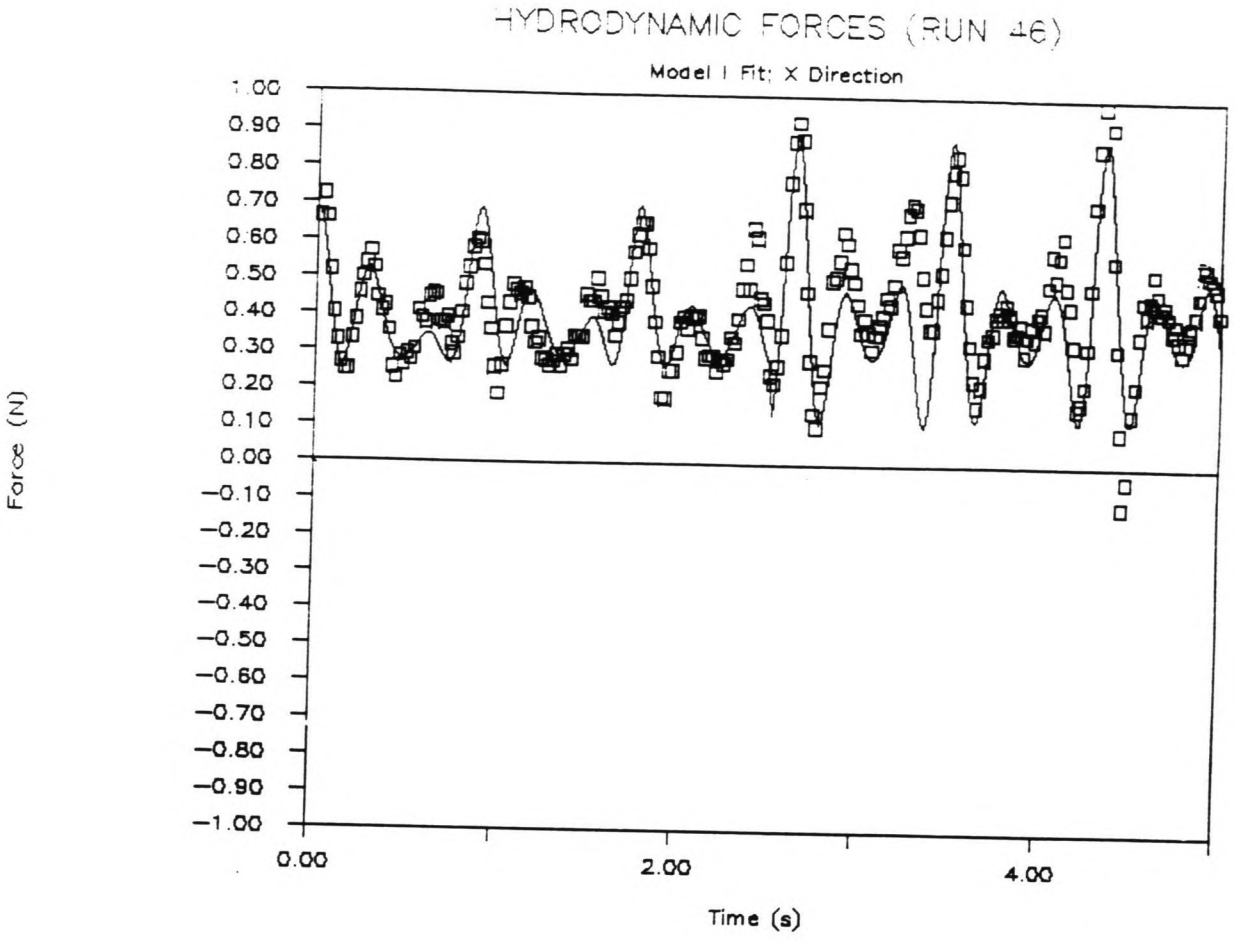

FIGURE 10.2.1

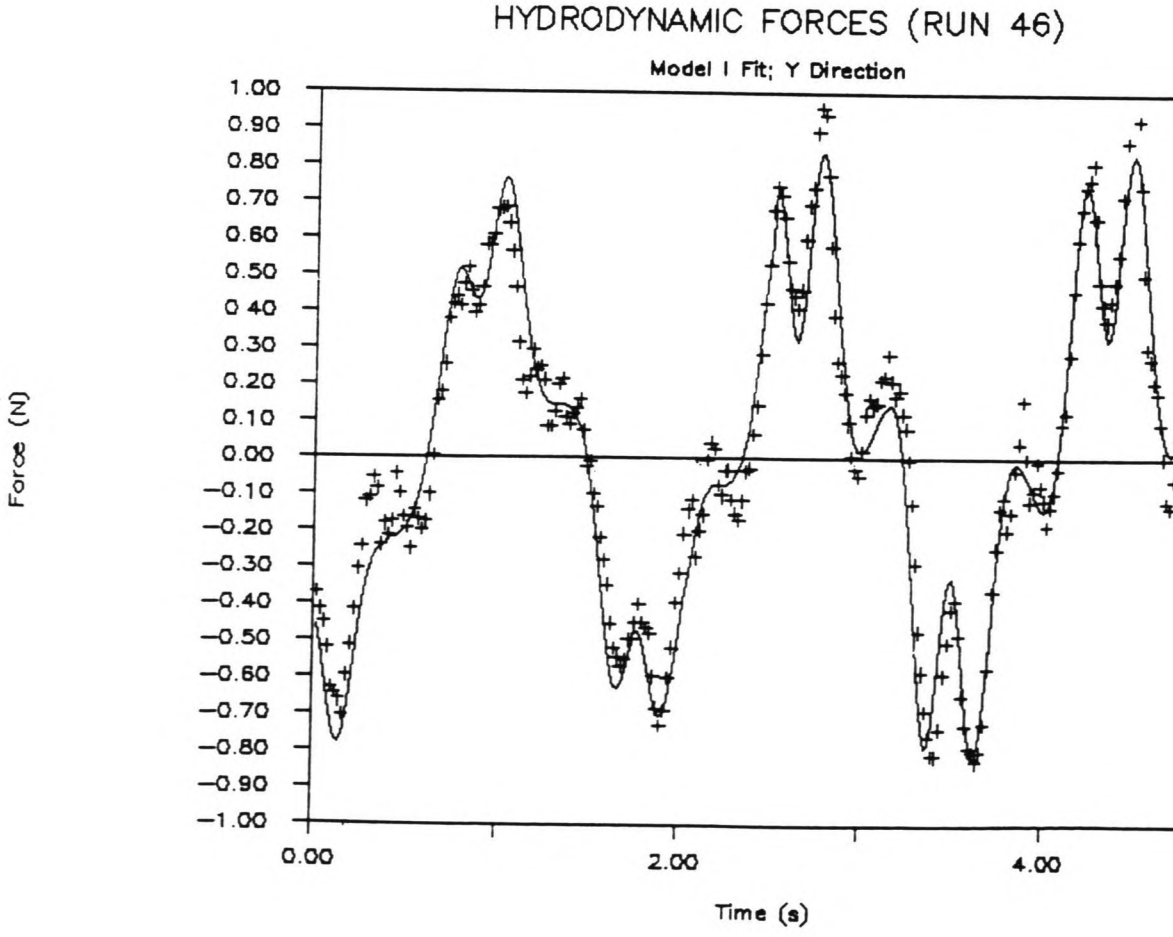

FIGURE 10.2.2

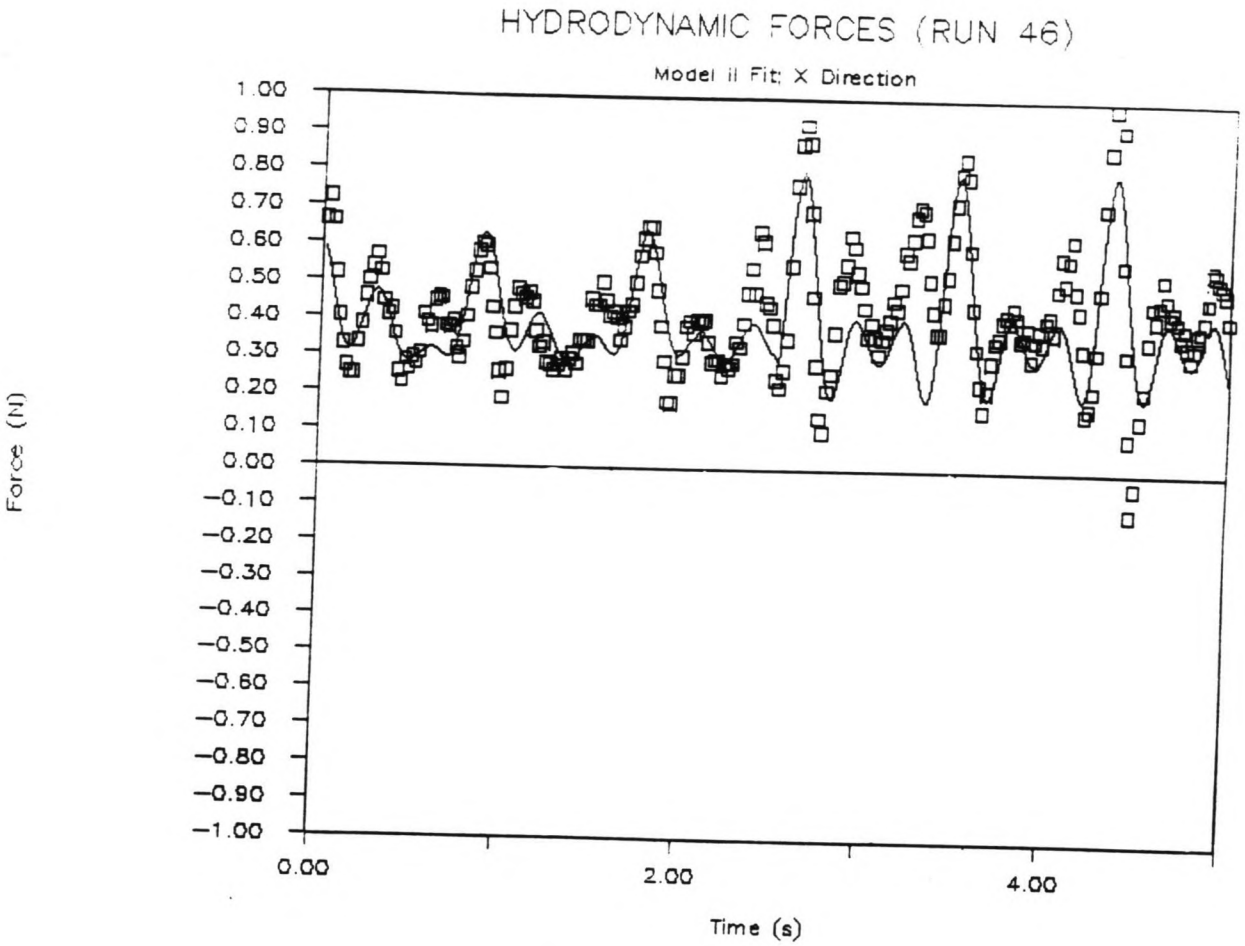

FIGURE 10.3.1

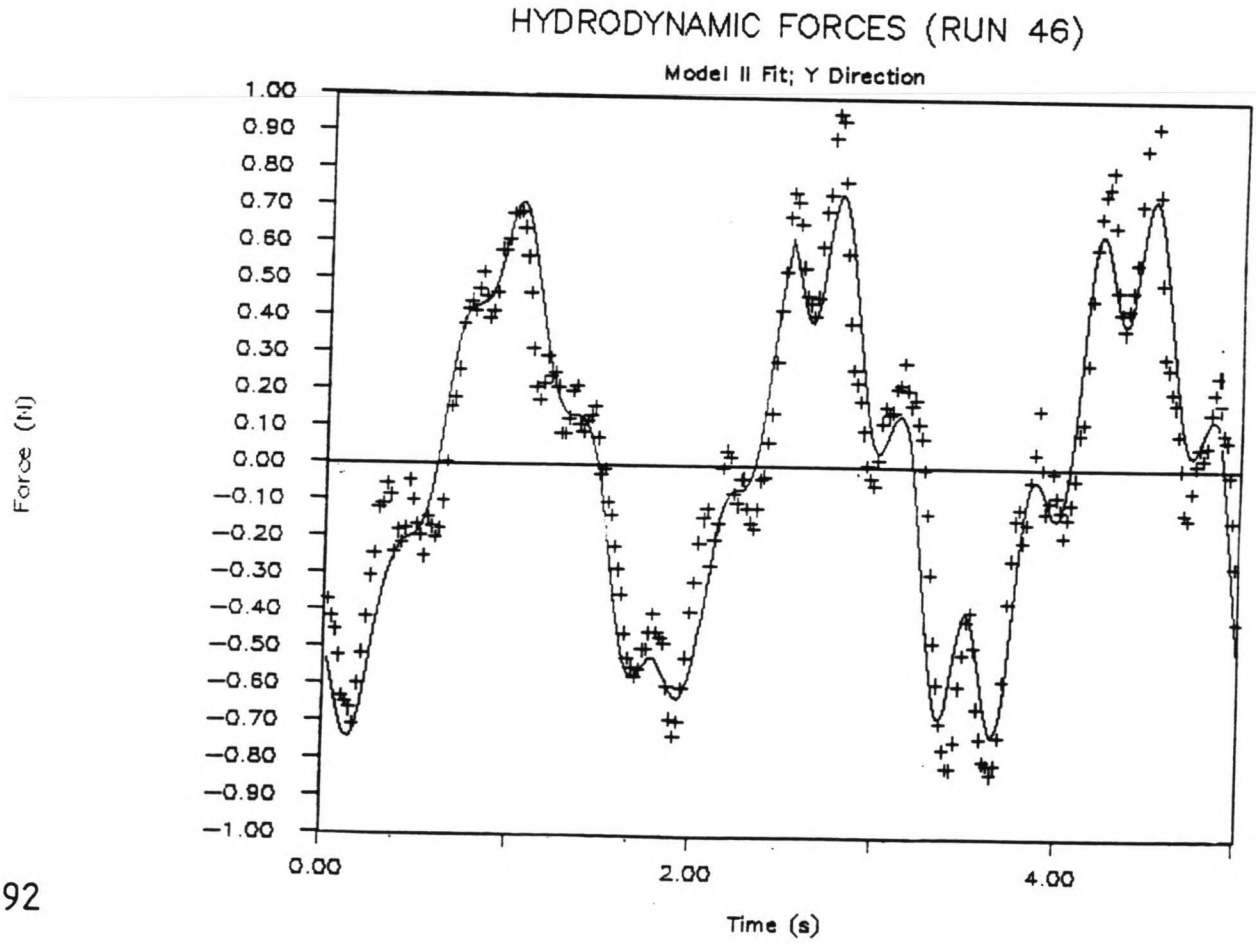

FIGURE 10.3.2

10.1.3 Spectral Analysis of Force Signals

The model spectra of run 46 are shown in the figures 10.4 and 10.5 (model I), and 10.6 and 10.7 (model II). Visual comparison confirms the conclusion that model I yields better results. The spectra of the other runs (mentioned in section 10.1.2) also indicate that model I is more accurate (figures in appendix G).

10.2 Interpretation of Model I Results

Using model I, the data analysis has been executed for all runs presented in chapter 7, figure 7.3.
In appendix G the output parameter values determined are presented in two forms:

- all parameters of all runs in a table like table 9.1;
- graphical versions of the results. In each graph one of the input parameters is kept at its standard value, the second is taken as the variable upon which one of the output parameters depends, and the third is given its minimum, standard and maximum value (see also section 7.3). Thus, for each output parameter are six graphs available.

From the graphical presentations the following (qualitative) observations can be made concerning:

- validity of the model (section 10.2.1);
- coefficient values (section 10.2.2),

as discussed below.

10.2.1 Validity of the Model

The criterium function values for the model forces in the x and the y direction give an indication of the validity of the theoretical model I. It appeared that:

for the X direction, a BETTER FIT is achieved for:

* an INCREASING stationary flow velocity V;
* an INCREASING oscillation period T;
* a DECREASING oscillation amplitude A.

for the Y direction, a BETTER FIT is achieved for:

* an INCREASING oscillation amplitude A.

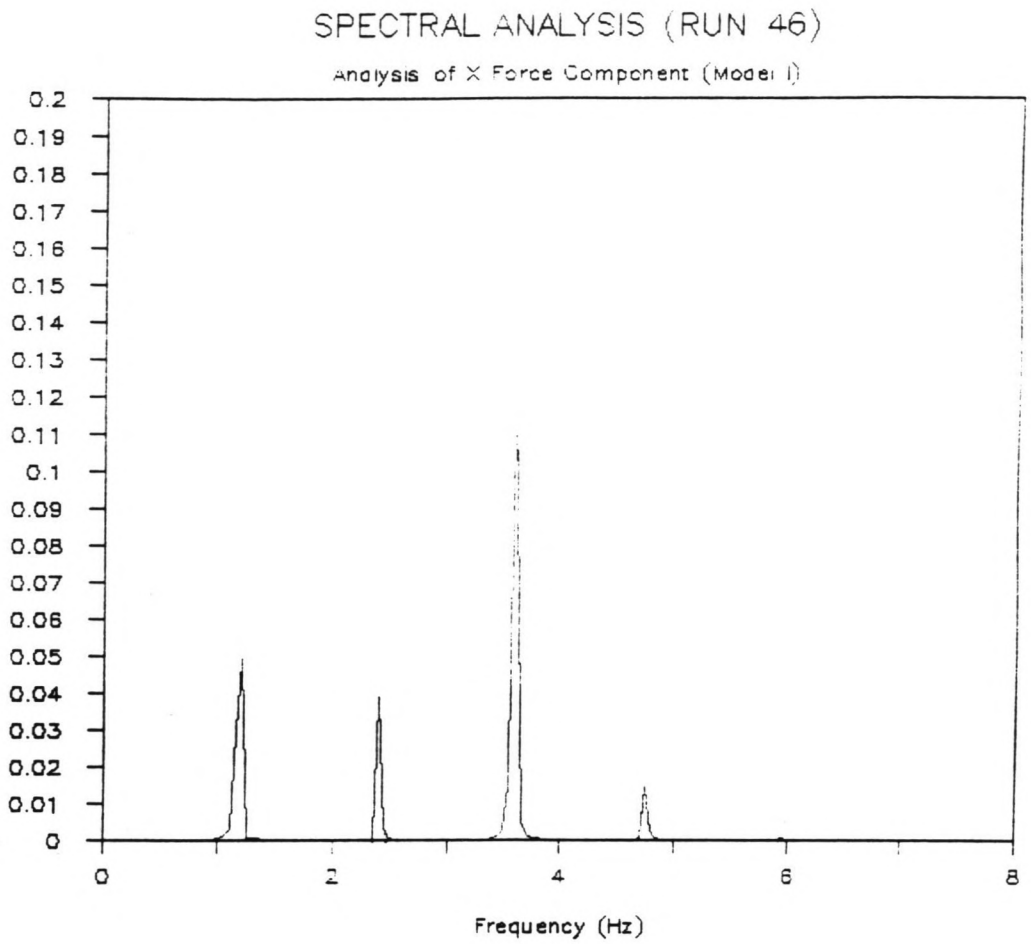

FIGURE 10.4.1

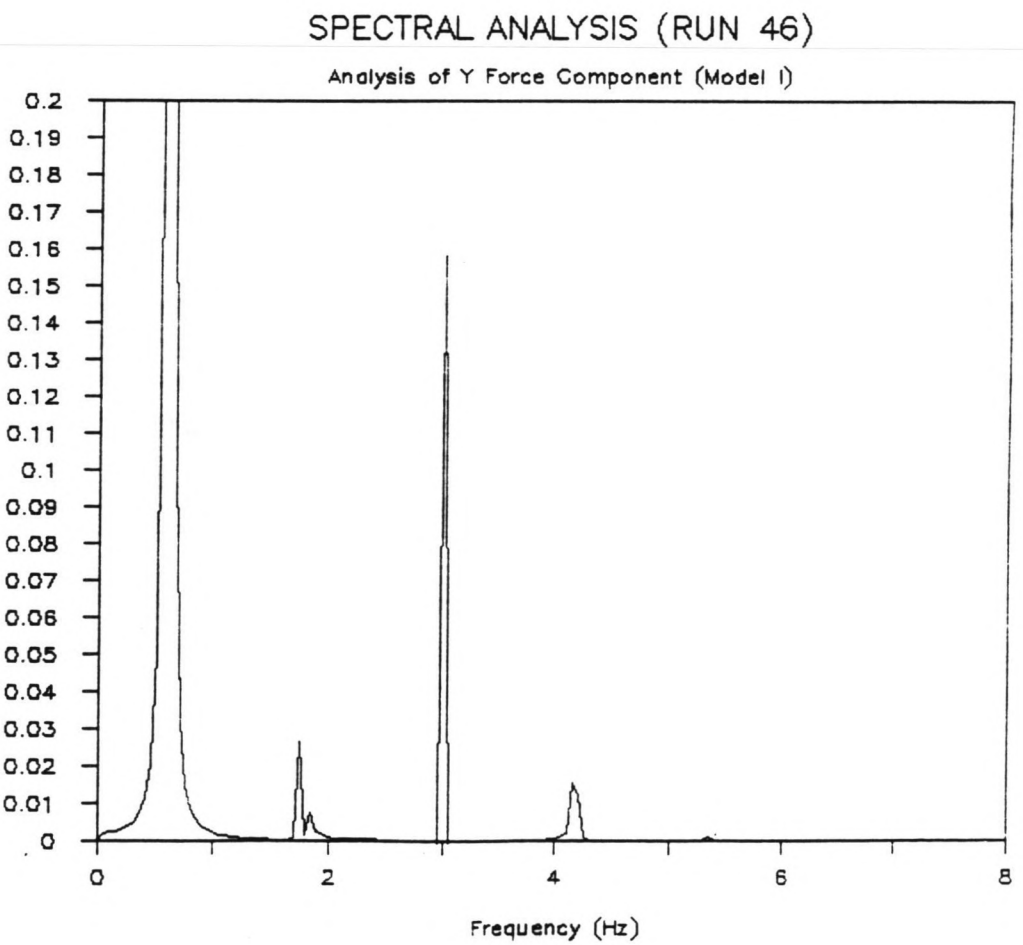

FIGURE 10.4.2

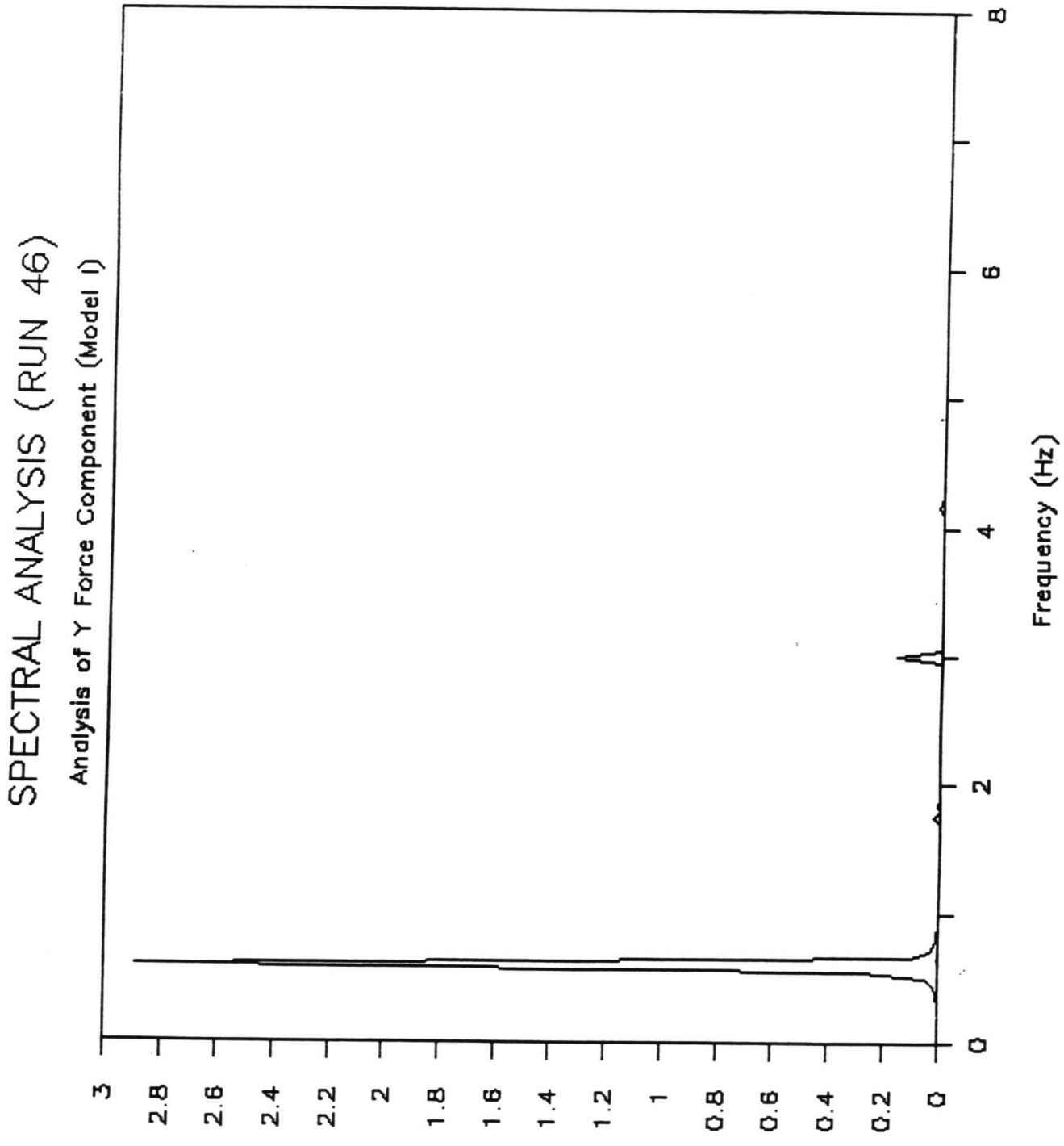
SPECTRAL ANALYSIS (RUN 46)
Analysis of Y Force Component (Model I)
3
2.8
2.6
2.4
2.2
2
1.8
1.6
1.4
1.2
1
0.8
0.6
0.4
0.2
0
0
2
4
6
8
Frequency (Hz)

FIGURE 10.5

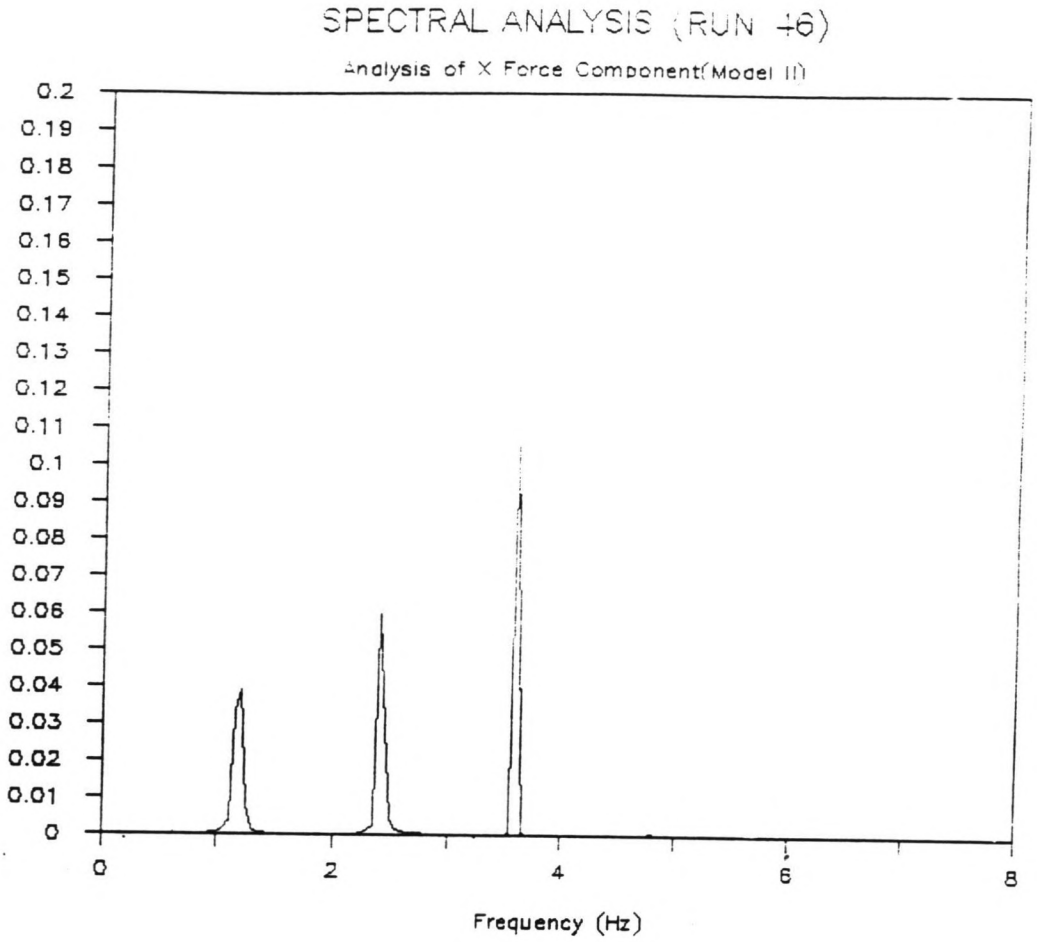

FIGURE 10.6.1

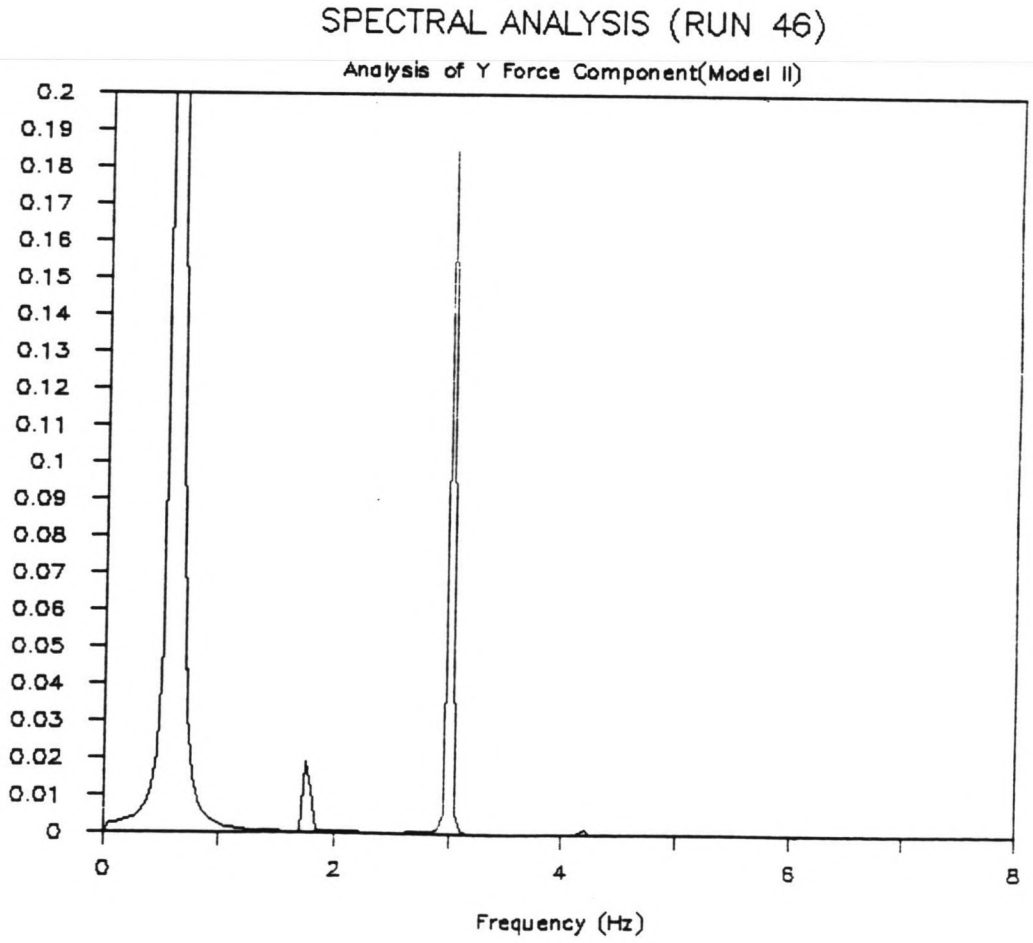

FIGURE 10.6.2

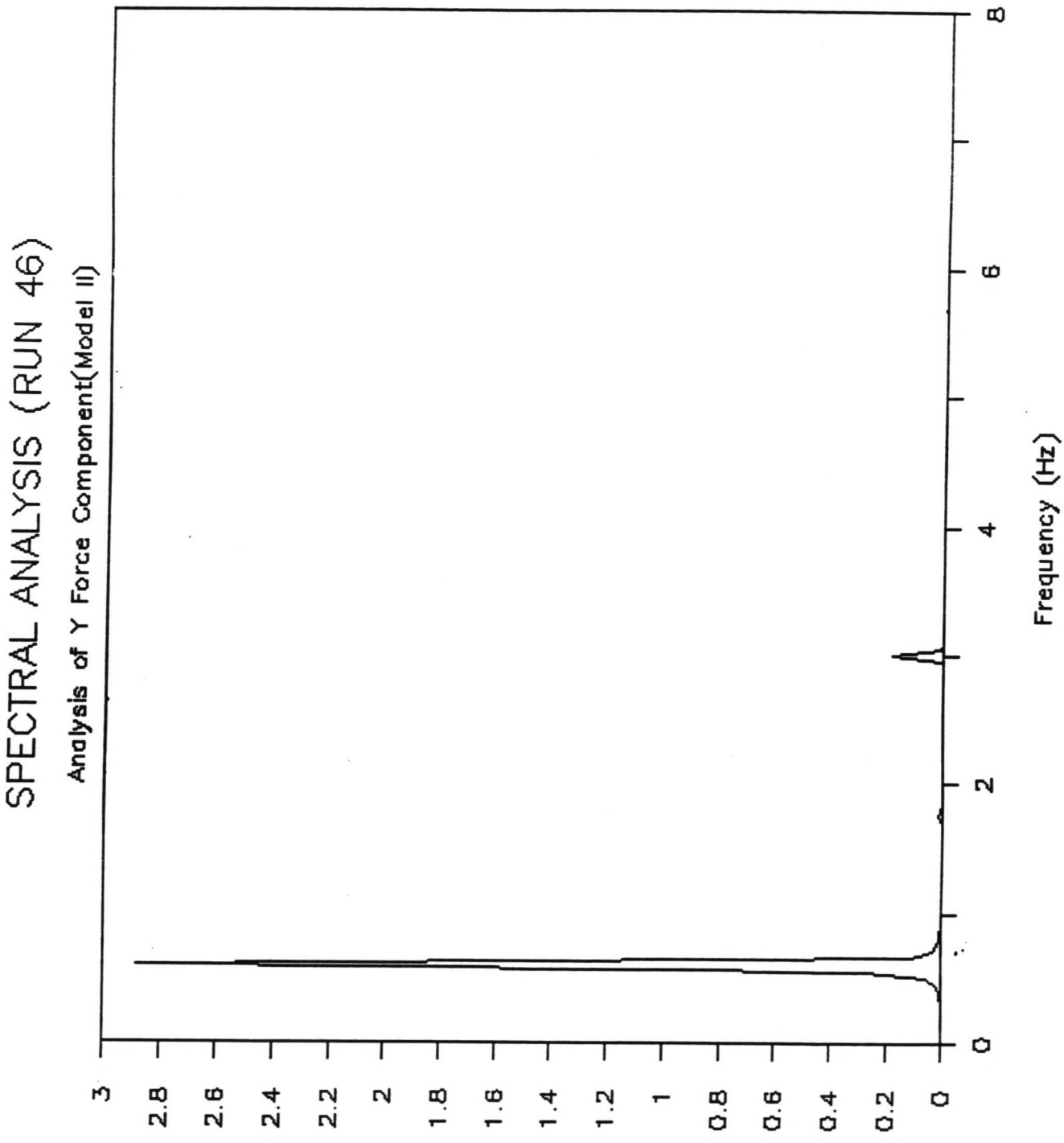
SPECTRAL ANALYSIS (RUN 46)
Analysis of Y Force Component(Model II)
3
2.8
2.6
2.4
2.2
2
1.8
1.6
1.4
1.2
1
0.8
0.6
0.4
0.2
0
0
2
4
6
8
Frequency (Hz)

FIGURE 10.7

This means for the x direction that the model fits better when the flow conditions are more nearly to a steady flow. For the y direction this effect is not that strong.

10.2.2 Coefficient Value Trends

For the Cd, Ca, Cl and St coefficients the following clear observations were made:

for the Cd coefficient:

* decreases when the stationary flow velocity V (> 0.50 m/s) increases;
* has a maximum value around V= 0.50 m/s (Re= 3.0E+4);
* not depending upon the oscillation amplitude A for higher oscillation periods T (T > 2.00 s).

for the Ca coefficient:

* increases when the stationary flow velocity V increases;

for the Cl coefficient:

* decreases when the stationary flow velocity V increases;
* increases for low oscillation periods T (T < 2.00 s) at low stationary flow velocities V (V < 0.75 m/s) or large oscillation amplitudes A (A/D > 2.00).

for the St coefficient:

* shows extremely low values for the combinations involving certain low stationary flow velocities V, large oscillation amplitudes A and short oscillation periods T.

10.3 Conclusions

- Comparing the values of the determined criterium functions of a number of runs, it appeared that for stationary flow conditions (runs 34, 36 and 37) both models give the same results (tables 10.1 and 10.2).

- For a stationary flow and an additional oscillation, model I describes the forces (much) more accurately than model II (figures 10.2 and 10.3). Also, the spectra of the forces calculated with model I look more like the spectra of the recorded forces than the spectra of model II (figures 10.4 to 10.7).

- It seems as if the error made by model I is in x direction depending upon A, V and T, but in Y direction only depending upon A (section 10.2.1).

- Both the Cd and the Ca coefficient depend primarily upon the stationary flow velocity V.

- The Cl value depends clearly upon all input parameters A, V and T, which indicates that the lift force amplitude formulation could be questioned.

- The Strouhal number shows for certain conditions extremely low values, indicating that the dependency of the vortex shedding frequency on the instantaneous velocity value in those conditions is not correct. However, even for those conditions, model I proves to be more accurate than model II (table 10.1 and 10.2).

11 GENERAL CONCLUSIONS

The following conclusions can be drawn from the study presented in this report concerning the hydrodynamic forces on slender cylinders oscillating transversely in a current:

- Vibrations of umbilical cables used to photograph the wreck of the Titanic have caused fatigue problems which have made the usable life of those cables unacceptably short.

- A literature study has revealed that little seems to be known about the hydrodynamic interaction of cylinders (cable segments) vibrating with large amplitudes in currents.

- The hydrodynamic forces model has been built up based upon literature information using a drag force component, an inertia force component and a lift force component.
  The drag and the inertia forces proved to be properly described by Morison's theory.
  The lift forces were described including a time varying vortex shedding frequency (analogous to the model of Verley [1982]); this was found to be more suitable than a constant frequency.
  The model is expected to describe the time domain hydrodynamic interaction of slender cylinders under a variety of flow conditions in the subcritical Reynolds regime.

- In the time domain this formulation includes five unknown coefficients:

  * Cd : drag coefficient;
  * Ca : inertia coefficient;
  * Cl : lift coefficient;
  * St : Strouhal number;
  * phi : lift force phase angle at the start of the record.

- The model has been verified by the comparison of measured and computed (model) forces. The measured forces came from a vertically mounted test cylinder that has been towed in still water with a constant velocity, while undergoing a forced oscillation transverse to the towing direction.

- The test cylinder used was able to measure (static) forces as low as 0.05 N in two perpendicular directions by means of four force transducers containing stain gages. The recorded signals of one transducer have been analysed.

- The experiments have included the following ranges of:

  * Reynolds Number Re:

    $3.0E+4 \leq Re \leq 9.0E+4 \quad (0.50 \leq V \leq 1.50 \text{ m/s})$;

  * Keulegan Carpenter Number KC:

    $12.3 \leq KC \leq 31.4 \quad (2.00 \leq A/D \leq 5.00)$;

  * Oscillation Period T:

    $1.50 \leq T \leq 3.00$ s.

  Lock in conditions were not included because of equipment limitations.

- An efficient procedure for determining the coefficients needed (Cd, Ca, Cl, St, phi) has been developed for the processing of the recorded force signals. The analysis was performed in three steps:
  First, the optimum Cd and Ca values were found, considering the high frequency lift force as "noise". Then the Cd and Ca force components were subtracted from the recorded signal.
  Next, for the remaining (lift) force signal the optimum St and phi values were determined, using an approximation of the Cl value.
  Finally, the optimum Cl value was determined using all four earlier determined coefficients.

- The measured lift forces showed so-called "beats"; this has been observed for both the steady flow conditions and the remaining (non stationary) experiments. Therefore, for a better reproduction of the measured force signals the recorded signal had to be segmented. Average values for the coefficients for one complete test run have been determined this way.

- The coefficient values found for degenerate cases like a stationary flow (Cd and St) or oscillatory flow (Cd and Ca) can be associated with already well known values, although the St values found (around 0.18) stay under the generally accepted value of 0.20.
  Most of the Cd, Ca and St coefficient values found for the other experiments were surprisingly close to those found by others (even though their flow conditions were different). This implies that currently accepted values of these coefficients can be used for the range of variables tested here as well.

- The model descibes the forces in the towing direction better for flow conditions close to a stationary flow. In the transverse direction this tendency is less strong.

- The lift force AMPLITUDE description contains a Cl coefficient that depends upon all input parameters and is by no means a constant value. Thus, a better description is needed for the lift force amplitude.

- For certain combinations of towing velocity, oscillation amplitude and period, the St values found in the analysis were extremely low (0.13), indicating that the lift force FREQUENCY description is not correct. The time varying lift force frequency description still appears to be more accurate than a constant lift force frequency, however.

- The residual error that indicated the accuracy of the model, appeared for some runs to be two orders of magnitude larger than for other runs. Generally, larger residual errors were associated with lower force situations; such errors are often attributed to instrumental noise.

12 FURTHER INVESTIGATIONS

The results from this study indicate that a lot of items are still there to be investigated. Regarding model I, the following aspects deserve further attention:

- Lift force description

  The results of the present study indicate that the dependency of the lift force amplitude upon the square of the velocity term can be questioned, since the determined Cl coefficients depended upon all input parameters.
  Also, for certain combinations of towing velocity, oscillation amplitude and period, the St values found in the analysis were low, indicating that the lift force frequency is overestimated here when using a constant St value.

- Cd and Ca coefficients

  The Cd and (surprisingly) the Ca coefficient appeared to be dependent upon the stationary flow velocity in the experiments carried out.

- Correlation between the (lift) forces along the cylinder axis.

  Axial correlation of lift forces is of major importance when simulating the dynamic behaviour of a series of finite elements of a slender cylinder. It is possibly solved by the model itself. Inserting an initial random phase in the lift force component for each element at the beginning of the simulation might give adequate results.

- Validity of the lift force description for higher cylinder oscillation frequencies than tested in the present study.

- Influence of the cylinder axis orientation

  The buoyancy and/or gravity should be included when the cylinder axis is not vertically orientated.
  Also, the effect on the hydrodynamic forces of the orientation of the cylinder axis with respect to the surrounding flow needs to be investigated.

- Possible relationship between the inter-segment phase shifts which were introduced when analysing the experimental time records.

  If there is any resemblance between them, then the model could perhaps be modified.

- Computer simulation of various flow conditions and cylinder geometries.

  With NOSDA (Non-linear Offshore Structure Dynamic Analyser; see Liu, P. and Massie, W.W., 1988), the (hydrodynamic) forces working on a series of finite elements of a cylinder and their response can be simulated in the time domain. The following questions could perhaps be answered afterwards:

  * How well does the developed model I describe the hydrodynamic forces when it is used in a more general relative motion situation?

  * Is it possible to simulate the lock-in phenomenon with the model developed?

  * A maximum amplitude of 1.5 cylinder diameters is mentioned in the literature for lock-in vibrations. Is this limit caused by equipment limitations or can it be explained hydrodynamically using model I?

APPENDIX A: NOTATIONS

APPENDIX A: NOTATIONS

.._i	subscript i (in text)	
A_..	coefficient	(-)
A	amplitude	(m)
B_..	coefficient	(-)
Ca	= C_A inertia force coefficient	(-)
Cd	= C_D drag force coefficient	(-)
Ci	= C_I = (1+Ca)	(-)
Cl	= C_L lift force coefficient	(-)
D	cylinder diameter	(m)
F	force	(N)
Fd	= F_D drag force	(N)
Fi	= F_I inertia force	(N)
Fl	= F_L lift force	(N)
Fp	= F_p pressure force	(N)
H	height	(m)
KC	Keulegan Carpenter Number	(-)
M	mass per unit length	(kg m^-1)
Re	Reynolds Number	(-)
Sc	Scruton Number	(-)
St	Strouhal Number	(-)
T	= T_o oscillation period	(s)
V	velocity	(m s^-1)
Vcur	= current velocity	(m s^-1)
Vt	= towing velocity	(m s^-1)
a	instantaneous acceleration direction	
dF	force	(N)
ds	cylinder element length	(m)
dz	cylinder element length	(m)
e	2.718	
f_e	excitation frequency	(Hz)
f_n	natural frequency	(Hz)
f_o	oscillation frequency	(Hz)
f_..	force in .. (x,y,r,n) direction	(N)
g	gravity constant (=9.81)	(m s^-2)
k	calibration factor	(m N^-1)
m	mass	(kg)
m	(subscript) model or mass	
max	(subscript) maximum value	
n	direction perpendicular to instantaneous velocity direction	
n	constant	
o	(subscript) oscillation	
p	(subscript) prototype	
t	time	(s)
r	instantaneous velocity direction	
v	(subscript) vortex shedding	
x	towing direction or stationary flow direction	
y	direction perpendicular to x	
β	= Re/KC	(-)
δ	damping ratio	
ν	viscosity (= 1.0 E-6)	(m^2 s^1)
π	3.1415	
ρ	density (of water: 1000)	(kg m^-3)
Φ, α, γ, ε	angle	(-)
ψ, φ	(phase) angle	(rad)
ω	angular frequency	(rad s^-1)
0	(zero) (subscript) starting value	

APPENDIX B: REFERENCES

APPENDIX B: REFERENCES

Alonso, M. and Finn, E.J.; Fundamental University Phisics; 1983; p. 288.

Bearman, P.W., Graham, J.M.R., Obasaju, E.D.; A Model Equation for the Transverse Forces on Cylinders in Oscillatory Flows; Applied Ocean Research, vol. 6, no. 3, 1984.

Berger, E.; On a Mechanism of Vortex Excited Oscillations of a Cylinder; Journal of Wind Engineering and Industrial Aerodynamics, vol. 28, no. 1, August 1988, p. 301-310.

Bernitsas, M.M.; Analysis of the Hydrodynamic Forces Exerted on a Harmonically Oscillating Circular Cylinder in any Direction Φ with respect to a Uniform Current; BOSS '79.

Bublitz, P.; The Periodic Normal Force on a Circular Cylinder in Cross-Flow - an Unsteady Magnus Effect; Z. Flugwiss. & Weltraumforsch., vol. 7, no. 4, July-August 1983, p. 253-262.

Chakrabarti, S.K.; Wave forces coefficients for rough vertical cylinders;Journal of Waterway, Port, Coastal and Ocean Division, ASCE, vol. 108, November 1982.

Chakrabarti, S.K.; Hydrodynamics of Offshore Structures, 1987, Chapter 6: Wave Forces on Small Structures.

Cohen, R.D., Walker, W.F.; Modeling the Boundary Layer Behaviour During Vortex Shedding; International Journal of Engineering Fluid Mechanics, vol. 2, no. 4, 1989, p. 331-342.

Dawson, T.H.; In-Line Forces on Vertical Cylinders in Deepwater Waves; ASME Journal of Energy Resourses Technology, vol. 107, no. 1, March 1985, p. 18-23.

Ericsson, L.E.; Karman Vortex Shedding and the Effect of Body Motion; AIAA Journal, vol. 18, no. 8, August 1980, p. 935-944.

Every, M.J., King, R., Griffin, O.M.; Hydrodynamic Loads on Flexible Marine Structures due to Vortex Shedding; Transactions of the ASME, Journal of Pressure Vessel Technology, vol. 104, December 1982, p. 330-336.

Fleischmann, S.T.; A Study of Flow-Induced Vibrations on Cylinders; Ocean Engineering, vol. 15, no. 3, 1988, p. 249-259.

Griffin, O.M.; Vortex-Excited Cross-Flow Vibrations of a Single Cylindrical Tube; Transactions of the ASME, Journal of Pressure Vessel Technology, vol. 102, May 1980, p. 158-166.

Iwagaki, Y., Asano, T., Nagai, F.; Hydrodynamic Forces on a Circular Cylinder Placed in Wave-Current Co-existing Fields; Memoires of the Faculty of Engineering, Kyoto University, Japan, vol. XLV, no. 1, January 1983, p. 11-23.

Kato, M., Abe, T., Tamiya, M., Kumakiri, K.; Drag Forces on Oscillating Cylinders in a Uniform Flow; ASME Journal of Energy Resourses Technology, vol. 107, no. 1, March 1985, p. 12-17.

Komatsu, S., Kobayashi, H.; Vortex-Induced Oscillation of Bluff Cylinders; Journal of Wind Engineering and Industrial Aerodynamics; vol. 6, 1980, p.335-362.

Liu, P. and Massie, W.W.; NOSDA - Nonlinear Dynamic Analysis Program for Offshore Structures; Research Report, Civil Engineering Faculty, Workgroup Offshore Technology, Delft University of Technology, 1988.

Low, H.T., Chew, Y.T., Tan, K.T.; Fluid Forces on a Cylinder Oscillating In Line with a Uniform Flow; Ocean Engineering, vol. 16, no. 3, 1989, p. 307-318.

Madsen, O.S.; Hydrodynamic Force on Circular Cylinders; Applied Ocean Research, vol. 8, no. 3, 1986, p. 151-155.

McConnell, K.G., Park, Y.S.; The Response and the Lift Force Analysis of an Elastically-Mounted Cylinder Oscillating in Still Water; Hemisphere Publishing Corp., Washington, U.S.A., vol. 2, Paper PH3.6, 1983, p. 671-680.

Moeller, M.J., Leehey, P.; Measurement of Fluctuating Forces on an Oscillating Cylinder in a Cross Flow; Hemisphere Publishing Corp., Washington, U.S.A., vol. 2, Paper PH3.6, 1983, p. 681-689.

Obasaju, E.D., Bearman, P.W., Graham, J.M.R.; A Study of Forces, Circulation and Vortex Patterns around a Circular Cylinder in Oscillating Flow; Journal of Fluid Mechanics, vol. 196, November 1988, p. 467-494.

Ruscheweyh, H.; Vortex-Excited Vibratios of Yawed Cantilevered Circular Cylinders with Different Scruton Numbers; Journal of Wind Engineering and Industrial Aerodynamics, vol. 23, no. 1-3, July 1986, p. 419-426.

Sarpkaya, T.; In-Line and Transverse Forces on Cylinders in Oscillating Flow at High Reynolds' Numbers; Proceedings of the Eighth Offshore Technology Conference, Houston, Texas, OTC Paper 2533, 1976, p. 95-108.

Thumann, V.M.; Eindverslag IO87: leren omgaan met vakwetenschappelijke informatie; (Literatuuronderzoek ten behoeve van het afstudeerwerk: "Hydrodynamic Forces on Slender Cylinders"); Delft, June 1990. (Dutch language).

Vandiver, J.K., Jong, J.-Y; The Relationship between In-Line and Cross-Flow Vortex-Induced Vibration of Cylinders; Journal of Fluids and Structures, vol. 1, no. 4, 1987, p.381-399.

Verley, R.L.P.; A Simple Model of Vortex-induced Forces in Waves and Oscillating Currents; Applied Ocean Research, vol. 4, no. 2, 1982, p. 117-120.

Verley, R.L.P., Johns, D.J.; Oscillations of Cylinders in Waves and Currents; Hemisphere Publishing Corp., Washington, U.S.A., vol. 2, Paper PH3.6, 1983, p. 690-701.

Williamson, C.H.K., Roshko, A.; Vortex Formation in the Wake of an Oscillating Cylinder; Journal of Fluids and Structures, vol. 2, no. 4, July 1988, p. 355-381.

APPENDIX C: TEST CYLINDER CALIBRATION

APPENDIX C: TEST CYLINDER CALIBRATION

C1 Calibration Factor Determination (data figures, tables and graphs in section C3)

The experiments described here have been executed on the test cylinder with and without a rubber skin; the rubber skin has been put on the day before the tests on the cylinder with skin were executed. For one orientation (IV) the significance of the time effect on the rubber skin was examined (see section 6.3.2); therefore measurements of this orientation have also been done shortly after the skin was put on.

In order to obtain the relationship between the electric signal and the exciting force, the cylinder has been mounted horizontally. All three transducers that are going to be used have been loaded vertically, each for four different orientations (fig.C1.1), by weights associated with masses of 0.1 kg from 0.0 kg up to 1.2 kg.
It has been tried to rotate the cylinder around its axis so that for each orientation only one, the x- or y-, direction of the force transducers was loaded. Of course, this is almost an impossible thing to do, and therefore the signals of both x- and y- direction have been registered in order to make corrections if necessary.
A linear regression on the data of two orientations (the second orientation is the one with the x and y axis rotated over 180 degrees) yields an average calibration factor for the loading direction (table C1 and C4).
The assumption is made that the x- and y- axis in each transducer are perpendicular to each other.
The calibration factor derived from orientation III and IV was used to determine the maximum force perpendicular to the loading direction when the cylinder had been given the orientation I and II, and vice versa. With this force and the maximum force in loading direction the rotation around the cylinder axis of each transducer could be determined quite accurately (table C2, C5 and figure C1.2). With this rotation a correction on the calibration factors could be made (table C3 and C6).
Also, an average value for the relative rotations between the transducers can be determined now, since for each orientation the difference in rotation of two transducers should be the same.

C2 Ring Mass Determination (table in section C3)

During the experiments a reference signal RFINF(t) that followed the oscillatory motion of the cylinder was recorded (see also section 7.1). The amplitude of this reference signal had the value 1.000, which means that the difference between force signal and reference signal is a factor $-A \bullet (2 \bullet \pi / T)^2$ at any time (equations I and II). The ring masses can be determined now according to equation III, or for discontinuous (digital)

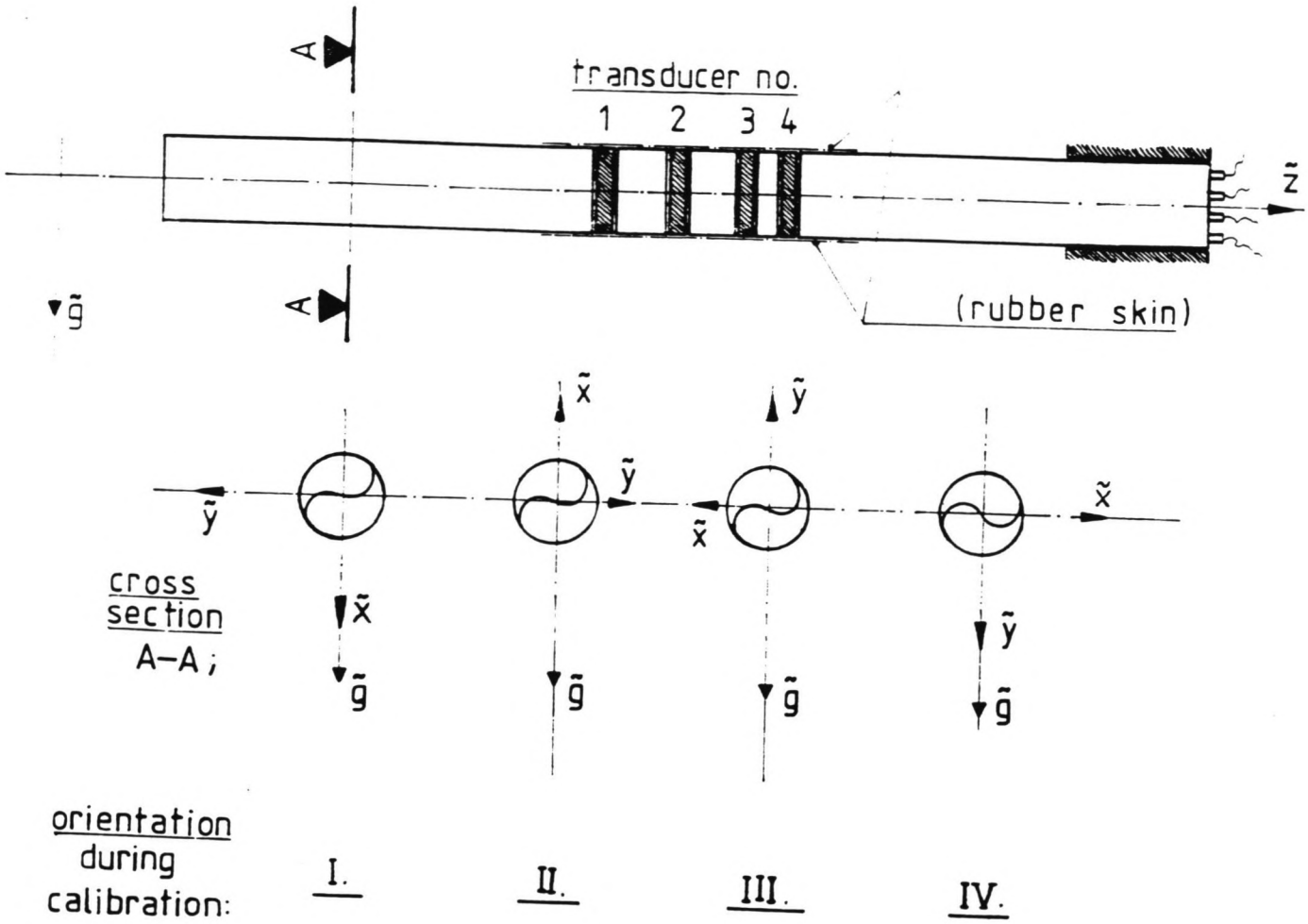

FIGURE C1.1

FIGURE C1.2

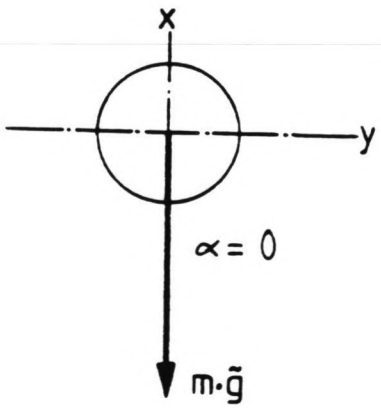

GIVEN: $\varepsilon_{x_o max}$, $\varepsilon_{y_o max}$ } for each loading direction (orientation)

k_{x_o}, k_{y_o} } from: $\varepsilon_{....} = k_{....} \cdot F_{....}$; $F_{....} = m \cdot \tilde{g}$; $\alpha = 0$

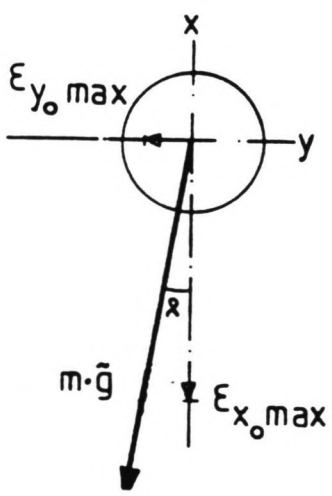

$$1 / F_{y_o max} \simeq k_{y_o} / \varepsilon_{y_o max}$$

$$\alpha = \arcsin(F_{y_o max} / mg)$$

$$k_x = k_{x_o} / \cos \alpha$$

recorded signals according to equation IV.

$$a(t) = -\left(\frac{2\cdot\pi}{T}\right)^2 \cdot A \cdot \sin\left(\frac{2\cdot\pi}{T}\cdot t\right) \qquad \text{(I)}$$

$$RFINF(t) = \sin\left(\frac{2\cdot\pi}{T}\cdot t\right) \qquad \text{(II)}$$

$$mass_{ring} = \frac{F(t)}{a(t)} = \frac{F(t)}{-\left(\frac{2\cdot\pi}{T}\right)^2 \cdot A \cdot RFINF(t)} \qquad \text{(III)}$$

$$mass_{ring} = \frac{\sum \| F(t_i) \|}{\sum \| \left(\frac{2\cdot\pi}{T}\right)^2 \cdot A \cdot RFINF(t_i) \|} \quad ; \quad i = 1(1)n \qquad \text{(IV)}$$

The masses have been determined by averaging the values obtained from the analysis (using the program RINGMASS; see appendix F) of three runs (table C7).
Figure C2.1 shows the measured forces and two curves: one represents the reference signal and the other represents the calculated force signal using the determined ring mass.

FIGURE C2.1

RING MASS DETERMINATION
Ring 2; m = .04073 kg
ref. signal
0.10
0.09
0.08
0.07
0.06
0.05
0.04
0.03
0.02
0.01
0.00
−0.01
−0.02
−0.03
−0.04
−0.05
−0.06
−0.07
−0.08
−0.09
−0.10
0.00
2.00
4.00
Time (s)
+ measured forces
Force Y Direction (N)

C3 Data Figures, Tables and Graphs

Table of Contents

k values: (1E-6 V/V/N)					max. strain: (5E-7 V/V)		
1	X I :	16.862			1	I Y :	-12.2
	X II :	16.958	I+II :	16.910		II Y :	4.1
	Y III :	15.414			*)	III X :	0.0
	Y IV :	15.649	III+IV :	15.532		IV X :	5.1
2	X I :	16.447			2	I Y :	-7.2
	X II :	16.426	I+II :	16.436		II Y :	3.5
	Y III :	15.227				III X :	-15.0
	Y IV :	15.499	III+IV :	15.363		IV X :	15.3
3	X I :	14.173			3	I Y :	-17.4
	X II :	14.220	I+II :	14.197		II Y :	11.4
	Y III :	14.755				III X :	-14.0
	Y IV :	14.799	III+IV :	14.777		IV X :	18.3

*) very poor relationship between strains measured

(table C1)

rotation: (rad)		
I	1	-0.0334
	2	-0.0199
	3	-0.0500
II	1	0.0112
	2	0.0097
	3	0.0328
III	1	0.0000
	2	-0.0388
	3	-0.0419
IV	1	0.0128
	2	0.0395
	3	0.0548

(table C2)

k values: (1E-6 V/V/N)				
1	X I :	16.871		
	X II :	16.959	I+II :	16.915
	Y III :	15.414		
	Y IV :	15.651	III+IV :	15.532
2	X I :	16.450		
	X II :	16.426	I+II :	16.438
	Y III :	15.239		
	Y IV :	15.511	III+IV :	15.375
3	X I :	14.191		
	X II :	14.227	I+II :	14.209
	Y III :	14.767		
	Y IV :	14.822	III+IV :	14.795

(table C3)

k values: (1E-6 V/V/N)					max. strain: (5E-7 V/V)		
1	X I :	16.102			1*) I Y :		0.0
	X II :	15.831	I+II :	15.966	*) II Y :		0.0
	Y III :	14.460			*) III X :		0.0
	Y IV :	15.230	III+IV :	14.845	IV X :		-6.8
2	X I :	15.743			2*) I Y :		0.0
	X II :	15.755	I+II :	15.749	II Y :		-2.3
	Y III :	14.320			III X :		-15.4
	Y IV :	14.251	III+IV :	14.285	*) IV X :		0.0
3	X I :	13.596			3*) I Y :		0.0
	X II :	13.928	I+II :	13.762	II Y :		11.1
	Y III :	13.863			III X :		-11.8
	Y IV :	14.037	III+IV :	13.950	IV X :		8.2

*) very poor relationship between strains measured

(table C4)

rotation: (rad)		
I	1	0.0000
	2	0.0000
	3	0.0000
II	1	0.0000
	2	-0.0068
	3	0.0338
III	1	0.0000
	2	-0.0415
	3	-0.0364
IV	1	-0.0181
	2	0.0000
	3	0.0253

(table C5)

k values: (1E-6 V/V/N)				
1	X I :	16.102		
	X II :	15.831	I+II :	15.966
	Y III :	14.460		
	Y IV :	15.232	III+IV :	14.846
2	X I :	15.743		
	X II :	15.755	I+II :	15.749
	Y III :	14.332		
	Y IV :	14.251	III+IV :	14.292
3	X I :	13.596		
	X II :	13.936	I+II :	13.766
	Y III :	13.872		
	Y IV :	14.042	III+IV :	13.957

(table C6)

run: (no.)	ring: (no.)	mass: (1E-3 kg)	ring: (no.)	mass: (1E-3 kg)	ring: (no.)	mass: (1E-3 kg)
18	1	40.78	2	41.07	3	42.65
20	1	40.08	2	40.43	3	42.13
23	1	39.93	2	40.70	3	42.39
average:	1	40.26	2	40.73	3	42.39

(table C7)

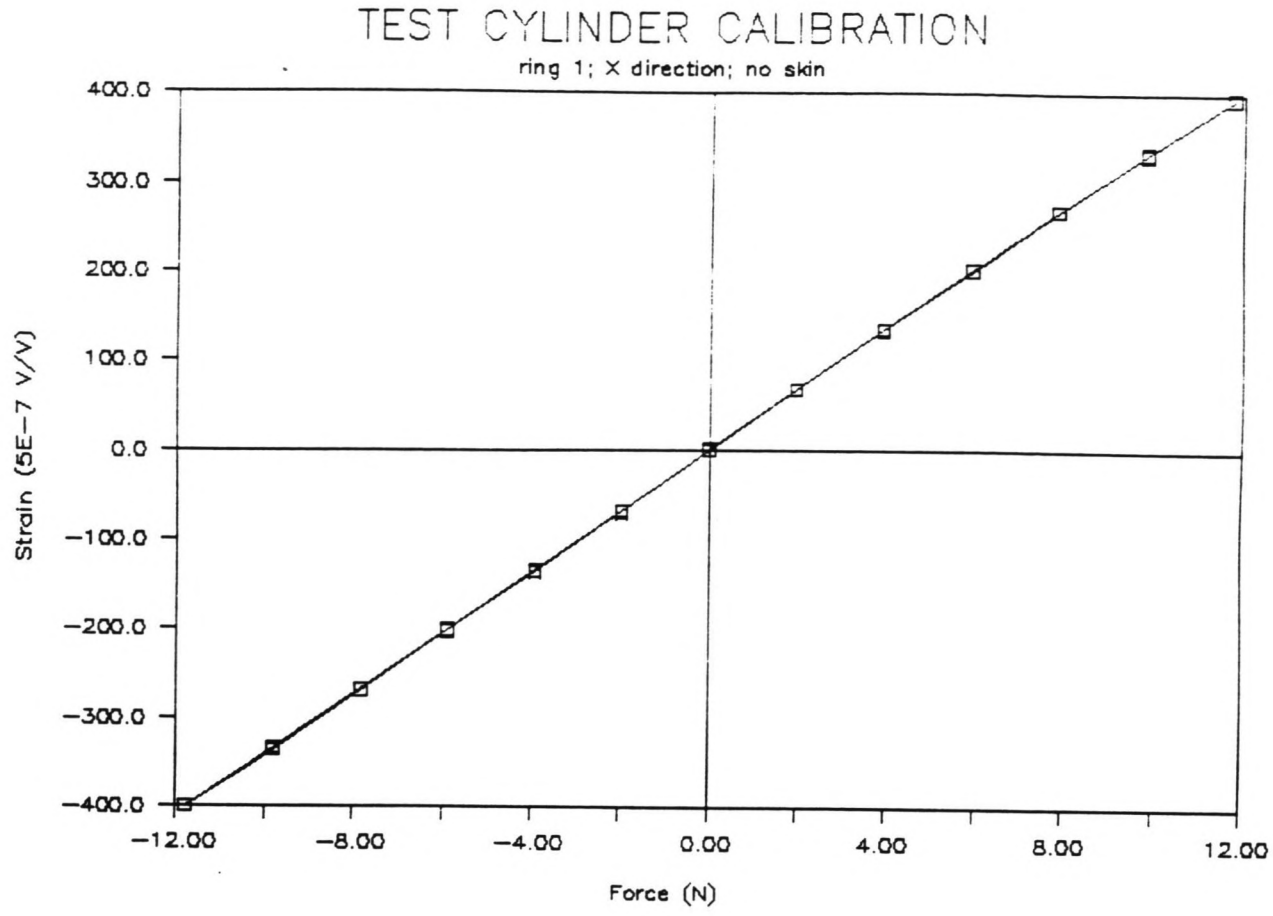

FIGURE C3.1.1

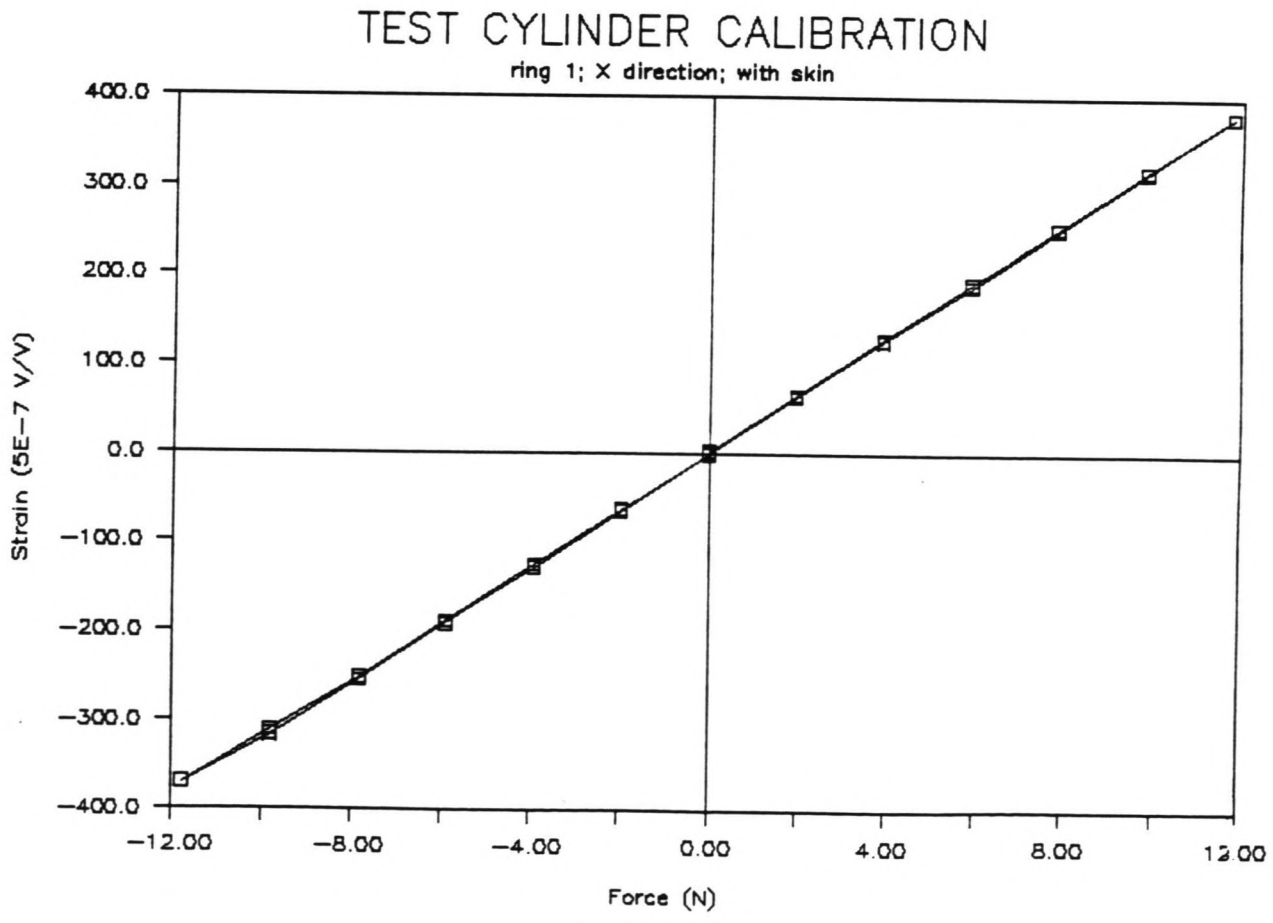

FIGURE C3.1.2

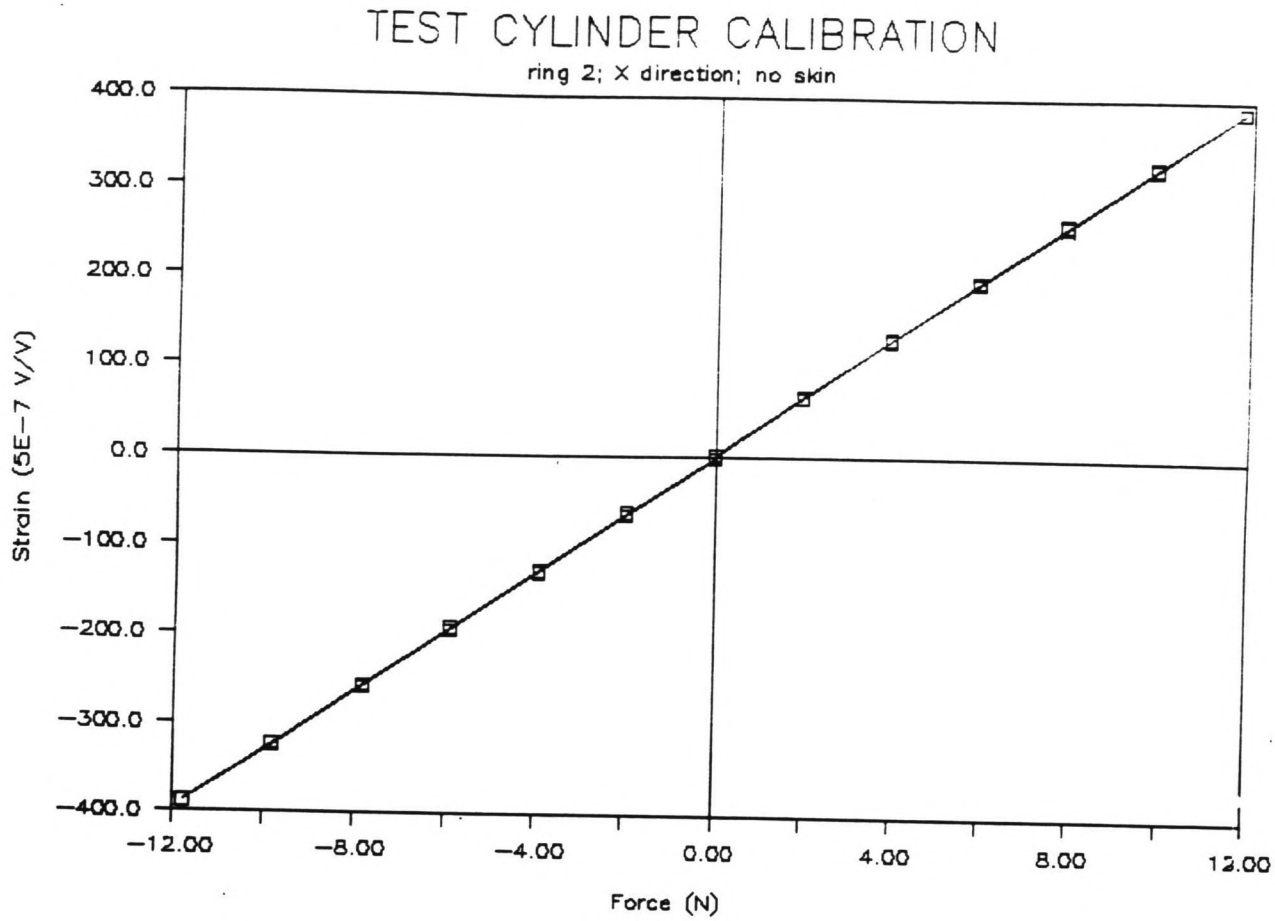

FIGURE C3.2.1

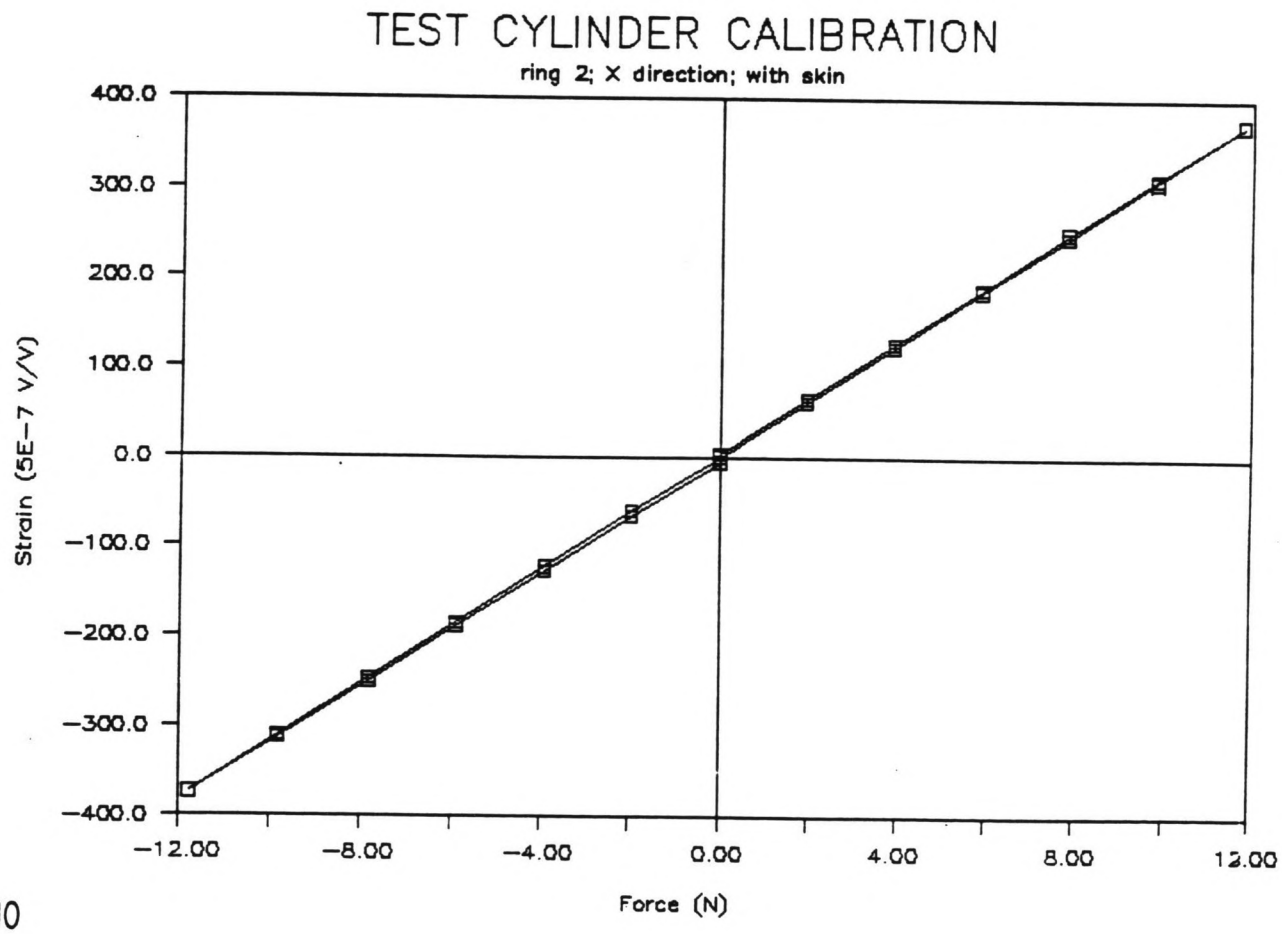

FIGURE C3.2.2

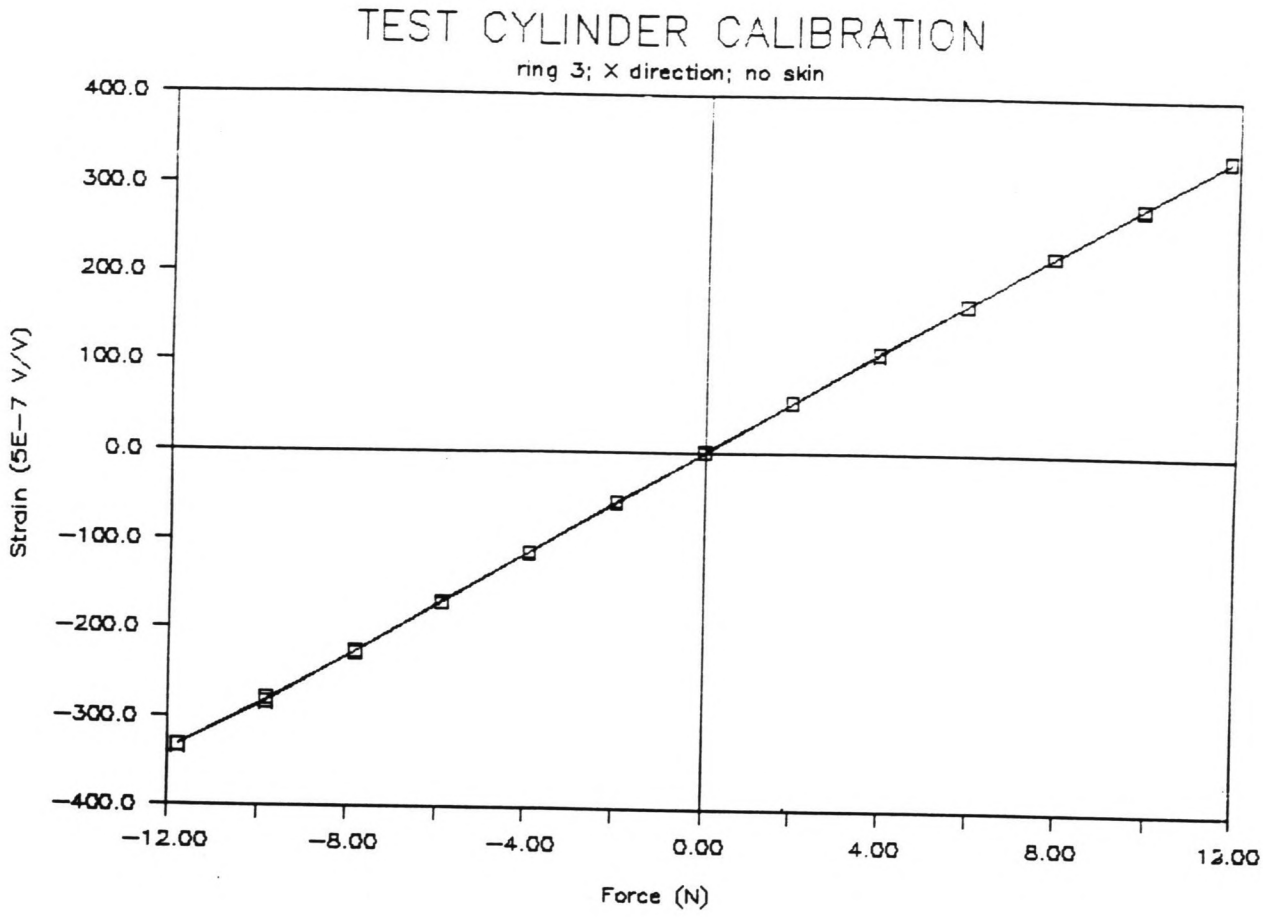

FIGURE C3.3.1

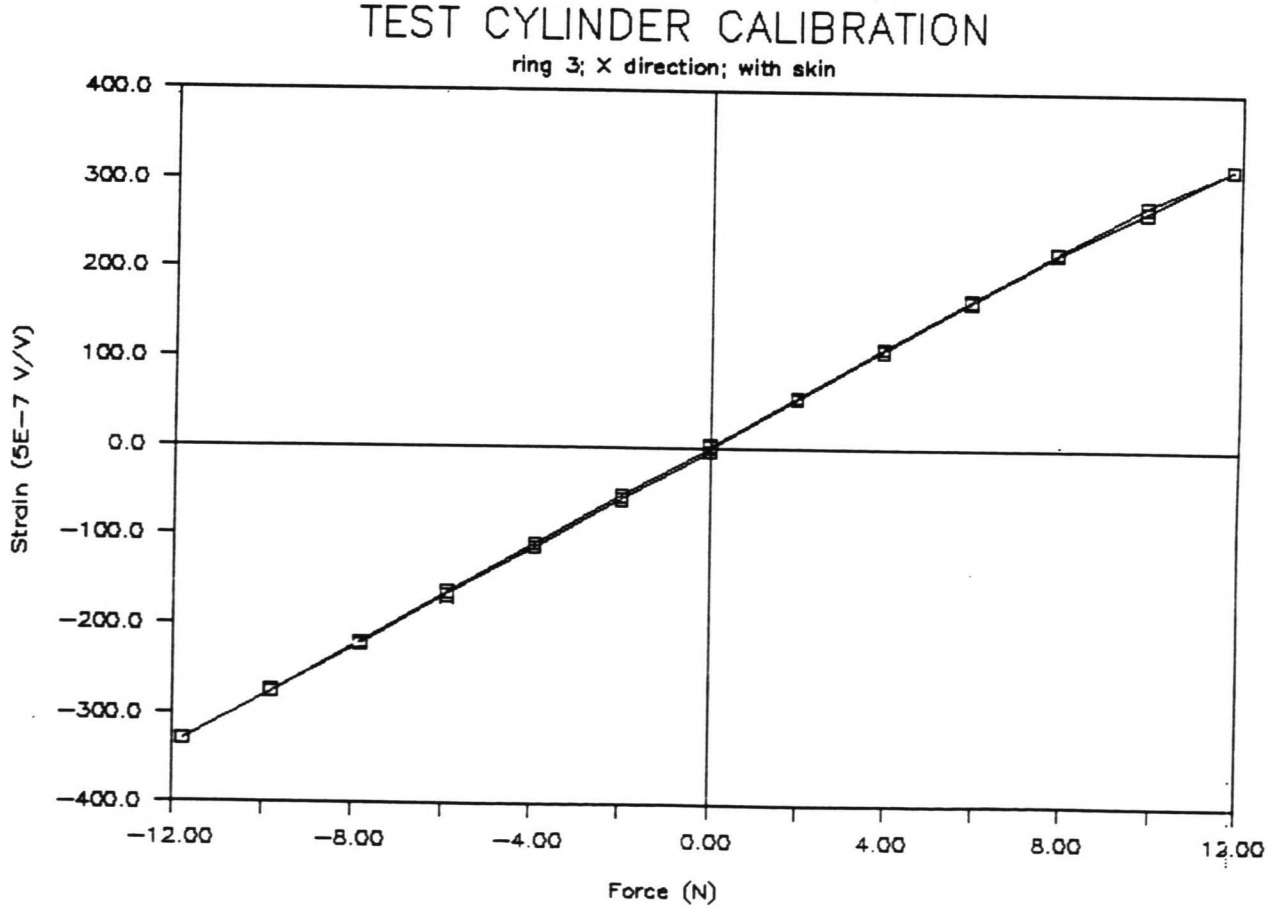

FIGURE C3.3.2

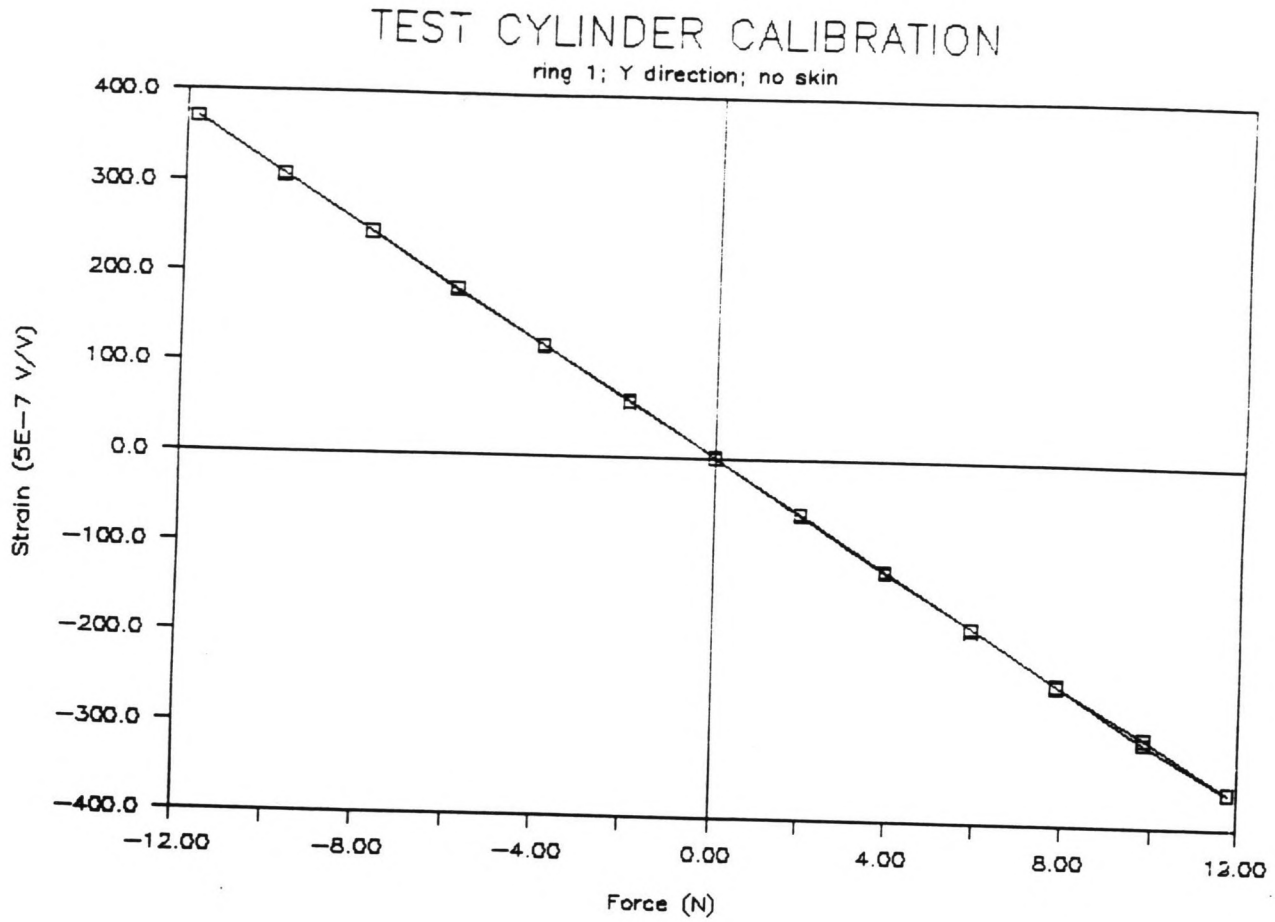

FIGURE C3.4.1

FIGURE C3.4.2

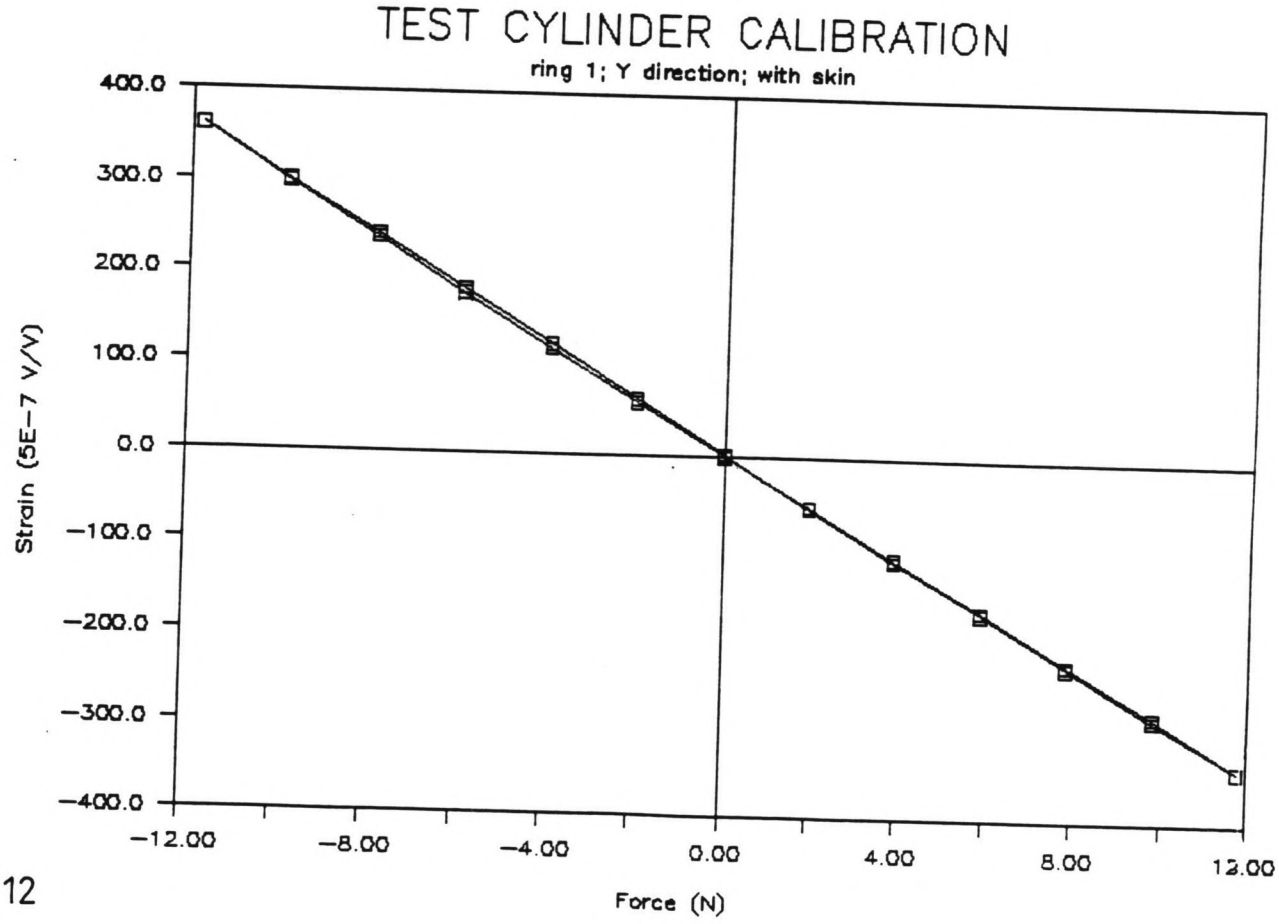

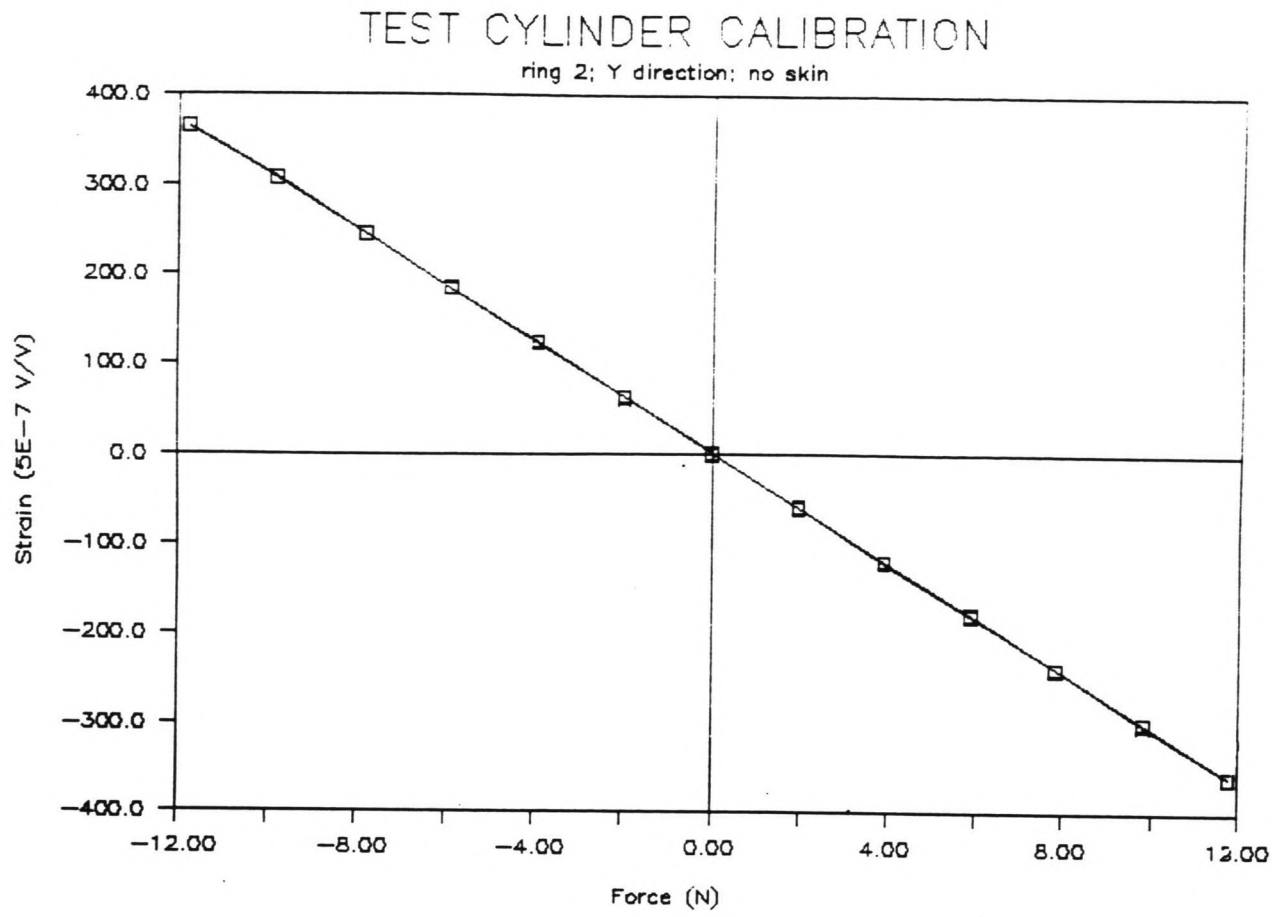

FIGURE C3.5.1

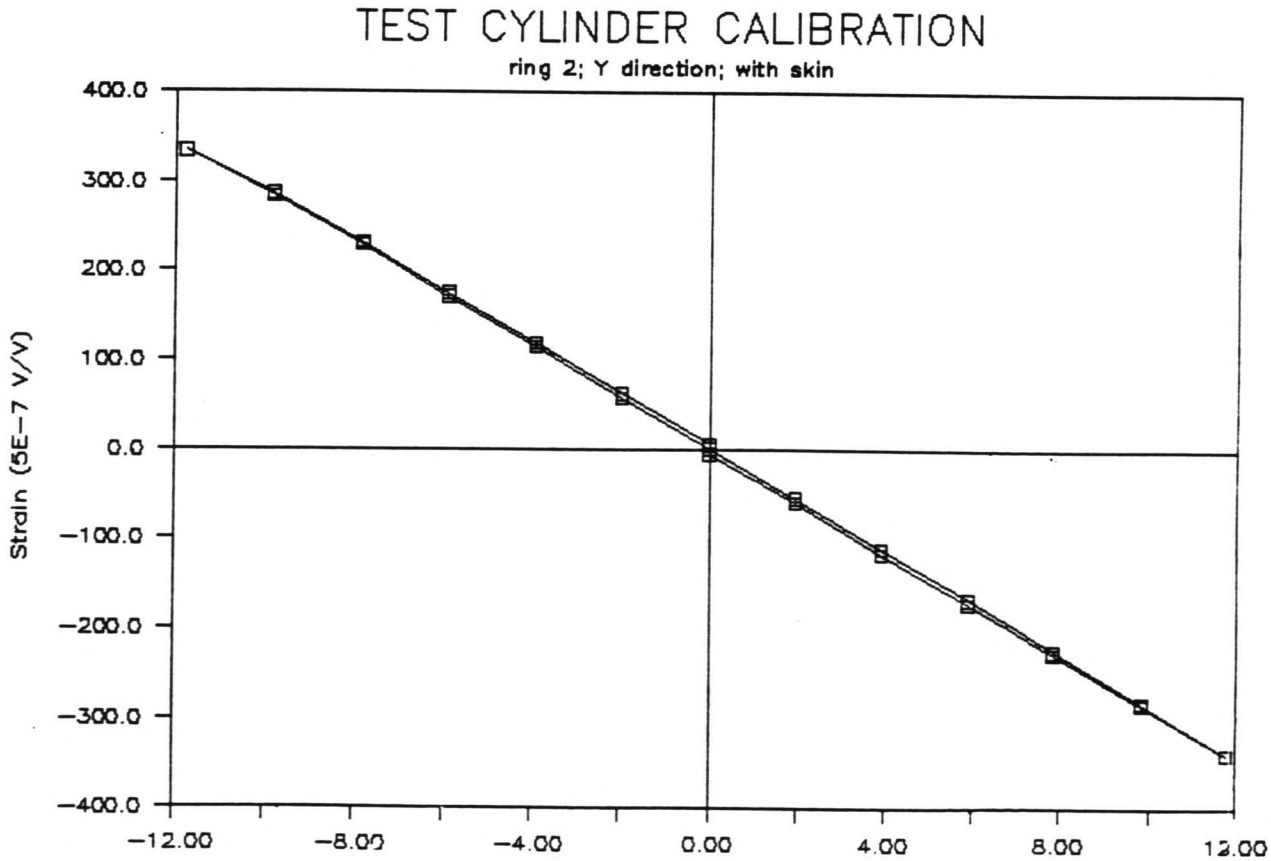

FIGURE C3.5.2

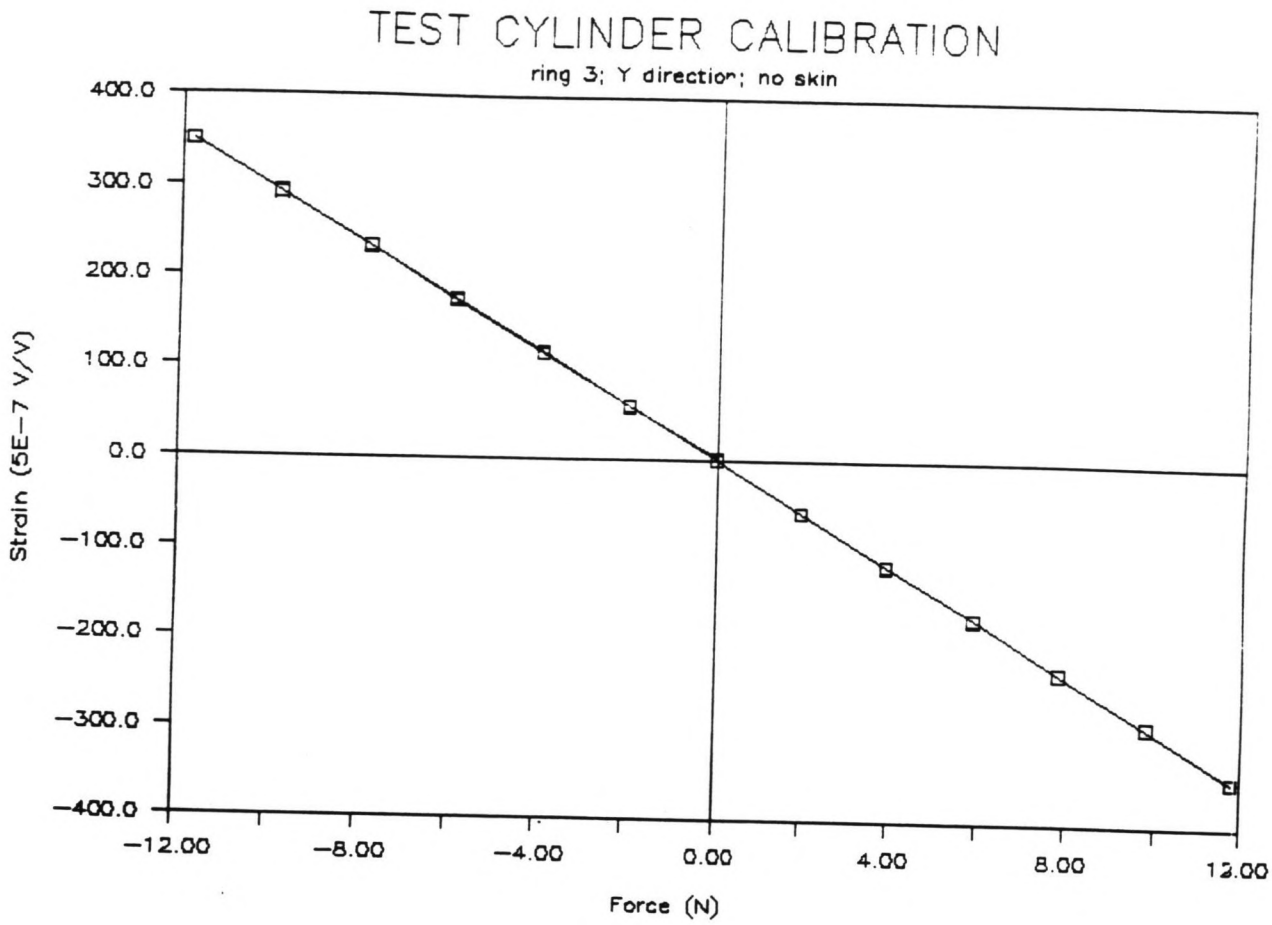

FIGURE C3.6.1

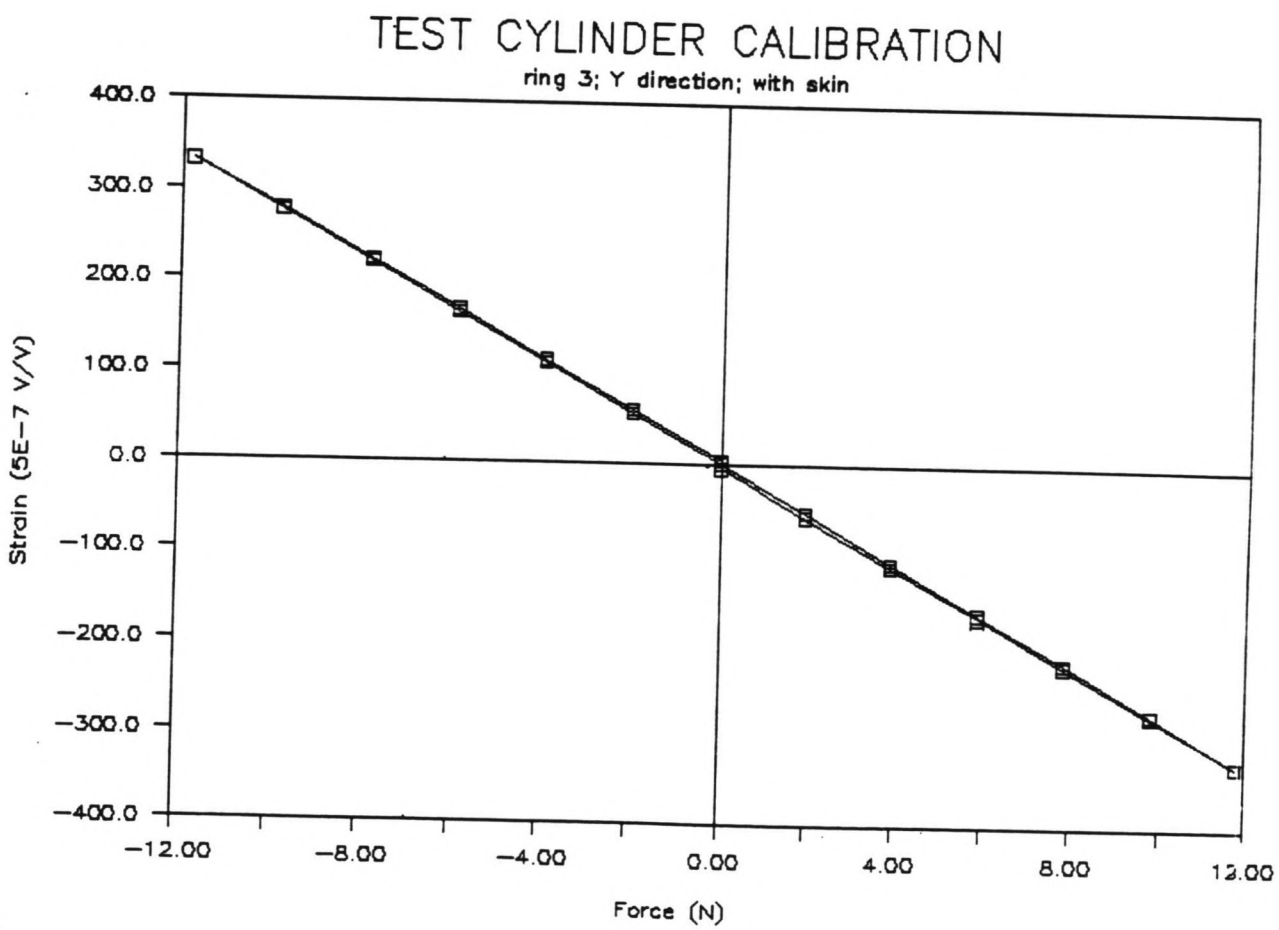

FIGURE C3.6.2

transducer : 1 loading direction : X
orientation : I / II skin : No

Mass: (kg)	Force: (N)	Strain: (5E-7 V/V)	rel. Stain: (5E-7 V/V)
0.000	0.000	55115.0	0.0
0.200	1.962	55182.2	67.2
0.400	3.924	55249.4	134.4
0.600	5.886	55316.2	201.2
0.800	7.848	55383.6	268.6
1.000	9.810	55446.2	331.2
1.200	11.772	55509.4	394.4
1.000	9.810	55448.0	333.0
0.800	7.848	55383.6	268.6
0.600	5.886	55316.8	201.8
0.400	3.924	55249.8	134.8
0.200	1.962	55182.4	67.4
0.000	0.000	55115.3	0.3
0.000	0.000	55038.6	0.0
0.200	-1.962	54970.3	-68.3
0.400	-3.924	54903.6	-135.0
0.600	-5.886	54837.4	-201.2
0.800	-7.848	54770.4	-268.2
1.000	-9.810	54705.1	-333.5
1.200	-11.772	54639.1	-399.5
1.000	-9.810	54703.5	-335.1
0.800	-7.848	54769.6	-269.0
0.600	-5.886	54835.9	-202.7
0.400	-3.924	54902.2	-136.4
0.200	-1.962	54969.2	-69.4
0.000	0.000	55037.6	-1.0

Regression Output:

Constant		1.6083
Std Err of Y Est		1.9104
R Squared		0.9998
No. of Observations		13
Degrees of Freedom		11
X Coefficient(s)	33.7240	
Std Err of Coef.	0.1431	

orientation I: k = 16.862 E-6 V/V/N

Regression Output:

Constant		-1.8302
Std Err of Y Est		1.1229
R Squared		0.9999
No. of Observations		13
Degrees of Freedom		11
X Coefficient(s)	33.9153	
Std Err of Coef.	0.0841	

orientation II: k = 16.958 E-6 V/V/N

orientation I + II: k = 16.910 E-6 V/V/N

(table C8.1)

transducer : 1 loading direction : X
orientation : I / II skin : Yes

Mass: (kg)	Force: (N)	Strain: (5E-7 V/V)	rel. Stain: (5E-7 V/V)
0.000	0.000	55115.1	0.0
0.200	1.962	55178.1	63.0
0.400	3.924	55241.3	126.2
0.600	5.886	55303.9	188.8
0.800	7.848	55367.7	252.6
1.000	9.810	55431.3	316.2
1.200	11.772	55494.9	379.8
1.000	9.810	55433.1	318.0
0.800	7.848	55369.6	254.5
0.600	5.886	55306.9	191.8
0.400	3.924	55243.4	128.3
0.200	1.962	55180.0	64.9
0.000	0.000	55117.2	2.1
0.000	0.000	55041.2	0.0
0.200	-1.962	54977.3	-63.9
0.400	-3.924	54914.7	-126.5
0.600	-5.886	54851.3	-189.9
0.800	-7.848	54788.7	-252.5
1.000	-9.810	54730.3	-310.9
1.200	-11.772	54671.4	-369.8
1.000	-9.810	54725.0	-316.2
0.800	-7.848	54785.9	-255.3
0.600	-5.886	54848.7	-192.5
0.400	-3.924	54911.8	-129.4
0.200	-1.962	54975.4	-65.8
0.000	0.000	55039.8	-1.4

Regression Output:

Constant		0.8917
Std Err of Y Est		1.1473
R Squared		0.9999
No. of Observations		13
Degrees of Freedom		11
X Coefficient(s)	32.2036	
Std Err of Coef.	0.0859	

orientation I: k = 16.102 E-6 V/V/N

Regression Output:

Constant		-2.9027
Std Err of Y Est		2.9153
R Squared		0.9995
No. of Observations		13
Degrees of Freedom		11
X Coefficient(s)	31.6622	
Std Err of Coef.	0.2184	

orientation II: k = 15.831 E-6 V/V/N

orientation I + II: k = 15.966 E-6 V/V/N

(table C8.2)

transducer : 2 loading direction : X
orientation : I / II skin : No

Mass: (kg)	Force: (N)	Strain: (5E-7 V/V)	rel. Stain: (5E-7 V/V)
0.000	0.000	55887.8	0.0
0.200	1.962	55952.3	64.5
0.400	3.924	56017.8	130.0
0.600	5.886	56081.9	194.1
0.800	7.848	56146.8	259.0
1.000	9.810	56210.6	322.8
1.200	11.772	56275.5	387.7
1.000	9.810	56212.4	324.6
0.800	7.848	56148.9	261.1
0.600	5.886	56084.2	196.4
0.400	3.924	56019.7	131.9
0.200	1.962	55954.1	66.3
0.000	0.000	55889.8	2.0
0.000	0.000	55814.5	0.0
0.200	-1.962	55750.8	-63.7
0.400	-3.924	55685.6	-128.9
0.600	-5.886	55621.2	-193.3
0.800	-7.848	55557.1	-257.4
1.000	-9.810	55491.4	-323.1
1.200	-11.772	55427.3	-387.2
1.000	-9.810	55490.0	-324.5
0.800	-7.848	55555.0	-259.5
0.600	-5.886	55619.0	-195.5
0.400	-3.924	55683.9	-130.6
0.200	-1.962	55748.2	-66.3
0.000	0.000	55811.9	-2.6

Regression Output:

Constant		1.3110
Std Err of Y Est		1.1643
R Squared		0.9999
No. of Observations		13
Degrees of Freedom		11
X Coefficient(s)	32.8938	
Std Err of Coef.	0.0872	

orientation I: k = 16.447 E-6 V/V/N

Regression Output:

Constant		-0.9442
Std Err of Y Est		1.1877
R Squared		0.9999
No. of Observations		13
Degrees of Freedom		11
X Coefficient(s)	32.8509	
Std Err of Coef.	0.0890	

orientation II: k = 16.425 E-6 V/V/N

orientation I + II: k = 16.436 E-6 V/V/N

(table C9.1)

transducer : 2 loading direction : X
orientation : I / II skin : Yes

Mass: (kg)	Force: (N)	Strain: (5E-7 V/V)	rel. Stain: (5E-7 V/V)
0.000	0.000	55877.7	0.0
0.200	1.962	55938.9	61.2
0.400	3.924	56000.1	122.4
0.600	5.886	56063.1	185.4
0.800	7.848	56124.1	246.4
1.000	9.810	56186.4	308.7
1.200	11.772	56250.0	372.3
1.000	9.810	56189.8	312.1
0.800	7.848	56128.5	250.8
0.600	5.886	56066.3	188.6
0.400	3.924	56004.5	126.8
0.200	1.962	55942.7	65.0
0.000	0.000	55881.4	3.7
0.000	0.000	55809.8	0.0
0.200	-1.962	55749.0	-60.8
0.400	-3.924	55687.3	-122.5
0.600	-5.886	55624.6	-185.2
0.800	-7.848	55562.7	-247.1
1.000	-9.810	55498.9	-310.9
1.200	-11.772	55436.6	-373.2
1.000	-9.810	55497.1	-312.7
0.800	-7.848	55558.5	-251.3
0.600	-5.886	55620.4	-189.4
0.400	-3.924	55681.8	-128.0
0.200	-1.962	55743.5	-66.3
0.000	0.000	55803.9	-5.9

Regression Output:

Constant		1.4970
Std Err of Y Est		2.0253
R Squared		0.9997
No. of Observations		13
Degrees of Freedom		11
X Coefficient(s)	31.4863	
Std Err of Coef.	0.1517	

orientation I: k = 15.743 E-6 V/V/N

Regression Output:

Constant		-2.1339
Std Err of Y Est		2.5235
R Squared		0.9996
No. of Observations		13
Degrees of Freedom		11
X Coefficient(s)	31.5092	
Std Err of Coef.	0.1890	

orientation II: k = 15.755 E-6 V/V/N

orientation I + II: k = 15.749 E-6 V/V/N

(table C9.2)

transducer : 3 loading direction : X
orientation : I / II skin : No

Mass: (kg)	Force: (N)	Strain: (5E-7 V/V)	rel. Stain: (5E-7 V/V)
0.000	0.000	55711.4	0.0
0.200	1.962	55767.0	55.6
0.400	3.924	55822.7	111.3
0.600	5.886	55878.7	167.3
0.800	7.848	55934.2	222.8
1.000	9.810	55989.6	278.2
1.200	11.772	56044.5	333.1
1.000	9.810	55990.4	279.0
0.800	7.848	55934.5	223.1
0.600	5.886	55878.4	167.0
0.400	3.924	55822.6	111.2
0.200	1.962	55767.2	55.8
0.000	0.000	55711.9	0.5
0.000	0.000	55645.9	0.0
0.200	-1.962	55589.5	-56.4
0.400	-3.924	55532.6	-113.3
0.600	-5.886	55476.1	-169.8
0.800	-7.848	55420.0	-225.9
1.000	-9.810	55366.8	-279.1
1.200	-11.772	55313.8	-332.1
1.000	-9.810	55363.4	-282.5
0.800	-7.848	55418.4	-227.5
0.600	-5.886	55475.3	-170.6
0.400	-3.924	55531.7	-114.2
0.200	-1.962	55588.4	-57.5
0.000	0.000	55645.2	-0.7

Regression Output:

Constant		0.2083
Std Err of Y Est		0.3908
R Squared		1.0000
No. of Observations		13
Degrees of Freedom		11
X Coefficient(s)	28.3468	
Std Err of Coef.	0.0293	

orientation I: k = 14.173 E-6 V/V/N

Regression Output:

Constant		-1.6060
Std Err of Y Est		1.9409
R Squared		0.9997
No. of Observations		13
Degrees of Freedom		11
X Coefficient(s)	28.4393	
Std Err of Coef.	0.1454	

orientation II: k = 14.220 E-6 V/V/N

orientation I + II: k = 14.197 E-6 V/V/N

(table C10.1)

transducer : 3 loading direction : X
orientation : I / II skin : Yes

Mass: (kg)	Force: (N)	Strain: (5E-7 V/V)	rel. Stain: (5E-7 V/V)
0.000	0.000	55729.4	0.0
0.200	1.962	55784.2	54.8
0.400	3.924	55838.9	109.5
0.600	5.886	55894.3	164.9
0.800	7.848	55949.1	219.7
1.000	9.810	55997.1	267.7
1.200	11.772	56044.7	315.3
1.000	9.810	56003.0	273.6
0.800	7.848	55950.9	221.5
0.600	5.886	55896.5	167.1
0.400	3.924	55841.9	112.5
0.200	1.962	55786.7	57.3
0.000	0.000	55731.6	2.2
0.000	0.000	55667.3	0.0
0.200	-1.962	55612.5	-54.8
0.400	-3.924	55558.0	-109.3
0.600	-5.886	55502.7	-164.6
0.800	-7.848	55447.2	-220.1
1.000	-9.810	55392.1	-275.2
1.200	-11.772	55338.0	-329.3
1.000	-9.810	55391.0	-276.3
0.800	-7.848	55444.9	-222.4
0.600	-5.886	55499.6	-167.7
0.400	-3.924	55553.9	-113.4
0.200	-1.962	55608.3	-59.0
0.000	0.000	55663.0	-4.3

Regression Output:

Constant		3.4940
Std Err of Y Est		3.7437
R Squared		0.9988
No. of Observations		13
Degrees of Freedom		11
X Coefficient(s)	27.1927	
Std Err of Coef.	0.2804	

orientation I: k = 13.596 E-6 V/V/N

Regression Output:

Constant		-2.2193
Std Err of Y Est		1.8038
R Squared		0.9997
No. of Observations		13
Degrees of Freedom		11
X Coefficient(s)	27.8563	
Std Err of Coef.	0.1351	

orientation II: k = 13.928 E-6 V/V/N

orientation I + II: k = 13.762 E-6 V/V/N

(table C10.2)

transducer : 1 loading direction : Y
orientation : III / IV skin : No

Mass: (kg)	Force: (N)	Strain: (5E-7 V/V)	rel. Stain: (5E-7 V/V)
0.000	0.000	54624.8	0.0
0.200	1.962	54564.2	-60.6
0.400	3.924	54502.7	-122.1
0.600	5.886	54441.6	-183.2
0.800	7.848	54380.2	-244.6
1.000	9.810	54323.4	-301.4
1.200	11.772	54265.1	-359.7
1.000	9.810	54317.8	-307.0
0.800	7.848	54379.1	-245.7
0.600	5.886	54440.6	-184.2
0.400	3.924	54501.4	-123.4
0.200	1.962	54563.2	-61.6
0.000	0.000	54624.2	-0.6
0.000	0.000	54694.8	0.0
0.200	-1.962	54756.0	61.2
0.400	-3.924	54816.6	121.8
0.600	-5.886	54877.9	183.1
0.800	-7.848	54939.6	244.8
1.000	-9.810	55001.8	307.0
1.200	-11.772	55063.6	368.8
1.000	-9.810	55002.0	307.2
0.800	-7.848	54939.9	245.1
0.600	-5.886	54878.9	184.1
0.400	-3.924	54817.6	122.8
0.200	-1.962	54756.7	61.9
0.000	0.000	54694.7	-0.1

Regression Output:

Constant		-1.2854
Std Err of Y Est		2.1654
R Squared		0.9997
No. of Observations		13
Degrees of Freedom		11
X Coefficient(s)	-30.8272	
Std Err of Coef.	0.1622	

orientation III: k = 15.414 E-6 V/V/N

Regression Output:

Constant		-0.2302
Std Err of Y Est		0.5262
R Squared		1.0000
No. of Observations		13
Degrees of Freedom		11
X Coefficient(s)	-31.2987	
Std Err of Coef.	0.0394	

orientation IV: k = 15.649 E-6 V/V/N

orientation III + IV: k = 15.531 E-6 V/V/N

(table C11.1)

transducer : 1 loading direction : Y
orientation : III / IV skin : Yes

Mass: (kg)	Force: (N)	Strain: (5E-7 V/V)	rel. Stain: (5E-7 V/V)
0.000	0.000	54625.9	0.0
0.200	1.962	54570.1	-55.8
0.400	3.924	54513.2	-112.7
0.600	5.886	54456.4	-169.5
0.800	7.848	54399.2	-226.7
1.000	9.810	54343.8	-282.1
1.200	11.772	54285.3	-340.6
1.000	9.810	54340.2	-285.7
0.800	7.848	54396.3	-229.6
0.600	5.886	54454.1	-171.8
0.400	3.924	54510.5	-115.4
0.200	1.962	54568.2	-57.7
0.000	0.000	54624.6	-1.3
0.000	0.000	54697.8	0.0
0.200	-1.962	54756.4	58.6
0.400	-3.924	54814.6	116.8
0.600	-5.886	54874.5	176.7
0.800	-7.848	54935.1	237.3
1.000	-9.810	54996.0	298.2
1.200	-11.772	55057.7	359.9
1.000	-9.810	54997.9	300.1
0.800	-7.848	54939.4	241.6
0.600	-5.886	54879.7	181.9
0.400	-3.924	54819.8	122.0
0.200	-1.962	54760.2	62.4
0.000	0.000	54699.4	1.6

Regression Output:

Constant		-0.4801
Std Err of Y Est		1.3952
R Squared		0.9999
No. of Observations		13
Degrees of Freedom		11
X Coefficient(s)	-28.9197	
Std Err of Coef.	0.1045	

orientation III: k = 14.460 E-6 V/V/N

Regression Output:

Constant		0.4389
Std Err of Y Est		2.1071
R Squared		0.9997
No. of Observations		13
Degrees of Freedom		11
X Coefficient(s)	-30.4592	
Std Err of Coef.	0.1578	

orientation IV: k = 15.230 E-6 V/V/N

orientation III + IV: k = 14.845 E-6 V/V/N

(table C11.2)

transducer : 2 loading direction : Y
orientation : III / IV skin : No

Mass: (kg)	Force: (N)	Strain: (5E-7 V/V)	rel. Stain: (5E-7 V/V)
0.000	0.000	54904.8	0.0
0.200	1.962	54845.3	-59.5
0.400	3.924	54785.4	-119.4
0.600	5.886	54725.8	-179.0
0.800	7.848	54665.9	-238.9
1.000	9.810	54605.9	-298.9
1.200	11.772	54545.6	-359.2
1.000	9.810	54604.9	-299.9
0.800	7.848	54664.6	-240.2
0.600	5.886	54724.0	-180.8
0.400	3.924	54784.0	-120.8
0.200	1.962	54843.7	-61.1
0.000	0.000	54903.4	-1.4
0.000	0.000	54972.9	0.0
0.200	-1.962	55035.3	62.4
0.400	-3.924	55096.2	123.3
0.600	-5.886	55157.2	184.3
0.800	-7.848	55218.0	245.1
1.000	-9.810	55279.0	306.1
1.200	-11.772	55336.6	363.7
1.000	-9.810	55279.3	306.4
0.800	-7.848	55218.5	245.6
0.600	-5.886	55158.2	185.3
0.400	-3.924	55097.3	124.4
0.200	-1.962	55036.0	63.1
0.000	0.000	54973.5	0.6

Regression Output:

Constant		-0.6189
Std Err of Y Est		0.7537
R Squared		1.0000
No. of Observations		13
Degrees of Freedom		11
X Coefficient(s)	-30.4544	
Std Err of Coef.	0.0564	

orientation III: k = 15.227 E-6 V/V/N

Regression Output:

Constant		1.6023
Std Err of Y Est		1.2112
R Squared		0.9999
No. of Observations		13
Degrees of Freedom		11
X Coefficient(s)	-30.9983	
Std Err of Coef.	0.0907	

orientation IV: k = 15.499 E-6 V/V/N

orientation III + IV: k = 15.363 E-6 V/V/N

(table C12.1)

transducer : 2 loading direction : Y
orientation : III / IV skin : Yes

Mass: (kg)	Force: (N)	Strain: (5E-7 V/V)	rel. Stain: (5E-7 V/V)
0.000	0.000	54901.6	0.0
0.200	1.962	54846.3	-55.3
0.400	3.924	54790.0	-111.6
0.600	5.886	54733.5	-168.1
0.800	7.848	54676.2	-225.4
1.000	9.810	54619.2	-282.4
1.200	11.772	54561.8	-339.8
1.000	9.810	54617.0	-284.6
0.800	7.848	54672.7	-228.9
0.600	5.886	54728.1	-173.5
0.400	3.924	54783.7	-117.9
0.200	1.962	54841.1	-60.5
0.000	0.000	54895.4	-6.2
0.000	0.000	54961.1	0.0
0.200	-1.962	55018.4	57.3
0.400	-3.924	55075.3	114.2
0.600	-5.886	55132.1	171.0
0.800	-7.848	55190.3	229.2
1.000	-9.810	55243.6	282.5
1.200	-11.772	55294.8	333.7
1.000	-9.810	55246.4	285.3
0.800	-7.848	55192.4	231.3
0.600	-5.886	55135.8	174.7
0.400	-3.924	55079.5	118.4
0.200	-1.962	55023.0	61.9
0.000	0.000	54965.4	4.3

Regression Output:

Constant		-2.4113
Std Err of Y Est		2.6597
R Squared		0.9995
No. of Observations		13
Degrees of Freedom		11
X Coefficient(s)	-28.6393	
Std Err of Coef.	0.1992	

orientation III: k = 14.320 E-6 V/V/N

Regression Output:

Constant		3.8963
Std Err of Y Est		2.9938
R Squared		0.9993
No. of Observations		13
Degrees of Freedom		11
X Coefficient(s)	-28.5019	
Std Err of Coef.	0.2242	

orientation IV: k = 14.251 E-6 V/V/N

orientation III + IV: k = 14.285 E-6 V/V/N

(table C12.2)

transducer : 3 loading direction : Y
orientation : III / IV skin : No

Mass: (kg)	Force: (N)	Strain: (5E-7 V/V)	rel. Stain: (5E-7 V/V)
0.000	0.000	55836.3	0.0
0.200	1.962	55778.3	-58.0
0.400	3.924	55720.4	-115.9
0.600	5.886	55662.8	-173.5
0.800	7.848	55604.5	-231.8
1.000	9.810	55546.7	-289.6
1.200	11.772	55488.5	-347.8
1.000	9.810	55546.4	-289.9
0.800	7.848	55603.8	-232.5
0.600	5.886	55662.5	-173.8
0.400	3.924	55719.8	-116.5
0.200	1.962	55777.9	-58.4
0.000	0.000	55835.5	-0.8
0.000	0.000	55901.8	0.0
0.200	-1.962	55960.1	58.3
0.400	-3.924	56018.0	116.2
0.600	-5.886	56076.3	174.5
0.800	-7.848	56134.7	232.9
1.000	-9.810	56192.4	290.6
1.200	-11.772	56250.2	348.4
1.000	-9.810	56193.4	291.6
0.800	-7.848	56135.3	233.5
0.600	-5.886	56077.7	175.9
0.400	-3.924	56019.5	117.7
0.200	-1.962	55961.0	59.2
0.000	0.000	55902.6	0.8

Regression Output:

Constant		-0.3246
Std Err of Y Est		0.3486
R Squared		1.0000
No. of Observations		13
Degrees of Freedom		11
X Coefficient(s)	-29.5090	
Std Err of Coef.	0.0261	

orientation III: k = 14.755 E-6 V/V/N

Regression Output:

Constant		0.6904
Std Err of Y Est		0.6398
R Squared		1.0000
No. of Observations		13
Degrees of Freedom		11
X Coefficient(s)	-29.5988	
Std Err of Coef.	0.0479	

orientation IV: k = 14.799 E-6 V/V/N

orientation III + IV: k = 14.777 E-6 V/V/N

(table C13.1)

transducer : 3 loading direction : Y
orientation : III / IV skin : Yes

Mass: (kg)	Force: (N)	Strain: (5E-7 V/V)	rel. Stain: (5E-7 V/V)
0.000	0.000	55841.6	0.0
0.200	1.962	55787.5	-54.1
0.400	3.924	55732.5	-109.1
0.600	5.886	55677.7	-163.9
0.800	7.848	55622.9	-218.7
1.000	9.810	55568.0	-273.6
1.200	11.772	55512.4	-329.2
1.000	9.810	55566.5	-275.1
0.800	7.848	55620.0	-221.6
0.600	5.886	55673.9	-167.7
0.400	3.924	55728.1	-113.5
0.200	1.962	55782.2	-59.4
0.000	0.000	55836.2	-5.4
0.000	0.000	55899.6	0.0
0.200	-1.962	55954.3	54.7
0.400	-3.924	56009.5	109.9
0.600	-5.886	56064.9	165.3
0.800	-7.848	56120.6	221.0
1.000	-9.810	56176.4	276.8
1.200	-11.772	56231.4	331.8
1.000	-9.810	56178.0	278.4
0.800	-7.848	56123.0	223.4
0.600	-5.886	56068.4	168.8
0.400	-3.924	56013.0	113.4
0.200	-1.962	55958.8	59.2
0.000	0.000	55903.4	3.8

Regression Output:

Constant		-2.5372
Std Err of Y Est		2.1559
R Squared		0.9996
No. of Observations		13
Degrees of Freedom		11
X Coefficient(s)	-27.7256	
Std Err of Coef.	0.1615	

orientation III: k = 13.863 E-6 V/V/N

Regression Output:

Constant		1.8103
Std Err of Y Est		1.7719
R Squared		0.9998
No. of Observations		13
Degrees of Freedom		11
X Coefficient(s)	-28.0746	
Std Err of Coef.	0.1327	

orientation IV: k = 14.037 E-6 V/V/N

orientation III + IV: k = 13.950 E-6 V/V/N

(table C13.2)

transducer : 1 loading direction : Y
orientation : IV skin : Yes
skin : Yes relaxation time : None / One day

Mass: (kg)	Force: (N)	Strain: (5E-7 V/V)	rel. Stain: (5E-7 V/V)
0.000	0.000	54697.9	0.0
0.200	-1.962	54754.5	56.6
0.400	-3.924	54811.1	113.2
0.600	-5.886	54868.7	170.8
0.800	-7.848	54925.9	228.0
1.000	-9.810	54985.3	287.4
1.200	-11.772	55044.5	346.6
1.000	-9.810	54986.4	288.5
0.800	-7.848	54928.8	230.9
0.600	-5.886	54870.9	173.0
0.400	-3.924	54812.9	115.0
0.200	-1.962	54755.4	57.5
0.000	0.000	54697.6	-0.3
0.000	0.000	54697.8	0.0
0.200	-1.962	54756.4	58.6
0.400	-3.924	54814.6	116.8
0.600	-5.886	54874.5	176.7
0.800	-7.848	54935.1	237.3
1.000	-9.810	54996.0	298.2
1.200	-11.772	55057.7	359.9
1.000	-9.810	54997.9	300.1
0.800	-7.848	54939.4	241.6
0.600	-5.886	54879.7	181.9
0.400	-3.924	54819.8	122.0
0.200	-1.962	54760.2	62.4
0.000	0.000	54699.4	1.6

Regression Output:

Constant		-0.7748
Std Err of Y Est		1.0941
R Squared		0.9999
No. of Observations		13
Degrees of Freedom		11
X Coefficient(s)	-29.4098	
Std Err of Coef.	0.0819	

relaxation time: None k = 14.705 E-6 V/V/N

Regression Output:

Constant		0.4389
Std Err of Y Est		2.1071
R Squared		0.9997
No. of Observations		13
Degrees of Freedom		11
X Coefficient(s)	-30.4592	
Std Err of Coef.	0.1578	

relaxation time: One day k = 15.230 E-6 V/V/N

(table C14)

transducer	: 2	loading direction	: Y
orientation	: IV	skin	: Yes
skin	: Yes	relaxation time	: None / One day

Mass: (kg)	Force: (N)	Strain: (5E-7 V/V)	rel. Stain: (5E-7 V/V)
0.000	0.000	54961.9	0.0
0.200	-1.962	55018.2	56.3
0.400	-3.924	55075.0	113.1
0.600	-5.886	55132.5	170.6
0.800	-7.848	55190.6	228.7
1.000	-9.810	55243.4	281.5
1.200	-11.772	55295.8	333.9
1.000	-9.810	55247.5	285.6
0.800	-7.848	55192.9	231.0
0.600	-5.886	55136.5	174.6
0.400	-3.924	55080.0	118.1
0.200	-1.962	55023.6	61.7
0.000	0.000	54966.0	4.1
0.000	0.000	54961.1	0.0
0.200	-1.962	55018.4	57.3
0.400	-3.924	55075.3	114.2
0.600	-5.886	55132.1	171.0
0.800	-7.848	55190.3	229.2
1.000	-9.810	55243.6	282.5
1.200	-11.772	55294.8	333.7
1.000	-9.810	55246.4	285.3
0.800	-7.848	55192.4	231.3
0.600	-5.886	55135.8	174.7
0.400	-3.924	55079.5	118.4
0.200	-1.962	55023.0	61.9
0.000	0.000	54965.4	4.3

Regression Output:

Constant	3.4385
Std Err of Y Est	3.0689
R Squared	0.9993
No. of Observations	13
Degrees of Freedom	11
X Coefficient(s)	-28.5211
Std Err of Coef.	0.2299

relaxation time: None k = 14.261 E-6 V/V/N

Regression Output:

Constant	3.8963
Std Err of Y Est	2.9938
R Squared	0.9993
No. of Observations	13
Degrees of Freedom	11
X Coefficient(s)	-28.5019
Std Err of Coef.	0.2242

relaxation time: One day k = 14.251 E-6 V/V/N

(table C15)

transducer	: 3	loading direction	: Y
orientation	: IV	skin	: Yes
skin	: Yes	relaxation time	: None / One day

Mass: (kg)	Force: (N)	Strain: (5E-7 V/V)	rel. Stain: (5E-7 V/V)
0.000	0.000	55900.5	0.0
0.200	-1.962	55954.6	54.1
0.400	-3.924	56008.8	108.3
0.600	-5.886	56063.5	163.0
0.800	-7.848	56118.2	217.7
1.000	-9.810	56173.9	273.4
1.200	-11.772	56228.4	327.9
1.000	-9.810	56175.5	275.0
0.800	-7.848	56121.0	220.5
0.600	-5.886	56067.3	166.8
0.400	-3.924	56012.5	112.0
0.200	-1.962	55958.3	57.8
0.000	0.000	55904.2	3.7
0.000	0.000	55899.6	0.0
0.200	-1.962	55954.3	54.7
0.400	-3.924	56009.5	109.9
0.600	-5.886	56064.9	165.3
0.800	-7.848	56120.6	221.0
1.000	-9.810	56176.4	276.8
1.200	-11.772	56231.4	331.8
1.000	-9.810	56178.0	278.4
0.800	-7.848	56123.0	223.4
0.600	-5.886	56068.4	168.8
0.400	-3.924	56013.0	113.4
0.200	-1.962	55958.8	59.2
0.000	0.000	55903.4	3.8

Regression Output:

Constant	1.5973
Std Err of Y Est	1.7546
R Squared	0.9998
No. of Observations	13
Degrees of Freedom	11
X Coefficient(s)	-27.7415
Std Err of Coef.	0.1314

relaxation time: None k = 13.871 E-6 V/V/N

Regression Output:

Constant	1.8103
Std Err of Y Est	1.7719
R Squared	0.9998
No. of Observations	13
Degrees of Freedom	11
X Coefficient(s)	-28.0746
Std Err of Coef.	0.1327

relaxation time: One day k = 14.037 E-6 V/V/N

(table C16)

APPENDIX D: RANGE FOR VARIABLE VALUES

APPENDIX D: RANGE FOR VARIABLE VALUES

D1 Towing in x Direction

Parameter values: Cd= 1.2, D= 0.060 m, ds= 0.015 m.

The force working in x direction on one of the transducers is given by:

$$F_D = \frac{1}{2} \cdot C_D \cdot \rho \cdot D \cdot \|V\| \cdot V \cdot ds \quad (N) \qquad \text{(I)}$$

When ‖F‖ should not exceed 10.0 N, the maximum allowed towing speed is 4.30 m/s.

D2 Cylinder Oscillation in y Direction: Forces Including Ring Mass

Additional parameter values: Cd= 0.9, A= 0.3 m, m= 0.040 kg, Ca= 0.5

When the cylinder displacement in oscillation direction is given by (II),

$$y(t) = A \cdot \sin(\omega \cdot t) \quad ; \quad \omega = 2 \cdot \pi \cdot f_o \qquad \text{(II)}$$

the force working in y direction on one of the transducers is given by (III),

$$F_y(t) = F_{Drag}(t) + F_{Inertia}(t) + F_{Mass}(t) \quad (N) \qquad \text{(III)}$$

with Fd, Fi and Fm as in (IV), (V) and (VI).

$$F_D = \frac{1}{2} \cdot C_D \cdot \rho \cdot D \cdot ds \cdot A^2 \cdot \omega^2 \cdot \cos(\omega \cdot t) \cdot \|\cos(\omega \cdot t)\| \quad (N) \qquad \text{(IV)}$$

$$F_I = -\frac{\pi}{4} \cdot \rho \cdot C_A \cdot D^2 \cdot ds \cdot A \cdot \omega^2 \cdot \sin(\omega \cdot t) \quad (N) \qquad \text{(V)}$$

$$F_M = -m \cdot A \cdot \omega^2 \cdot \sin(\omega \cdot t) \quad (N) \qquad \text{(VI)}$$

It is here assumed that the maxima of these forces occur simultaneously. When ‖F‖ should not exceed 10.0 N, the parameter values inserted in equations (IV), (V) and (VI) yield for the maximum allowed oscillation frequency f_o:

$$f\_o < 2.15 \text{ Hz}$$

APPENDIX E: EXPERIMENT LOG

APPENDIX E: EXPERIMENT LOG

E1 Run Numbers and their Variable Values

RUN:	A (m):	V(m/s):	T(s):	date:	env:	
1	0.000	0.00	0.00	4/12	air	{*
2	0.000	0.00	0.00	4/12	air	cylinder res-
3	0.000	0.00	0.00	4/12	air	ponse *}
4	0.000	0.00	0.00	5/12	air	{*
5	0.250	0.00	3.00	5/12	air	wrong calibra-
6	0.250	0.00	2.00	5/12	air	tion factors
7	0.250	0.00	1.50	5/12	air	used *}
8				5/12	air	{*
9				5/12	air	dynamic
10				5/12	air	response
11				5/12	air	of rings
12				5/12	air	
13				5/12	air	
14				5/12	air	
15				5/12	air	
16				5/12	air	
17				5/12	air	*}
18	0.300	0.00	1.50	5/12	air	
19	0.300	0.00	2.00	5/12	air	
20	0.300	0.00	3.00	5/12	air	
21	0.300	0.00	2.50	5/12	air	
22	0.300	0.00	1.85	5/12	air	
23	0.300	0.00	1.70	5/12	air	
24	0.300	0.00	1.60	5/12	air	
25	0.300	0.00	1.55	5/12	air	
26	0.270	0.00	1.50	5/12	air	
27	0.240	0.00	1.50	5/12	air	
28	0.180	0.00	1.50	5/12	air	
29	0.000	0.00	0.00	5/12	air	{* step load
30	0.000	0.00	0.00	5/12	air	(rope)
31	0.000	0.00	0.00	5/12	air	*}
32	0.180	0.00	1.50	6/12	water	
33	0.180	0.50	1.50	6/12	water	
34	0.000	0.50	0.00	6/12	water	
35	0.000	1.00	0.00	6/12	water	
36	0.000	0.75	0.00	6/12	water	
37	0.000	1.50	0.00	6/12	water	
38	0.300	0.00	1.50	6/12	water	{* short run *}
39	0.300	0.10	1.50	6/12	water	
40	0.300	0.25	1.50	6/12	water	

RUN:	A (m):	V(m/s):	T(s):	date:	env:
41	0.300	0.50	1.50	6/12	water
42	0.300	0.75	1.50	6/12	water
43	0.300	1.00	1.50	6/12	water
44	0.300	1.50	1.50	6/12	water
45	0.270	0.10	1.70	6/12	water
46	0.270	0.75	1.70	6/12	water
47	0.270	0.50	1.70	6/12	water
48	0.270	1.00	1.70	6/12	water
49	0.270	1.50	1.70	6/12	water
50	0.270	0.75	1.60	6/12	water
51	0.270	0.75	1.50	6/12	water
52	0.270	0.75	1.85	6/12	water
53	0.270	0.75	2.00	6/12	water
54	0.270	0.75	2.50	6/12	water
55	0.270	0.75	3.00	6/12	water
56	0.300	0.10	1.70	6/12	water
57	0.300	0.75	1.70	6/12	water
58	0.285	0.10	1.70	6/12	water
59	0.285	0.75	1.70	6/12	water
60	0.255	0.10	1.70	6/12	water
61	0.255	0.75	1.70	6/12	water
62	0.240	0.10	1.70	6/12	water
63	0.240	0.75	1.70	6/12	water
64	0.210	0.10	1.70	6/12	water
65	0.210	0.75	1.70	6/12	water
66	0.180	0.10	1.70	6/12	water
67	0.180	0.75	1.70	6/12	water
68	0.120	0.10	1.70	6/12	water
69	0.120	0.75	1.70	6/12	water
70	0.000	0.10	0.00	6/12	water
71	0.270	0.50	3.00	7/12	water
72	0.270	0.50	2.50	7/12	water
73	0.270	0.50	2.00	7/12	water
74	0.270	0.50	1.85	7/12	water
75	0.270	0.50	1.70	7/12	water
76	0.270	0.50	1.60	7/12	water
77	0.270	0.50	1.50	7/12	water
78	0.270	1.50	3.00	7/12	water
79	0.270	1.50	2.50	7/12	water
80	0.270	1.50	2.00	7/12	water

RUN:	A (m):	V(m/s):	T(s):	date:	env:	
81	0.270	1.50	1.85	7/12	water	
82	0.270	1.50	1.70	7/12	water	
83	0.270	0.75	1.50	7/12	water	
84	0.270	1.50	1.60	7/12	water	
85	0.270	1.00	1.50	7/12	water	
86	0.270	1.50	1.50	7/12	water	
87	0.270	0.75	3.00	7/12	water	
88	0.270	1.00	3.00	7/12	water	
89	0.240	0.75	1.85	7/12	water	
90	0.210	0.75	2.00	7/12	water	
91	0.180	0.75	2.50	7/12	water	
92	0.120	0.75	3.00	7/12	water	
97	0.300	0.50	1.70	7/12	water	
98	0.300	0.75	1.70	7/12	water	
99	0.300	1.00	1.70	7/12	water	
100	0.300	0.75	3.00	7/12	water	
101	0.300	1.50	1.70	7/12	water	
102	0.300	0.75	2.00	7/12	water	
103	0.300	0.75	2.50	7/12	water	
104	0.300	0.75	1.85	7/12	water	
105	0.300	0.75	1.60	7/12	water	
106	0.300	0.75	1.50	7/12	water	
107	0.120	0.75	2.50	7/12	water	{*
108	0.120	0.75	2.00	7/12	water	perhaps 0.21
109	0.120	0.75	1.85	7/12	water	
110	0.120	0.75	1.70	7/12	water	
111	0.120	0.75	1.60	7/12	water	
112	0.120	0.75	1.50	7/12	water	
113	0.120	0.50	1.70	7/12	water	
114	0.120	1.00	1.70	7/12	water	
115	0.120	1.50	1.70	7/12	water	installed *}
116	0.180	0.00	1.70	7/12	water	
117	0.180	0.50	1.70	7/12	water	
118	0.180	1.50	1.70	7/12	water	
119	0.180	0.75	3.00	7/12	water	
120	0.180	0.75	1.50	7/12	water	
121	0.210	0.00	1.70	7/12	water	
122	0.210	0.50	1.70	7/12	water	
123	0.210	1.50	1.70	7/12	water	
124	0.210	0.75	3.00	7/12	water	
125	0.210	0.75	1.50	7/12	water	
126	0.240	0.00	1.70	7/12	water	
127	0.240	0.50	1.70	7/12	water	
128	0.240	1.50	1.70	7/12	water	
129	0.240	0.75	3.00	7/12	water	
130	0.240	0.75	1.50	7/12	water	

RUN:	A (m):	V(m/s):	T(s):	date:	env:
131	0.255	0.00	1.70	7/12	water
132	0.255	0.50	1.70	7/12	water
133	0.255	1.50	1.70	7/12	water
134	0.255	0.75	3.00	7/12	water
135	0.255	0.75	1.50	7/12	water
136	0.270	0.00	1.70	7/12	water
137	0.270	0.50	1.70	7/12	water
138	0.270	1.50	1.70	7/12	water
139	0.270	0.75	3.00	7/12	water
140	0.270	0.75	1.50	7/12	water
141	0.285	0.00	1.70	7/12	water
142	0.285	0.50	1.70	7/12	water
143	0.285	1.50	1.70	7/12	water
144	0.285	0.75	3.00	7/12	water
145	0.285	0.75	1.50	7/12	water
146	0.000	0.00	0.00	7/12	water
147	0.270	0.00	1.70	10/12	water
148	0.270	0.10	1.70	10/12	water
149	0.270	0.50	1.70	10/12	water
150	0.270	0.75	1.70	10/12	water
151	0.270	1.00	1.70	10/12	water
152	0.270	1.50	1.70	10/12	water
153	0.270	0.75	1.50	10/12	water
154	0.270	0.75	1.60	10/12	water
155	0.270	0.75	1.85	10/12	water
156	0.270	0.75	2.00	10/12	water
157	0.270	0.75	2.50	10/12	water
158	0.270	0.75	3.00	10/12	water
159	0.000	0.00	0.00	10/12	water
161	0.300	0.75	1.70	10/12	water
162	0.285	0.75	1.70	10/12	water
163	0.255	0.75	1.70	10/12	water
164	0.240	0.75	1.70	10/12	water
165	0.210	0.75	1.70	10/12	water
166	0.180	0.75	1.70	10/12	water
167	0.120	0.75	1.70	10/12	water
168	0.000	0.50	0.00	10/12	water
169	0.000	0.75	0.00	10/12	water
170	0.000	1.00	0.00	10/12	water
171	0.000	1.50	0.00	10/12	water
172	0.000	2.00	0.00	10/12	water

E2 Variable Values and their Run Numbers

A/D (-):	V (m/s):	fo (Hz):	RUN:			
4.50	0.75	0.33	55	139	87	158
		0.40	54			157
		0.50	53			156
		0.54	52			155
		0.59	46			
		0.63	50			154
		0.67	51	83	140	153
2.00	0.75	0.59	69	110		167
3.00			67			166
3.50			65			165
4.00			63			164
4.25			61			163
4.50				46		
4.75			59			162
5.00			57	98		161
4.50	0.50	0.59	47	75	137	149
	0.75			46		150
	1.00		48			151
	1.50		49	138	82	152
4.50	0.50	0.33	71			
		0.40	72			
		0.50	73			
		0.54	74			
		0.59	75	137	47	
		0.63	76			
		0.67	77			
2.00	0.75	0.33	92			
3.00			119			
3.50			124			
4.00			129			
4.25			134			
4.50			139	87	55	
4.75			144			
5.00			100			
4.50	0.50	0.33		71		
	0.75		87		55	
	1.00		88			
	1.50			78		

A/D (-):	V (m/s):	fo (Hz):	RUN:		
5.00	0.75	0.33		100	
		0.40	103		
		0.50	102		
		0.54	104		
		0.59	98		57
		0.63	105		
		0.67	42	106	
2.00	1.50	0.59		115	
3.00			118		
3.50			123		
4.00			128		
4.25			133		
4.50			138	82	49
4.75			143		
5.00			101		
5.00	0.50	0.59	97		
	0.75			98	57
	1.00		99		
	1.50			101	
2.00	0.10	0.59	68		
3.00			66		
3.50			64		
4.00			62		
4.25			60		
4.50			45		148
4.75			58		
5.00			56		
2.00	0.00	0.59			
3.00			116		
3.50			121		
4.00			126		
4.25			131		
4.50			136		147
4.75			141		
5.00					
0.00	0.00	0.00	146		159
	0.10		70		
	0.50		34		168
	0.75		36		169
	1.00		35		170
	1.50		37		171
	2.00				172

A/D (-):	V (m/s):	fo (Hz):	RUN:		
4.50	1.50	0.33	78		
		0.40	79		
		0.50	80		
		0.54	81		
		0.59	82	138	49
		0.63	84		
		0.67	86		
2.00	0.75	0.67		112	
3.00			120		
3.50			125		
4.00			130		
4.25			135		
4.50			83	140	51
4.75			145		
5.00			106	42	
4.50	0.50	0.67	77		
	0.75		140	83	51
	1.00		85		
	1.50			86	
2.00	0.75	0.33		92	
		0.40	107		
		0.50	108		
		0.54	109		
		0.59	110		69
		0.63	111		
		0.67	112		
2.00	0.50	0.59	113		
3.00			117		
3.50			122		
4.00			127		
4.25			132		
4.50			137	75	47
4.75			142		
5.00			97		
2.00	0.50	0.59	113		
	0.75		110	69	
	1.00		114		
	1.50		115		

E3 Miscelleneous Parameters

Channel numbers and signals recorded:

1: towing velocity;
2: force in x-direction of transducer no. 1;
3: force of y-direction of transducer no. 1;
4: force in x-direction of transducer no. 2;
5: force of y-direction of transducer no. 2;
6: force in x-direction of transducer no. 3;
7: force of y-direction of transducer no. 3;
8: reference signal in phase with oscillator motion;
9: reference signal 90 degrees out of phase with oscillator motion.

Oscillator setting versus in phase/out of phase signal:

0 degrees: maximum positive: out of phase;
90 degrees: maximum positive: in phase;
180 degrees: maximum negative: out of phase;
270 degrees: maximum negative: in phase.

Time interval of each run : 20 seconds.
Sample interval : 0.020 seconds (number of samples: 1000).
Filtering frequency : 20 Hz (low pass filter).
Water temperature : 16 degrees Celcius.

APPENDIX F: COMPUTER PROGRAMS LISTINGS

F1 DEVELOPED COMPUTER PROGRAMS

All programs for the analysis of the experiments of the present study have been written in FORTRAN. The output files were designed in such way that spreadsheet software like SYMPHONY could easily be applied. The author is aware of the fact that more efficient pragamming would probably reduce the length of the listings considerably.
Six programs have been developed:

- Program ANALYSIS

  This program determines the required coefficients of Model I.

- Program DATA1

  This program summarises the output of ANALYSIS in such way that a table like table G1 in appendix G occurs.

- Program RESULTS

  This program rearranges the table mentioned above (i.e. the output of DATA1) in such a way that the values of one coefficient for identical input parameters are put together. Now, graphs like those in appendix G, figures G1 to G6, can easily be made with spreadsheet software.

- Program RINGMASS

  This program determines the ring mass that is responsible for the forces that have been recorded during air oscillations.

- Program RELEVAT5

  This program gives the same results as ANALYSIS, but now for the Model II.

- Program DATA5

  This program manipulates the output of RELEVAT5 in the same way as DATA1.

```
      PROGRAM ANALYSIS

      CHARACTER INPHASE*15,OUTPHASE*15,FORCEX*15,FORCEY*15,
     +RUNNUMBER*3,AOUTF*12,PART*1
      REAL HINF(145,7),HOUT(145,7),HFX(145,7),HFY(145,7),
     +RINF(1000),ROUT(1000),FX(1000),FY(1000),
     +XLIFT(1000),YLIFT(1000),
     +NSTEP(4),STEP(4),
     +CDMIN(0:4),CAMIN(0:4),TCLMIN(0:4),STRMIN(0:4),TPHIMIN(0:4),
     +CRITFSTRPHI(9),CRITFCL(9),STR(9),PHIMIN(9),CLMIN(9),
     +ENDPHI(9),CRITFCDCA(9)
      OPEN(10,FILE='INVOER1',STATUS='UNKNOWN')
      OPEN(15,FILE='UITVOER1',STATUS='UNKNOWN',IOSTAT=IOOPEN)
      PRINT*,IOOPEN
      READ(10,*)NUMBEROFRUNS
      READ(10,*)RMASS,RHO
      DO 10000 NUMBEROFRUN=1,NUMBEROFRUNS
        READ(10,*)RUNNUMBER,PIECES
        READ(10,*)INPHASE,OUTPHASE,FORCEX,FORCEY
        READ(10,*)A,V,T
        OPEN(11,FILE=INPHASE,STATUS='UNKNOWN')
        OPEN(12,FILE=OUTPHASE,STATUS='UNKNOWN')
        OPEN(13,FILE=FORCEX,STATUS='UNKNOWN')
        OPEN(14,FILE=FORCEY,STATUS='UNKNOWN')
        REWIND 11
        REWIND 12
        REWIND 13
        REWIND 14
        PI=3.1415927
        READ(11,*)CHI,R,DTI
        READ(12,*)CHO,R,DTO
        READ(13,*)CHX,R,DTX
        READ(14,*)CHY,R,DTY
        WRITE(*,*)'Analysis of RUN ',RUNNUMBER,':'
        WRITE(*,*)'Reading files ....'
        DO 10 I=1,142
          READ(11,*)(HINF(I,J),J=1,7)
          READ(12,*)(HOUT(I,J),J=1,7)
          READ(13,*)(HFX(I,J),J=1,7)
          READ(14,*)(HFY(I,J),J=1,7)
          DO 5 J=1,7
            RINF((I-1)*7+J)=HINF(I,J)
            ROUT((I-1)*7+J)=HOUT(I,J)
            FX((I-1)*7+J)=HFX(I,J)
            HFY(I,J)=HFY(I,J)-(RMASS*HINF(I,J)*A*(2*PI/T)**2)
            FY((I-1)*7+J)=HFY(I,J)
5       CONTINUE
10    CONTINUE
        READ(11,*)(HINF(143,J),J=1,6)
        READ(12,*)(HOUT(143,J),J=1,6)
        READ(13,*)(HFX(143,J),J=1,6)
        READ(14,*)(HFY(143,J),J=1,6)
```

```
      DO 20 J=1,6
        RINF(994+J)=HINF(143,J)
        ROUT(994+J)=HOUT(143,J)
        FX(994+J)=HFX(143,J)
        HFY(143,J)=HFY(143,J)-(RMASS*HINF(143,J)*A*(2*PI/T)**2)
        FY(994+J)=HFY(143,J)
 20     CONTINUE
      WRITE(*,*)'                    .... completed.',
      + ' (Ring Mass Force has been subtracted from Y-FORCE
      + signal).'
      NSAMPLES=INT(R)
      TELLER=AINT((NSAMPLES/PIECES))
      NTELLER=INT(TELLER)
      NPIECES=INT(PIECES)
      PART=CHAR(NPIECES+48)
      WRITE(15,IOSTAT=IOWRTE,FMT=999)RUNNUMBER
 999  FORMAT(A3)
      PRINT*,IOWRTE
      WRITE(15,1100)NPIECES,NTELLER
 1100   FORMAT(I3,I5)
      WRITE(15,1110)A,V,T
 1110   FORMAT(F8.3,F8.3,F8.3)
      NSTEP(1)=4
      NSTEP(2)=5
      NSTEP(3)=5
      NSTEP(4)=4
      STEP(1)=.2
      STEP(2)=.04
      STEP(3)=.008
      STEP(4)=.002
      CDMIN(0)=1.1
      CAMIN(0)=1.1
      WRITE(*,*)'Optimum values for Cd and Ca:'
      DO 100 I=1,4
        CDMIN(I)=CDMIN(I-1)
        CAMIN(I)=CAMIN(I-1)
        DO 150 L=-NSTEP(I),NSTEP(I)
          CD=CDMIN(I-1)+L*STEP(I)
          DO 200 J=-NSTEP(I),NSTEP(I)
            CA=CAMIN(I-1)+J*STEP(I)
            CRITF=0
            DO 300 K=1,NSAMPLES

          ALPHA=ATAN((2*PI*A*ROUT(K)/T)/V)
          FDMODEL=0.45*CD*(V**2+(2*PI*A*ROUT(K)/T)**2)*RHO/1000.
          FAMODEL=-0.042412*(2*PI/T)**2*A*RINF(K)*CA*RHO/1000.
          FXMODEL=FDMODEL*COS(ALPHA)
          FYMODEL=FAMODEL-FDMODEL*SIN(ALPHA)
          CRITF=CRITF+(FXMODEL-FX(K))**2+(FYMODEL-FY(K))**2

 300        CONTINUE
            IF ((I .EQ. 1) .AND. (L .EQ. -NSTEP(1))) THEN
              CRITFMIN=CRITF
            ENDIF
```

```
            IF (CRITF .LT. CRITFMIN) THEN
              CRITFMIN=CRITF
              CDMIN(I)=CD
              CAMIN(I)=CA
            ENDIF
200       CONTINUE
150     CONTINUE
        WRITE(*,1300)'Cd = ',CDMIN(I)
        WRITE(*,1300)'Ca = ',CAMIN(I)
100   CONTINUE
      YMAX1=0
      DO 400 K=1,NSAMPLES

    ALPHA=ATAN((2*PI*A*ROUT(K)/T)/V)
    FDMODEL=0.45*CDMIN(4)*(V**2+(2*PI*A*ROUT(K)/T)**2)*RHO/1000.
    FAMODEL=-0.042412*(2*PI/T)**2*A*RINF(K)*CAMIN(4)*RHO/1000.
    FXMODEL=FDMODEL*COS(ALPHA)
    FYMODEL=FAMODEL-FDMODEL*SIN(ALPHA)
    XLIFT(K)=FX(K)-FXMODEL
    YLIFT(K)=FY(K)-FYMODEL
    CLGUESS=MAX(ABS(YLIFT(K)/(.45*(V**2+(2*PI*A/T)*
       +       *2))*RHO/1000.),YMAX1)
    YMAX1=CLGUESS

400   CONTINUE
      WRITE(15,1140)CDMIN(4),CAMIN(4)
1140    FORMAT(F8.3,F8.3)
      WRITE(*,*)'Approximation for Cl:'
      WRITE(*,1300)'Cl ~ ',CLGUESS
      DO 500 II=1,NPIECES
        IF (NPIECES .GT. 1) THEN
          WRITE(*,1250)'Analysis of part ',II,' of the record:'
        ENDIF
1250    FORMAT(A18,I2,A16)
        NSTEP(1)=3
        NSTEP(2)=3
        NSTEP(3)=4
        NSTEP(4)=4
        STEP(1)=.02
        STEP(2)=.005
        STEP(3)=.001
        STEP(4)=.0002
        WRITE(*,*)'Optimum values for St and Phi(t=t0):'
        STRMIN(0)=.2
        CRITFMIN=1.E35
        DO 520 I=1,4
          STRMIN(I)=STRMIN(I-1)
          DO 540 J=-NSTEP(I),NSTEP(I)
            STR(II)=STRMIN(I-1)+J*STEP(I)
            DO 560 L=-5,6
              PHI=L*PI/6
              CRITF=0
```

```
              DO 580 K=((II-1)*NTELLER+1),(II*NTELLER)

     ALPHA=ATAN((2*PI*A*ROUT(K)/T)/V)
     PHI=PHI+(2*PI*STR(II)*SQRT(V**2+(2*PI*A*ROUT(K)/T)**2)/3)
     FLMODEL=0.45*CLGUESS*(V**2+(2*PI*A*ROUT(K)/T)**2)*
    +          SIN(PHI)*RHO/1000.

                IF (V .GT. .15) THEN
                  CRITF=CRITF+(YLIFT(K)-FLMODEL*COS(ALPHA))**2
                ELSE
                  CRITF=CRITF+(XLIFT(K)-FLMODEL*SIN(ALPHA))**2
                ENDIF
580           CONTINUE
              IF (CRITF .LT. CRITFMIN) THEN
                CRITFMIN=CRITF
                PHIMIN(II)=L*PI/6
                STRMIN(I)=STRMIN(I-1)+J*STEP(I)
              ENDIF
560         CONTINUE
540       CONTINUE
          WRITE(*,1300)'St = ',STRMIN(I)
          WRITE(*,1300)'Phi= ',PHIMIN(II)
520     CONTINUE
        STR(II)=STRMIN(4)
        WRITE(*,*)'Optimum value for Phi(t=t0):'
        NSTEP(1)=4
        NSTEP(2)=3
        NSTEP(3)=2
        STEP(1)=PI/30
        STEP(2)=PI/120
        STEP(3)=PI/360
        CRITFMIN=1.E35
        TPHIMIN(0)=PHIMIN(II)
        DO 600 I=1,3
          TPHIMIN(I)=TPHIMIN(I-1)
          DO 610 J=-NSTEP(I),NSTEP(I)
            CRITF=0
            PHI=TPHIMIN(I-1)+J*STEP(I)
            DO 620 K=((II-1)*NTELLER+1),(II*NTELLER)

      ALPHA=ATAN((2*PI*A*ROUT(K)/T)/V)
      PHI=PHI+(2*PI*STR(II)*SQRT(V**2+(2*PI*A*ROUT(K)/T)**2)/3)
      FLMODEL=0.45*CLGUESS*(V**2+(2*PI*A*ROUT(K)/T)**2)*
       +        SIN(PHI)*RHO/1000.

              IF (V .GT. .15) THEN
                CRITF=CRITF+(YLIFT(K)-FLMODEL*COS(ALPHA))**2
              ELSE
                CRITF=CRITF+(XLIFT(K)-FLMODEL*SIN(ALPHA))**2
              ENDIF
620         CONTINUE
            IF (CRITF .LT. CRITFMIN) THEN
              CRITFMIN=CRITF
              TPHIMIN(I)=TPHIMIN(I-1)+J*STEP(I)
              ENDPHI(II)=MOD(PHI,2*PI)
```

```
            IF (ENDPHI(II) .GT. (PI/2.)) THEN
              ENDPHI(II)=ENDPHI(II)-(1.5*PI)
            ELSE
              ENDPHI(II)=ENDPHI(II)+(.5*PI)
            ENDIF
          ENDIF
610      CONTINUE
         WRITE(*,1300)'Phi( t=t0 ) = ',TPHIMIN(I)
         WRITE(*,1300)'Phi(t=t0+P) = ',ENDPHI(II)
600    CONTINUE
1300   FORMAT(A15,F10.4)
       PHIMIN(II)=TPHIMIN(3)
       CRITFSTRPHI(II)=CRITFMIN
       WRITE(*,*)'Optimum value for Cl:'
       STEP(1)=.2
       STEP(2)=.05
       STEP(3)=.01
       STEP(4)=.002
       NSTEP(1)=5
       NSTEP(2)=3
       NSTEP(3)=4
       NSTEP(4)=4
       TCLMIN(0)=1.
       CRITFMIN=1.E35
       DO 700 I=1,4
         TCLMIN(I)=TCLMIN(I-1)
         DO 720 J=-NSTEP(I),NSTEP(I)
           CL=TCLMIN(I-1)+J*STEP(I)
           CRITF=0
           PHI=PHIMIN(II)
           DO 740 K=((II-1)*NTELLER+1),(II*NTELLER)

     ALPHA=ATAN((2*PI*A*ROUT(K)/T)/V)
     PHI=PHI+(2*PI*STR(II)*SQRT(V**2+(2*PI*A*ROUT(K)/T)**2)/3)
     FLMODEL=0.45*CL*(V**2+(2*PI*A*ROUT(K)/T)**2)*SIN(PHI)*
      +       RHO/1000.

             IF (V .GT. .15) THEN
               CRITF=CRITF+(YLIFT(K)-FLMODEL*COS(ALPHA))**2
             ELSE
               CRITF=CRITF+(XLIFT(K)-FLMODEL*SIN(ALPHA))**2
             ENDIF
740        CONTINUE
           IF (CRITF .LT. CRITFMIN) THEN
             CRITFMIN=CRITF
             TCLMIN(I)=TCLMIN(I-1)+J*STEP(I)
           ENDIF
720      CONTINUE
         WRITE(*,1300)'Cl = ',TCLMIN(I)
700    CONTINUE
       CLMIN(II)=TCLMIN(4)
       CRITFCL(II)=CRITFMIN
       WRITE(15,1120)CLMIN(II),STR(II),PHIMIN(II),ENDPHI(II)
1120   FORMAT(F8.3,F8.4,F10.6,F10.6)
500  CONTINUE
```

```
      AOUTF='FORCE'//RUNNUMBER//'.EX'//PART
      OPEN(16,FILE=AOUTF,STATUS='UNKNOWN',IOSTAT=IO16)
      PRINT*,'IO16=',IO16
      AOUTF='FORCE'//RUNNUMBER//'.MD'//PART
      OPEN(17,FILE=AOUTF,STATUS='UNKNOWN',IOSTAT=IO17)
      PRINT*,'IO17=',IO17
      STARTALPHA=ATAN((2*PI*A*ROUT(1)/T)/V)
      DO 800 I=1,2
        AVGSTR=0.
        AVGCL=0.
        WRITE((15+I),IOSTAT=IOWRTE,FMT=999)RUNNUMBER
        WRITE((15+I),'(2(5X,I5))')NPIECES,NTELLER
        WRITE((15+I),'(4(5X,F10.5))')A,V,T,RMASS
        WRITE((15+I),'(4(5X,F10.3))')CDMIN(4),
     +                                CAMIN(4),STARTALPHA,RHO
        DO 810 II=1,NPIECES
          WRITE((15+I),1120)CLMIN(II),STR(II),PHIMIN(II),
     +                      ENDPHI(II)
          AVGCL=AVGCL+CLMIN(II)
          AVGSTR=AVGSTR+STR(II)
810     CONTINUE
        AVGCL=AVGCL/NPIECES
        AVGSTR=AVGSTR/NPIECES
        WRITE((15+I),1130)AVGCL,AVGSTR
800   CONTINUE
      WRITE(15,1130)AVGCL,AVGSTR
1130    FORMAT(F10.3,F10.4)
      TCRITFX=0.
      TCRITFY=0.
      TSUMFX=0.
      TSUMFY=0.
      DO 830 K=1,NPIECES
        CRITFX=0.
        CRITFY=0.
        CRITFCDCA(K)=0.
        SUMCDCA=0.
        SUMFX=0.
        SUMFY=0.
        SUMCL=0.
        PHI=PHIMIN(K)
          DO 820 I=((K-1)*NTELLER+1),(K*NTELLER)
          WRITE(16,1500)(I*.02),FX(I),FY(I)

      ALPHA=ATAN((2*PI*A*ROUT(I)/T)/V)
      PHI=PHI+(2*PI*STR(K)*SQRT(V**2+(2*PI*A*ROUT(I)/T)**2)/3)
      FLMODEL=0.45*CLMIN(K)*(V**2+(2*PI*A*ROUT(I)/T)*
     +     *2)*SIN(PHI)*RHO/1000.
      FDMODEL=0.45*CDMIN(4)*(V**2+(2*PI*A*ROUT(I)/T)*
     +     *2)*RHO/1000.
        FAMODEL=-0.042412*(2*PI/T)*
     +       *2*A*RINF(I)*CAMIN(4)*RHO/1000.
        FXMODEL=FDMODEL*COS(ALPHA)+FLMODEL*SIN(ALPHA)
        FYMODEL=FAMODEL-FDMODEL*SIN(ALPHA)+FLMODEL*COS(ALPHA)
        CRITFCDCA(K)=CRITFCDCA(K)+XLIFT(I)**2+YLIFT(I)**2
```

```
      CRITFX=CRITFX+(FX(I)-FXMODEL)**2
      TCRITFX=TCRITFX+(FX(I)-FXMODEL)**2
      CRITFY=CRITFY+(FY(I)-FYMODEL)**2
      TCRITFY=TCRITFY+(FY(I)-FYMODEL)**2
      SUMCDCA=SUMCDCA+(FX(I)-XLIFT(I))**2+(FY(I)-YLIFT(I))**2
      SUMCL=SUMCL+(FLMODEL*COS(ALPHA))**2
      SUMFX=SUMFX+FXMODEL**2
      TSUMFX=TSUMFX+FXMODEL**2
      SUMFY=SUMFY+FYMODEL**2
      TSUMFY=TSUMFY+FYMODEL**2
      WRITE(17,1500)(I*.02),FXMODEL,FYMODEL
      WRITE(18,*)(I*.02),FY(I)
      WRITE(19,*)(I*.02),XLIFT(I)
      WRITE(20,*)(I*.02),YLIFT(I)
      WRITE(21,*)(I*.02),FY(I)-FYMODEL
      WRITE(22,*)(I*.02),FX(I)-FXMODEL
1500      FORMAT(F6.2,F8.4,F8.4)
820   CONTINUE
    CDCACRITF=CRITFCDCA(K)/SUMCDCA
    STRPHICRITF=CRITFSTRPHI(K)/SUMCL
    CLCRITF=CRITFCL(K)/SUMCL
    WRITE(15,1510)CDCACRITF,STRPHICRITF,CLCRITF
    CRITFX=CRITFX/SUMFX
    CRITFY=CRITFY/SUMFY
    WRITE(15,1520)CRITFX,CRITFY
    WRITE(*,1520)CRITFX,CRITFY
1510    FORMAT(E10.3,E10.3,E10.3)
1520    FORMAT(E10.3,E10.3)
830 CONTINUE
  TCRITFX=TCRITFX/TSUMFX
  TCRITFY=TCRITFY/TSUMFY
  WRITE(*,1520)TCRITFX,TCRITFY
  WRITE(15,1520)TCRITFX,TCRITFY
10000 CONTINUE
      WRITE(*,*)'Program ANALYSIS has been executed.'
      END
```

```
      PROGRAM DATA1

      REAL A(150),V(150),T(150),CD(150),CA(150),CL(150),
     +PHISHIFT(9),STR(150),CRITFX(150),CRITFY(150)
      INTEGER RUNNUMBER(150)
      OPEN(10,FILE='UITVOER1',STATUS='UNKNOWN')
      OPEN(11,FILE='UITVOER2',STATUS='UNKNOWN')
      OPEN(12,FILE='UITVOER3',STATUS='UNKNOWN')
      DO 100 N=1,150
        READ(10,*,END=10000)RUNNUMBER(N)
        WRITE(*,*)N
        READ(10,*)PIECES,TELLER
        NPIECES=INT(PIECES)
        NN=INT(PIECES*TELLER)
        READ(10,*)A(N),V(N),T(N)
        READ(10,*)CD(N),CA(N)
        PHI0=0.
        PI=3.1415927
        DO 10 I=1,NPIECES
          READ(10,*)DUMMY1,DUMMY2,PHI1,PHI2
          PHISHIFT(I)=PHI1-PHI0
          IF (ABS(PHISHIFT(I)) .GT. PI) THEN
            IF (PHISHIFT(I) .LT. 0.) THEN
              PHISHIFT(I)=PHISHIFT(I)+2*PI
            ELSE
              PHISHIFT(I)=PHISHIFT(I)-2*PI
            ENDIF
          ENDIF
          PHI0=PHI2
10      CONTINUE
        WRITE(12,'(I3,9(1X,F7.4))')RUNNUMBER(N),
     +        (PHISHIFT(J),J=1,NPIECES)
        READ(10,*)CL(N),STR(N)
        DO 20 I=1,NPIECES
          READ(10,*)DUMMY3
          READ(10,*)DUMMY4
20      CONTINUE
        READ(10,*)CRITFX(N),CRITFY(N)
100   CONTINUE
10000 CONTINUE
      DO 200 I=1,(N-1)
        WRITE(11,1100)RUNNUMBER(I),CD(I),CA(I),CL(I),STR(I),
     +        A(I),V(I),T(I),CRITFX(I),CRITFY(I)
200   CONTINUE
1100  FORMAT(I3,F6.3,F6.3,F6.3,F7.4,F6.3,F6.3,F6.3,
     +      E10.3,E10.3)
      WRITE(*,*)'Program DATA1 has been executed.'
      END
```

```
      PROGRAM RESULTS

      CHARACTER INPUTF*12
      REAL FX(150,6),X(150,3),CONSTANT(5,3),Y(3,150,5),
     +GY(3,150,6),COLUMN(0:3,150,6)
      INTEGER JMAX(3)
      OPEN(10,FILE='INVOER6',STATUS='UNKNOWN',IOSTAT=IOOPEN)
      WRITE(*,*)IOOPEN
      OPEN(12,FILE='UITVOER8',STATUS='UNKNOWN',IOSTAT=IOOPEN)
      WRITE(*,*)IOOPEN
      READ(10,*)NUMBEROFFILES
      DO 5 I=1,3
        READ(10,*)(CONSTANT(I,L),L=1,3)
5     CONTINUE
      DO 10 I=4,5
        DO 15 L=1,3
          CONSTANT(I,L)=CONSTANT((I-3),L)
15      CONTINUE
10    CONTINUE
      DO 20000 NUMBEROFFILE=1,NUMBEROFFILES
        READ(10,*)INPUTF
        OPEN(11,FILE=INPUTF,STATUS='UNKNOWN',IOSTAT=IOOPEN)
        WRITE(*,*)IOOPEN
        REWIND 11
        DO 25 J=1,150
          READ(11,*,END=30)NUMBEROFRUN,(FX(J,I),I=1,4),
     +              (X(J,I),I=1,3),(FX(J,I),I=5,6)
25      CONTINUE
30      CONTINUE
        NRUNS=J-1
        WRITE(*,*)NRUNS
        DO 35 I=1,3
          J=0
          DO 40 N=1,NRUNS
            IF (ABS(X(N,I)-CONSTANT(I,2)) .LT. .005) THEN
              J=J+1
              DO 45 L=1,3
                Y(I,J,L)=X(N,L)
45            CONTINUE
              DO 50 L=4,5
                Y(I,J,L)=X(N,(L-3))
50            CONTINUE
              DO 55 K=1,6
                GY(I,J,K)=FX(N,K)
55            CONTINUE
            ENDIF
40        CONTINUE
          JMAX(I)=J
35      CONTINUE
        OPEN(13,FILE='UITVOER8.CON',STATUS='UNKNOWN',
     +       IOSTAT=IOOPEN)
        WRITE(*,*)IOOPEN
        OPEN(14,FILE='UITVOER8.STR',STATUS='UNKNOWN',
     +       IOSTAT=IOOPEN)
        WRITE(*,*)IOOPEN
```

```
      OPEN(15,FILE='UITVOER8.CRT',STATUS='UNKNOWN',
     +       IOSTAT=IOOPEN)
      WRITE(*,*)IOOPEN
      DO 60 I=1,3
        DO 65 L=1,2
          NN=INT(2./L)
          WRITE(13,1210)CONSTANT(I,2),(CONSTANT((
     +                    I+NN),J),J=1,3)
          WRITE(14,1210)CONSTANT(I,2),(CONSTANT((
     +                    I+NN),J),J=1,3)
          WRITE(15,1210)CONSTANT(I,2),(CONSTANT((
     +                    I+NN),J),J=1,3)
          WRITE(13,*)' '
          WRITE(14,*)' '
          WRITE(15,*)' '
          DO 70 N=1,JMAX(I)
            DO 72 K=1,6
              COLUMN(0,N,K)=Y(I,N,(I+L))
              DO 75 J=1,3
                IF (ABS(Y(I,N,(I+NN))-CONSTANT((
     +                I+NN),J)) .LT. .005) THEN
                  COLUMN(J,N,K)=GY(I,N,K)
                ELSE
                  COLUMN(J,N,K)=-1.
                ENDIF
75            CONTINUE
72          CONTINUE
70        CONTINUE
          NMAX=N-1
          DO 90 K=1,3
            DO 110 N=1,NMAX
              WRITE(13,1210)(COLUMN(J,N,K),J=0,3)
110         CONTINUE
            WRITE(13,*)' '
90        CONTINUE
          DO 130 N=1,NMAX
            WRITE(14,1230)(COLUMN(J,N,4),J=0,3)
130       CONTINUE
          WRITE(14,*)' '
          DO 100 K=5,6
            DO 120 N=1,NMAX
              WRITE(15,1240)(COLUMN(J,N,K),J=0,3)
120         CONTINUE
            WRITE(15,*)' '
100       CONTINUE
65      CONTINUE
60    CONTINUE
1210  FORMAT(F7.3,F10.3,F10.3,F10.3)
1230  FORMAT(F7.3,F10.4,F10.4,F10.4)
1240  FORMAT(F7.3,E10.3,E10.3,E10.3)
20000 CONTINUE
      WRITE(*,*)'Program RESULTS has been executed.'
      END
```

```
      PROGRAM RINGMASS

      CHARACTER INPUTF*12,OUTPUTF*12,RUNNUMBER*3,RING*1
      REAL RINF(1000),FY(1000),HINF(145,7),HFY(145,7),MASS
      OPEN(10,FILE='INVOER5',STATUS='UNKNOWN')
      PI=3.1415927
      DO 9999 NUMBEROFRUNS=1,150
        READ(10,*,END=10000)RUNNUMBER,RING,A,T
        INPUTF='RFINF'//RUNNUMBER//'.ASC'
        OPEN(11,FILE=INPUTF,STATUS='UNKNOWN')
        REWIND 11
        INPUTF='Y'//RING//'R'//RUNNUMBER//'.ASC'
        OPEN(12,FILE=INPUTF,STATUS='UNKNOWN')
        REWIND 12
        READ(11,*)DUMMY1,R
        READ(12,*)DUMMY2,R
        NSAMPLES=INT(R)
        SUMFACCELERATION=0.
        SUMFMEASURED=0.
        DO 10 I=1,142
          READ(11,*)(HINF(I,J),J=1,7)
          READ(12,*)(HFY(I,J),J=1,7)
          DO 5 J=1,7
            RINF((I-1)*7+J)=HINF(I,J)
            FY((I-1)*7+J)=HFY(I,J)
5         CONTINUE
10      CONTINUE
        READ(11,*)(HINF(143,J),J=1,6)
        READ(12,*)(HFY(143,J),J=1,6)
        DO 15 J=1,6
          RINF(994+J)=HINF(143,J)
          FY(994+J)=HFY(143,J)
15      CONTINUE
        DO 20 I=1,NSAMPLES
          SUMFMEASURED=SUMFMEASURED+ABS(FY(I))
          SUMFACCELERATION=SUMFACCELERATION+
     +      ABS((2*PI/T)**2*A*RINF(I))
20      CONTINUE
        MASS=SUMFMEASURED/SUMFACCELERATION
        OUTPUTF='RNG'//RING//'R'//RUNNUMBER//'.MAS'
        OPEN(13,FILE=OUTPUTF,STATUS='UNKNOWN')
        WRITE(13,*)RUNNUMBER,RING,MASS
        WRITE(*,*)RUNNUMBER,RING,MASS
        DO 500 I=1,NSAMPLES
          RINGMASSFORCE=-(2*PI/T)**2*A*RINF(I)*MASS
          WRITE(13,*)(.02*I),RINF(I),FY(I),RINGMASSFORCE
500     CONTINUE
9999  CONTINUE
10000 CONTINUE
      END
```

PROGRAM RELEVAT5

This program is almost the same as ANALYSIS. The differences are:

- The variable FREQ (and fellow variables) is used instead of STR;
- The output file UITVOER5 is used instead of UITVOER1;
- The following description of the lift force phase has been used:
  PHI=PHI+(2*PI*FREQ(K)*0.02)
  instead of:
  PHI=PHI+(2*PI*STR(K)*SQRT(V**2+(2*PI*A*ROUT(I)/T)**2)/3);
- The values for NSTEP and STEP where the lift force frequency is determined are different:

I	NSTEP	STEP
1	7	0.2
2	3	0.05
3	4	0.01
4	4	0.002

FREQMIN(0)=3.0

- The output file *.FR has been used instead of *.MD.

PROGRAM DATA5

This program differs only from DATA1 where the output files are defined. DATA5 uses UITVOER5, UITVOER6 and UITVOER7 instead of UITVOER1, UITVOER2 and UITVOER3, respectively.

APPENDIX G: RESULTS OF ANALYSIS

APPENDIX G: RESULTS OF ANALYSIS

TABLE OF CONTENTS

Listing of Output Parameters (Model I)

Run: (no.)	Cd: (-)	Ca: (-)	Cl: (-)	St: (-)	A: (m)	V: (m/s)	T: (s)	CritfX: (-)	CritfY: (-)
46	1.140	.574	.511	.1773	.270	.750	1.700	.695E-01	.628E-01
45	1.086	.052	.638	.1778	.270	.100	1.700	.106E+01	.137E+00
55	1.000	.636	.276	.1865	.270	.750	3.000	.251E-01	.733E-01
51	1.210	.772	.722	.1828	.270	.750	1.500	.603E-01	.493E-01
57	1.126	.530	.497	.1636	.300	.750	1.700	.927E-01	.846E-01
69	.926	.696	.226	.1797	.120	.750	1.700	.154E-01	.714E-01
49	.854	.744	.106	.1841	.270	1.500	1.700	.102E-01	.402E-01
47	1.306	.370	.825	.1330	.270	.500	1.700	.293E+00	.641E-01
36	.900	.300	.185	.1874	.000	.750	1.700	.706E-02	.487E+00
56	1.074	.052	.525	.1661	.300	.100	1.700	.172E+01	.120E+00
68	1.904	1.014	2.198	.1228	.120	.100	1.700	.901E+00	.949E-01
71	1.074	.464	.391	.1813	.270	.500	3.000	.599E-01	.549E-01
77	1.288	.146	1.000	.1344	.270	.500	1.500	.251E+00	.567E-01
78	.744	.814	.050	.1628	.270	1.500	3.000	.389E-02	.646E-01
86	.802	.752	.072	.1780	.270	1.500	1.500	.112E-01	.438E-01
92	.974	.806	.159	.1895	.120	.750	3.000	.895E-02	.148E+00
97	1.210	.236	.529	.1529	.300	.500	1.700	.352E+00	.645E-01
100	.956	.490	.172	.1794	.300	.750	3.000	.266E-01	.502E-01
101	.786	.708	.075	.1736	.300	1.500	1.700	.100E-01	.391E-01
106	1.102	.582	.492	.1767	.300	.750	1.500	.818E-01	.379E-01
112	1.012	.612	.248	.1866	.120	.750	1.500	.155E-01	.748E-01
113	1.226	.190	1.015	.1799	.120	.500	1.700	.363E-01	.593E-01
115	.716	.762	.035	.1618	.120	1.500	1.700	.389E-02	.145E+00
136	.944	.052	.624	.2106	.270	.005	1.700	.890E+00	.132E+00
54	.942	.610	.189	.1800	.270	.750	2.500	.203E-01	.501E-01
53	.984	.590	.264	.1921	.270	.750	2.000	.340E-01	.494E-01
52	1.032	.624	.311	.1761	.270	.750	1.850	.482E-01	.610E-01
50	1.162	.586	.607	.1791	.270	.750	1.600	.599E-01	.570E-01
67	.980	.692	.291	.1886	.180	.750	1.700	.234E-01	.637E-01
65	1.014	.618	.372	.1881	.210	.750	1.700	.292E-01	.479E-01
63	1.034	.596	.357	.1764	.240	.750	1.700	.392E-01	.603E-01
61	1.056	.554	.423	.1831	.255	.750	1.700	.551E-01	.574E-01
59	1.102	.560	.460	.1723	.285	.750	1.700	.720E-01	.652E-01
48	.982	.626	.224	.1892	.270	1.000	1.700	.222E-01	.541E-01
72	1.184	.346	.699	.1751	.270	.500	2.500	.658E-01	.569E-01
73	1.158	.460	.477	.1790	.270	.500	2.000	.111E+00	.471E-01
74	1.182	.378	.536	.1549	.270	.500	1.850	.238E+00	.663E-01
76	1.276	.052	.906	.1356	.270	.500	1.600	.307E+00	.693E-01
119	.914	.558	.170	.1843	.180	.750	3.000	.183E-01	.100E+00
124	.916	.518	.164	.1844	.210	.750	3.000	.177E-01	.682E-01
129	.922	.572	.197	.1778	.240	.750	3.000	.243E-01	.685E-01
134	.920	.506	.170	.1902	.255	.750	3.000	.224E-01	.566E-01
144	.896	.514	.187	.1889	.285	.750	3.000	.214E-01	.390E-01
88	.870	.594	.134	.1810	.270	1.000	3.000	.807E-02	.578E-01
103	.966	.464	.217	.1831	.300	.750	2.500	.269E-01	.379E-01
102	.988	.428	.239	.1863	.300	.750	2.000	.488E-01	.472E-01
104	1.010	.454	.280	.1769	.300	.750	1.850	.613E-01	.517E-01
105	1.110	.412	.524	.1705	.300	.750	1.600	.107E+00	.604E-01
118	.730	.852	.043	.1628	.180	1.500	1.700	.520E-02	.678E-01
123	.722	.818	.032	.1617	.210	1.500	1.700	.507E-02	.489E-01

Listing of Output Parameters (Model I)

Run: (no.)	Cd: (-)	Ca: (-)	Cl: (-)	St: (-)	A: (m)	V: (m/s)	T: (s)	CritfX: (-)	CritfY: (-)
79	.752	.758	.051	.1651	.270	1.500	2.500	.505E-02	.548E-01
80	.774	.744	.063	.1699	.270	1.500	2.000	.502E-02	.431E-01
81	.758	.756	.048	.1720	.270	1.500	1.850	.693E-02	.410E-01
84	.776	.700	.056	.1717	.270	1.500	1.600	.832E-02	.357E-01
120	.940	.524	.198	.1809	.180	.750	1.500	.283E-01	.604E-01
125	1.012	.556	.376	.1851	.210	.750	1.500	.556E-01	.732E-01
130	1.028	.606	.415	.1905	.240	.750	1.500	.490E-01	.644E-01
135	1.032	.596	.390	.1839	.255	.750	1.500	.594E-01	.671E-01
145	1.056	.560	.426	.1786	.285	.750	1.500	.555E-01	.410E-01
85	.944	.506	.262	.1791	.270	1.000	1.500	.325E-01	.657E-01
107	.980	.536	.179	.1836	.120	.750	2.500	.226E-01	.120E+00
108	1.004	.626	.231	.1838	.120	.750	2.000	.218E-01	.938E-01
109	.970	.614	.149	.1857	.120	.750	1.850	.121E-01	.750E-01
111	.998	.584	.209	.1873	.120	.750	1.600	.127E-01	.715E-01
117	1.290	.168	.978	.1590	.180	.500	1.700	.103E+00	.834E-01
122	1.276	.222	.974	.1459	.210	.500	1.700	.157E+00	.700E-01
127	1.280	.180	.985	.1377	.240	.500	1.700	.194E+00	.718E-01
132	1.216	.282	.744	.1366	.255	.500	1.700	.285E+00	.575E-01
142	1.164	.346	.554	.1509	.285	.500	1.700	.284E+00	.567E-01
114	.830	.626	.132	.1822	.120	1.000	1.700	.796E-02	.817E-01
34	.886	.252	.232	.1864	.000	.500	1.700	.189E-01	.478E+00
37	.748	.060	.068	.1739	.000	1.500	1.700	.469E-02	.671E+00
35	.842	.052	.105	.1837	.000	1.000	1.700	.504E-02	.845E+00
172	.728	.052	.049	.1505	.000	2.000	1.700	.102E-01	.211E+01
128	.746	.762	.060	.1637	.240	1.500	1.700	.648E-02	.417E-01
133	.742	.728	.062	.1685	.255	1.500	1.700	.895E-02	.387E-01
143	.752	.746	.059	.1738	.285	1.500	1.700	.881E-02	.405E-01
99	.892	.464	.160	.1818	.300	1.000	1.700	.300E-01	.490E-01
66	1.388	.306	.804	.2146	.180	.100	1.700	.166E+01	.124E+00
64	1.234	.190	.651	.1800	.210	.100	1.700	.168E+01	.151E+00
62	1.182	.104	.642	.1711	.240	.100	1.700	.101E+01	.138E+00
60	1.106	.052	.722	.1833	.255	.100	1.700	.822E+00	.147E+00
58	1.050	.146	.634	.1981	.285	.100	1.700	.157E+01	.138E+00
116	1.238	.052	.810	.1816	.180	.005	1.700	.120E+01	.152E+00
121	1.102	.052	.725	.2050	.210	.005	1.700	.103E+01	.143E+00
126	1.042	.052	.636	.1949	.240	.005	1.700	.102E+01	.142E+00
131	.946	.052	.660	.2129	.255	.005	1.700	.107E+01	.144E+00
141	.886	.052	.517	.2171	.285	.005	1.700	.129E+01	.148E+00

(table G1)

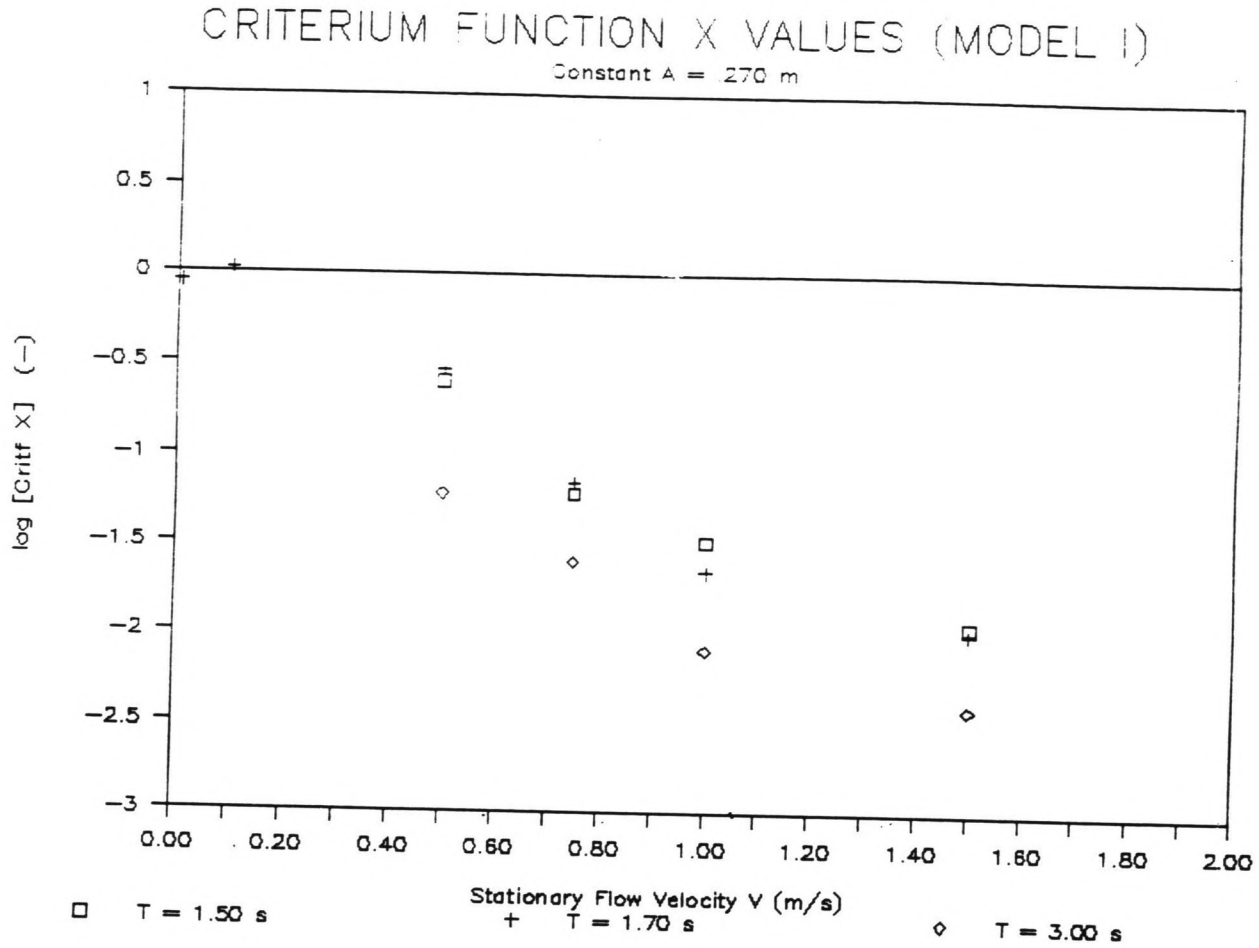

FIGURE G1.1

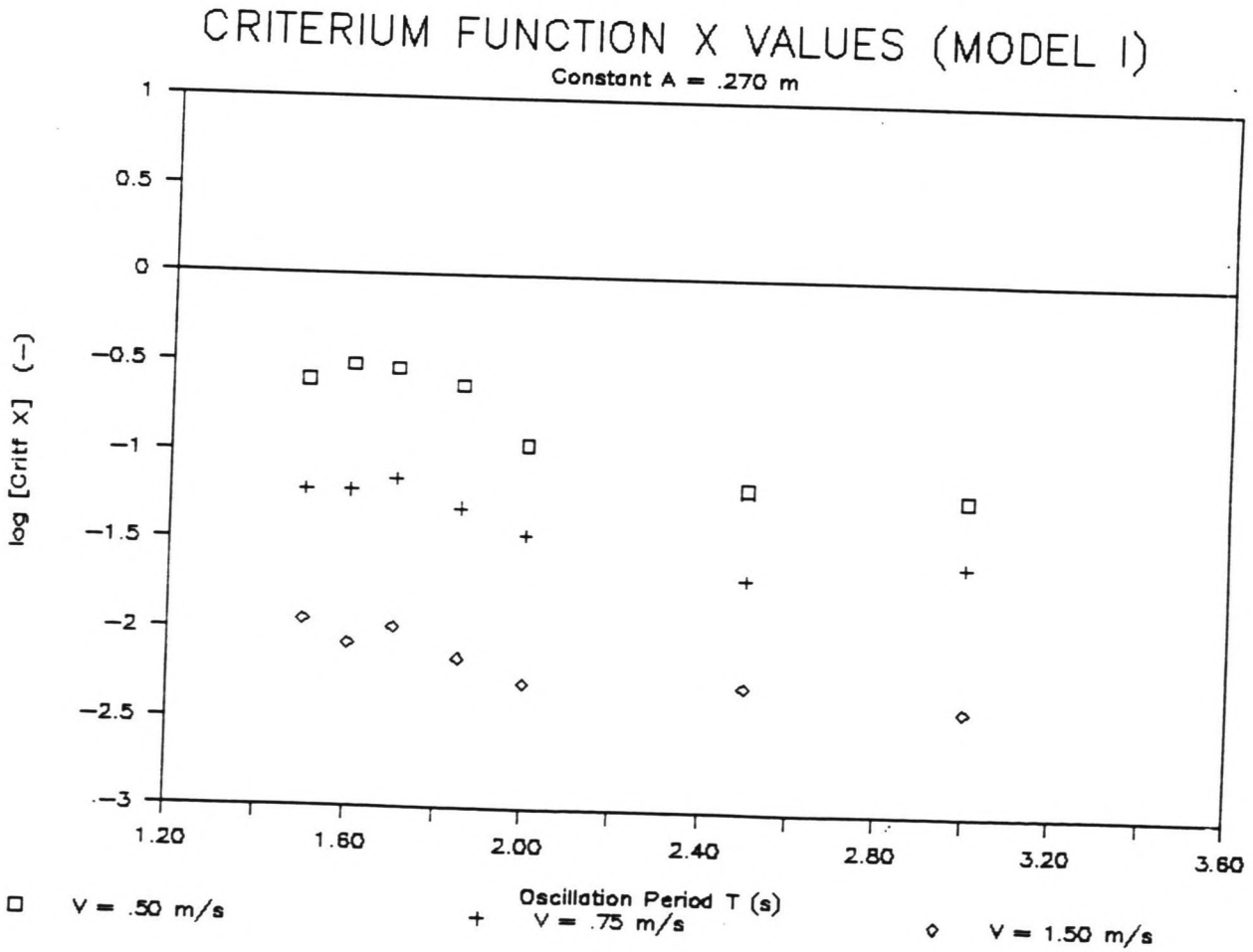

FIGURE G1.2

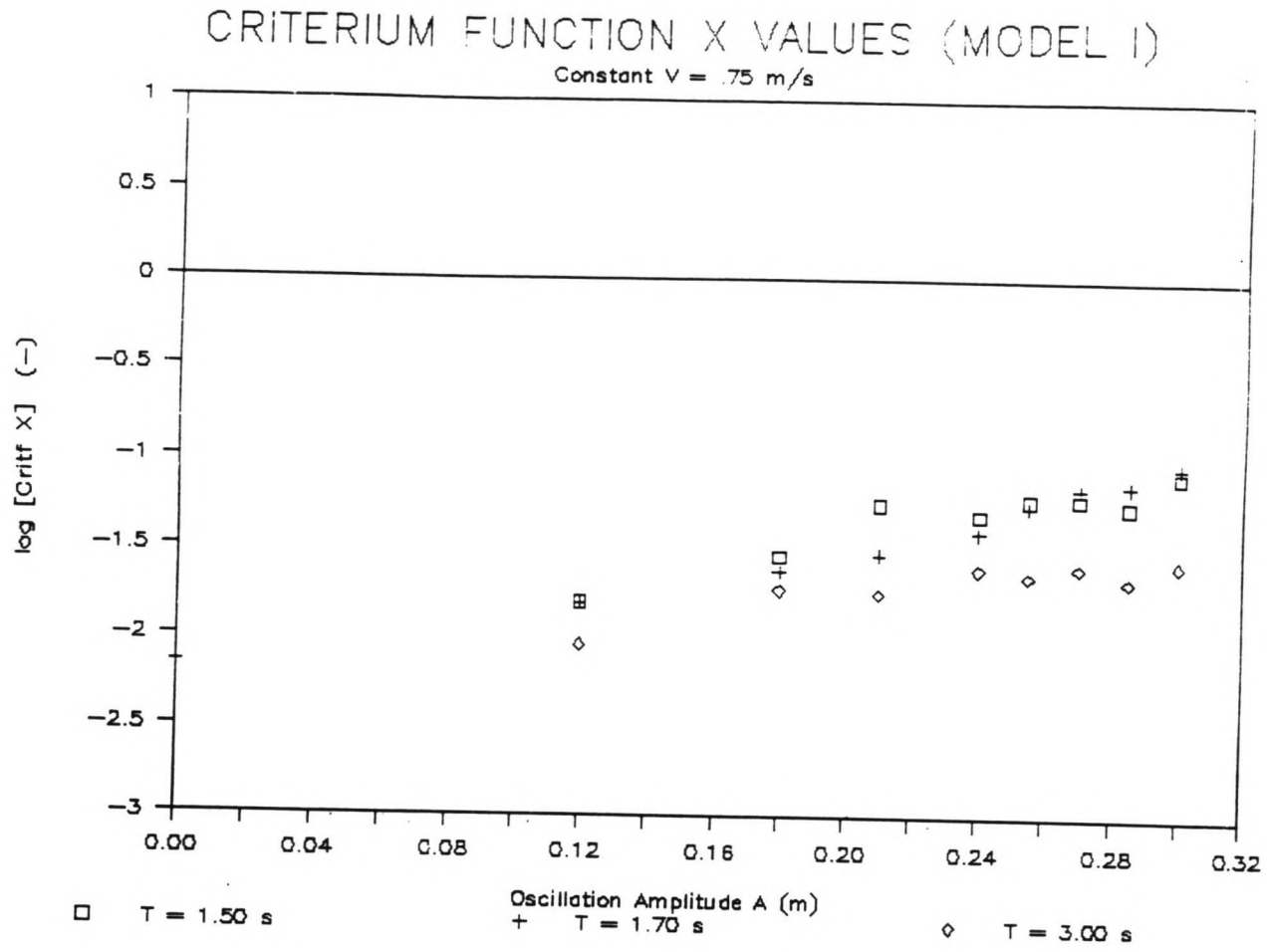

FIGURE G1.3

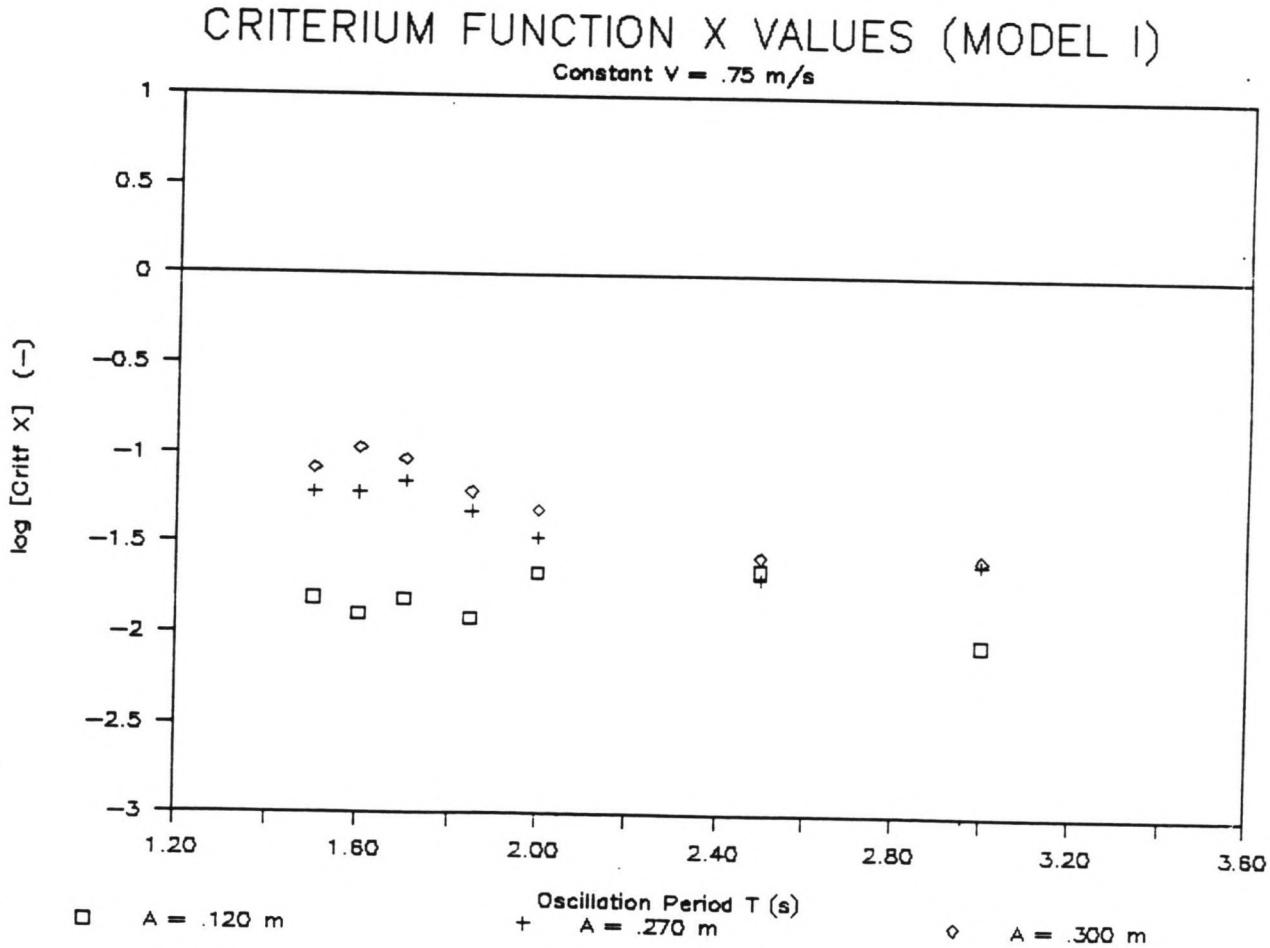

FIGURE G1.4

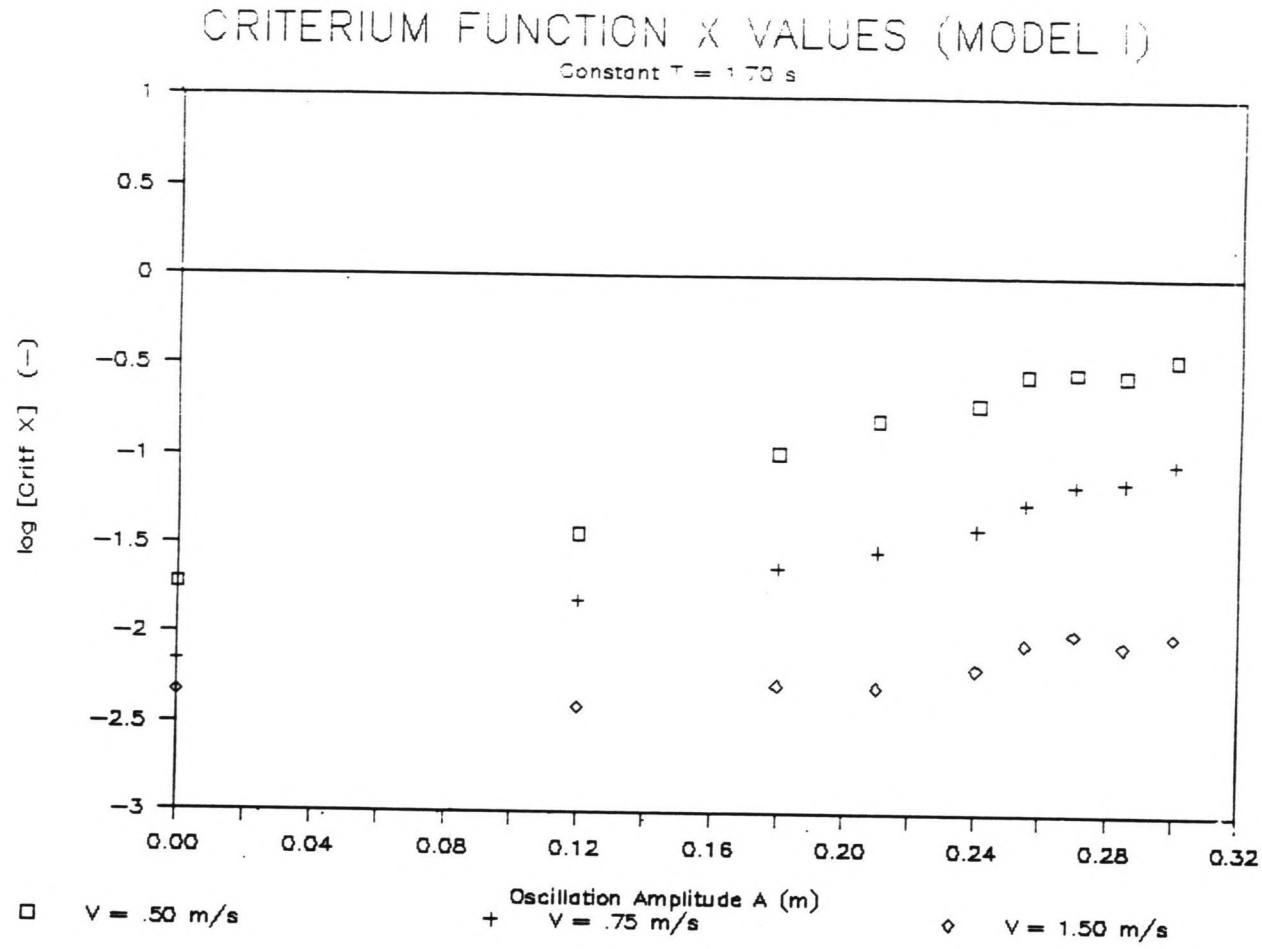

FIGURE G1.5

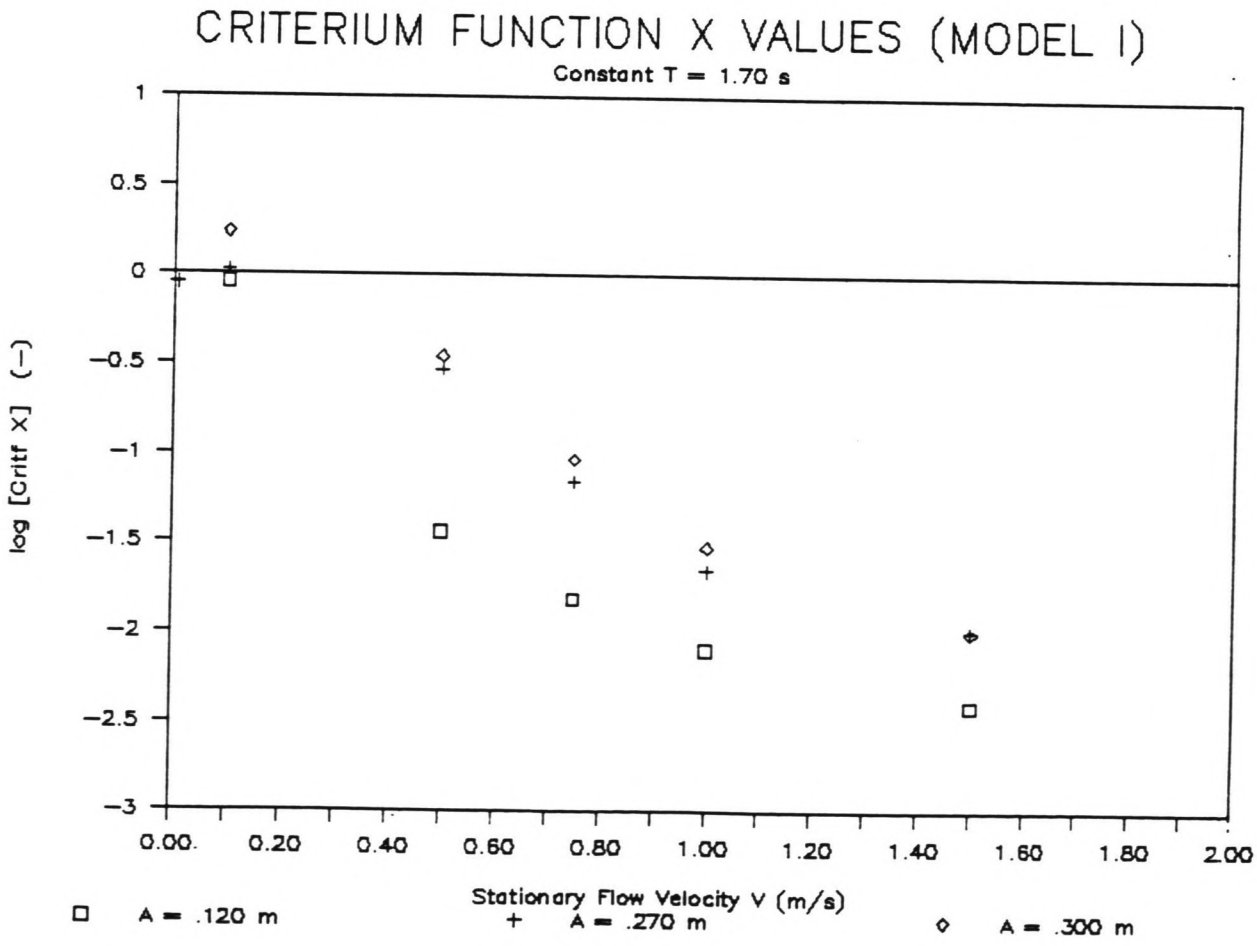

FIGURE G1.6

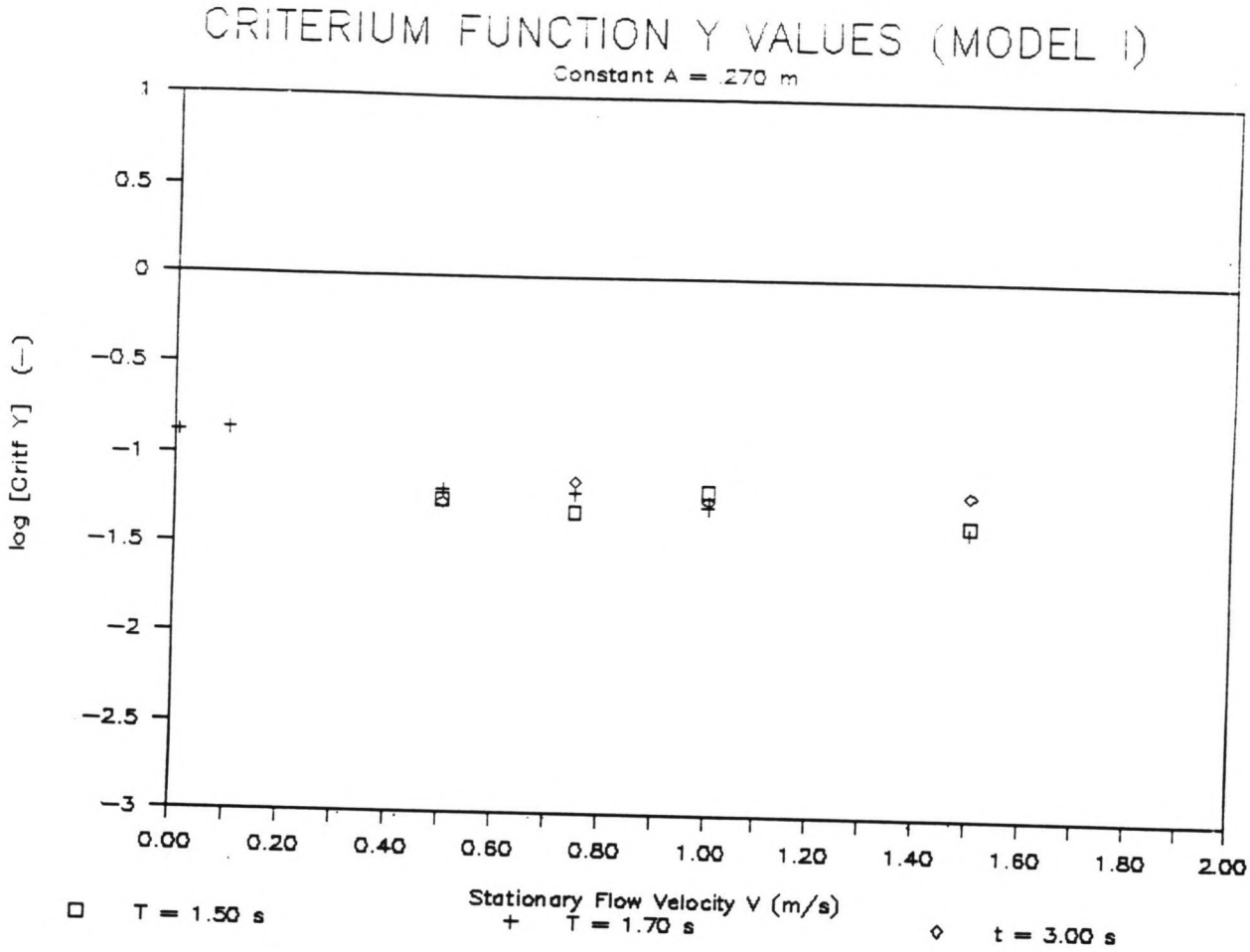

FIGURE G2.1

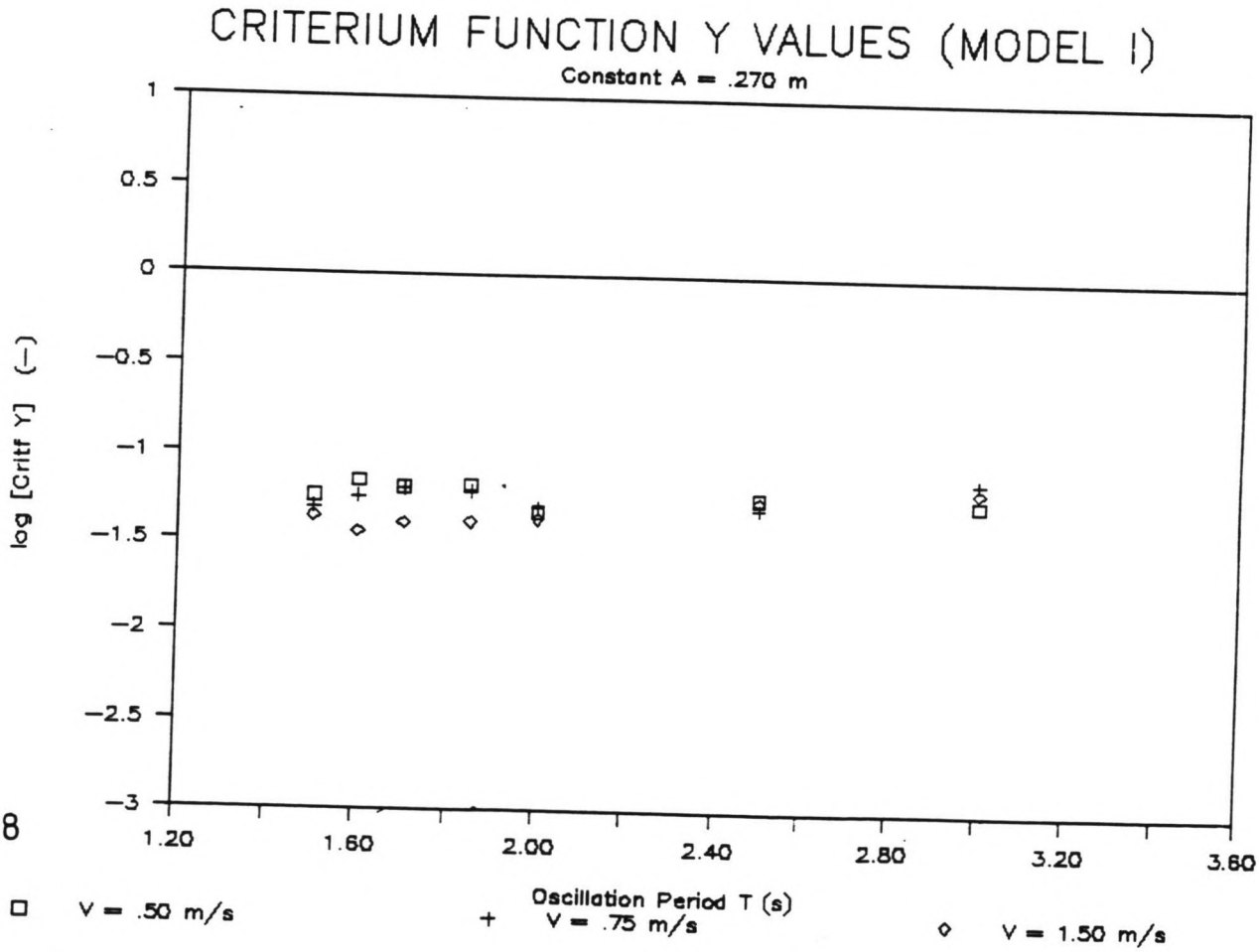

FIGURE G2.2

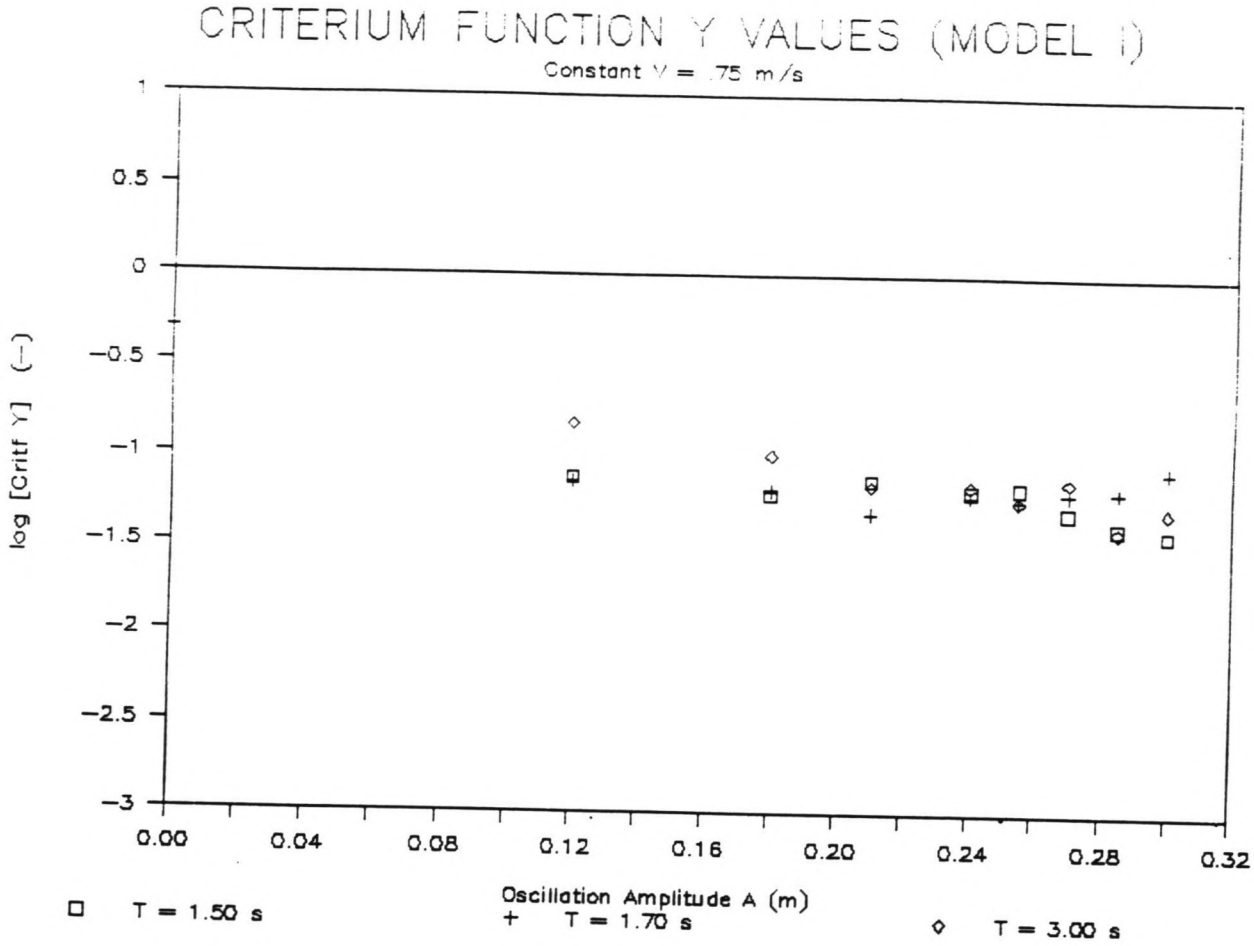

FIGURE G2.3

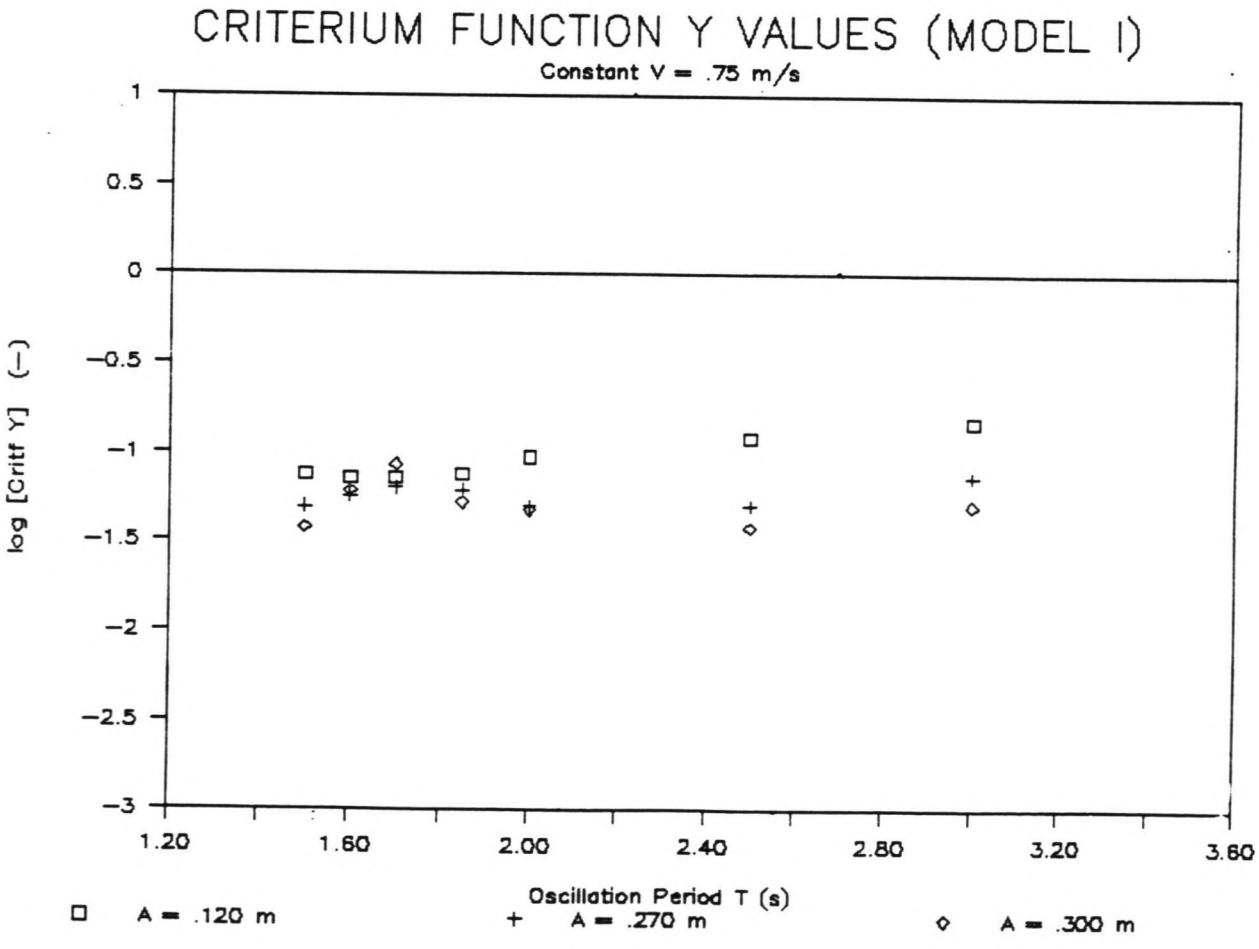

FIGURE G2.4

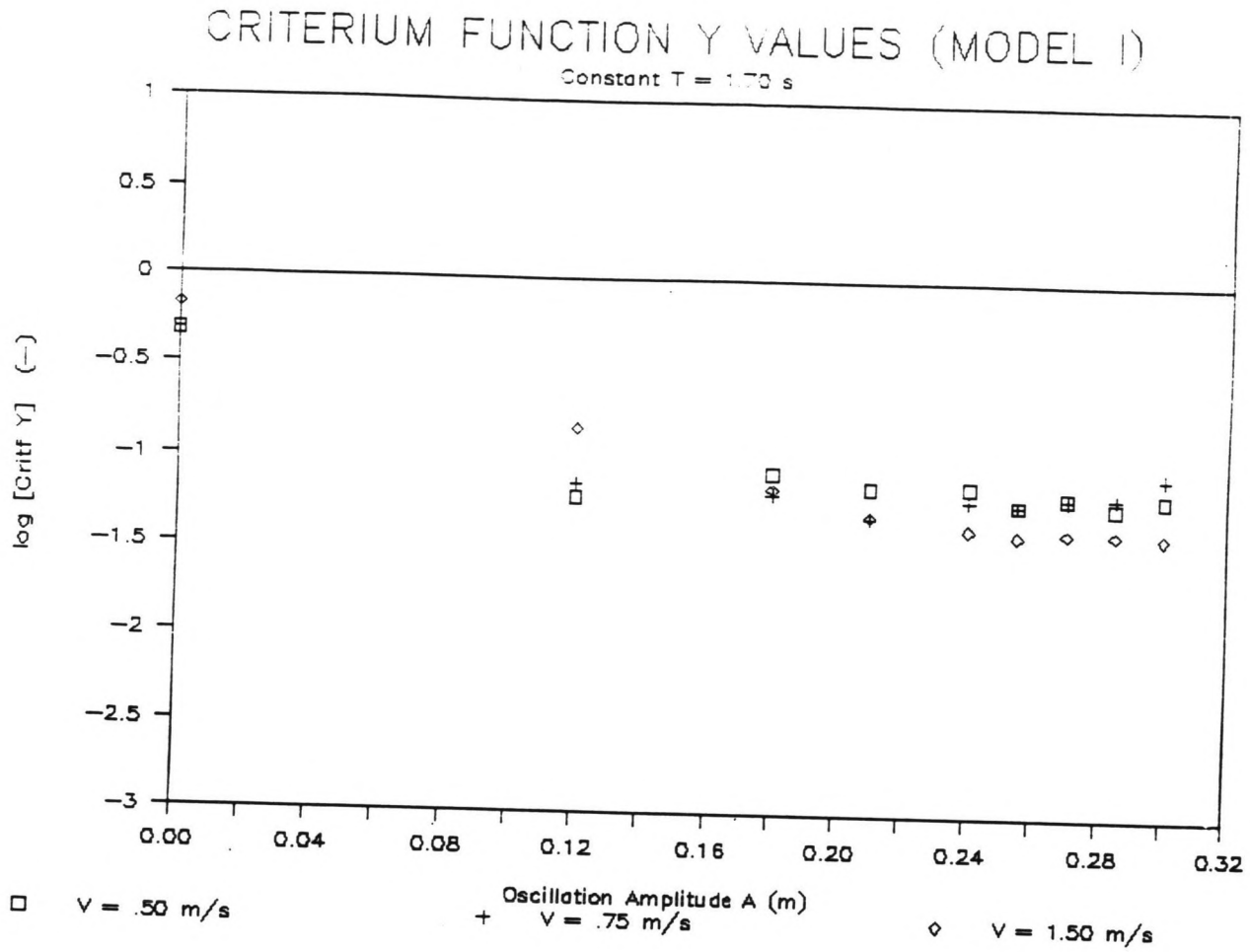

FIGURE G2.5

FIGURE G2.6

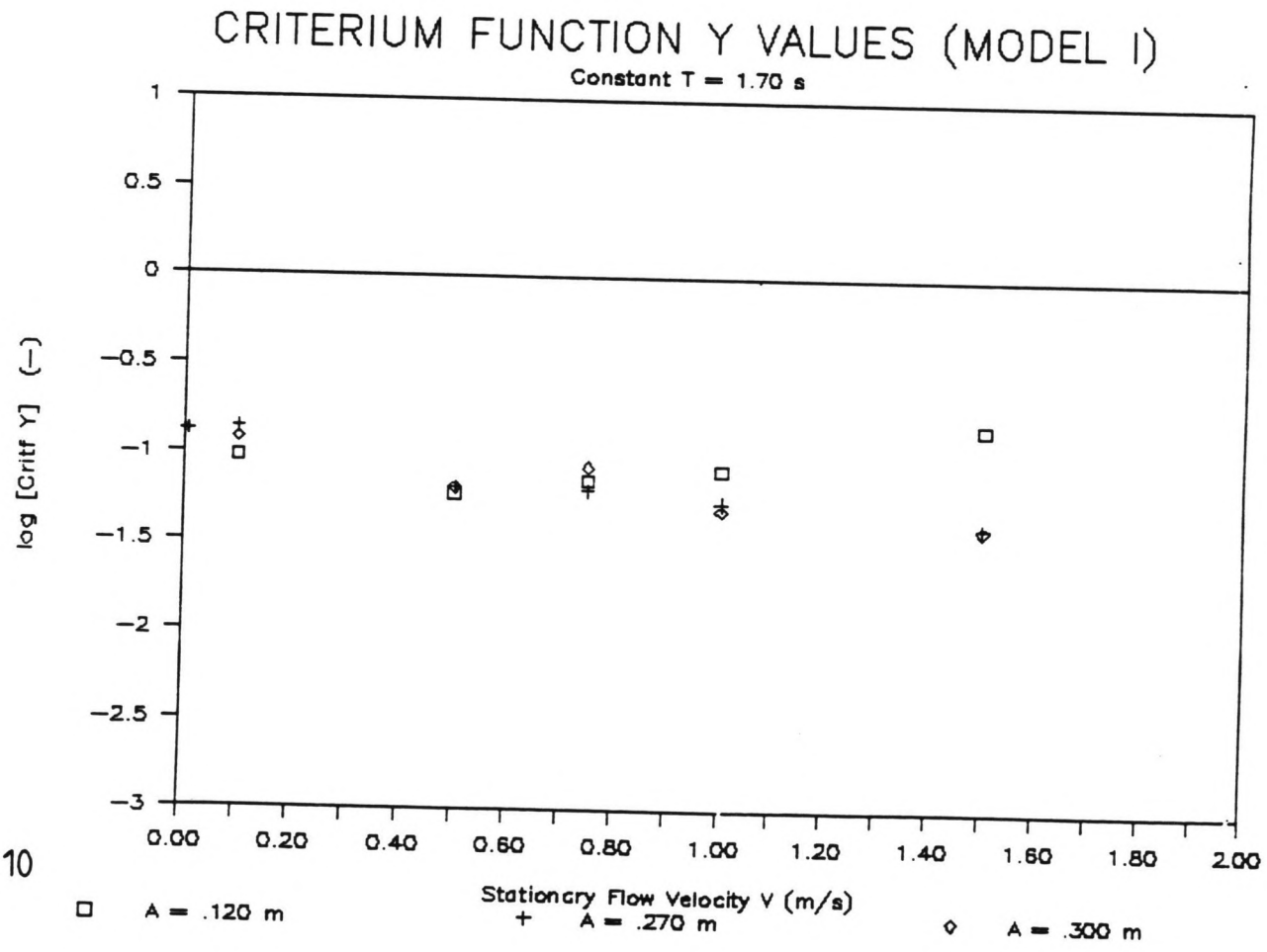

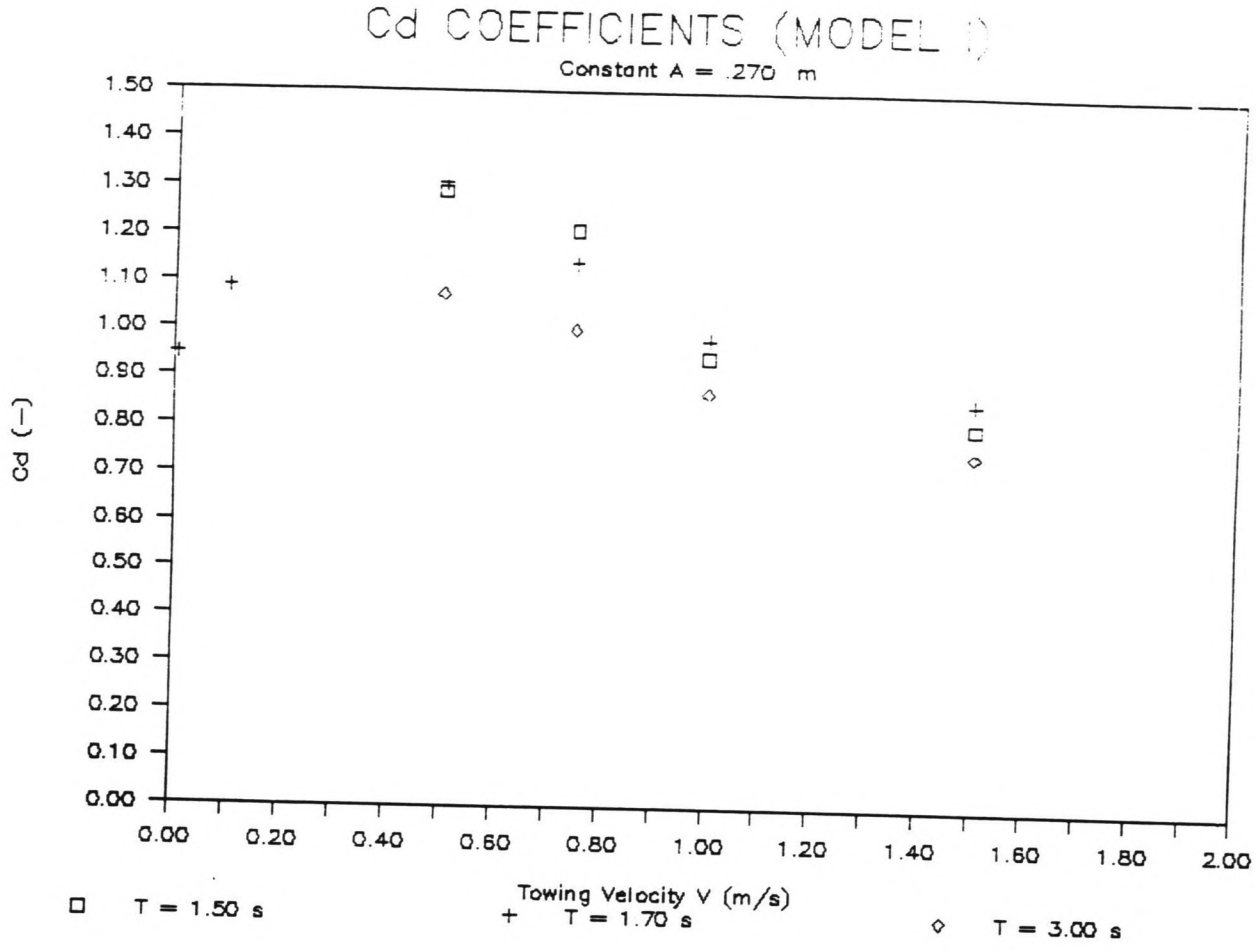

FIGURE G3.1

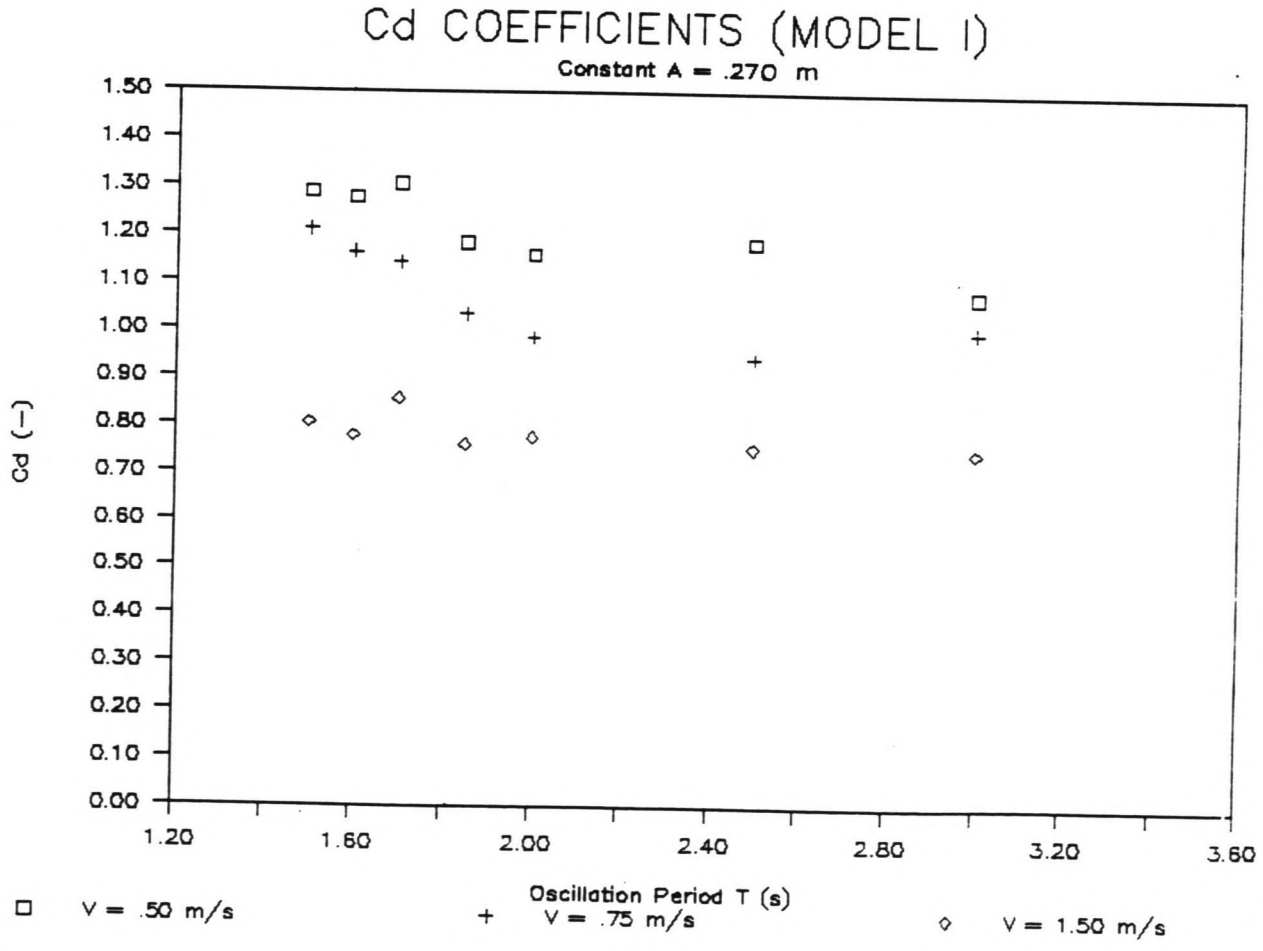

FIGURE G3.2

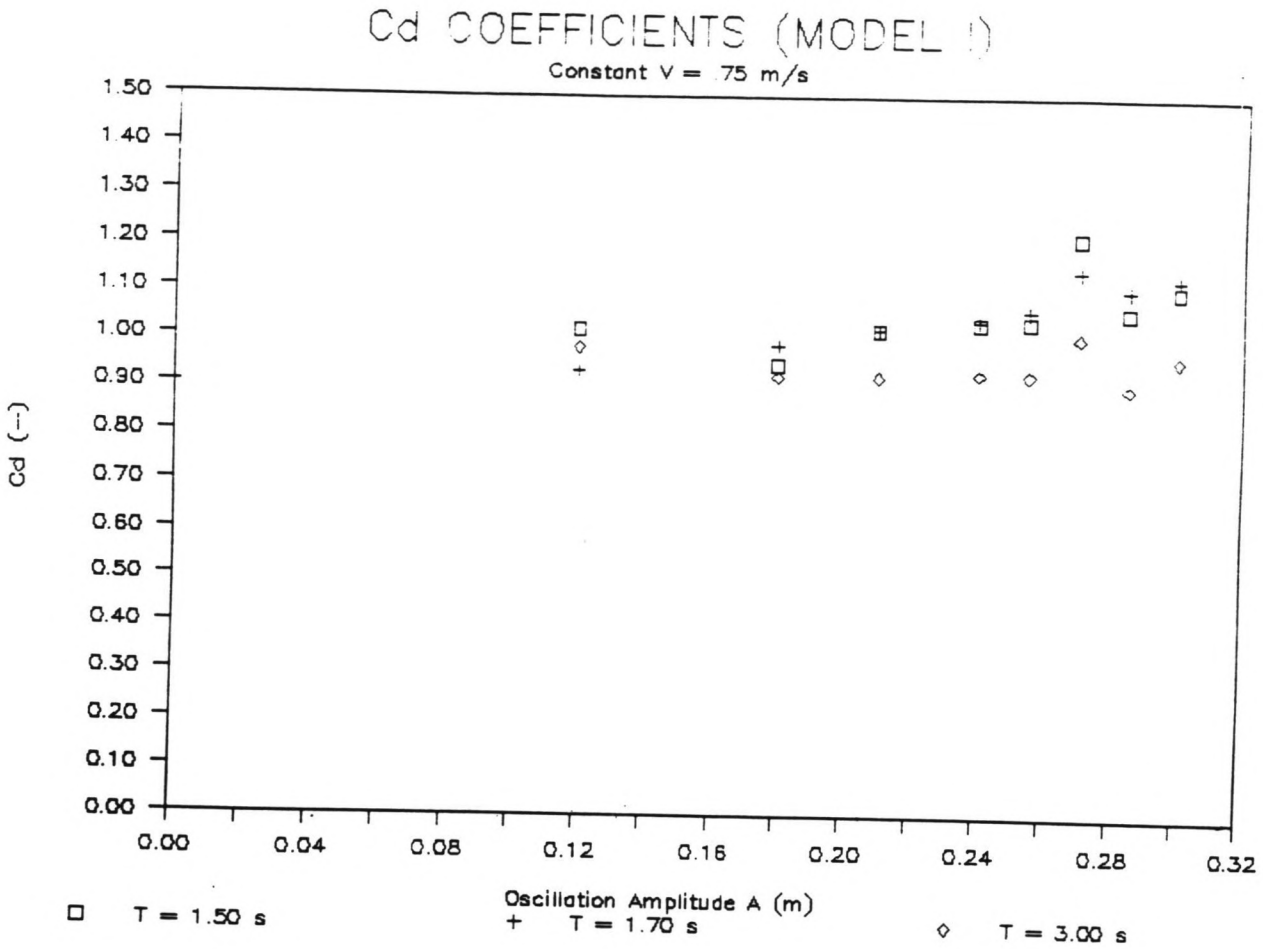

FIGURE G3.3

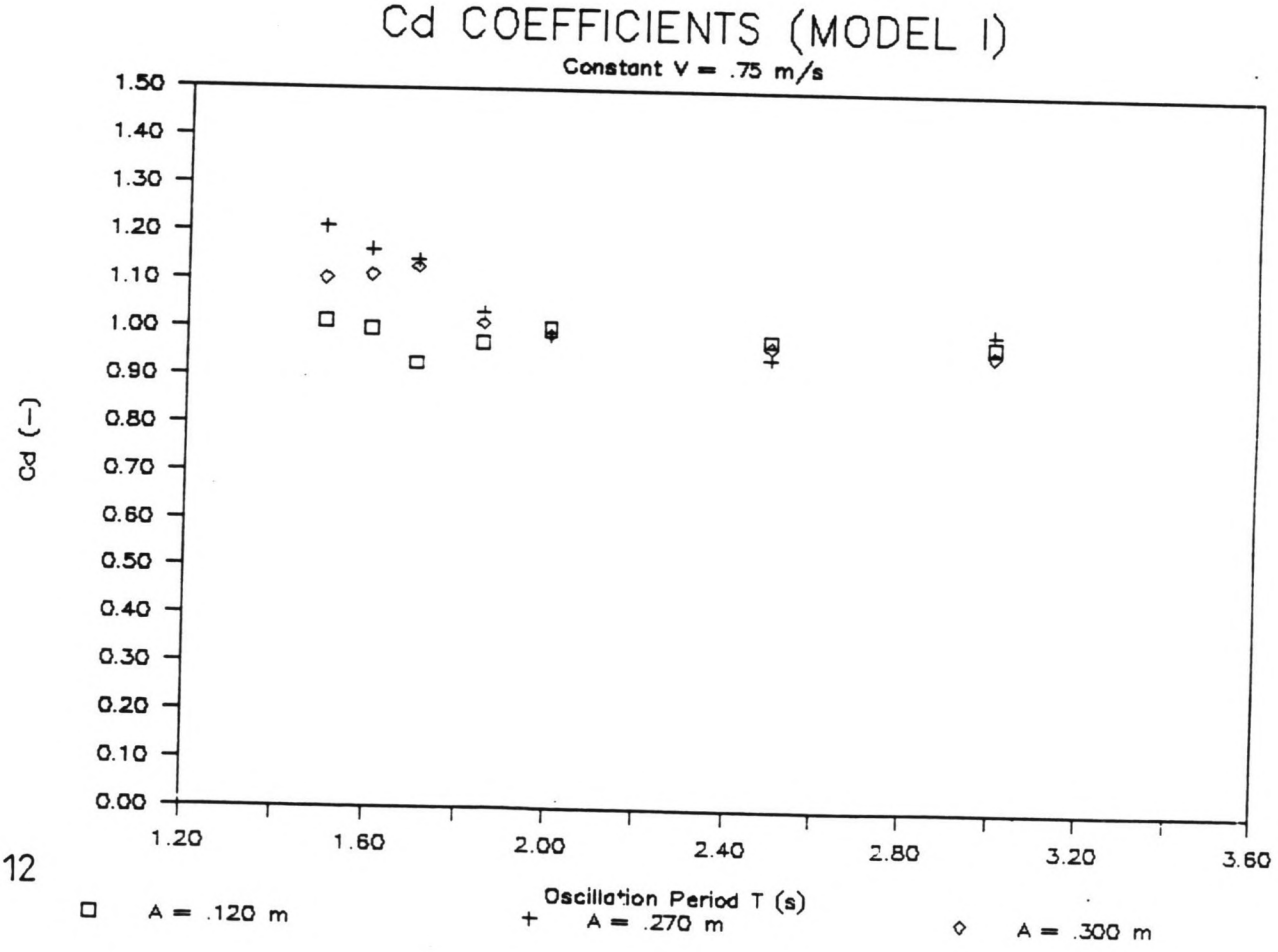

FIGURE G3.4

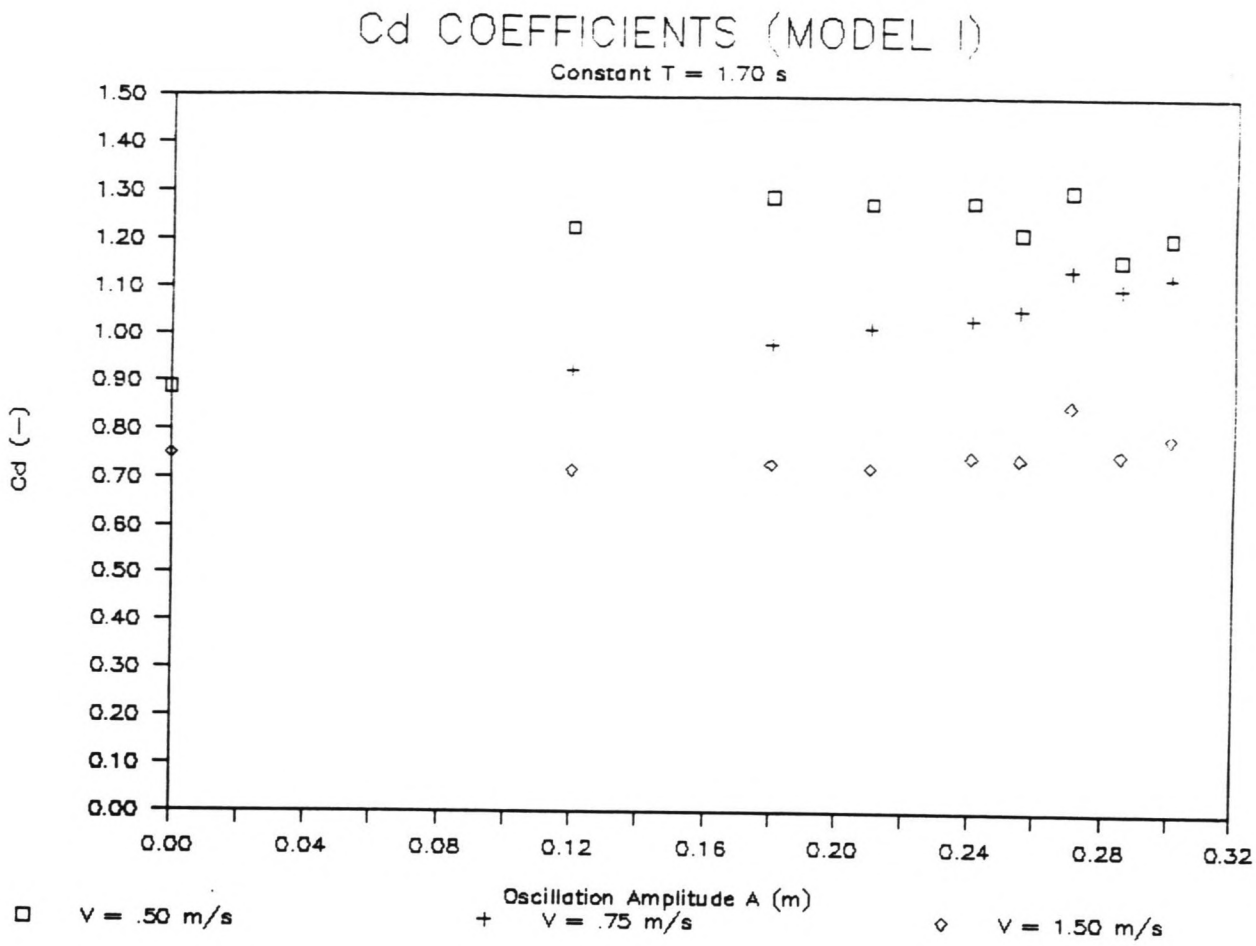

FIGURE G3.5

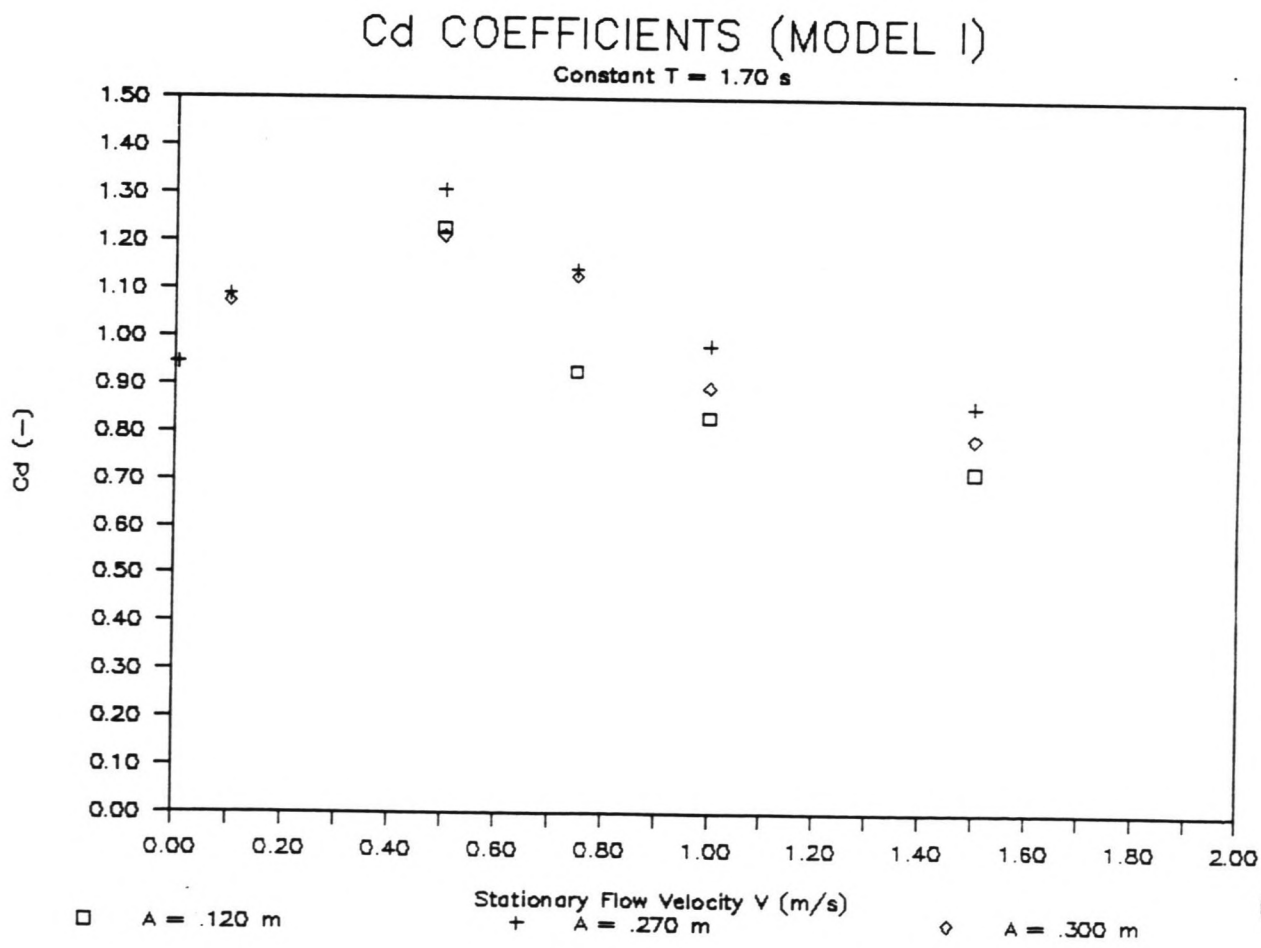

FIGURE G3.6

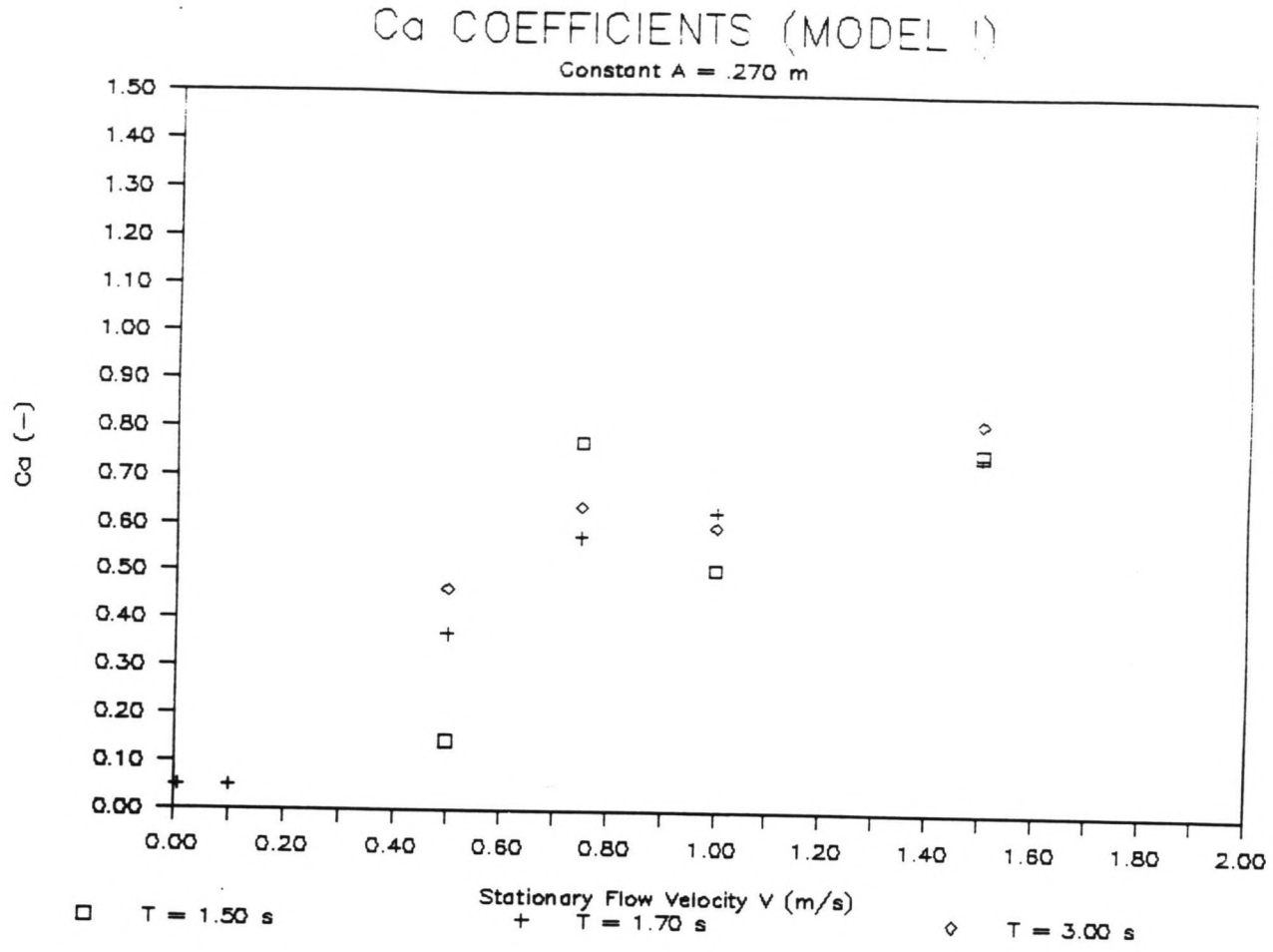

FIGURE G4.1

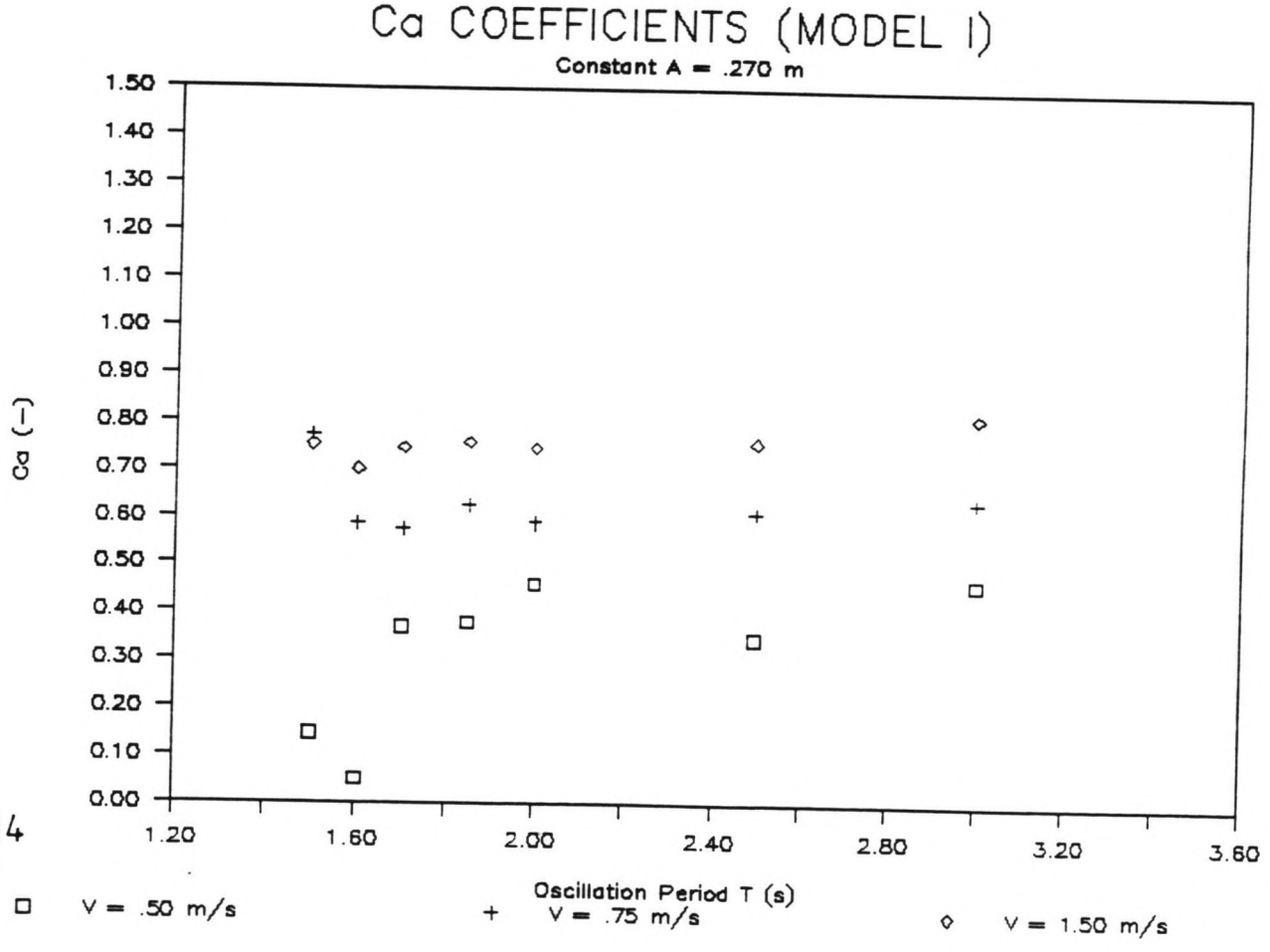

FIGURE G4.2

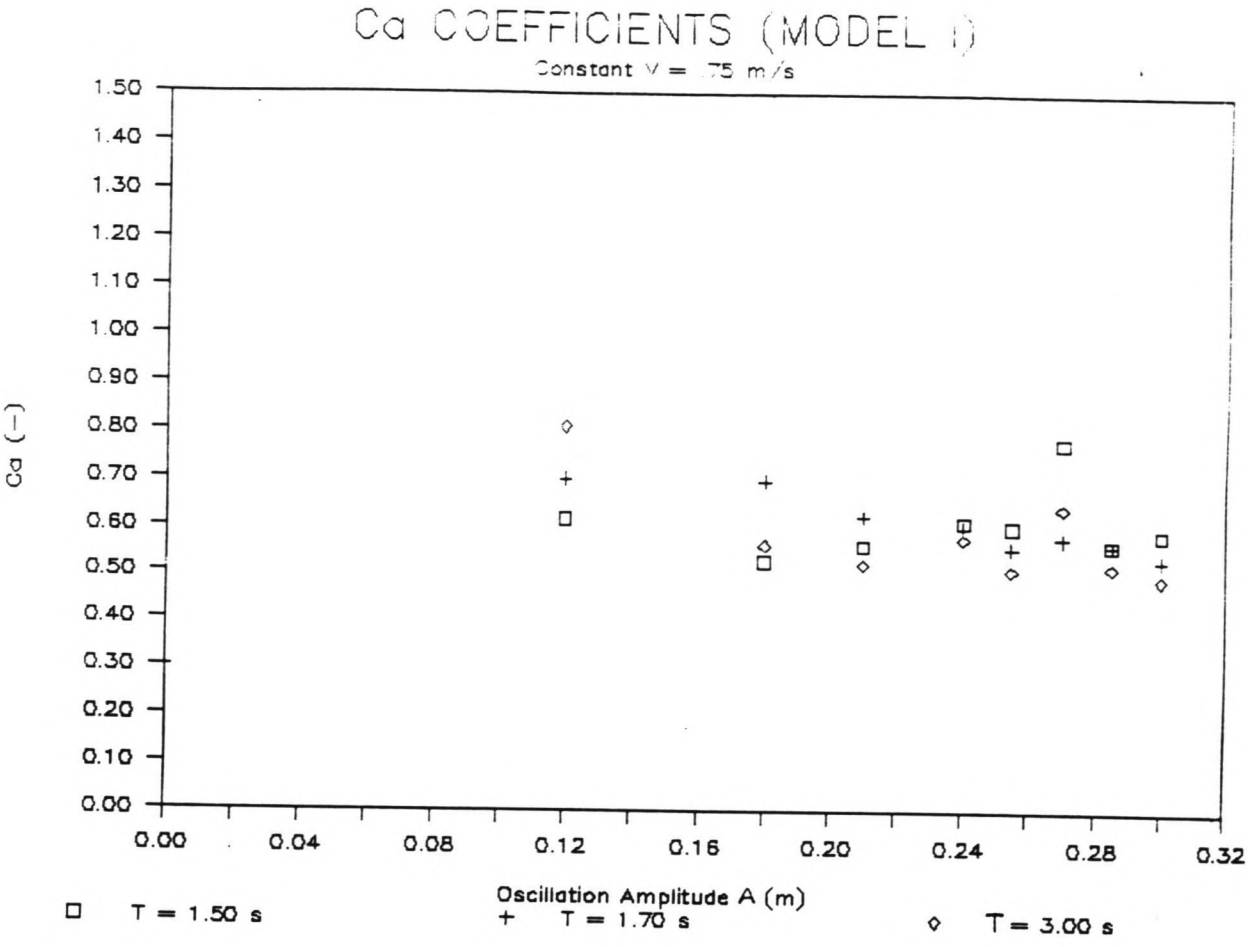

FIGURE G4.3

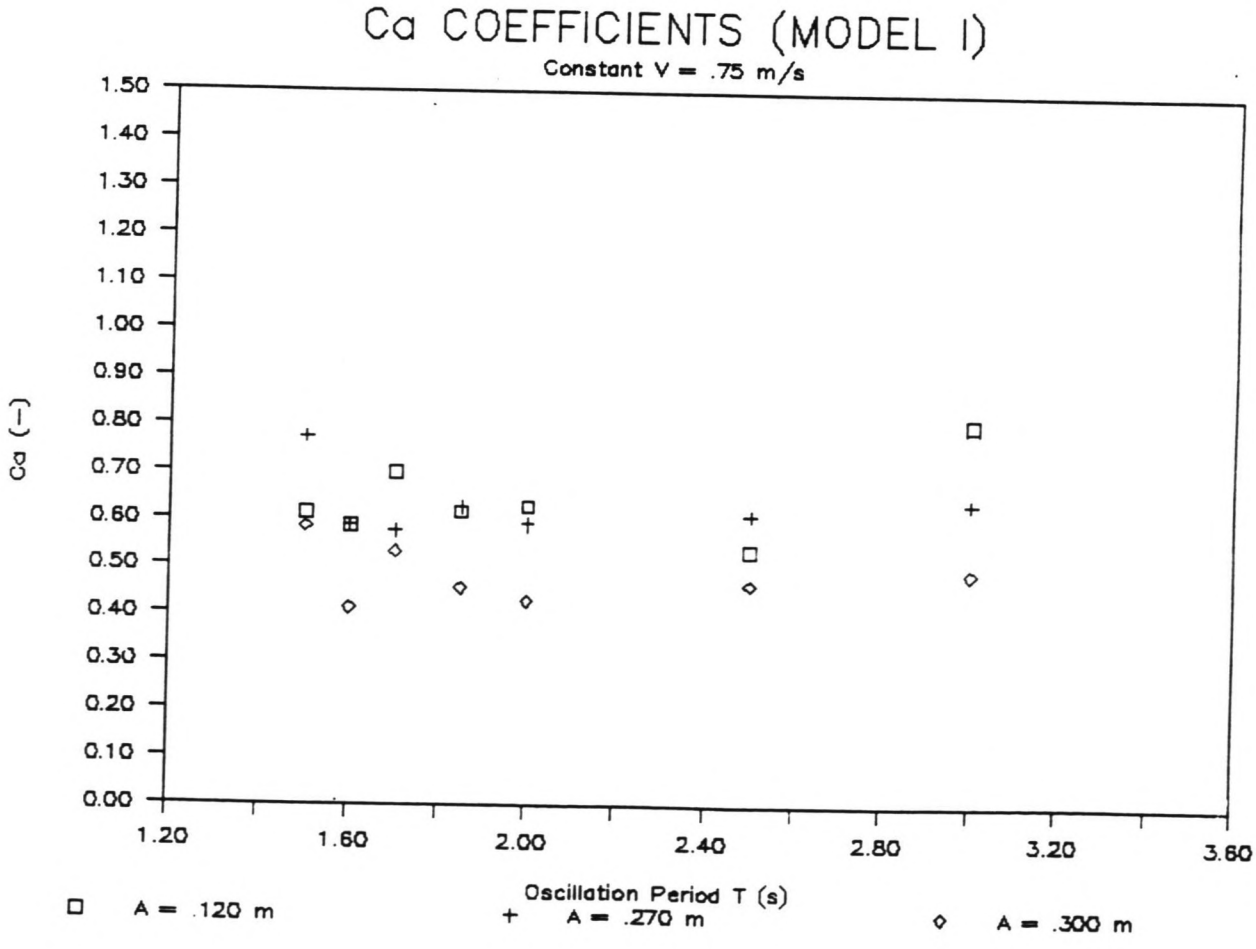

FIGURE G4.4

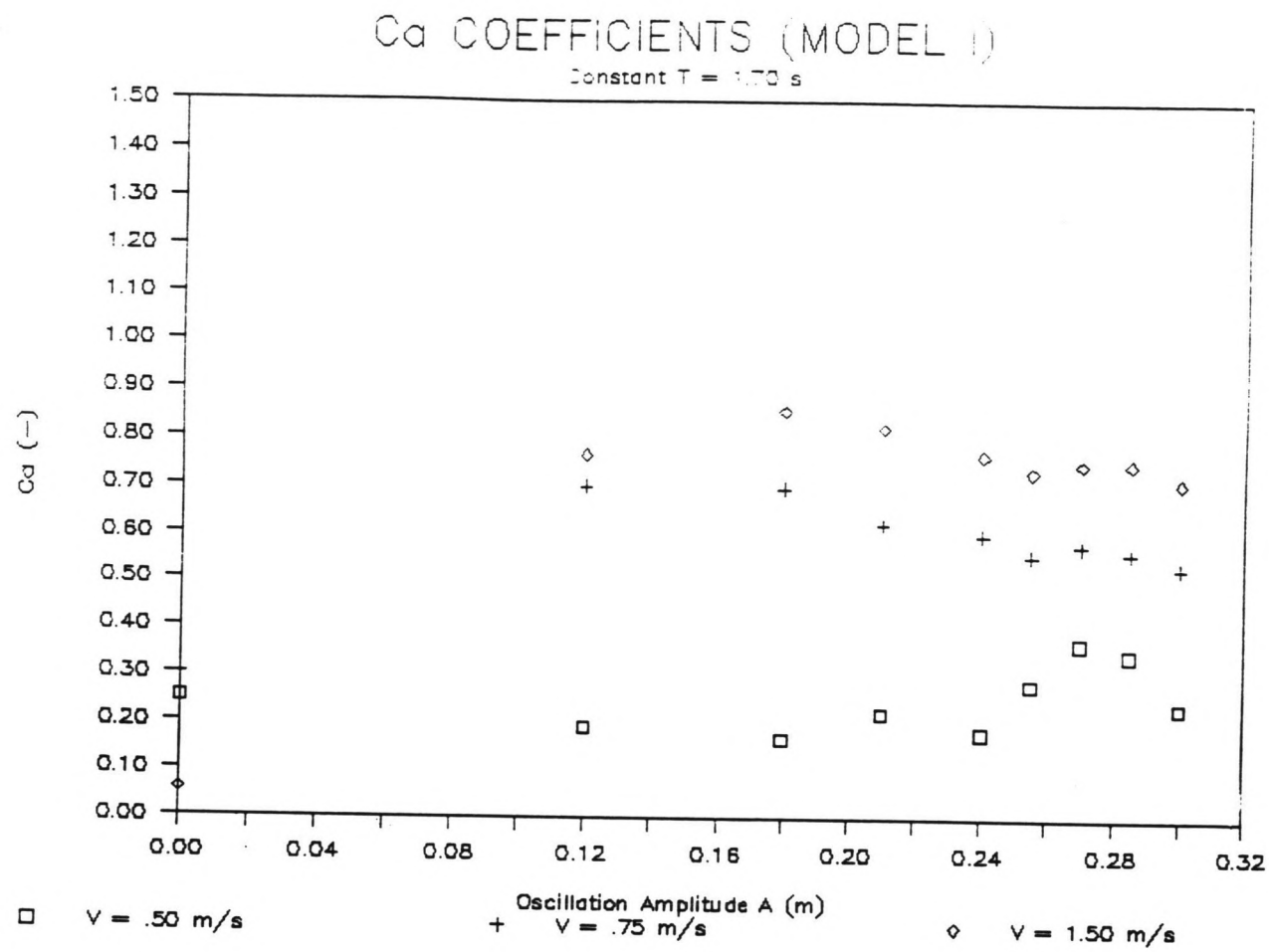

FIGURE G4.5

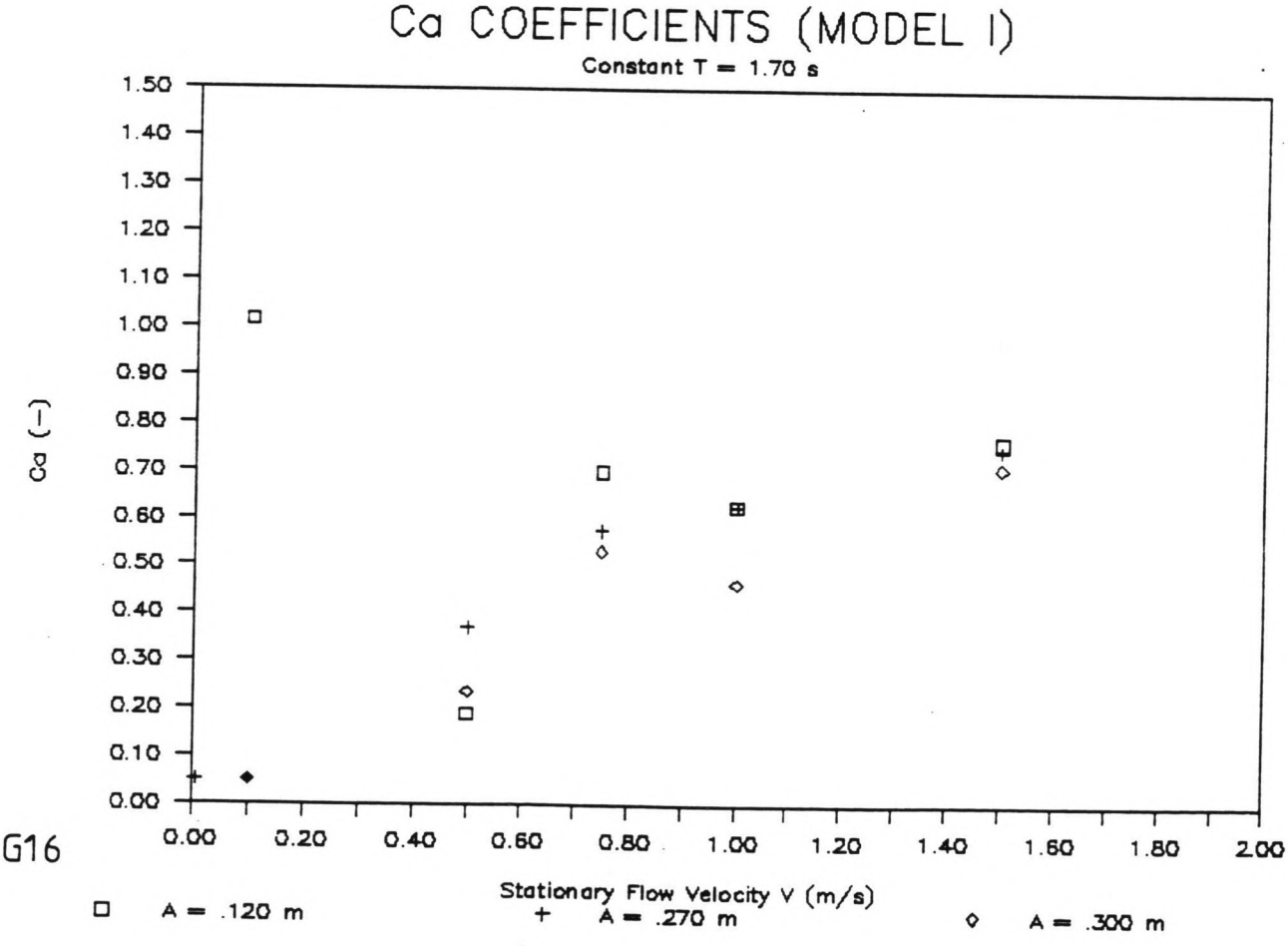

FIGURE G4.6

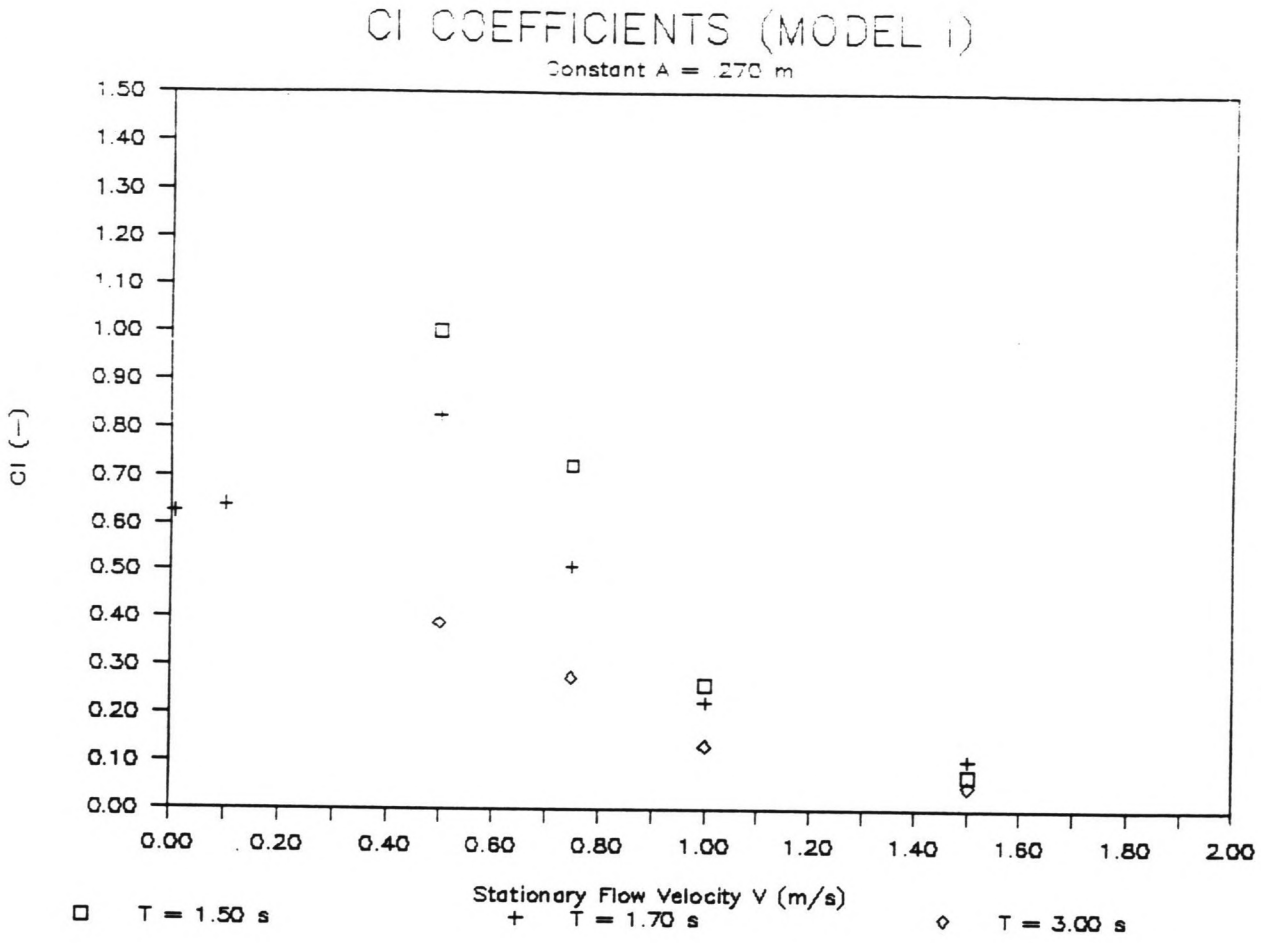

FIGURE G5.1

FIGURE G5.2

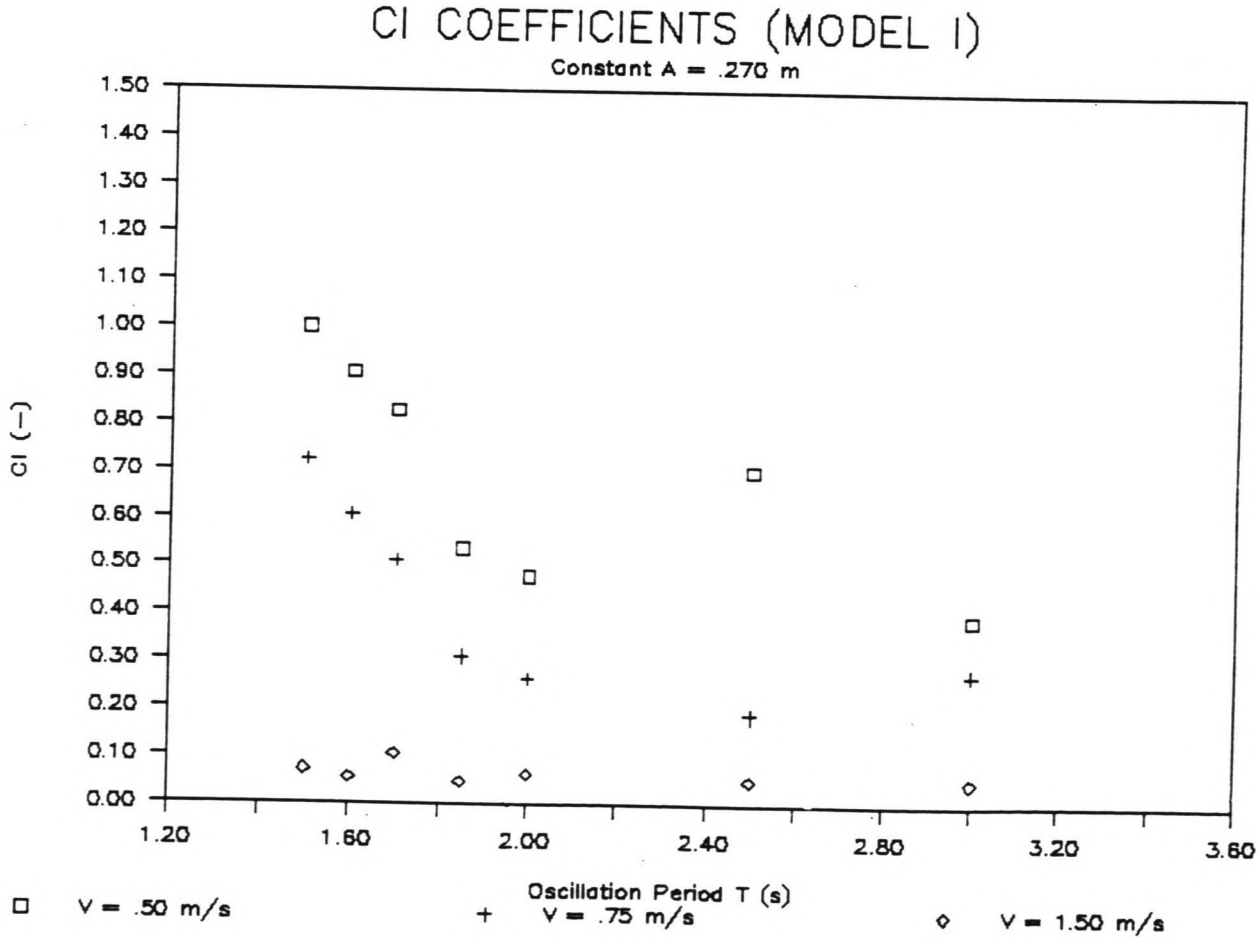

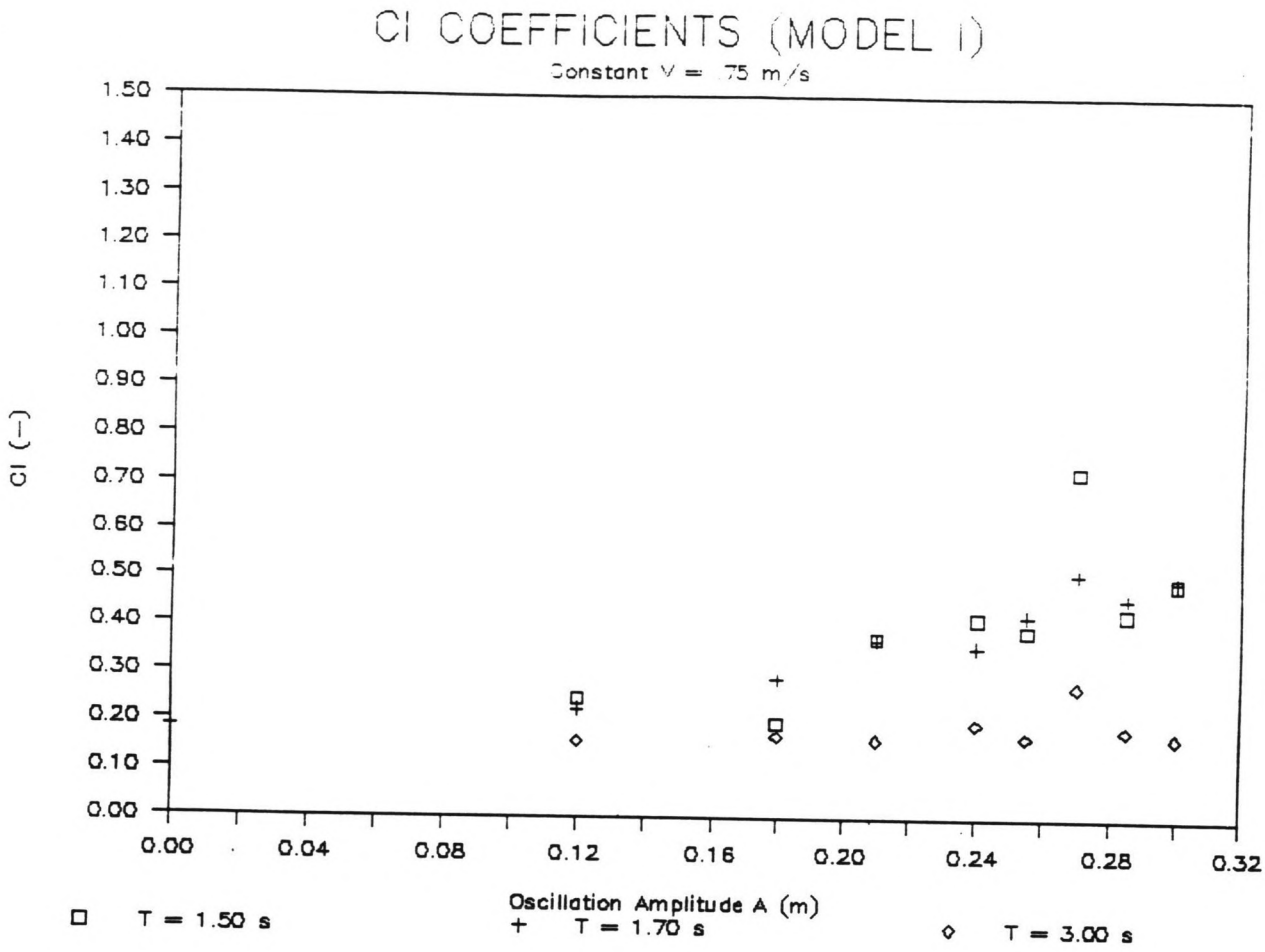

FIGURE G5.3

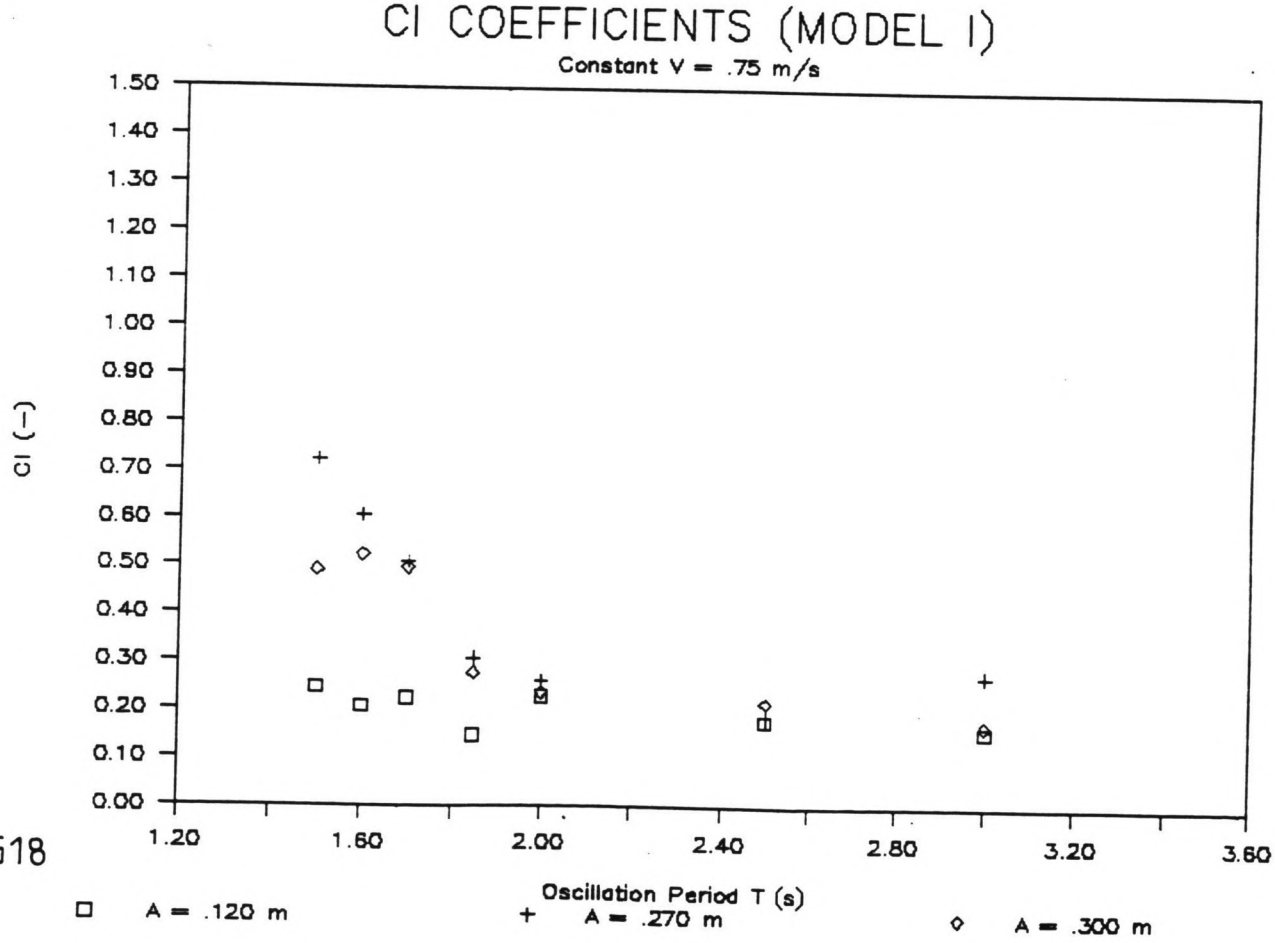

FIGURE G5.4

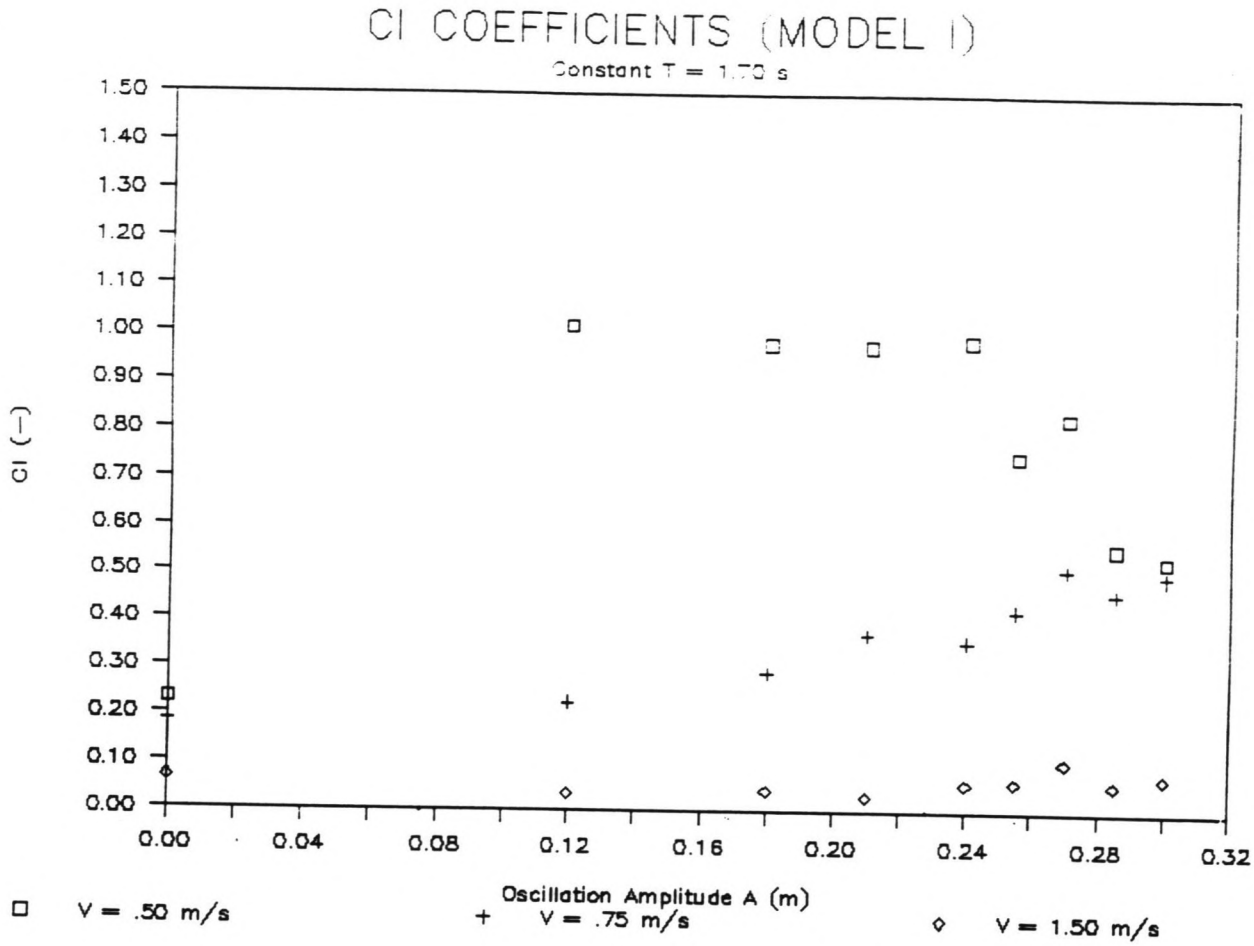

FIGURE G5.5

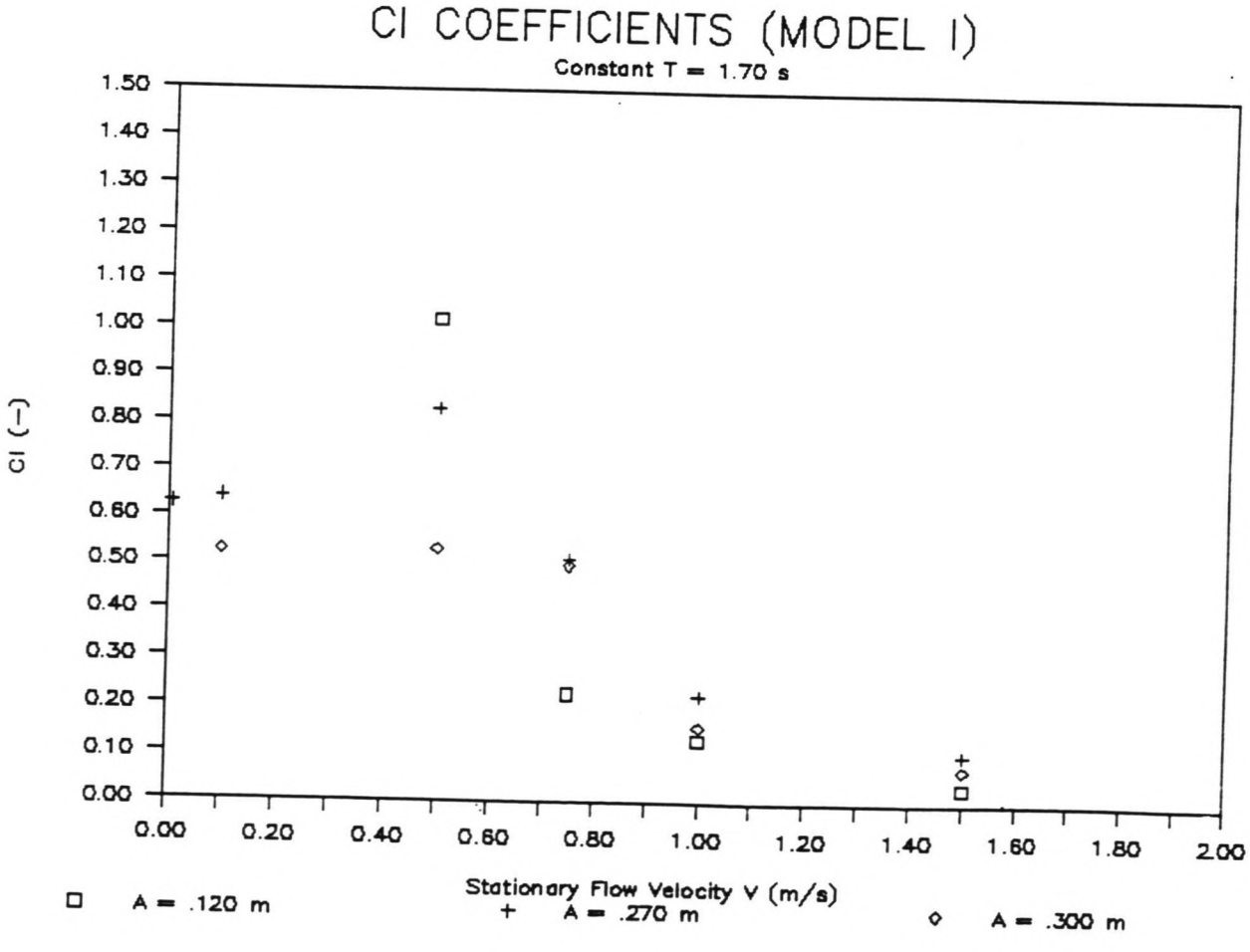

FIGURE G5.6

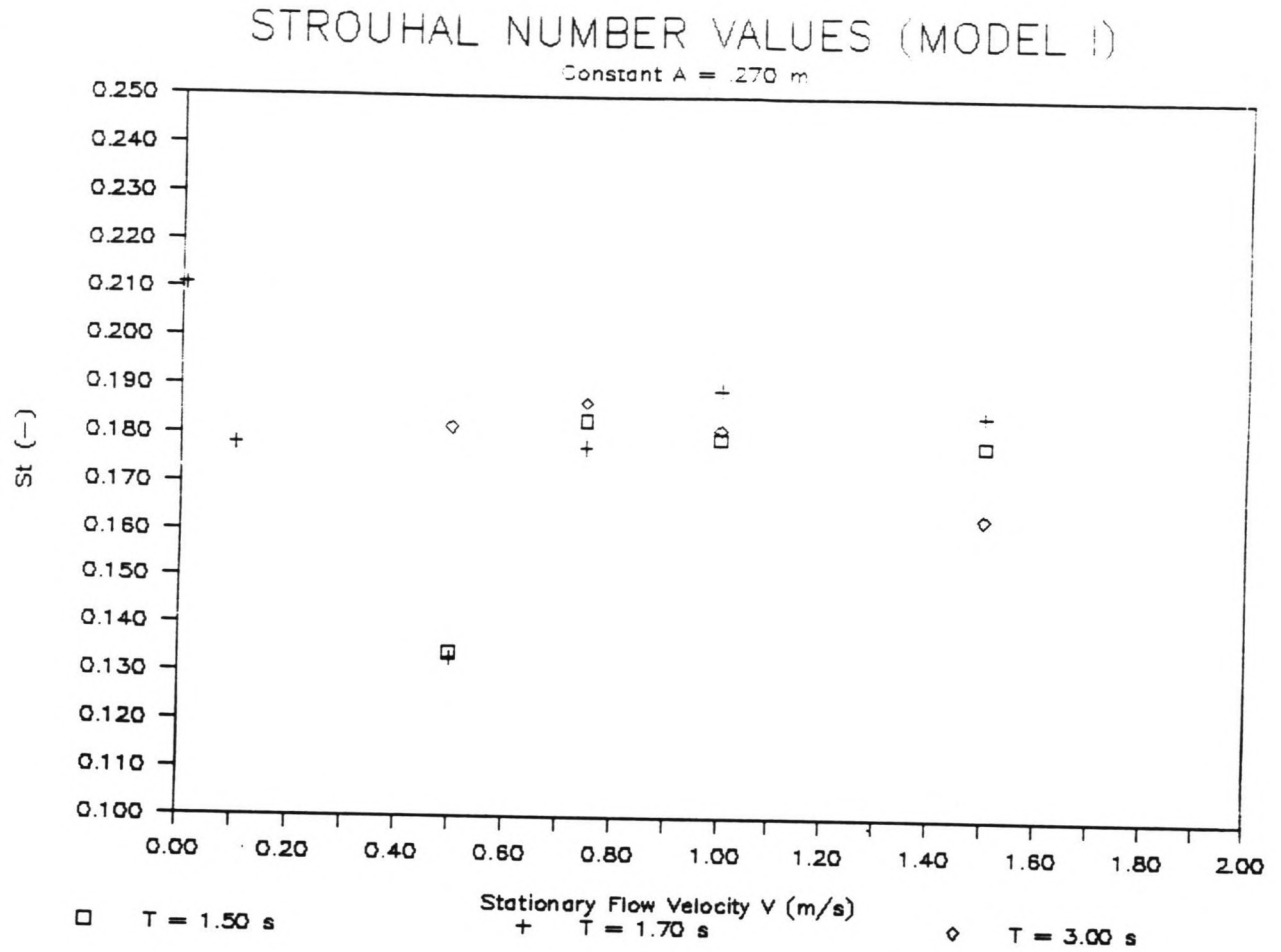

FIGURE G6.1

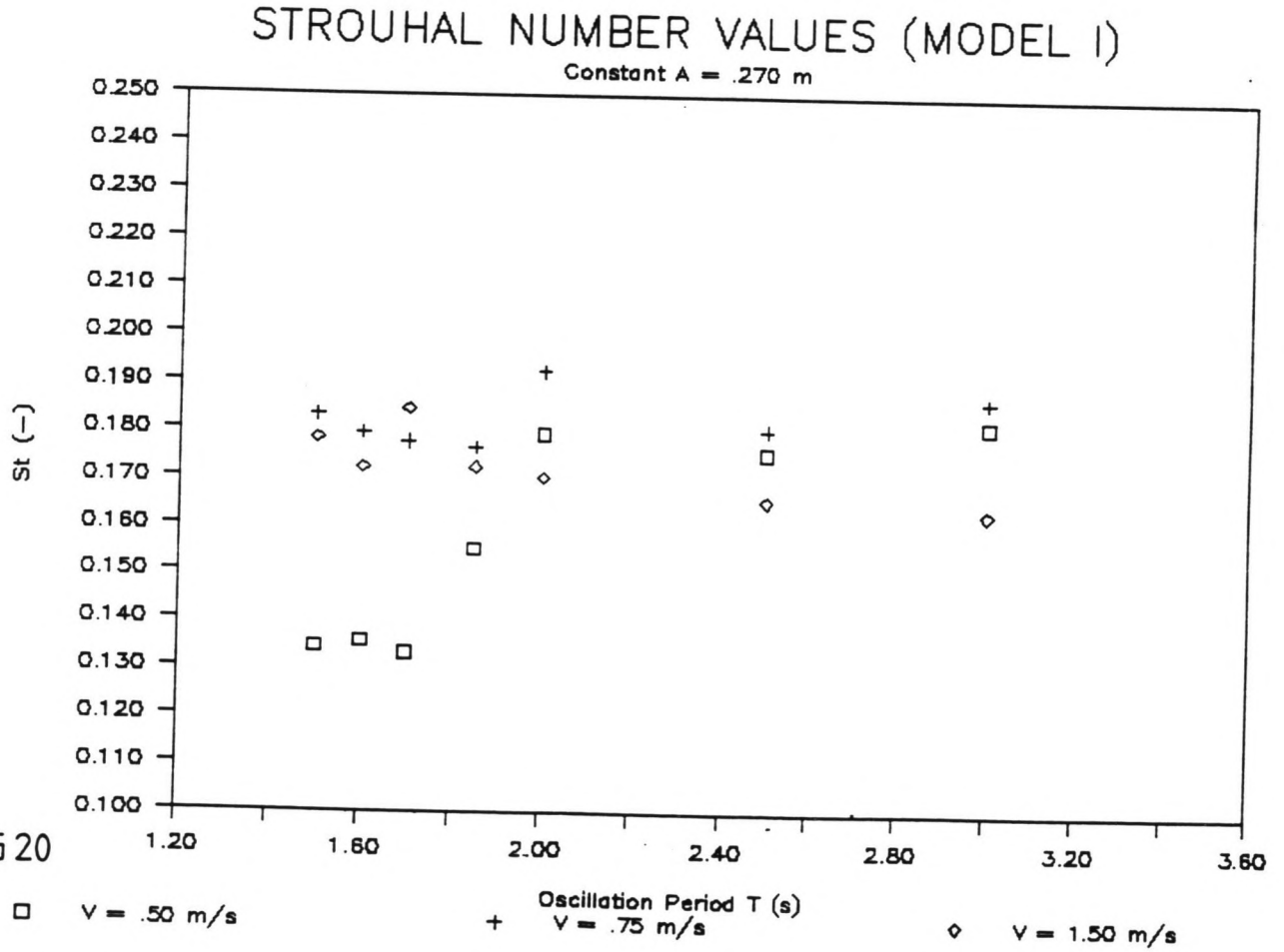

FIGURE G6.2

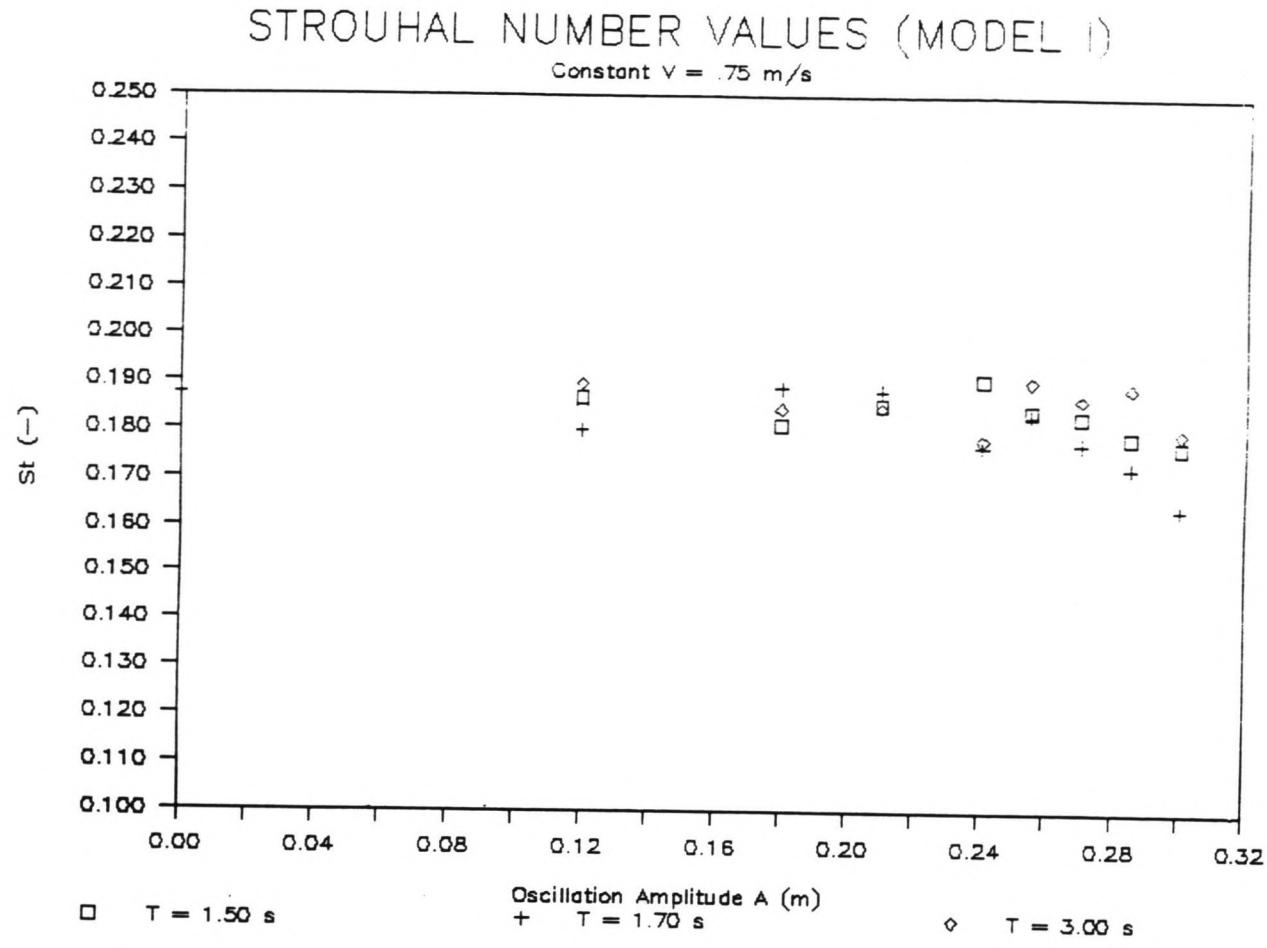

FIGURE G6.3

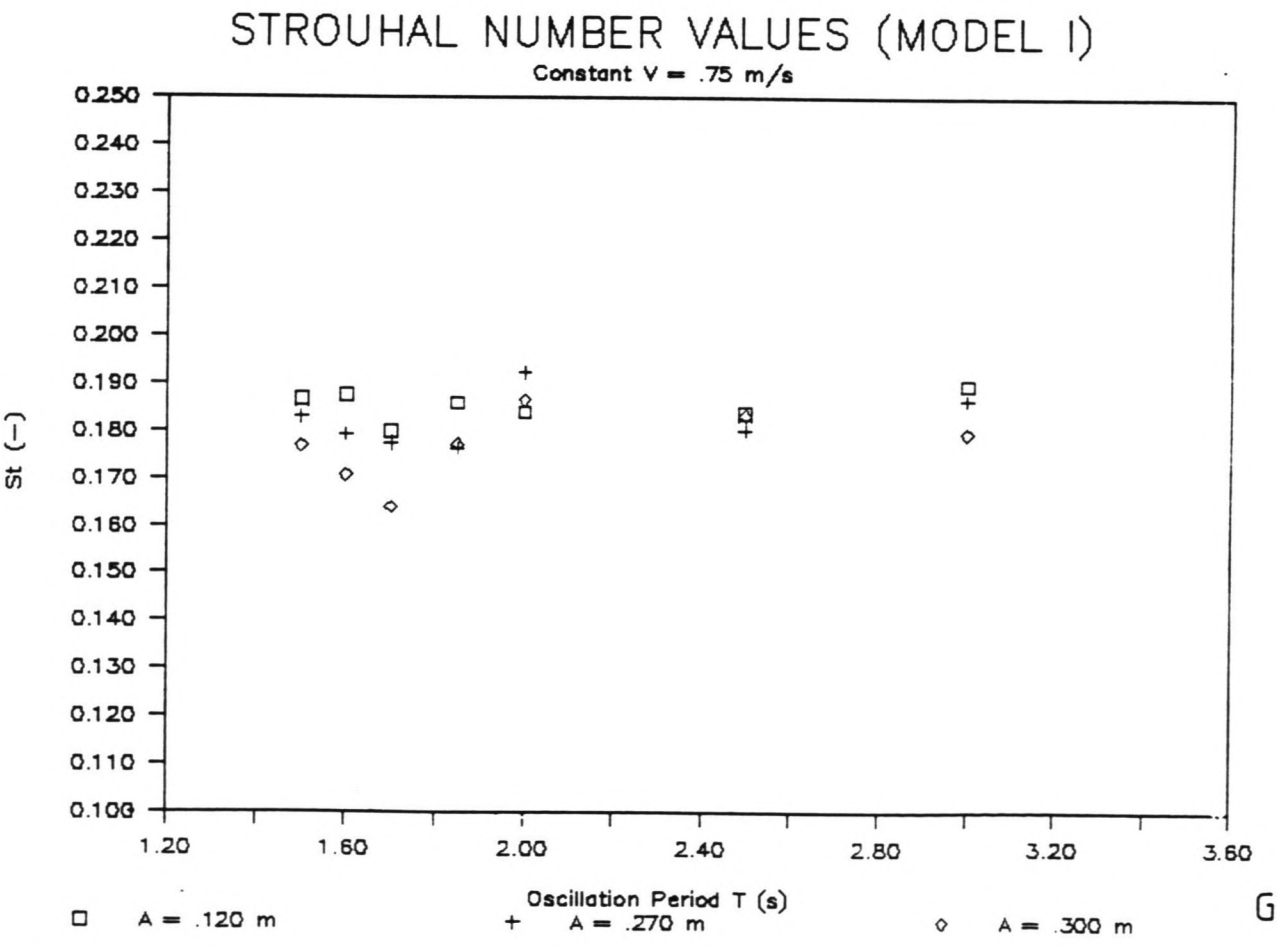

FIGURE G6.4

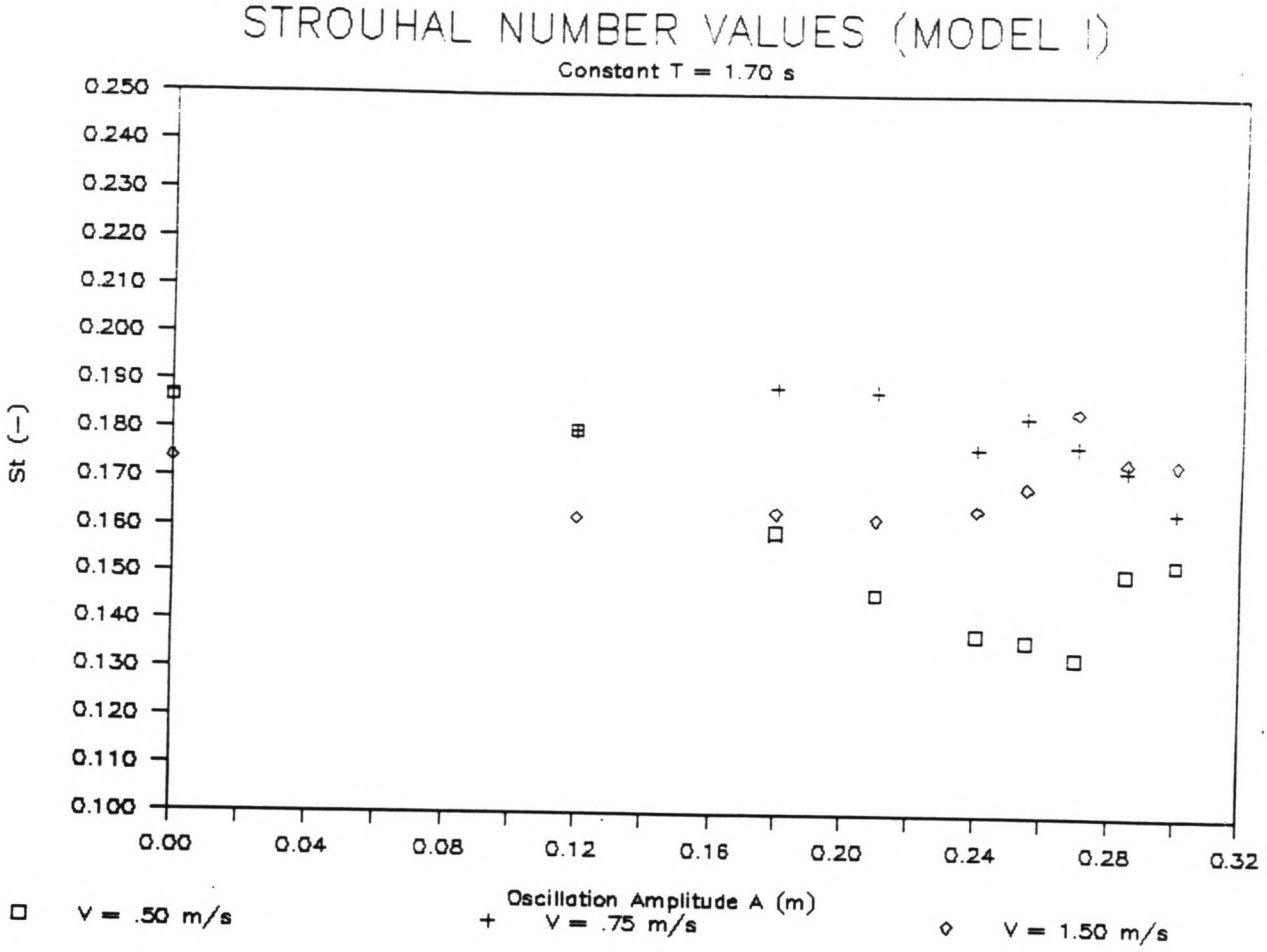

FIGURE G6.5

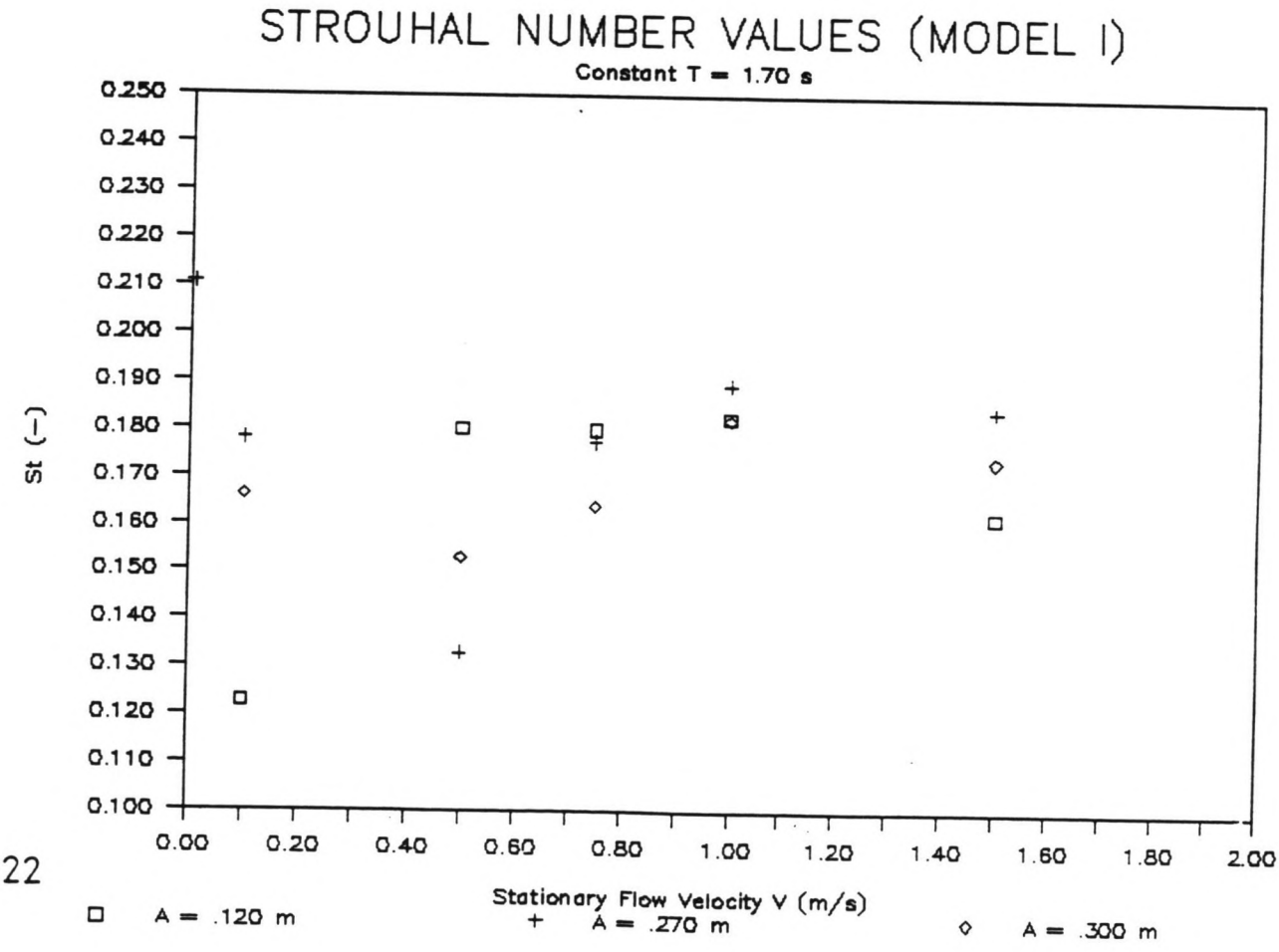

FIGURE G6.6

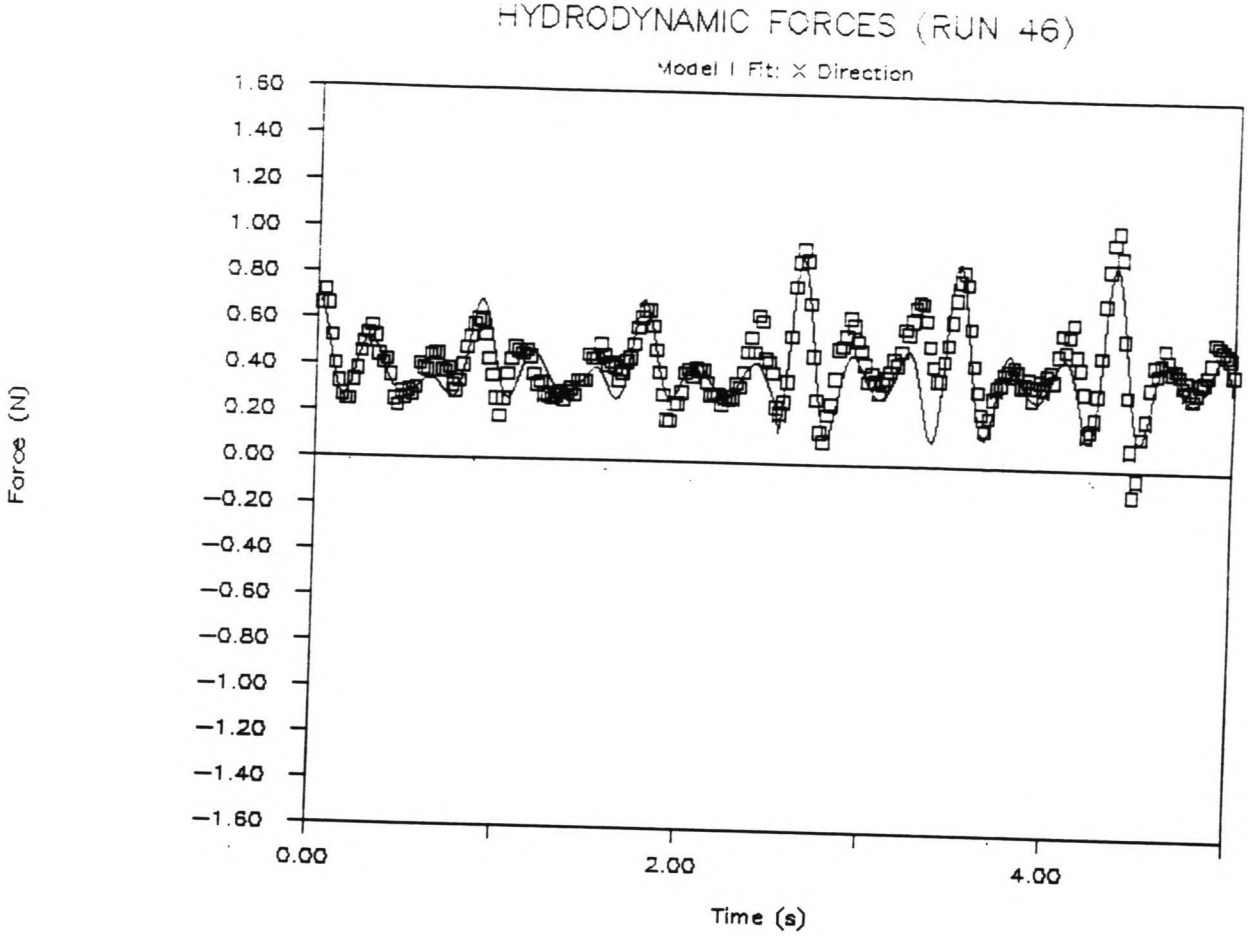

FIGURE G7.1.1

FIGURE G7.1.2

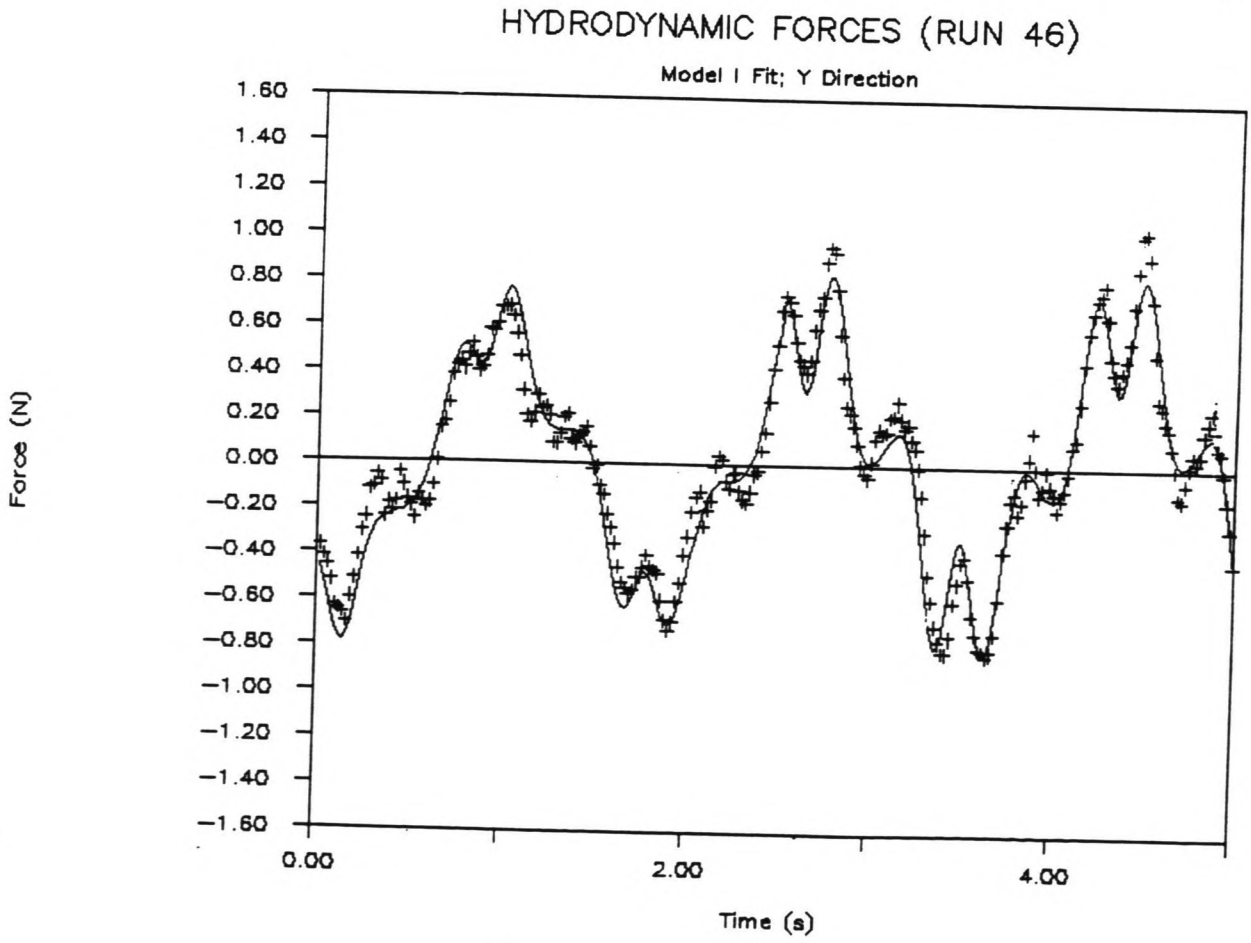

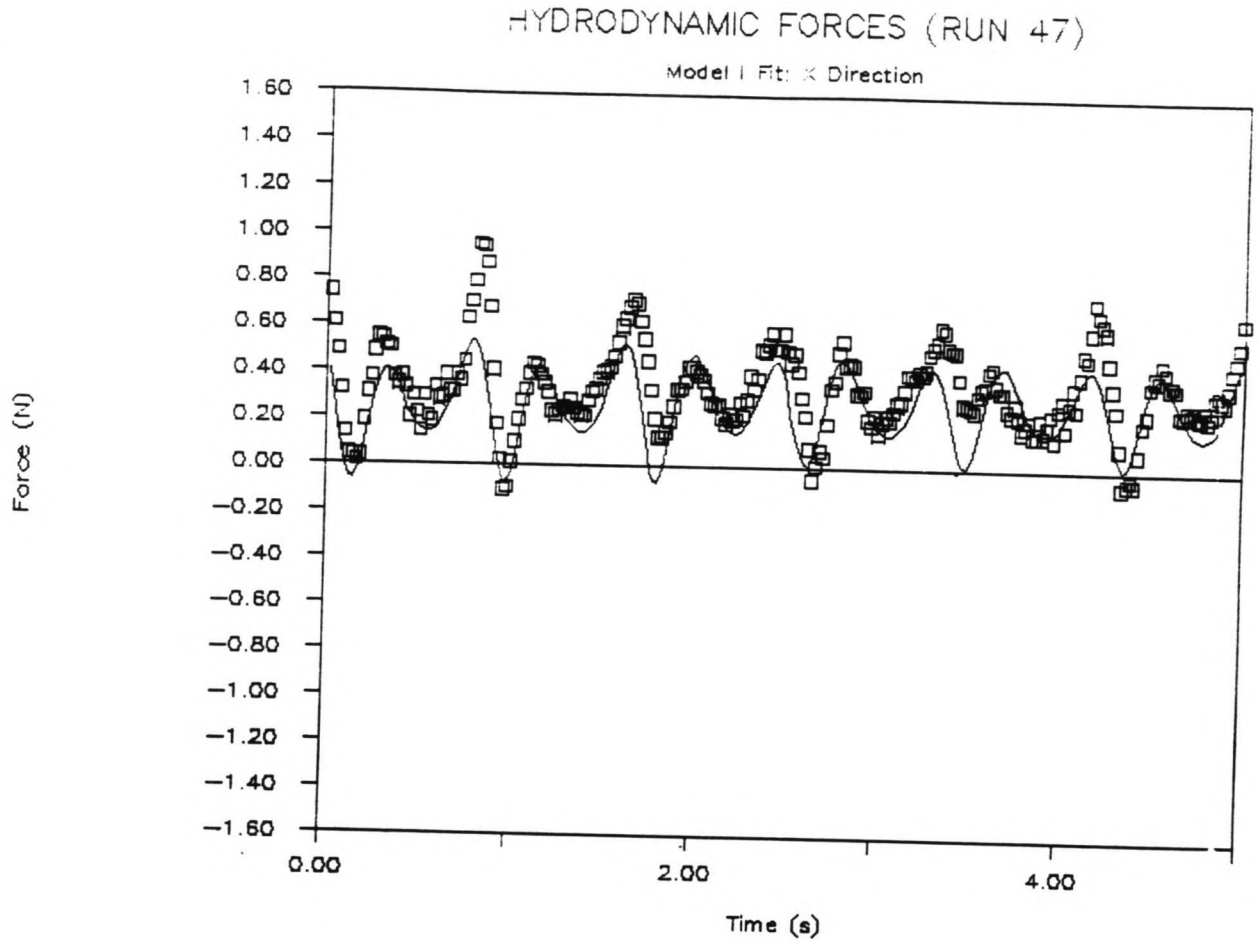

FIGURE G7.2.1

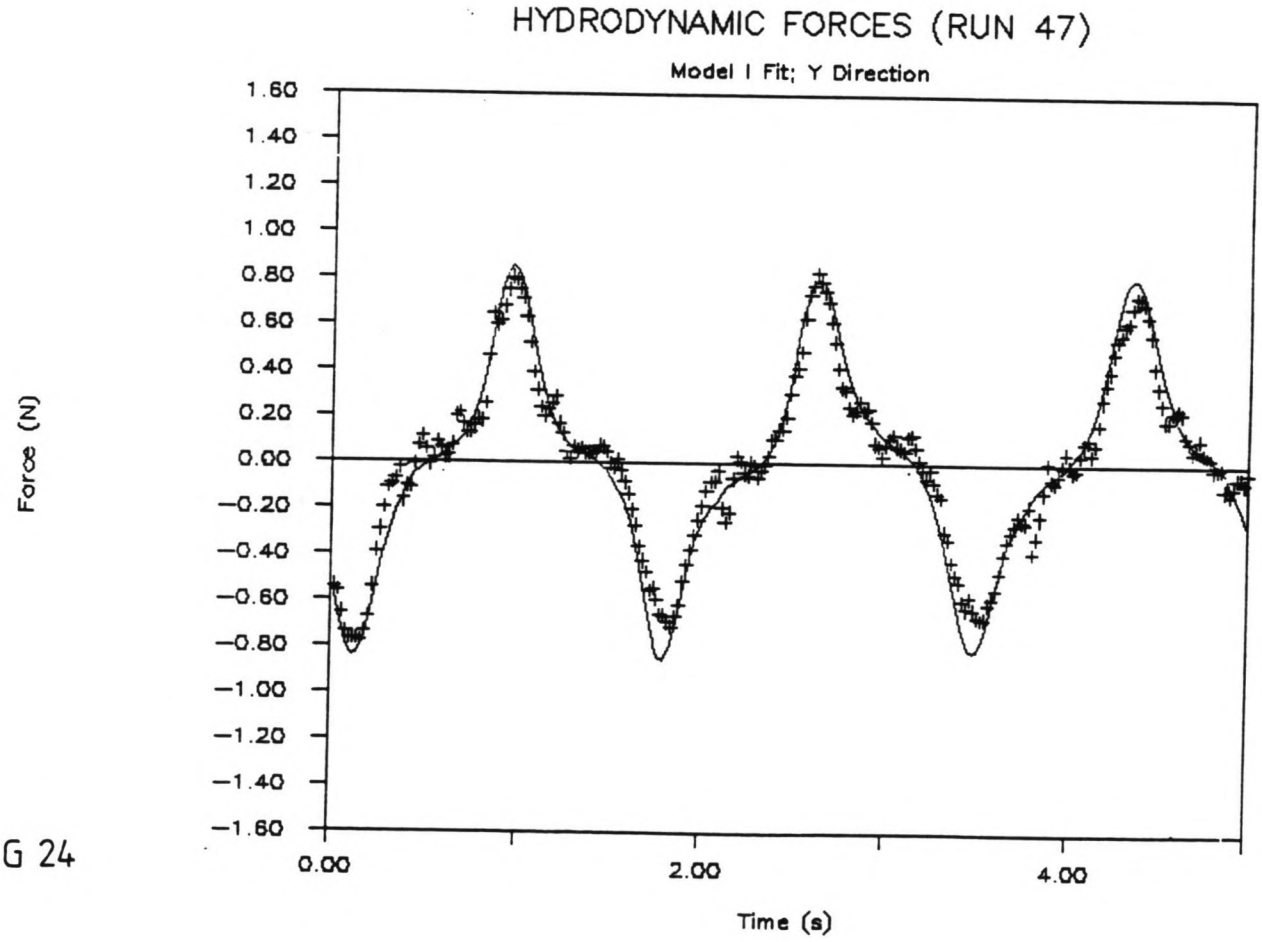

FIGURE G7.2.2

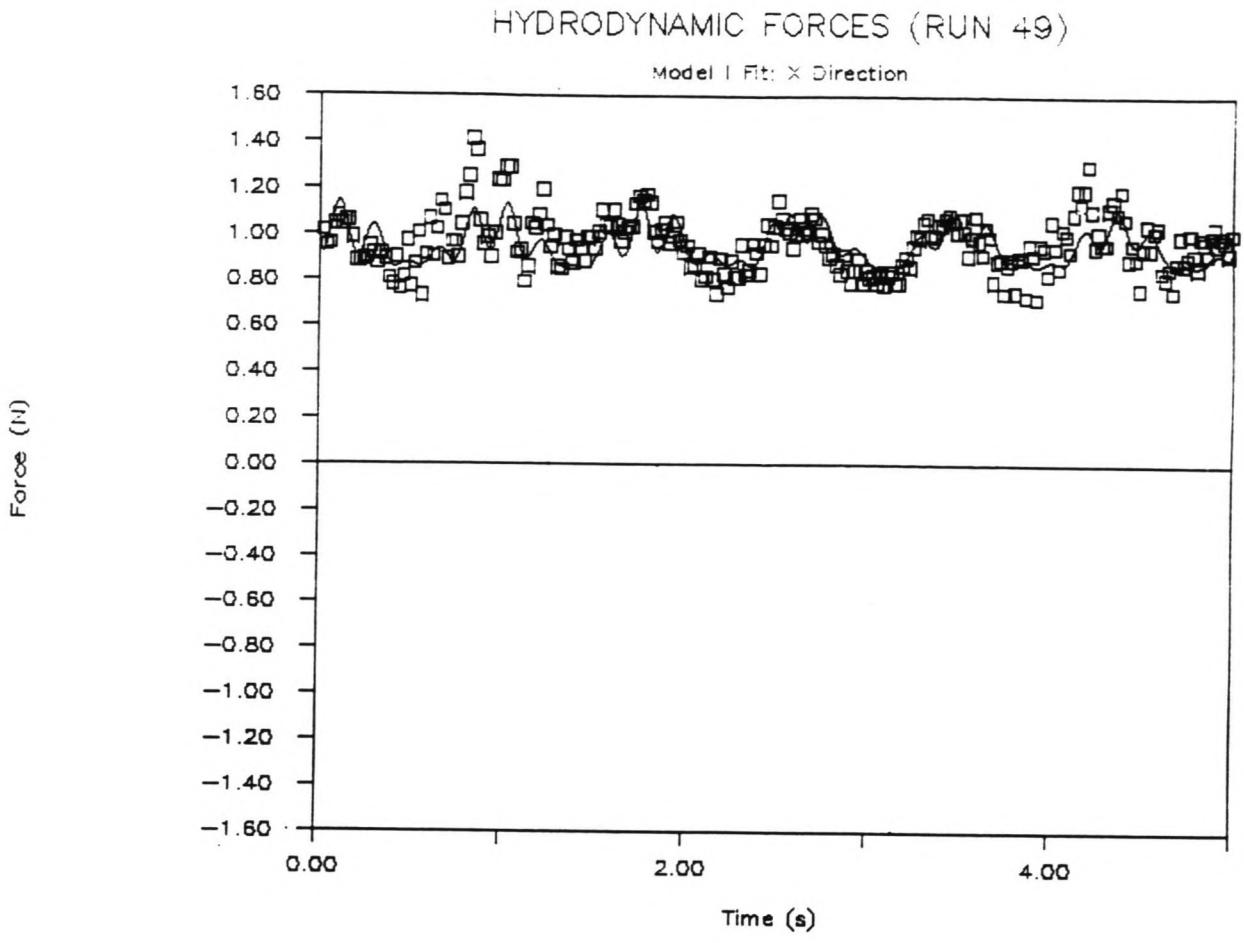

FIGURE G7.3.1

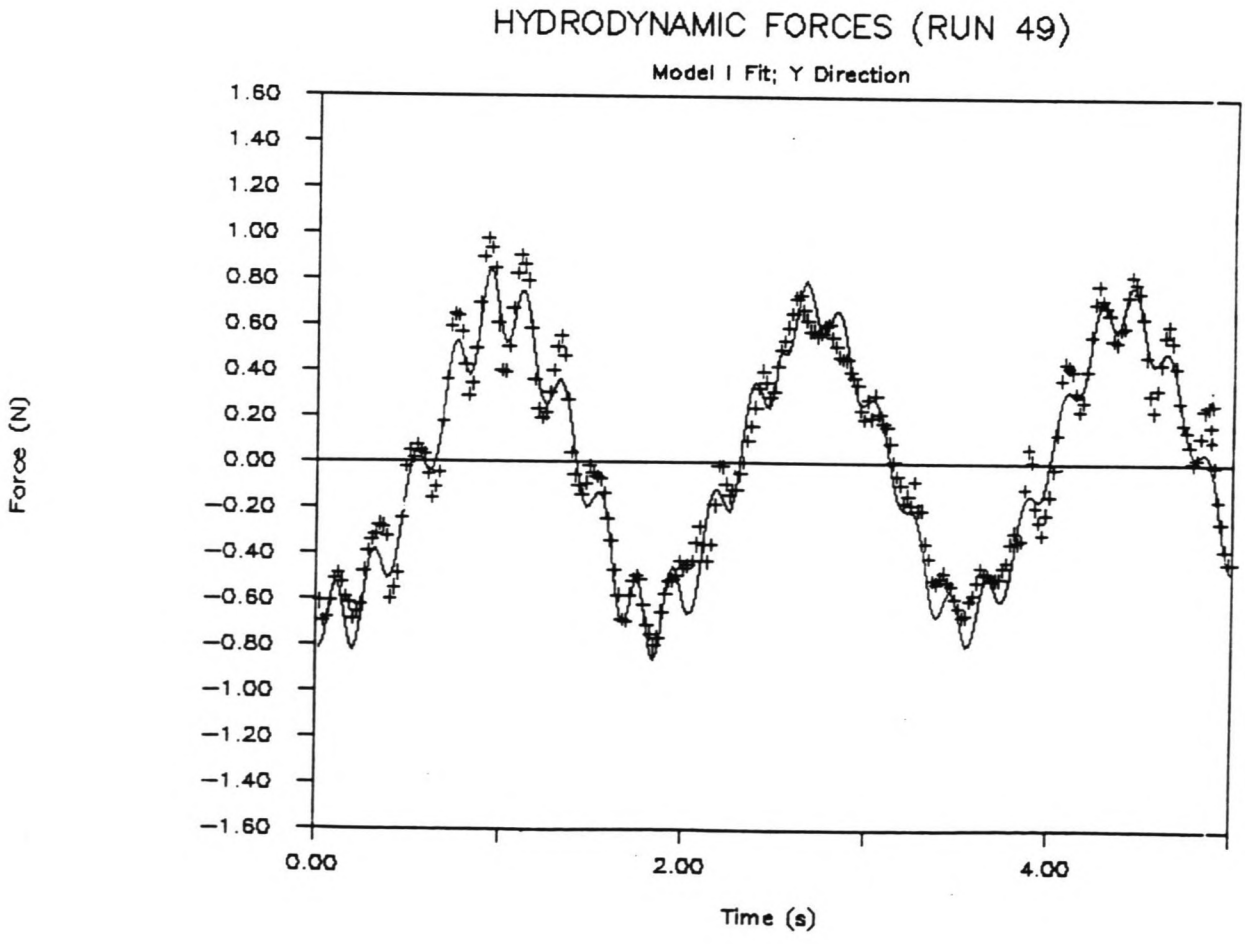

FIGURE G7.3.2

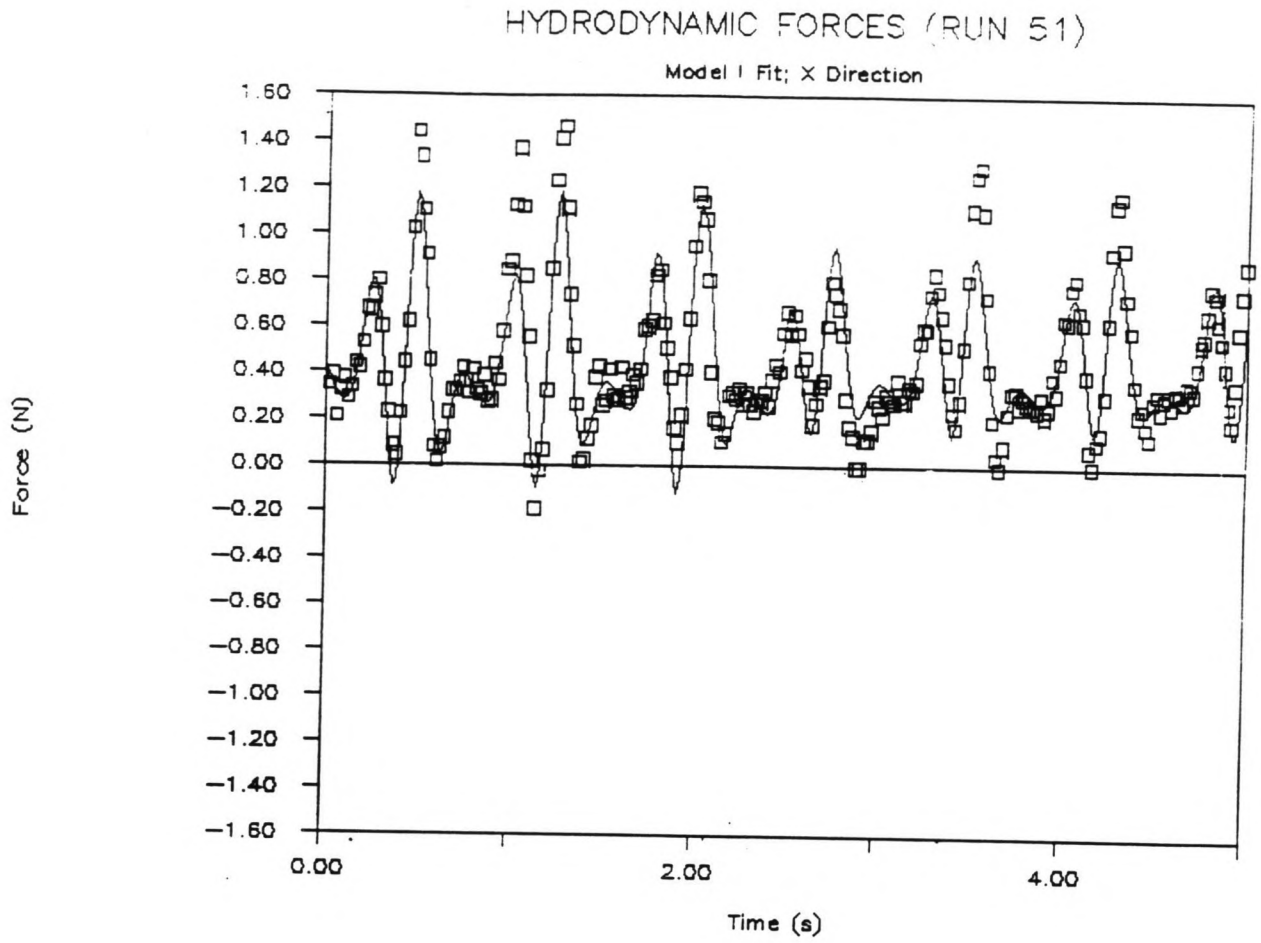

FIGURE G7.4.1

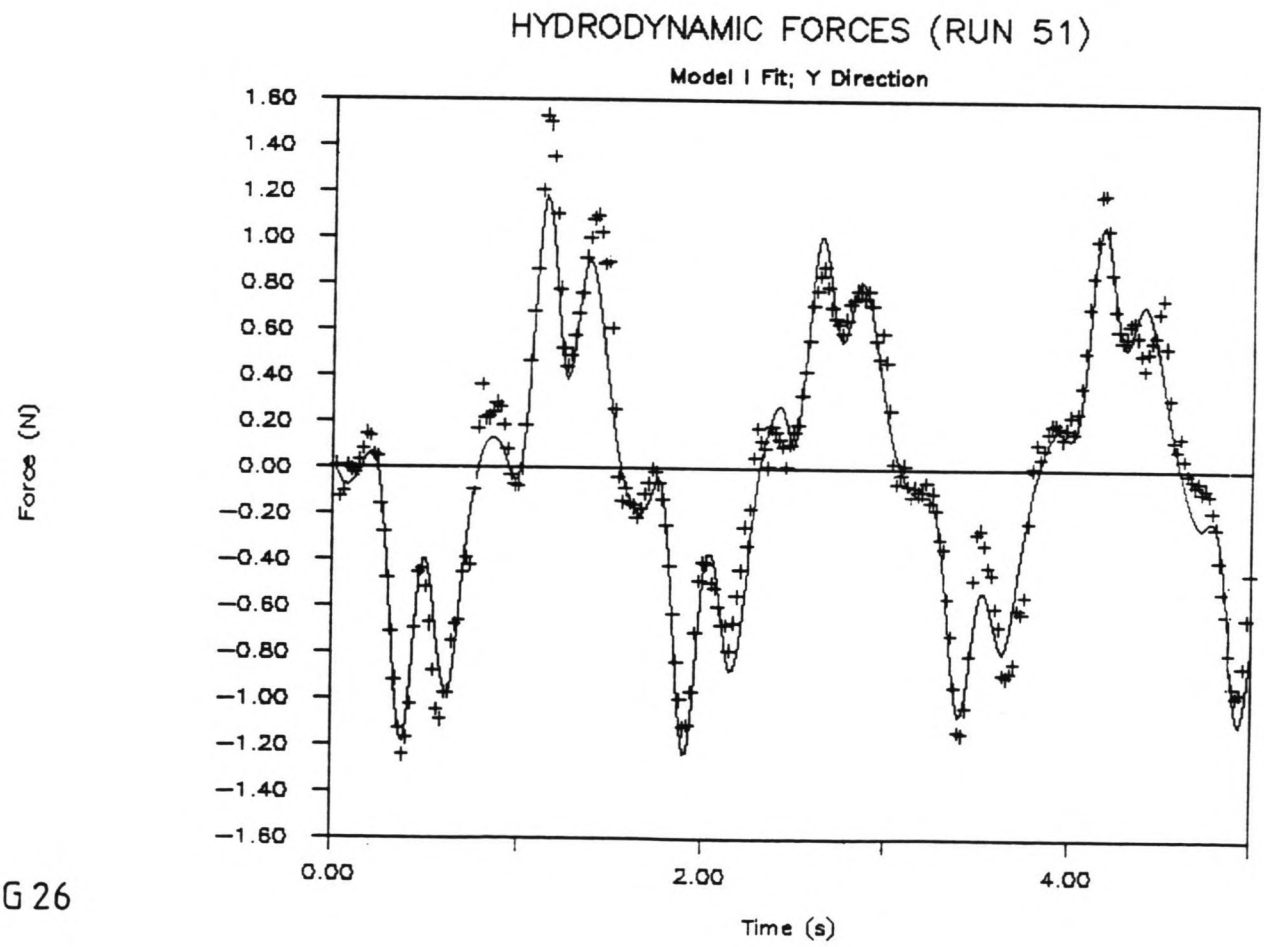

FIGURE G7.4.2

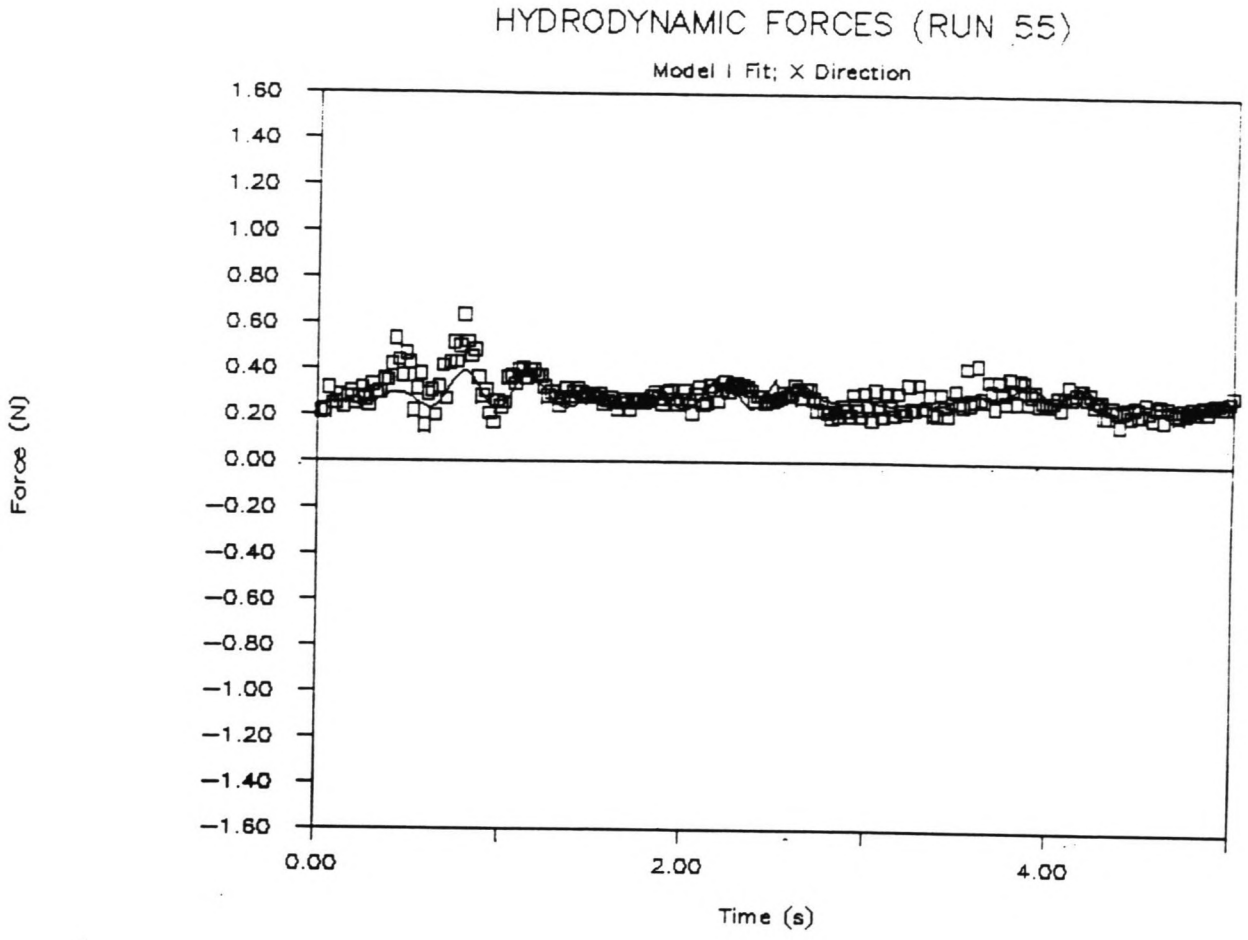

FIGURE G7.5.1

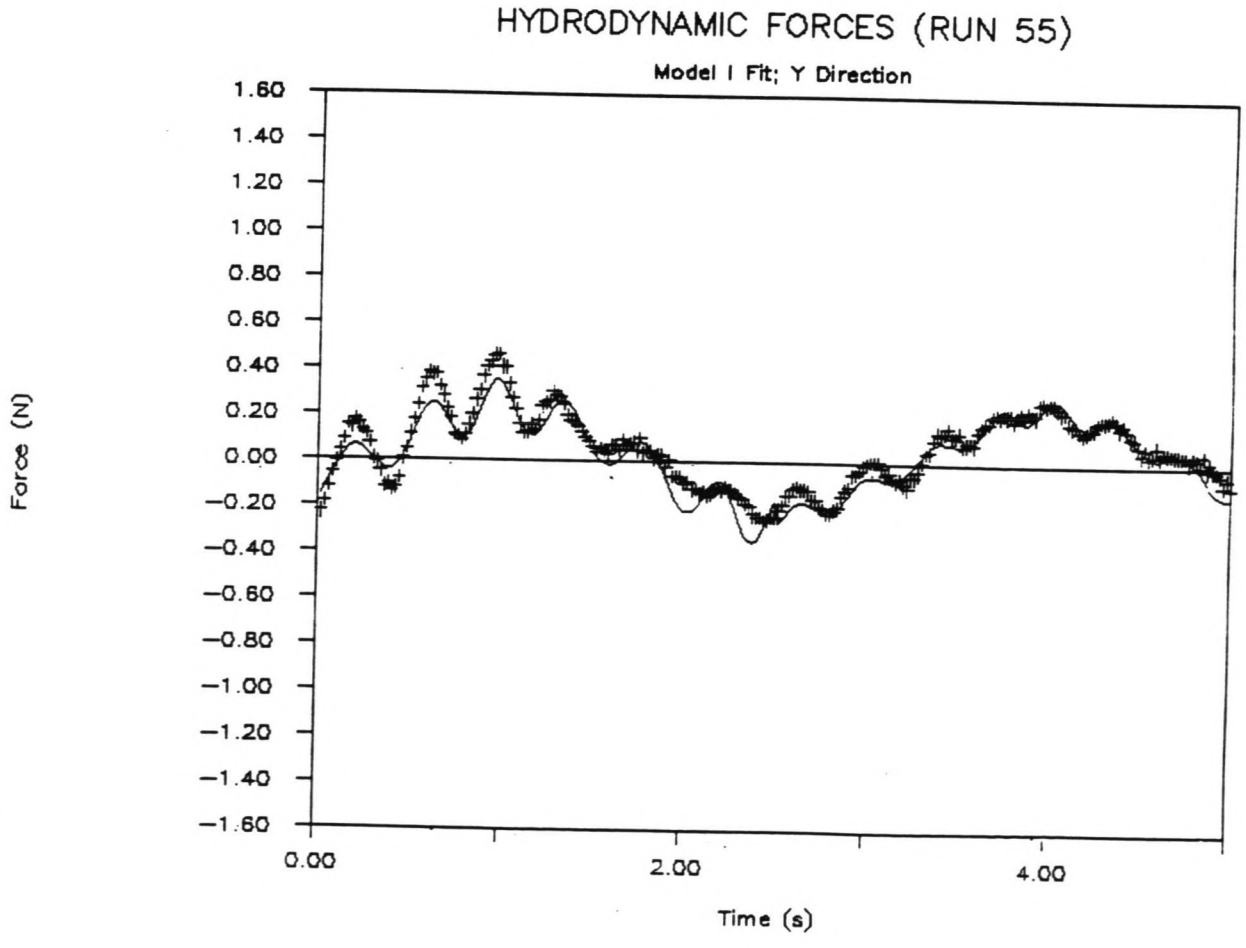

FIGURE G7.5.2

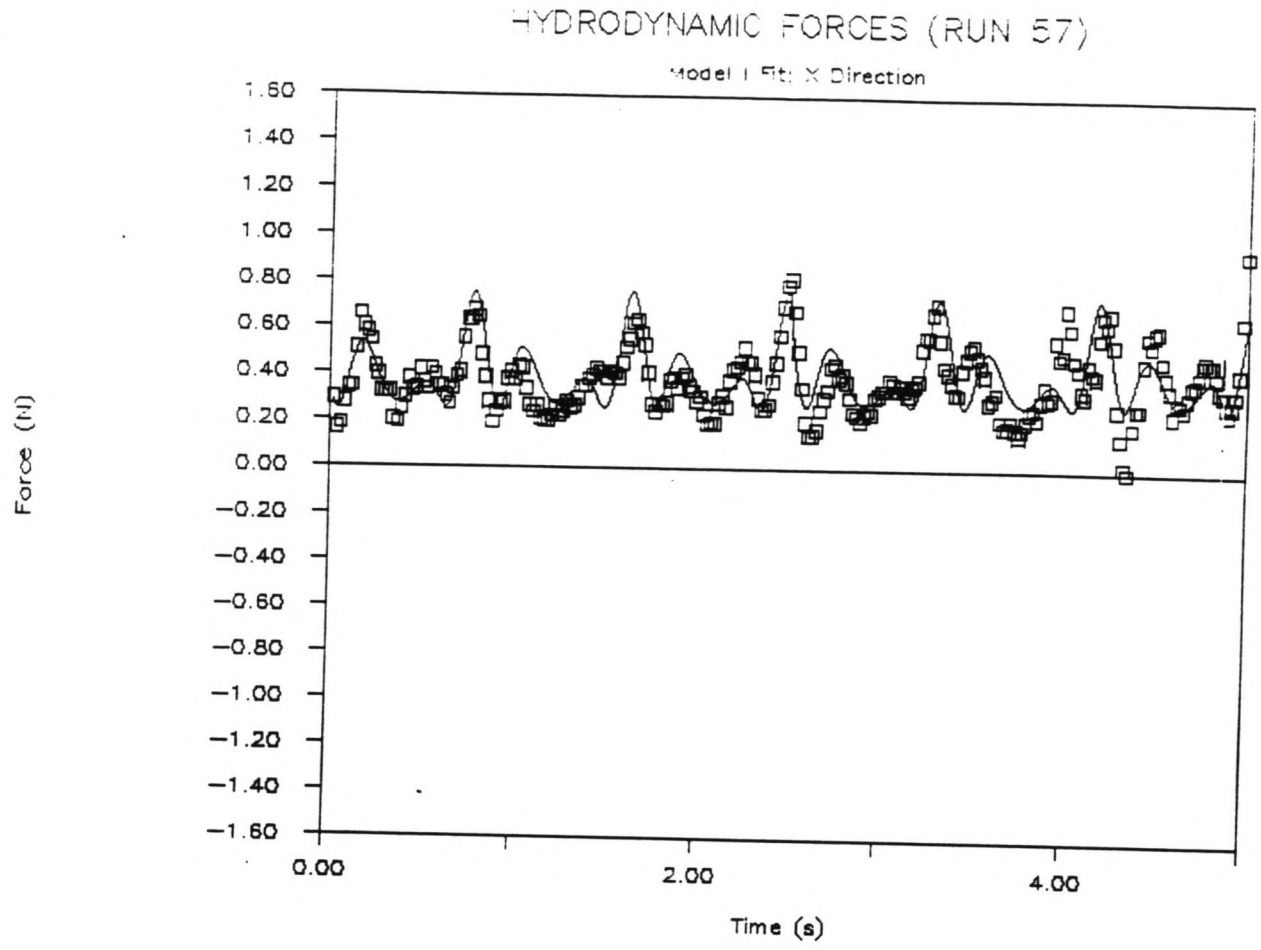

FIGURE G7.6.1

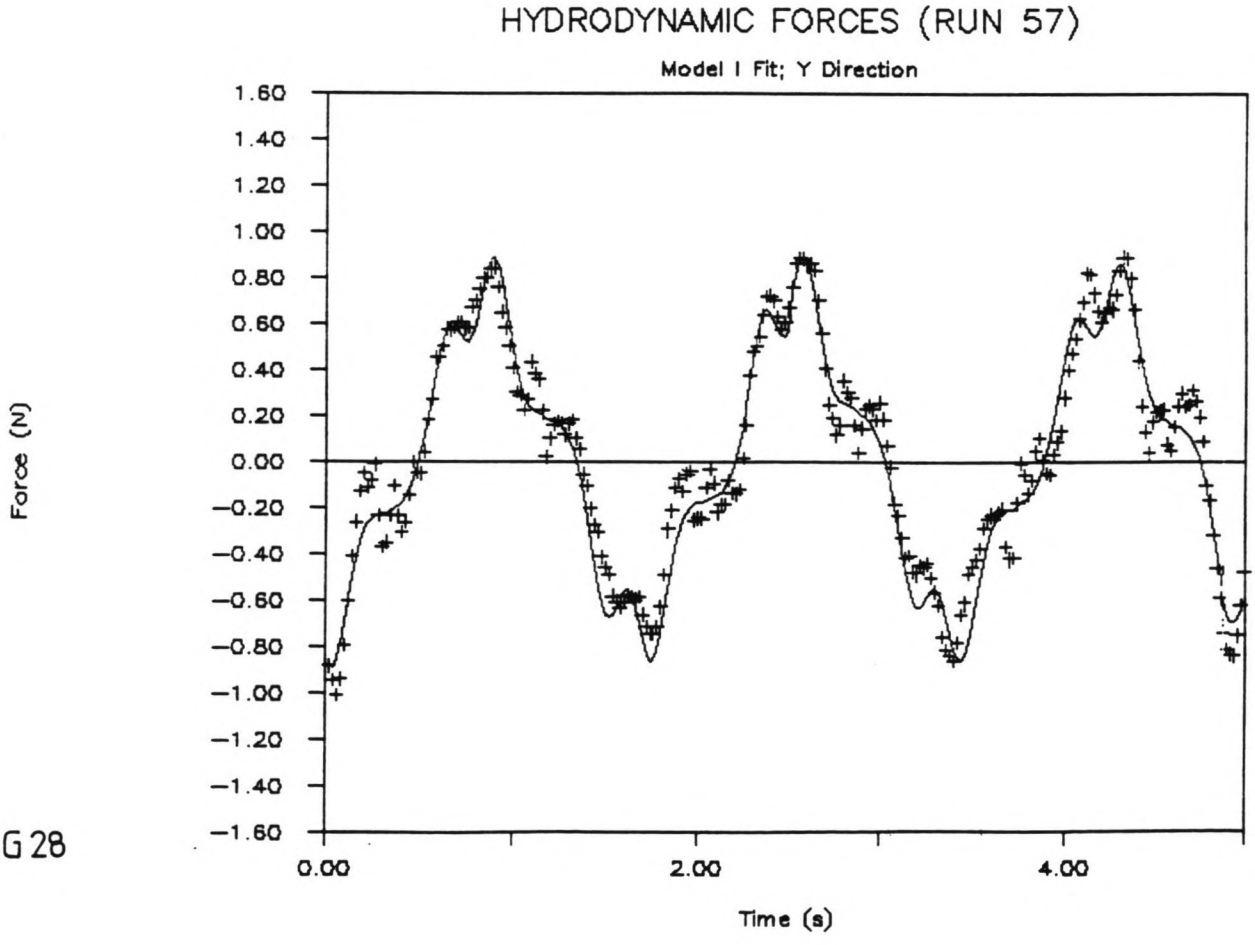

FIGURE G7.6.2

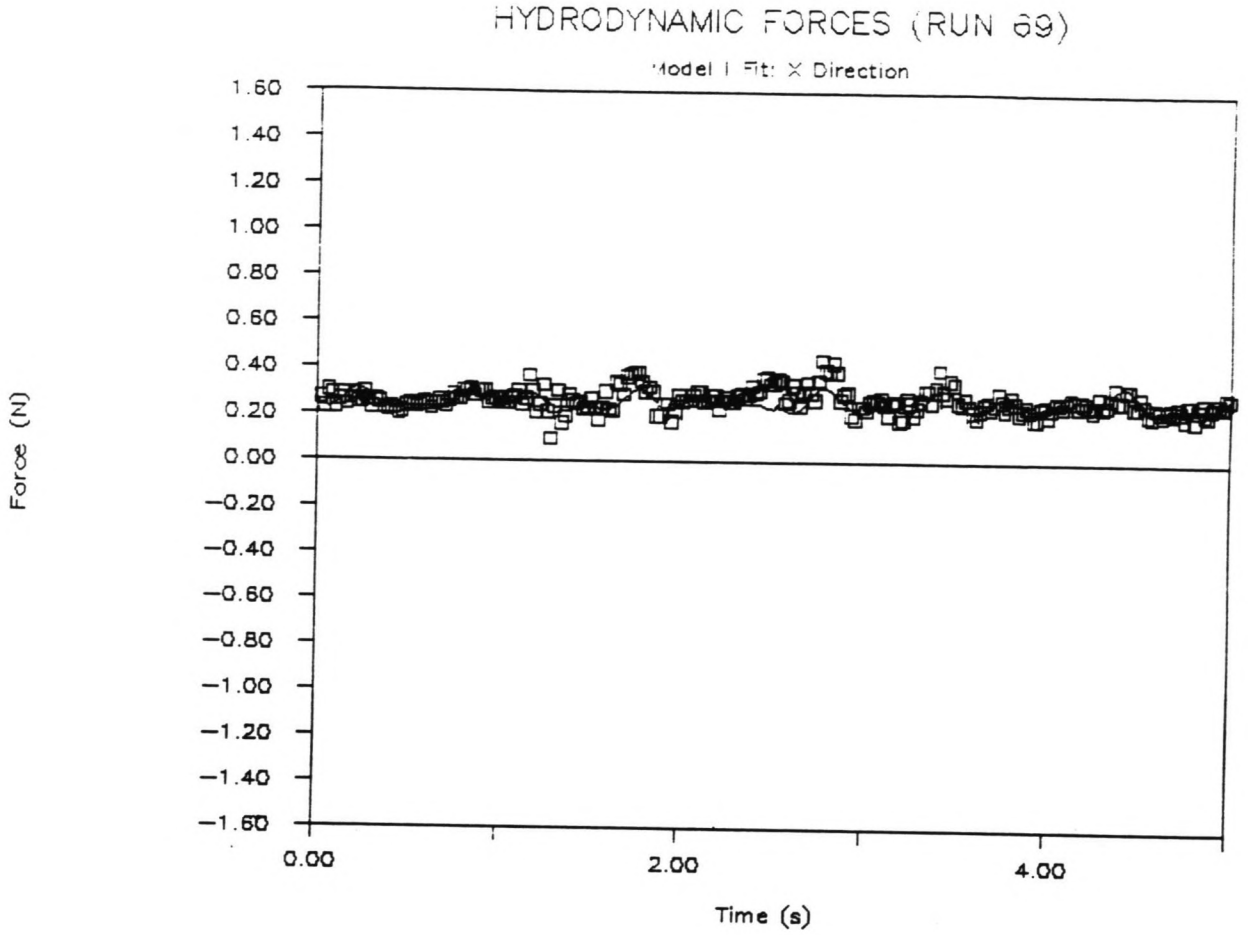

FIGURE G7.7.1

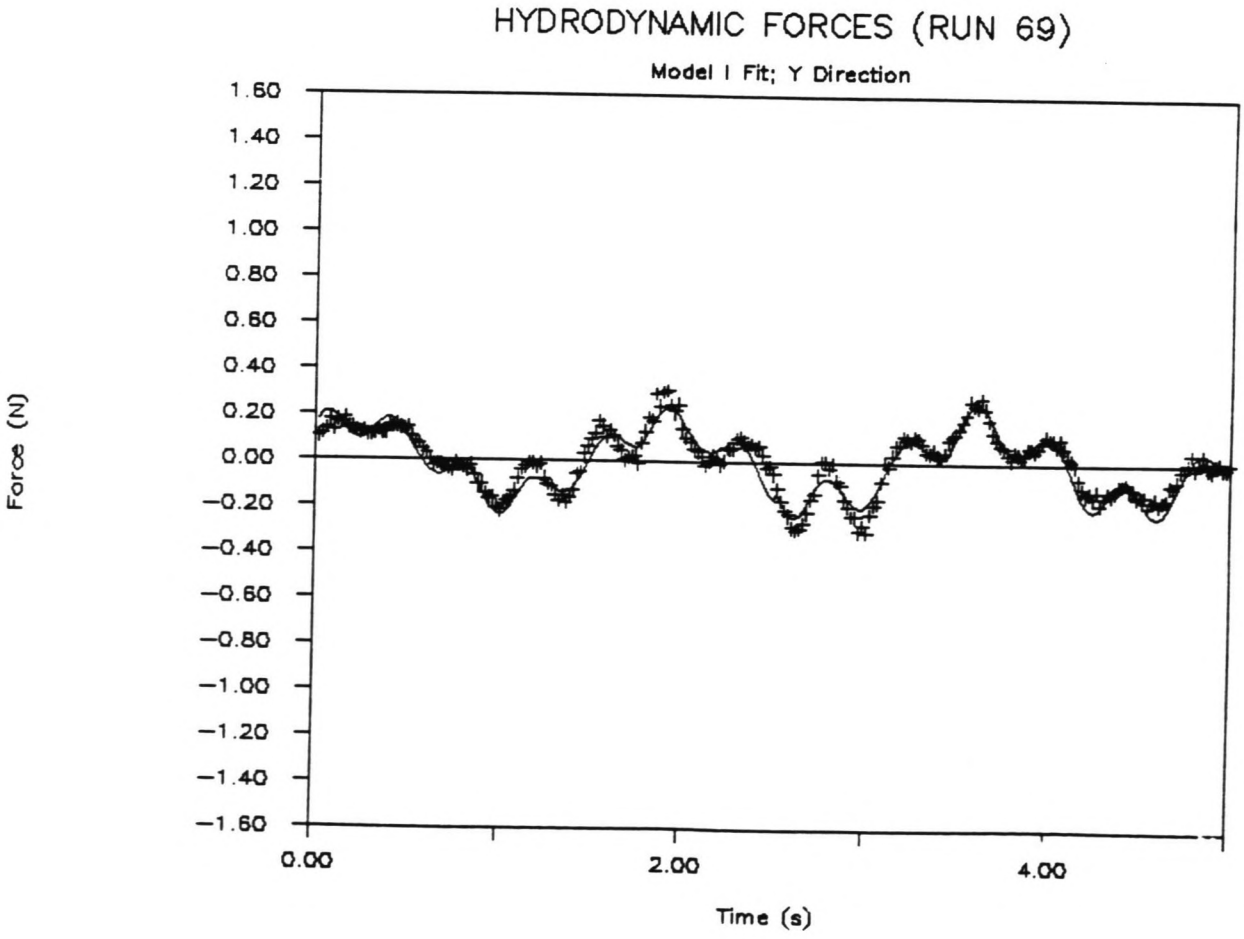

FIGURE G7.7.2

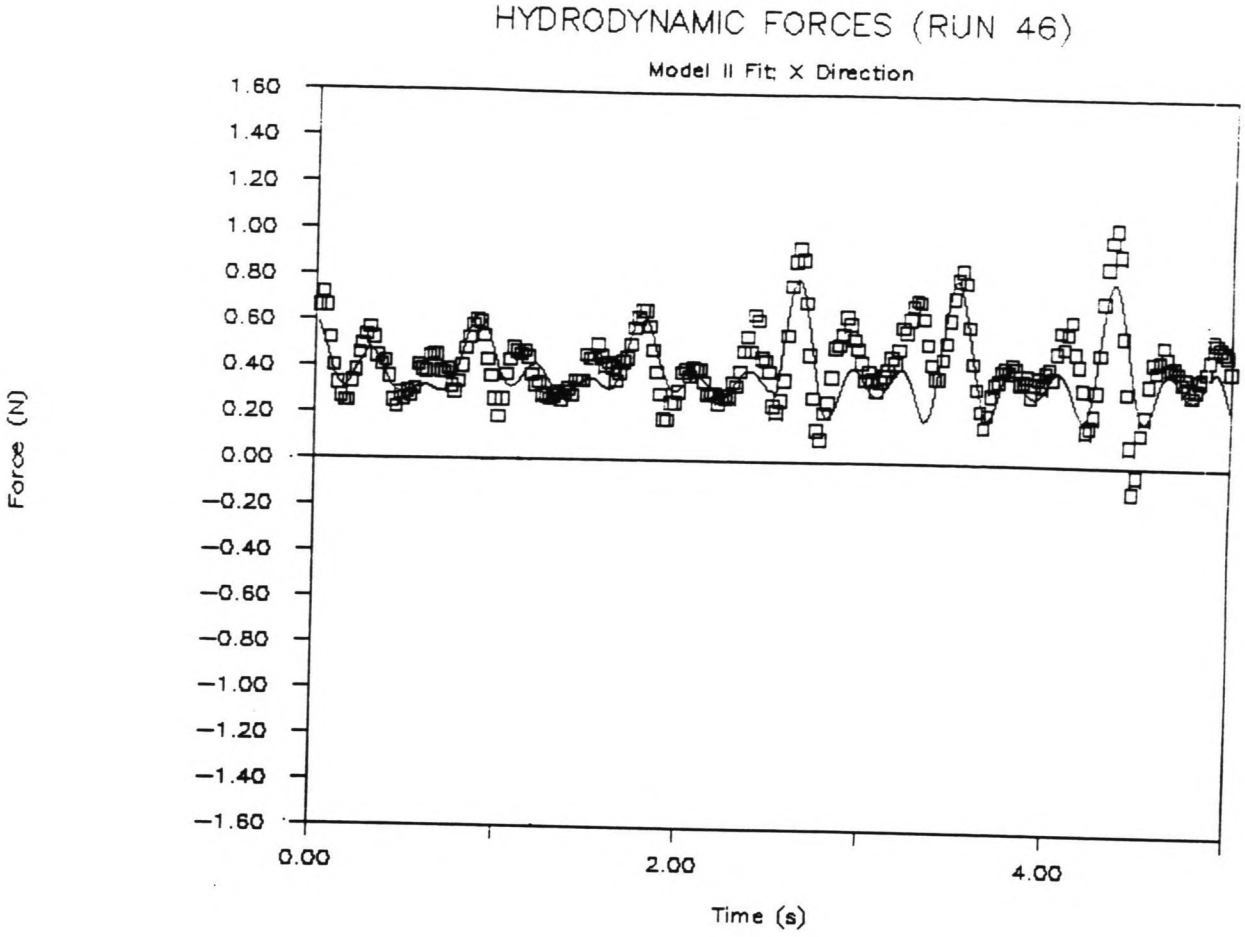

FIGURE G8.1.1

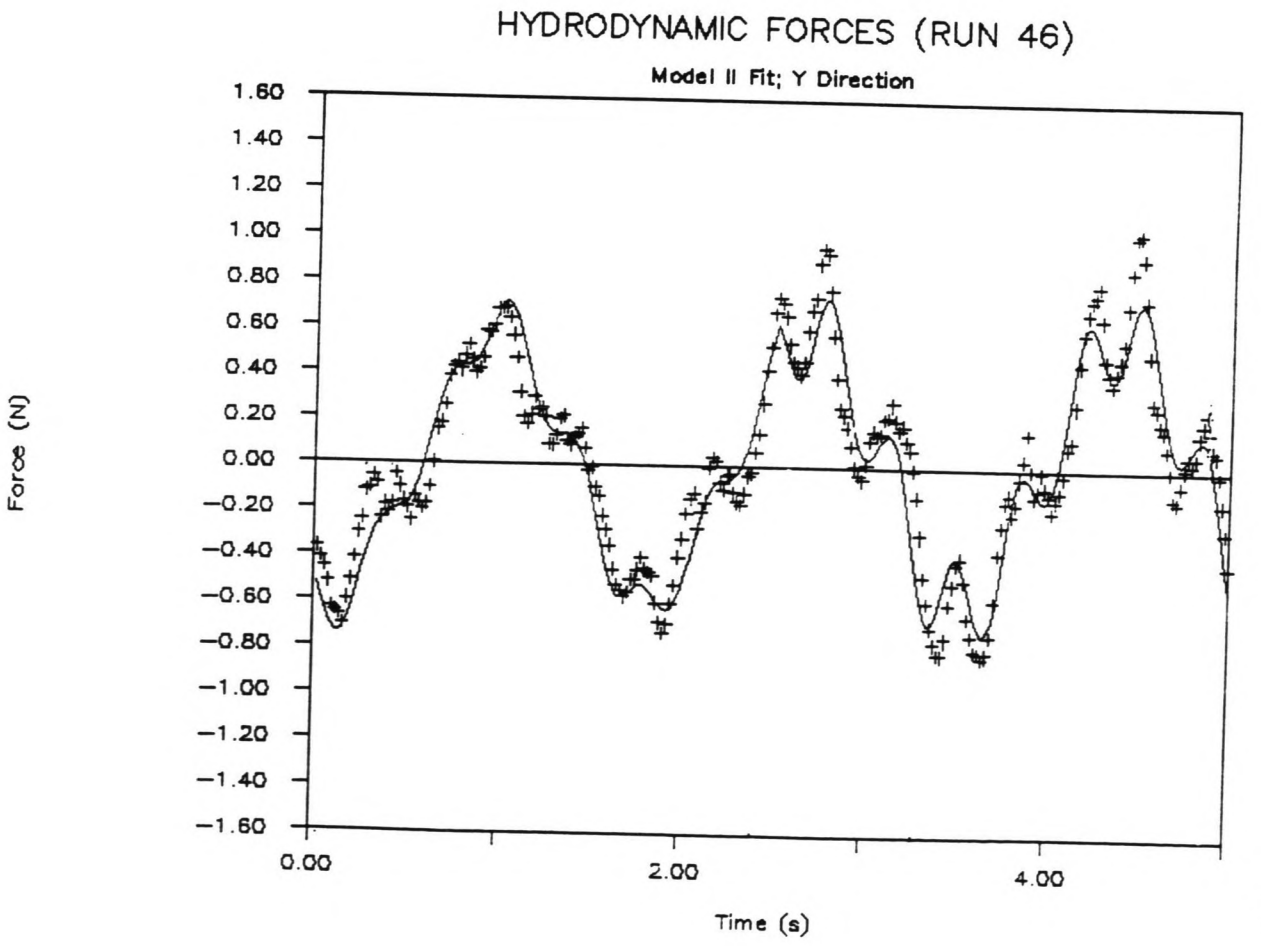

FIGURE G8.1.2

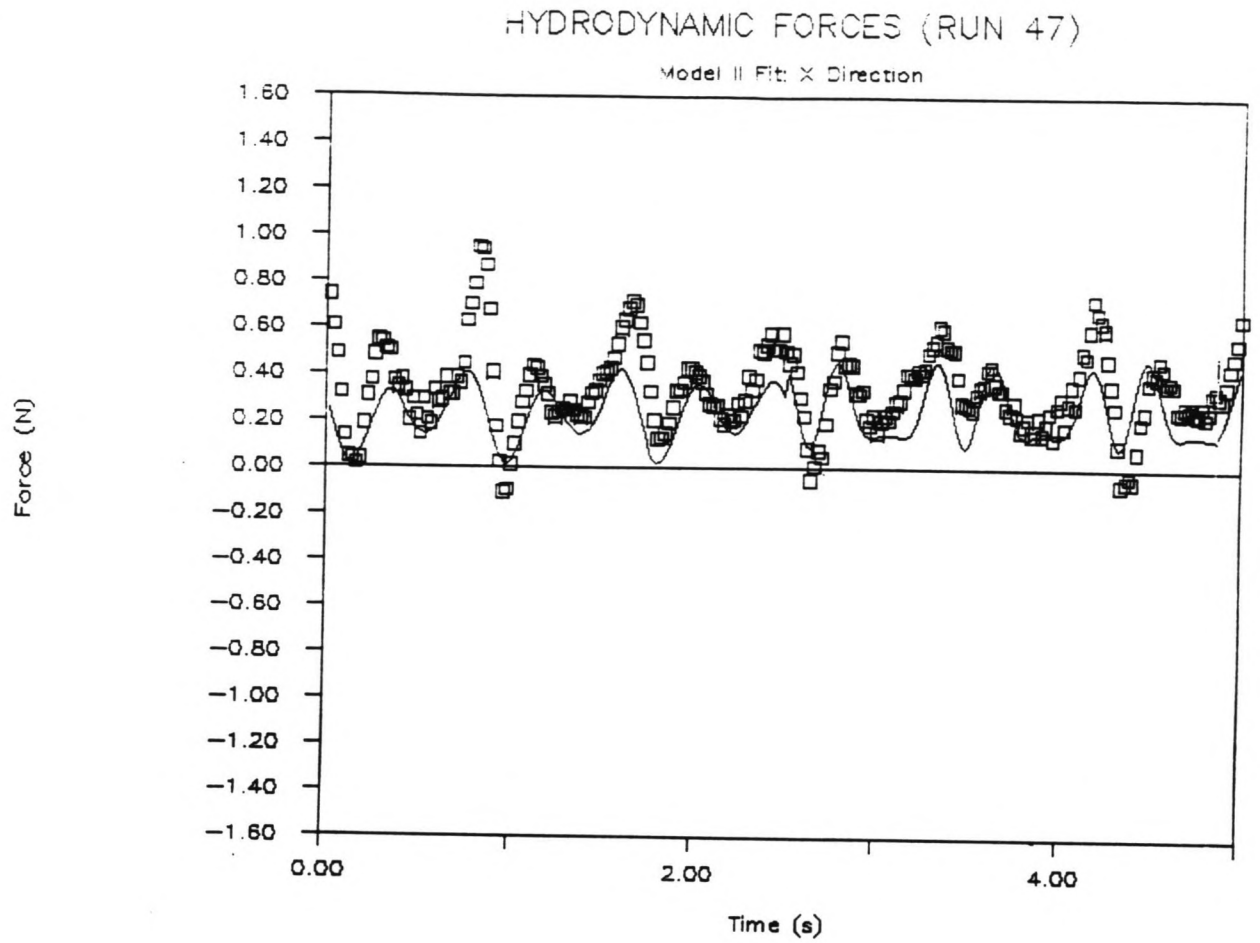

FIGURE G8.2.1

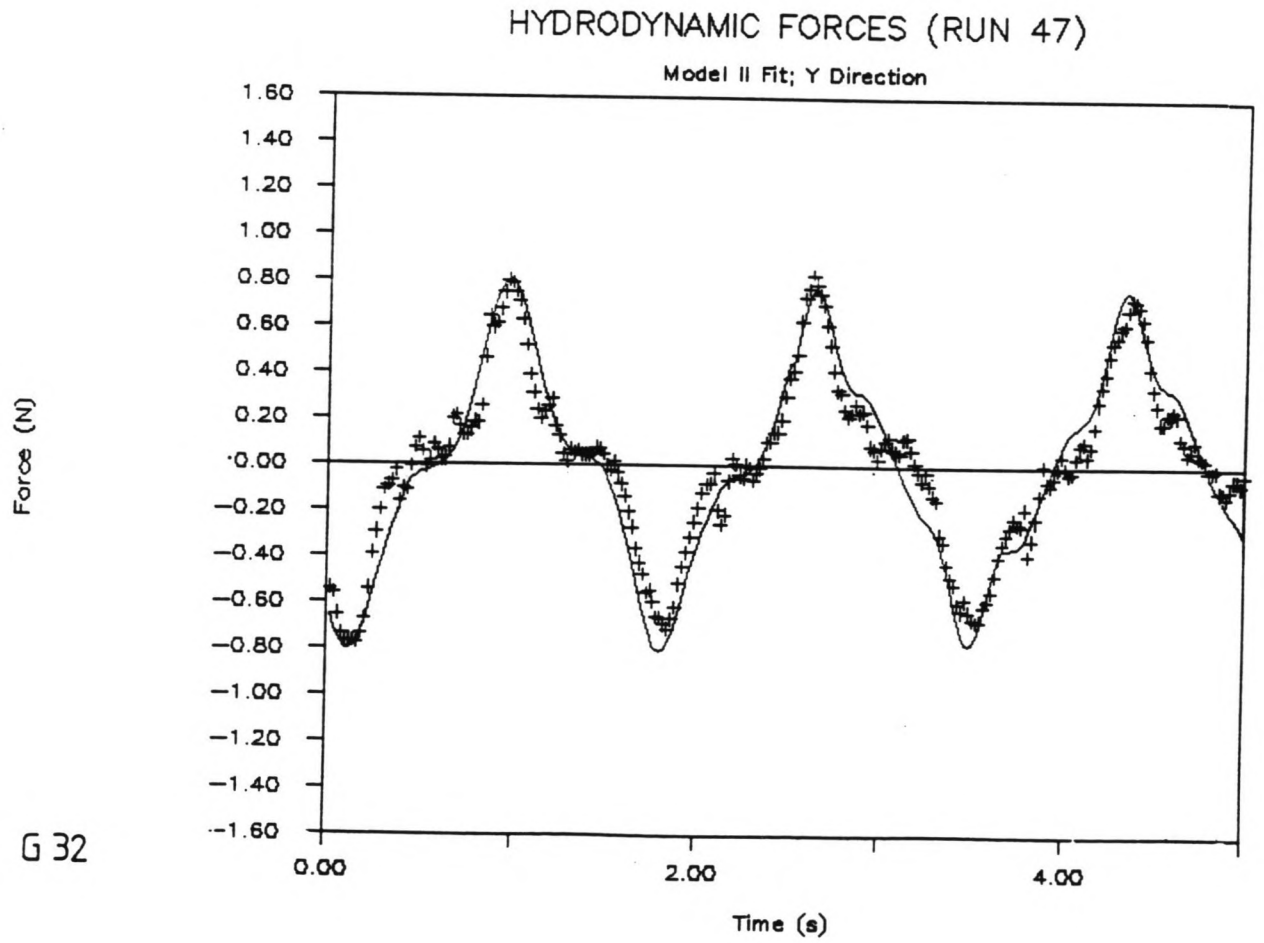

FIGURE G8.2.2

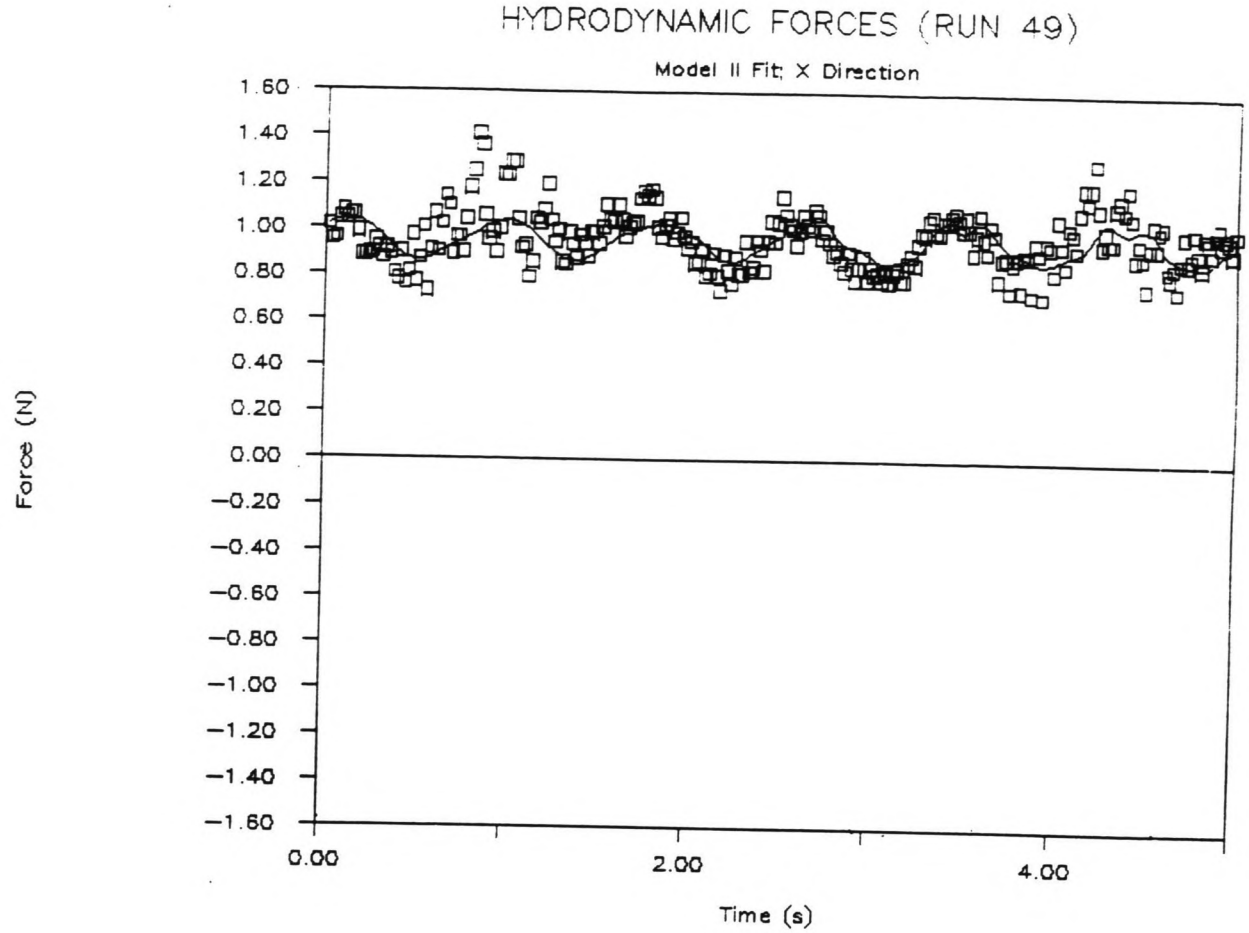

FIGURE G8.3.1

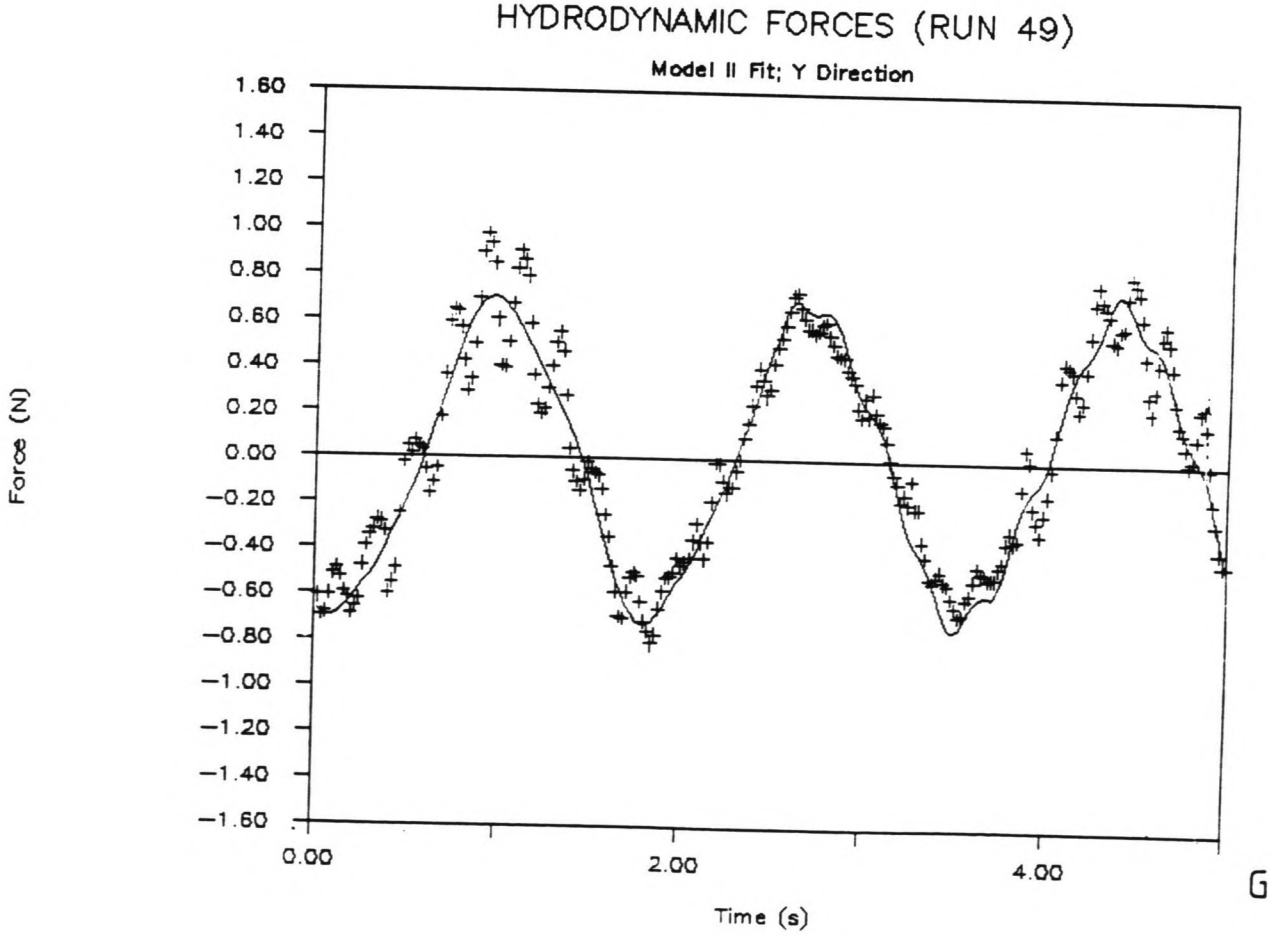

FIGURE G8.3.2

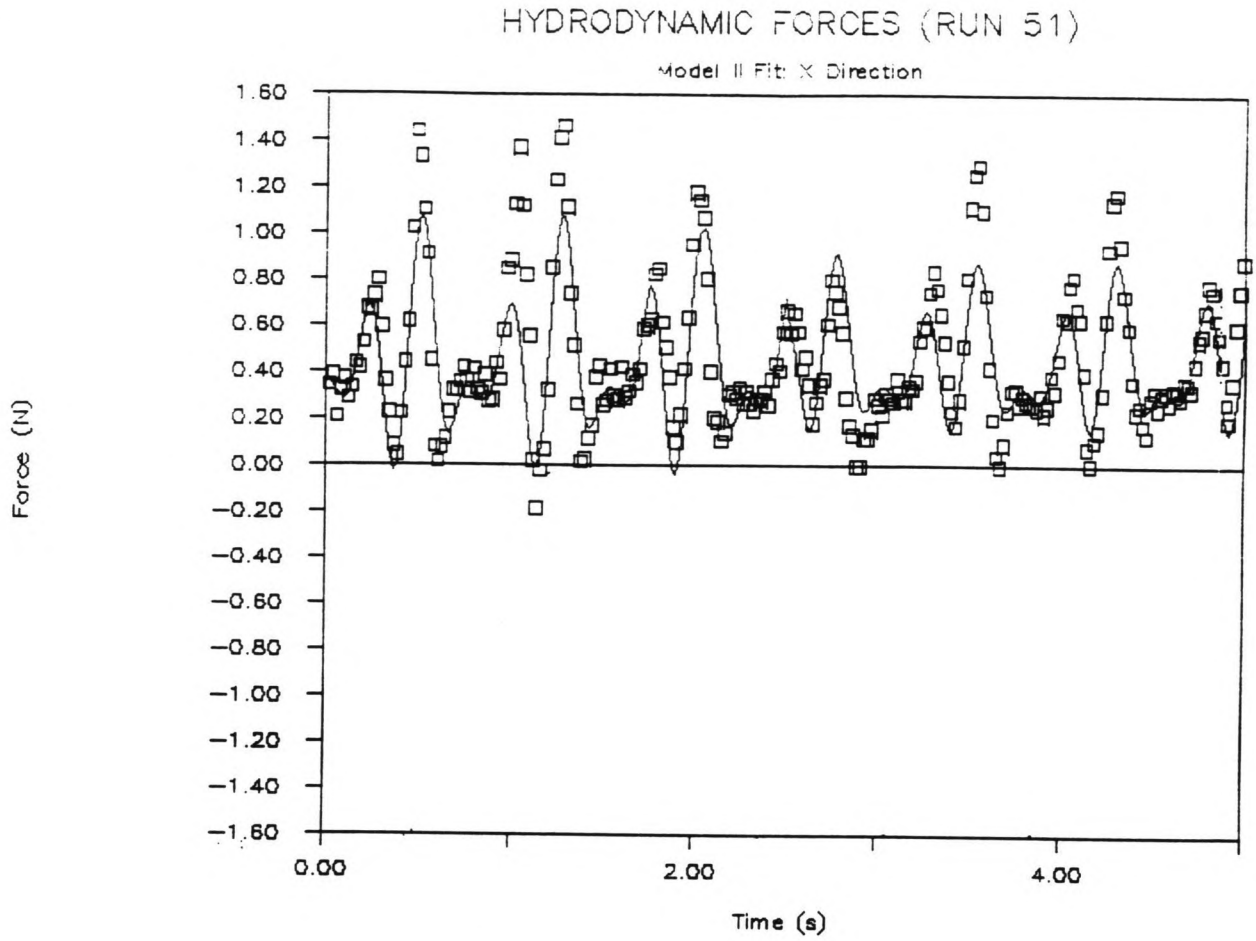

FIGURE G8.4.1

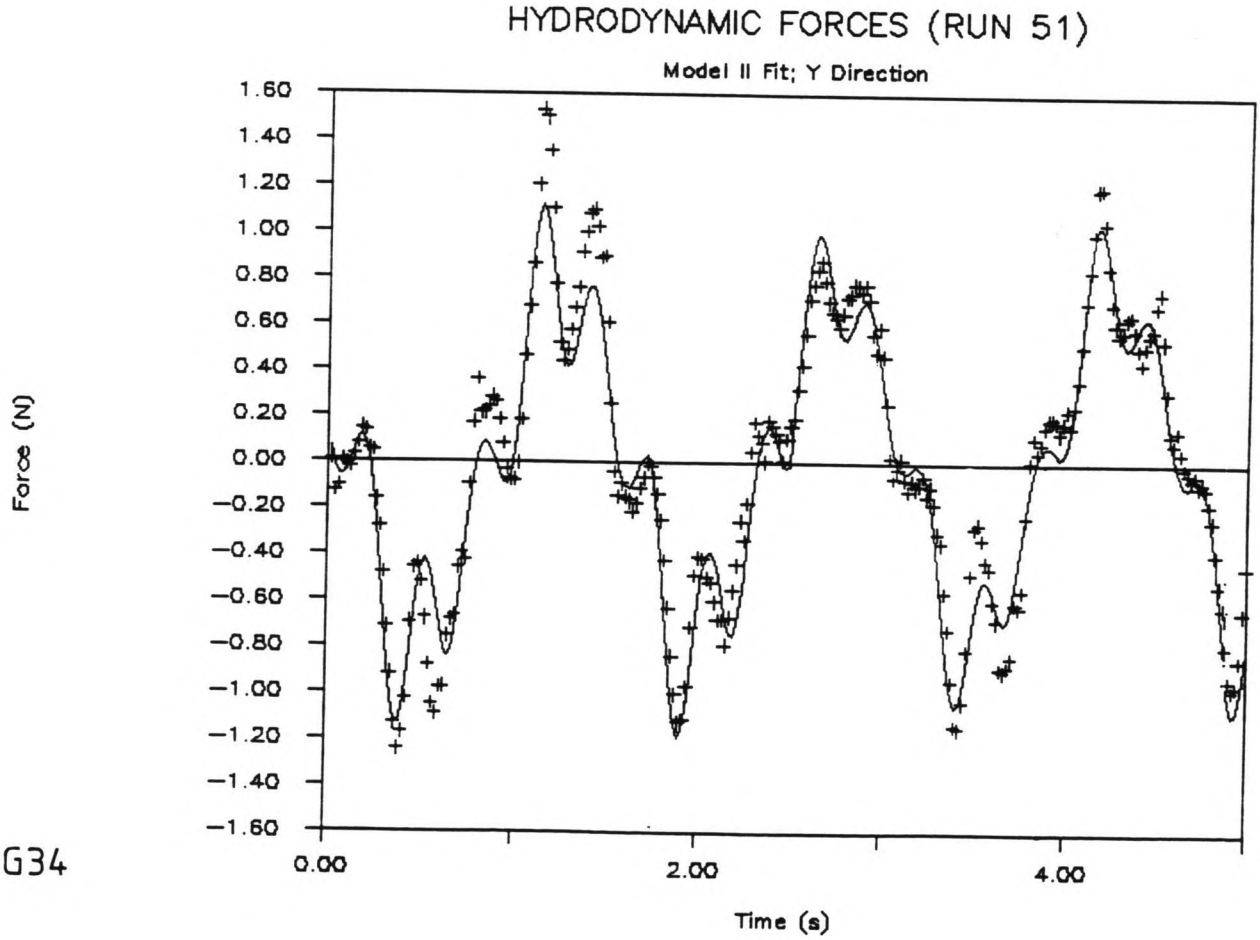

FIGURE G8.4.2

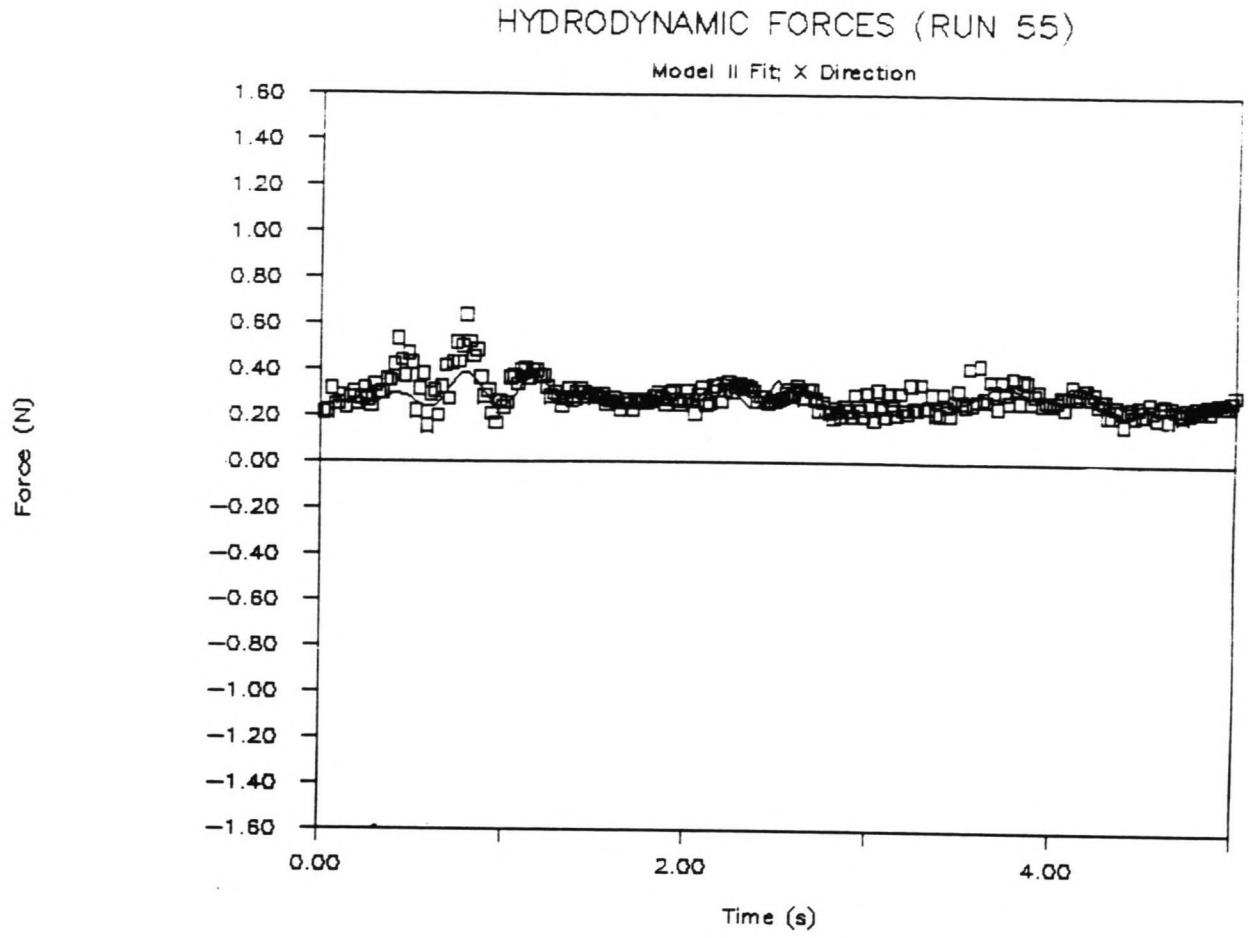

FIGURE G8.5.1

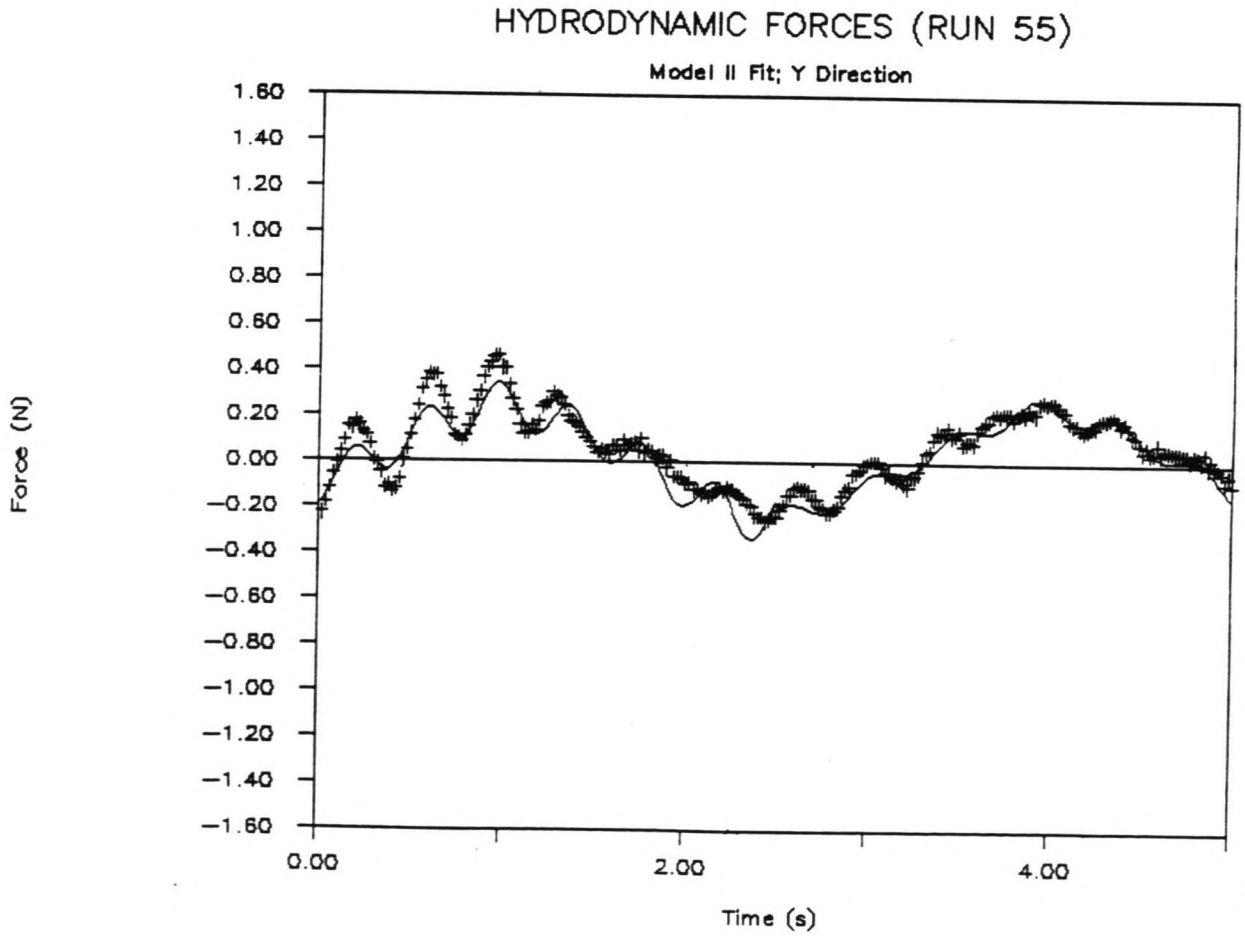

FIGURE G8.5.2

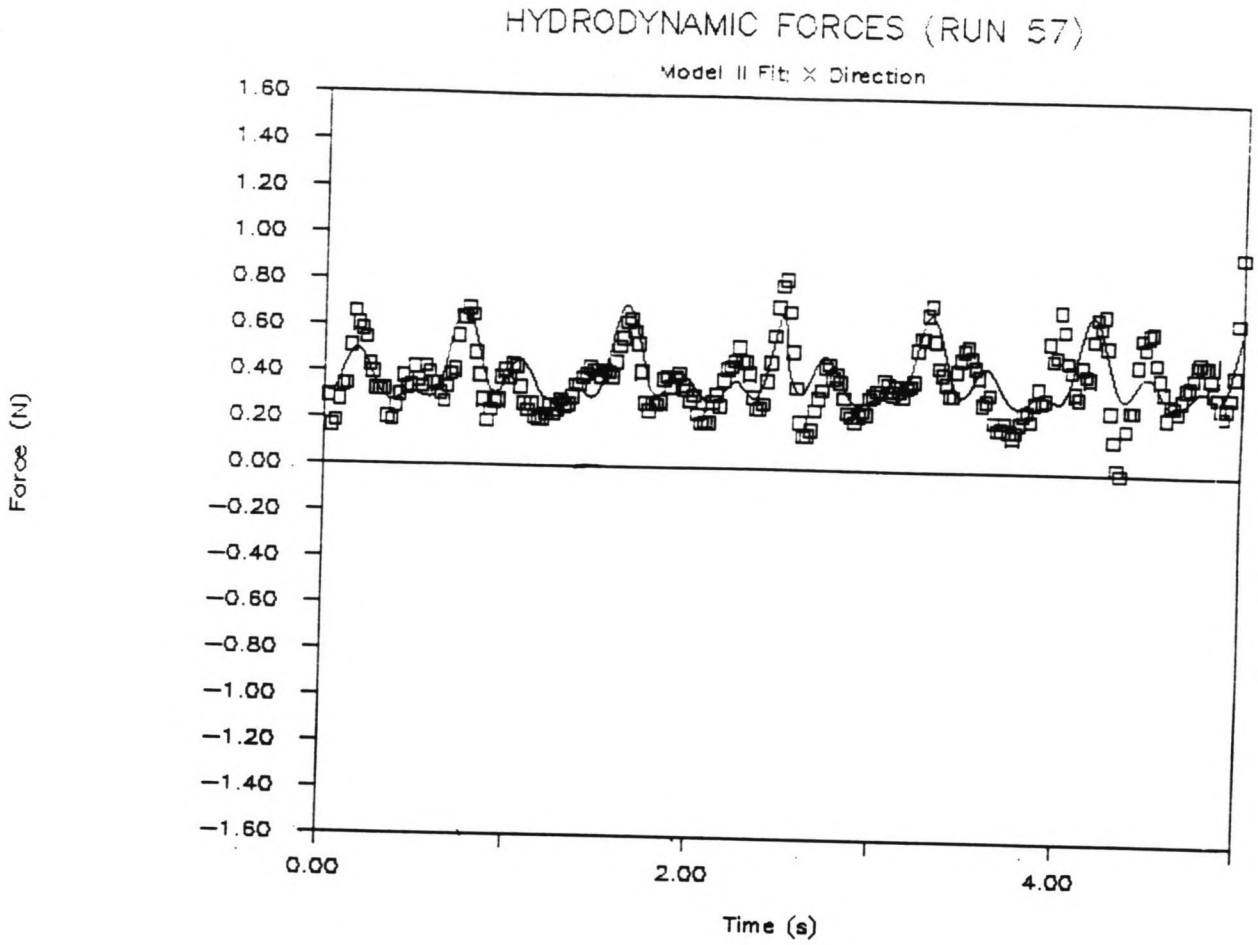

FIGURE G8.6.1

FIGURE G8.6.2

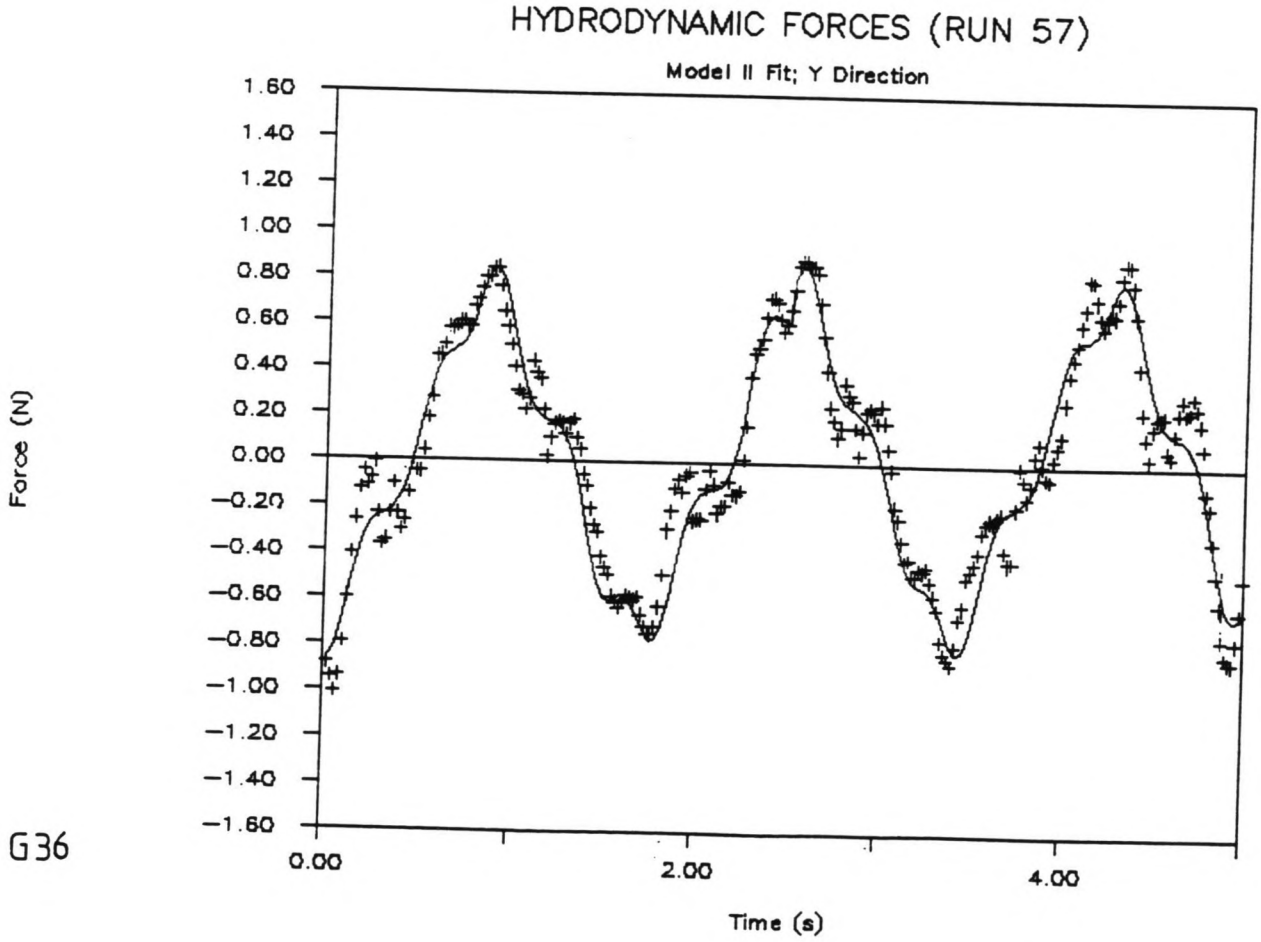

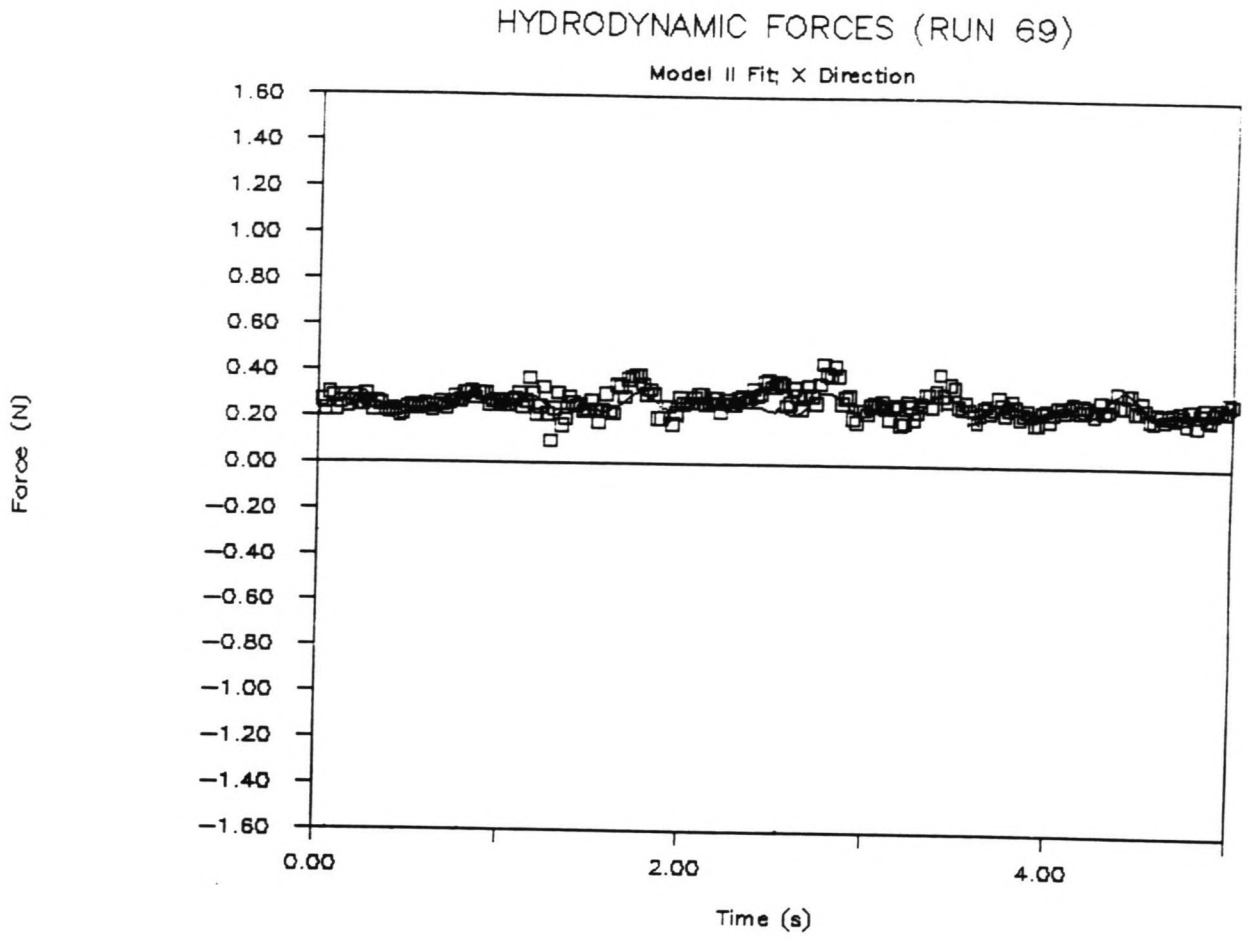

FIGURE G8.7.1

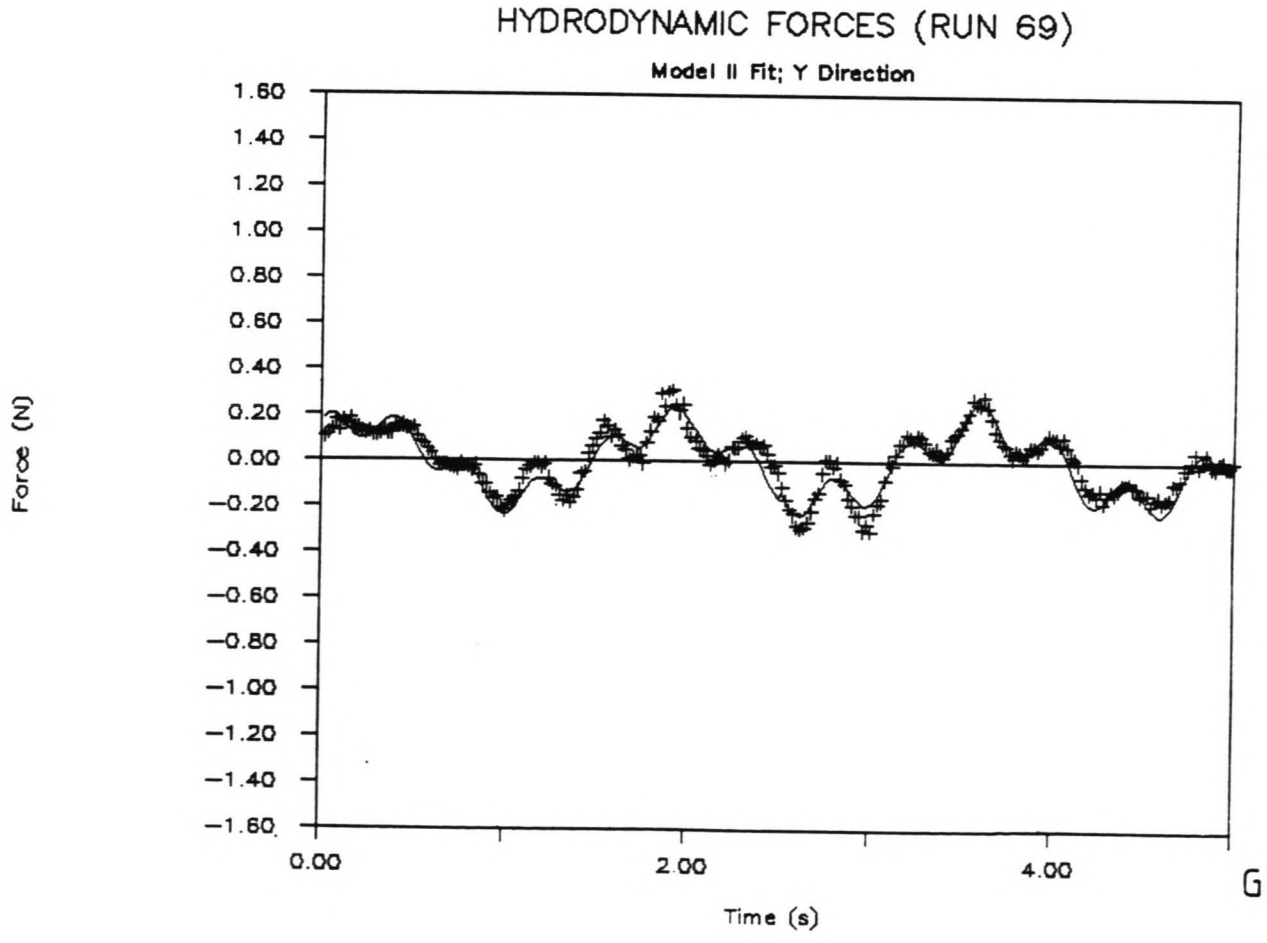

FIGURE G8.7.2

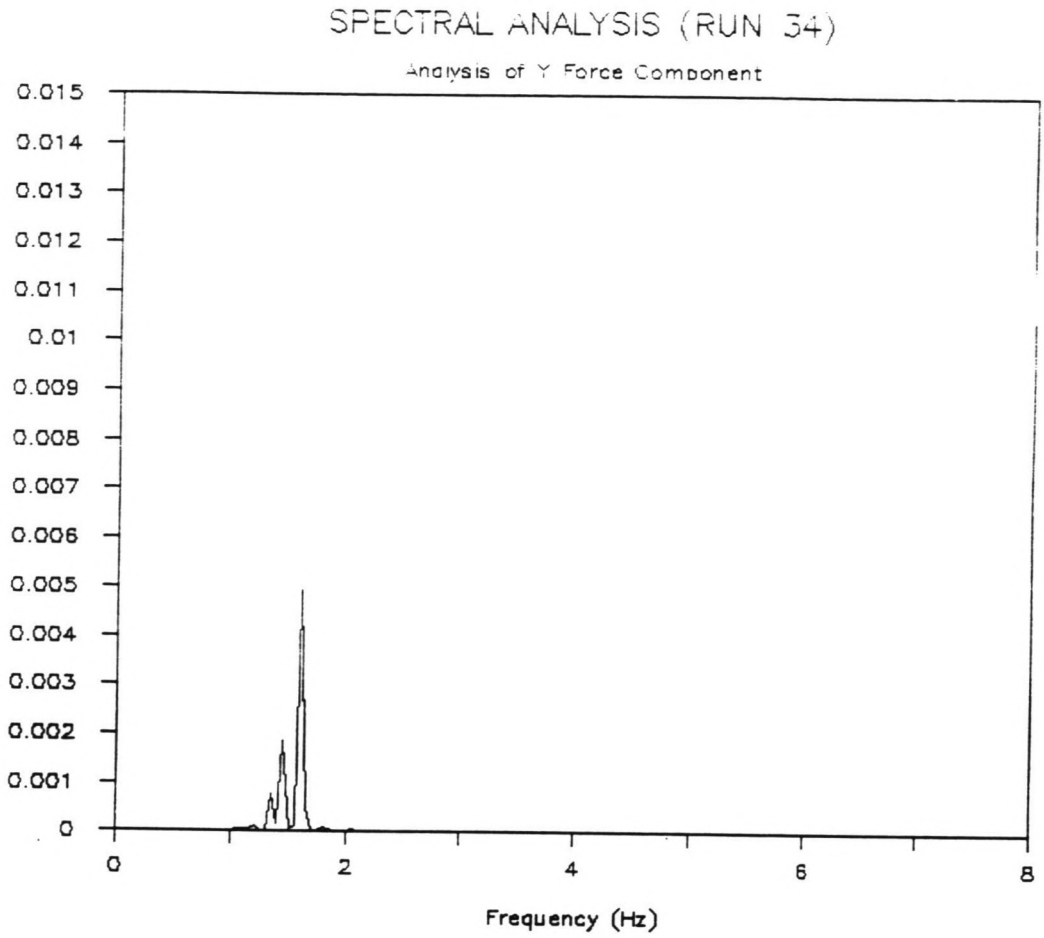

FIGURE G9.1

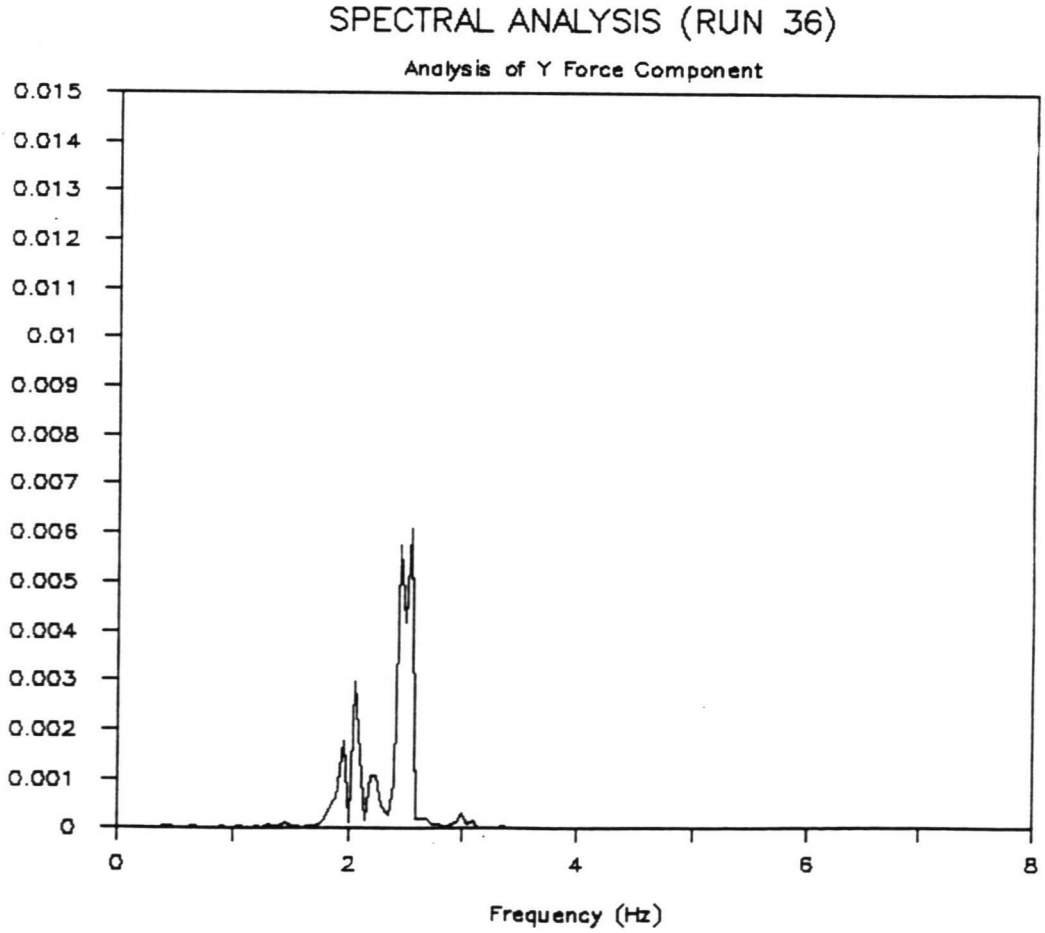

FIGURE G9.2

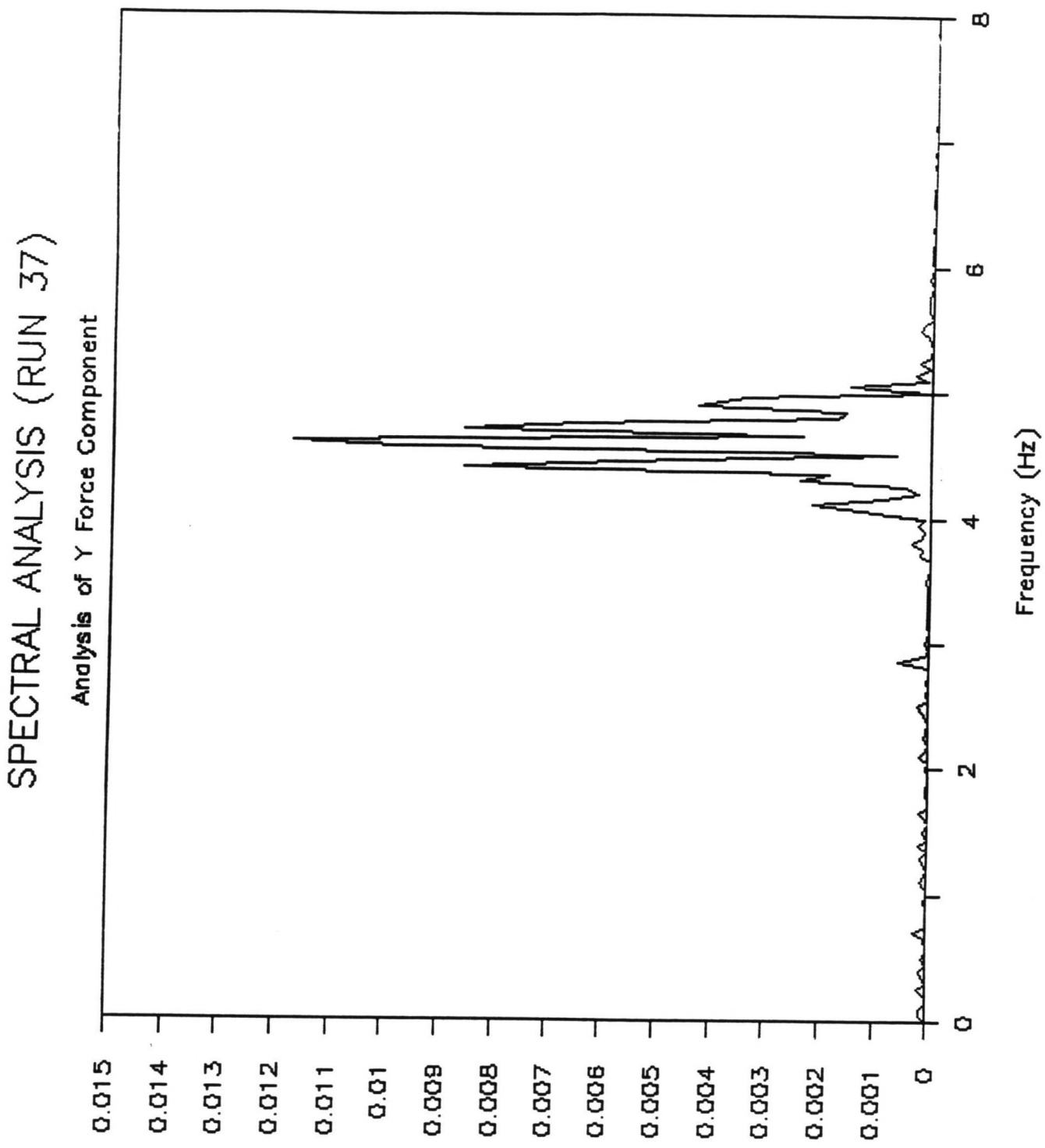
SPECTRAL ANALYSIS (RUN 37)
Analysis of Y Force Component
0.015
0.014
0.013
0.012
0.011
0.01
0.009
0.008
0.007
0.006
0.005
0.004
0.003
0.002
0.001
0
0
2
4
6
8
Frequency (Hz)

FIGURE G9.3

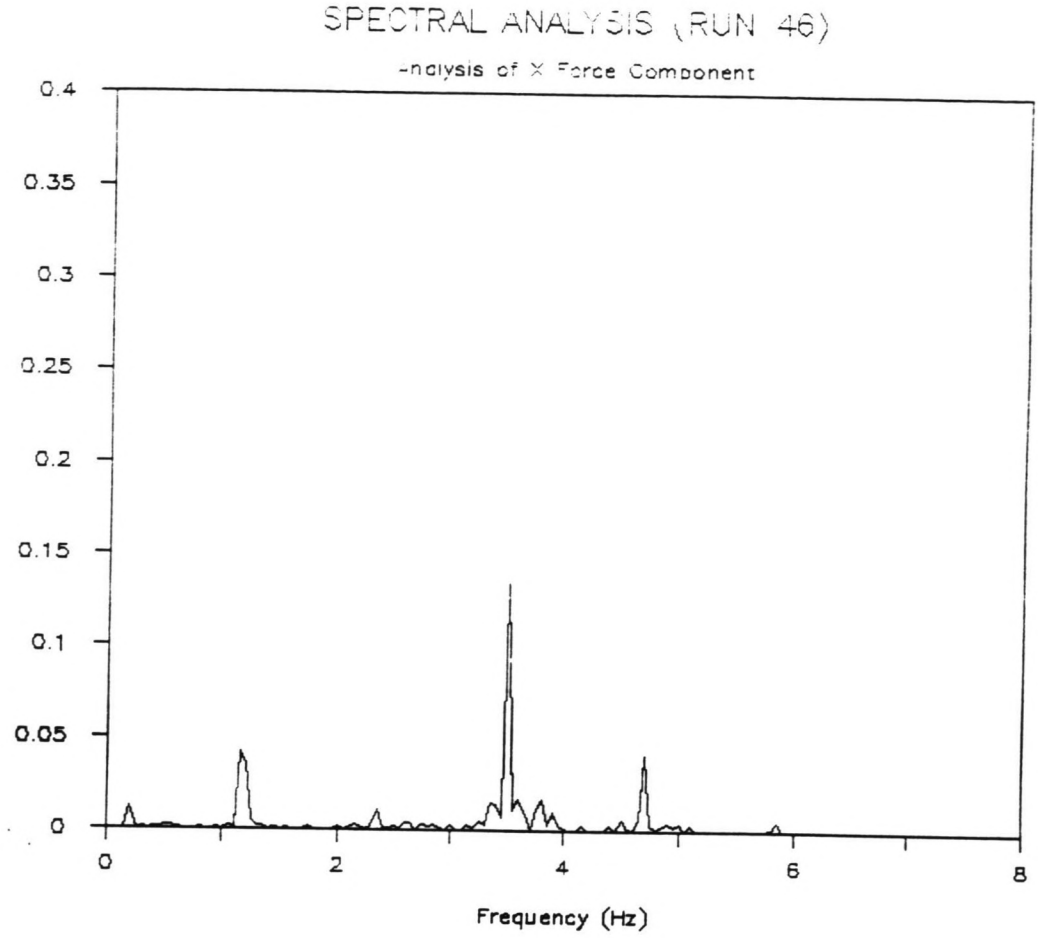

FIGURE G9.4.1

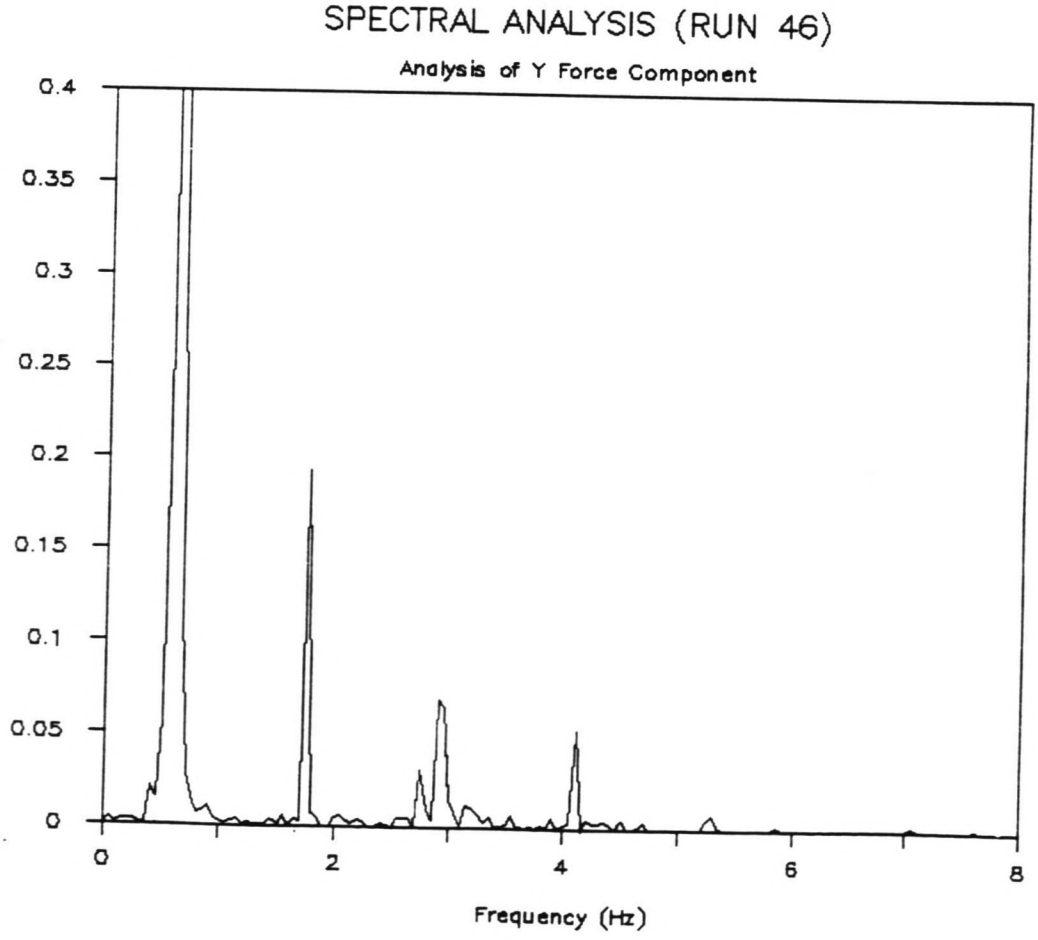

FIGURE G9.4.2

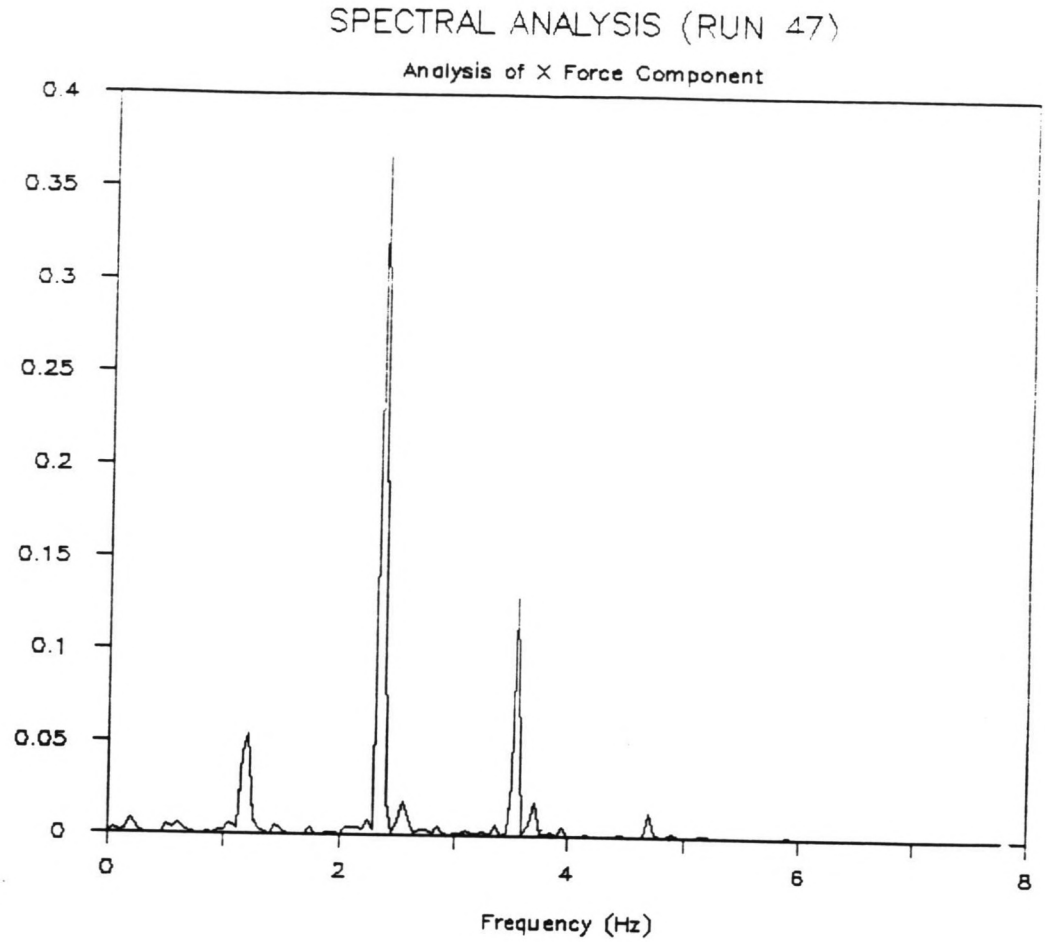

FIGURE G9.5.1

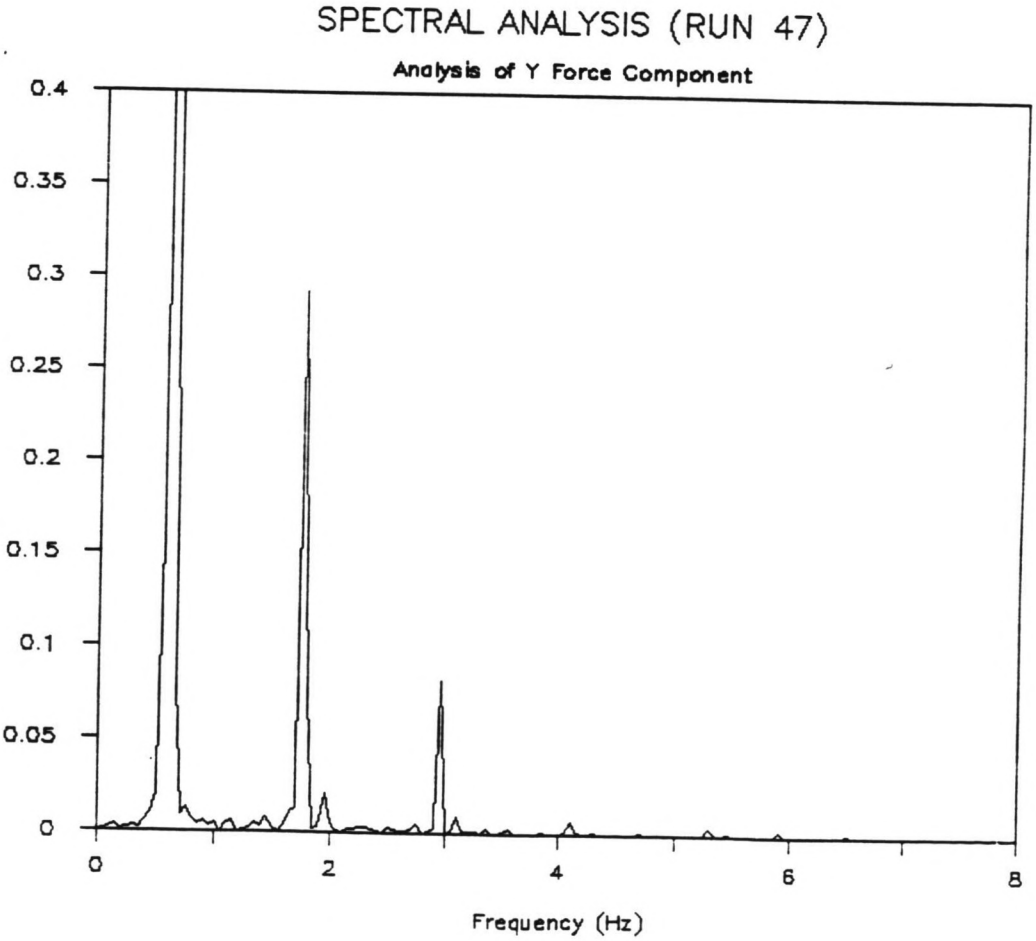

FIGURE G9.5.2

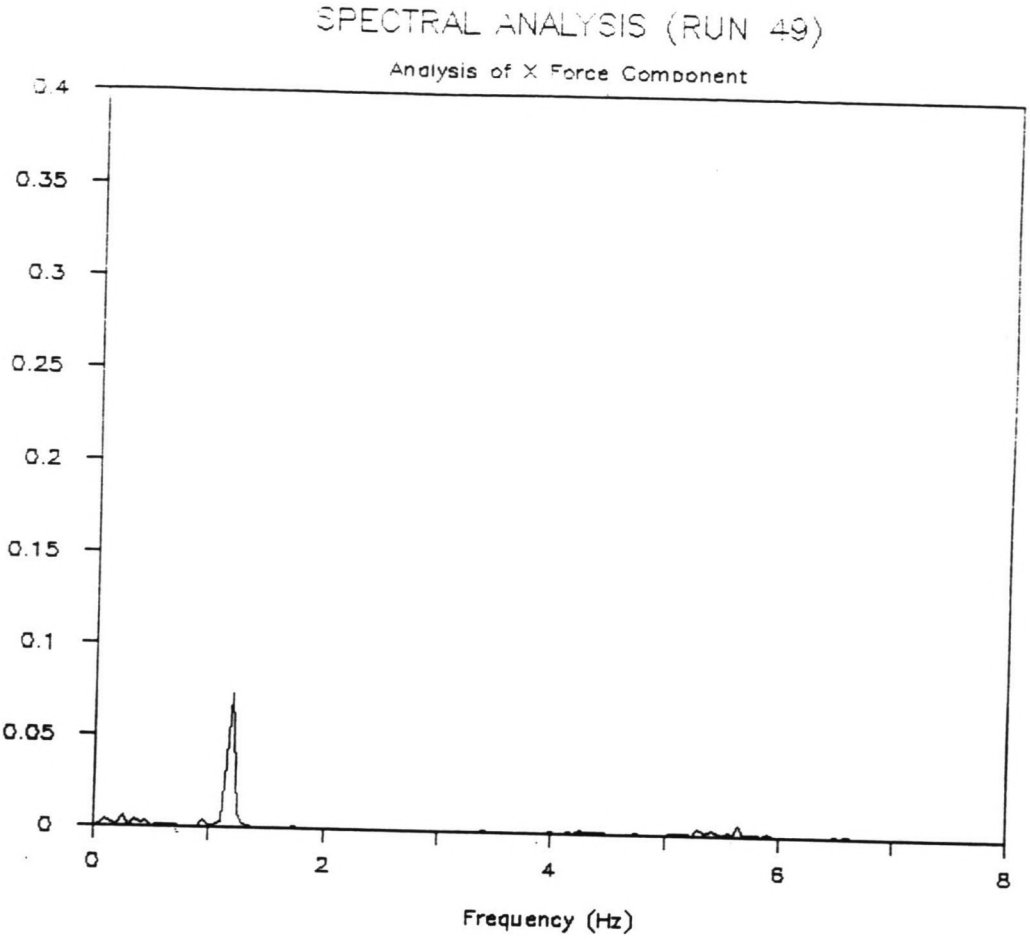

FIGURE G9.6.1

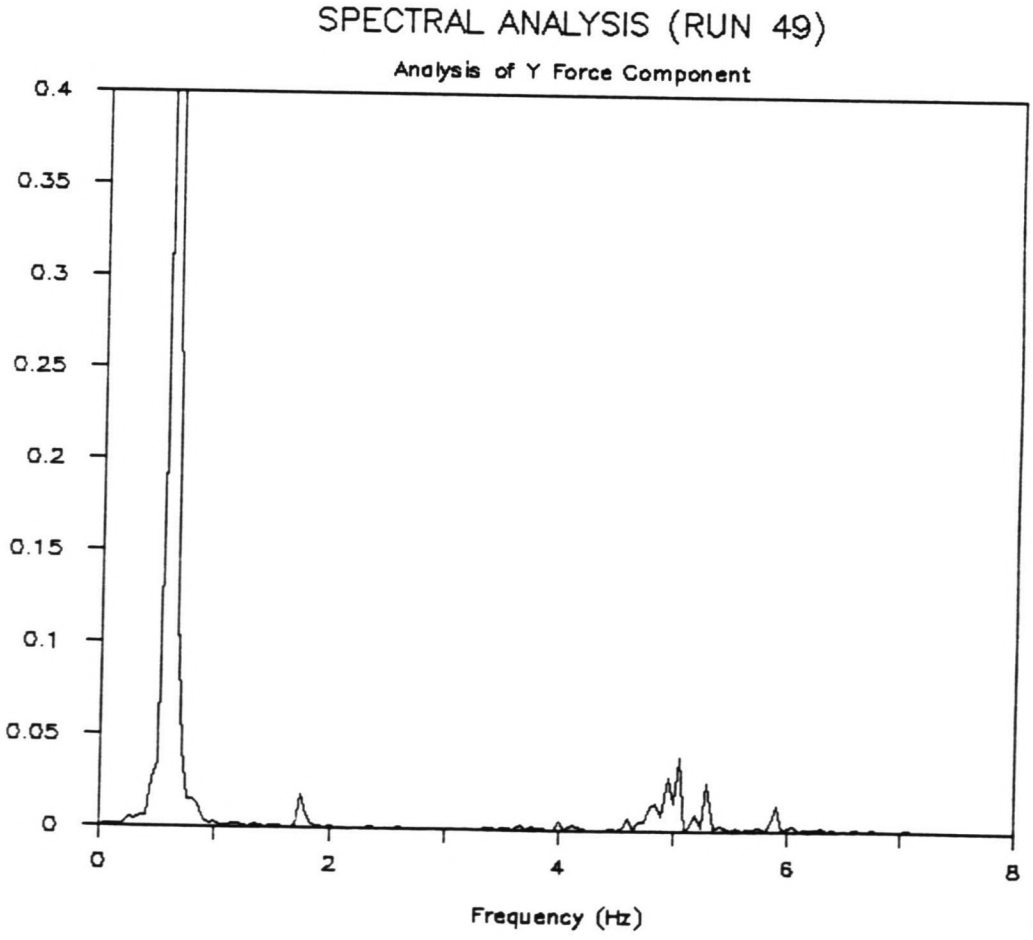

FIGURE G9.6.2

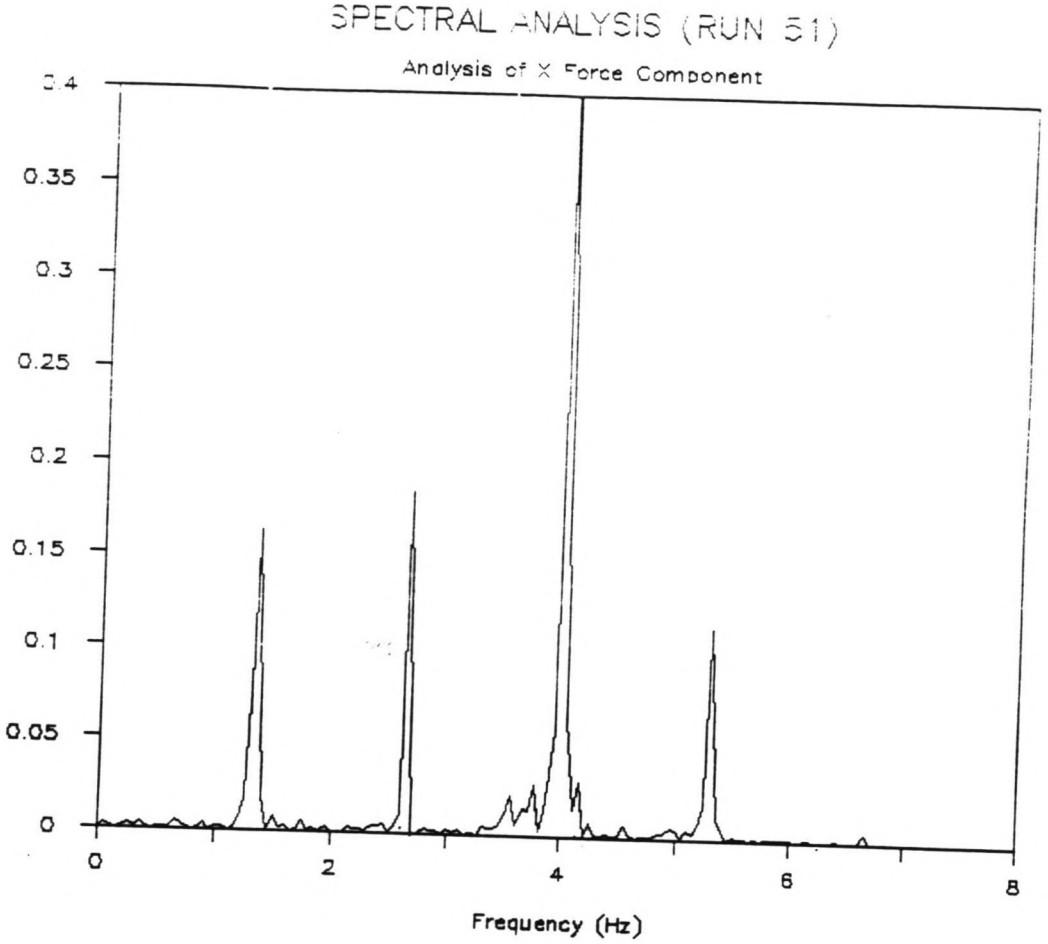

FIGURE G9.7.1

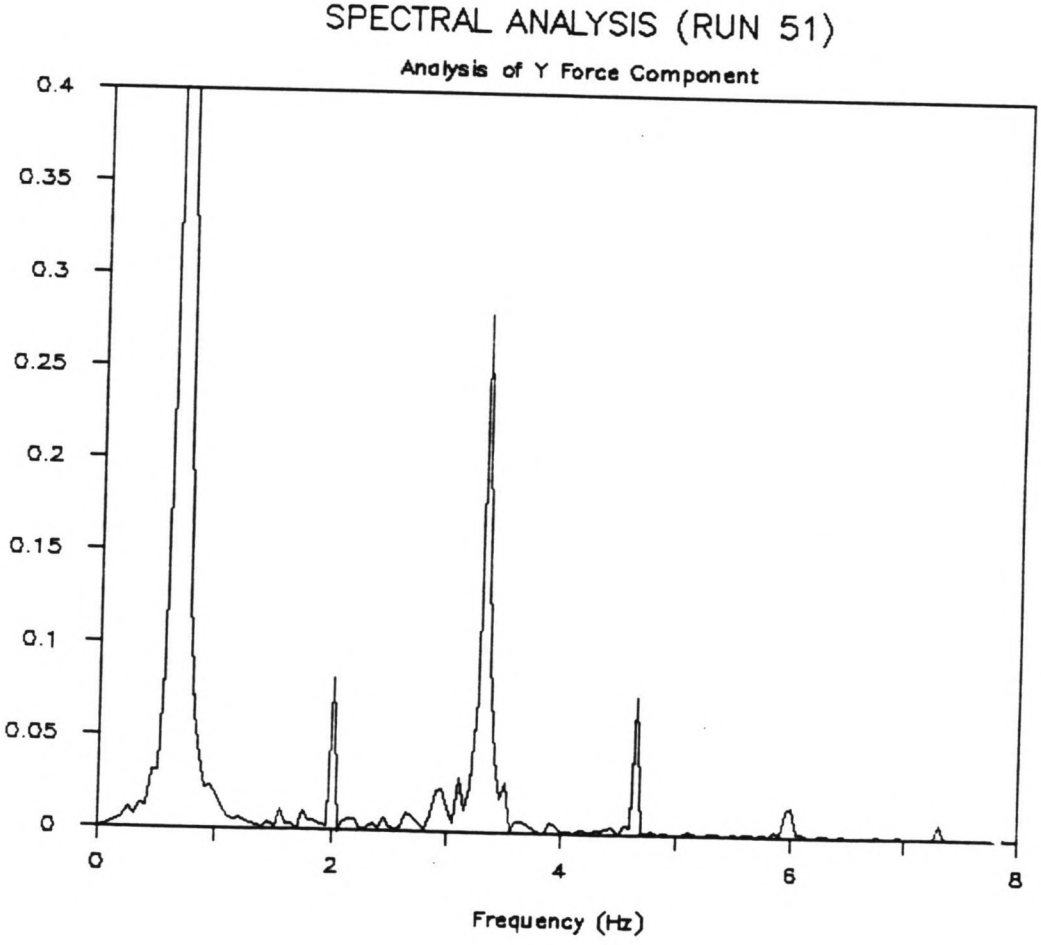

FIGURE G9.7.2

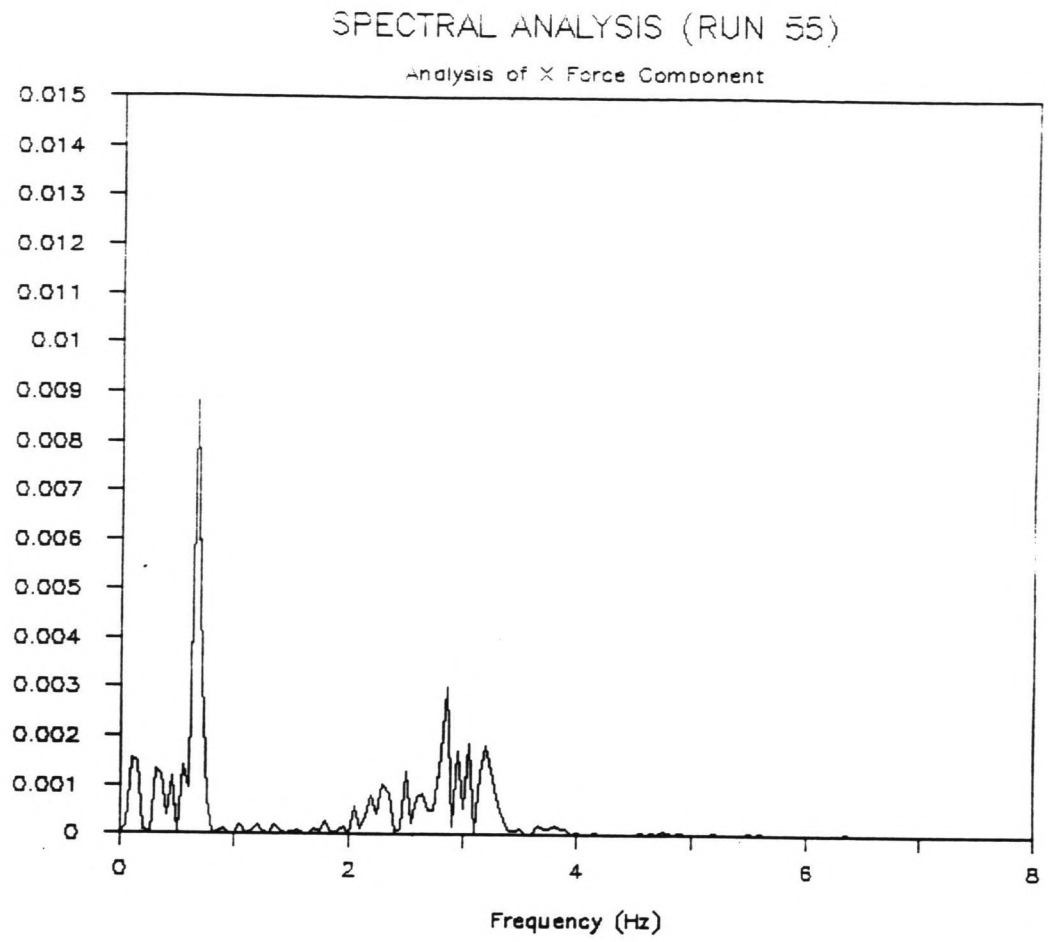

FIGURE G9.8.1

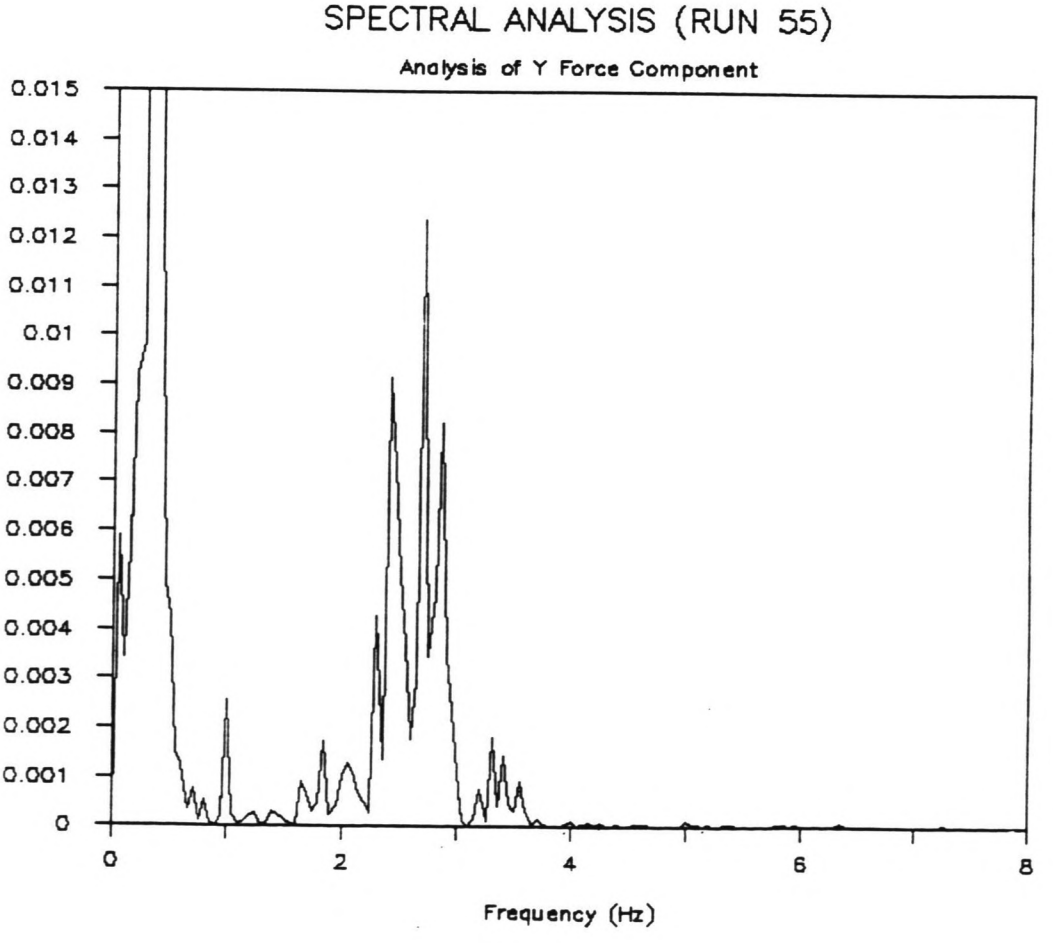

FIGURE G9.8.2

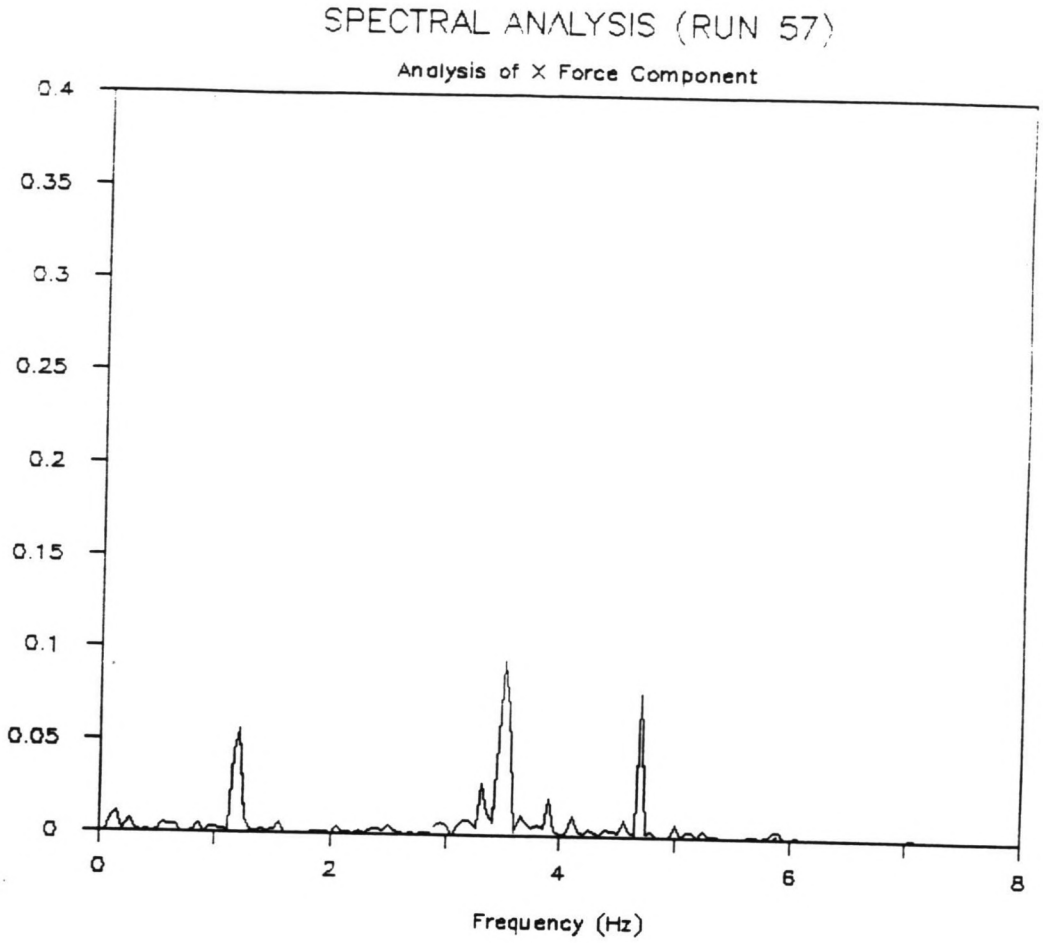

FIGURE G9.9.1

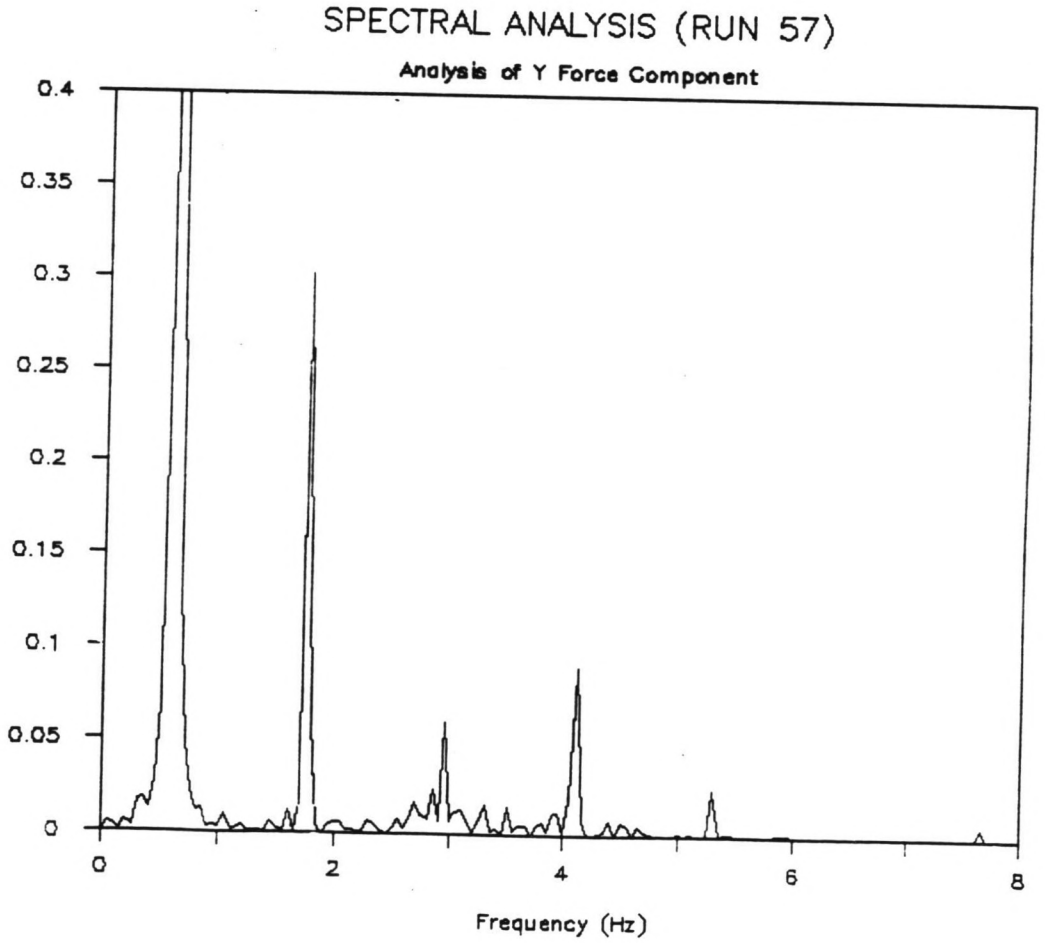

FIGURE G9.9.2

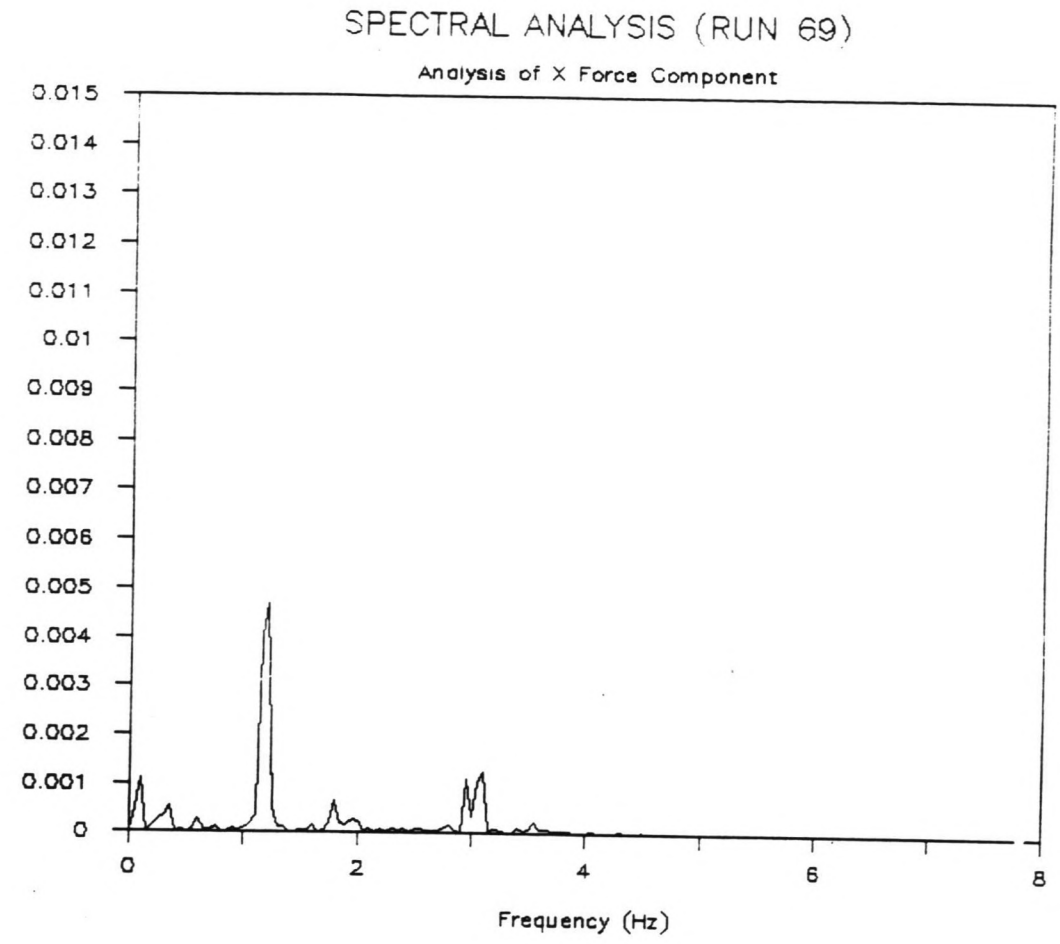

FIGURE G9.10.1

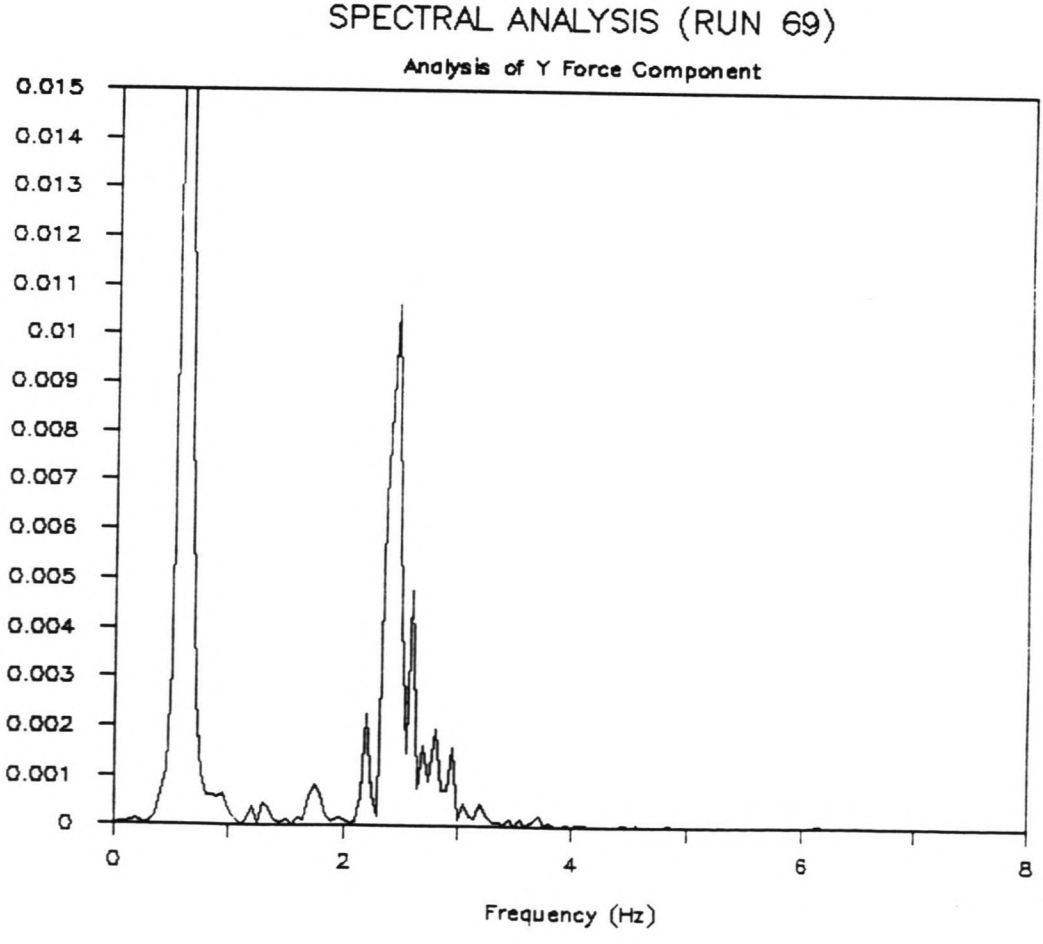

FIGURE G9.10.2

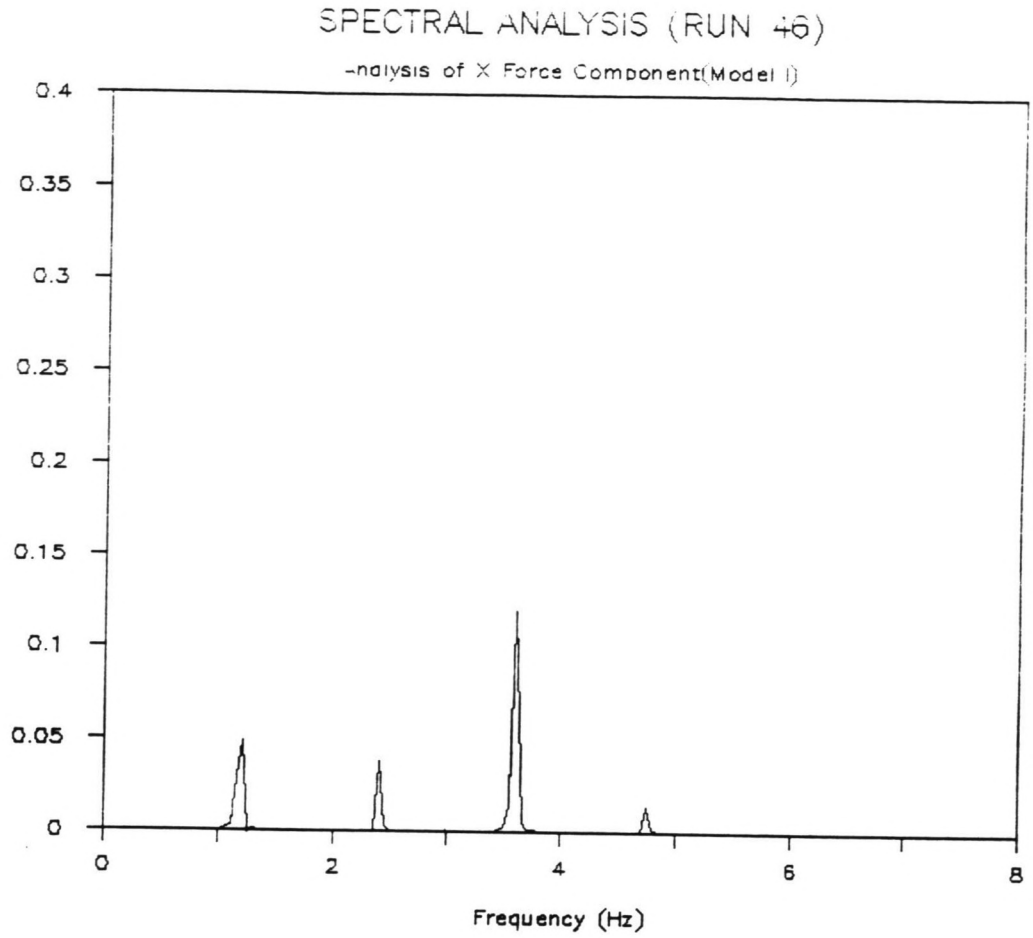

FIGURE G10.1.1

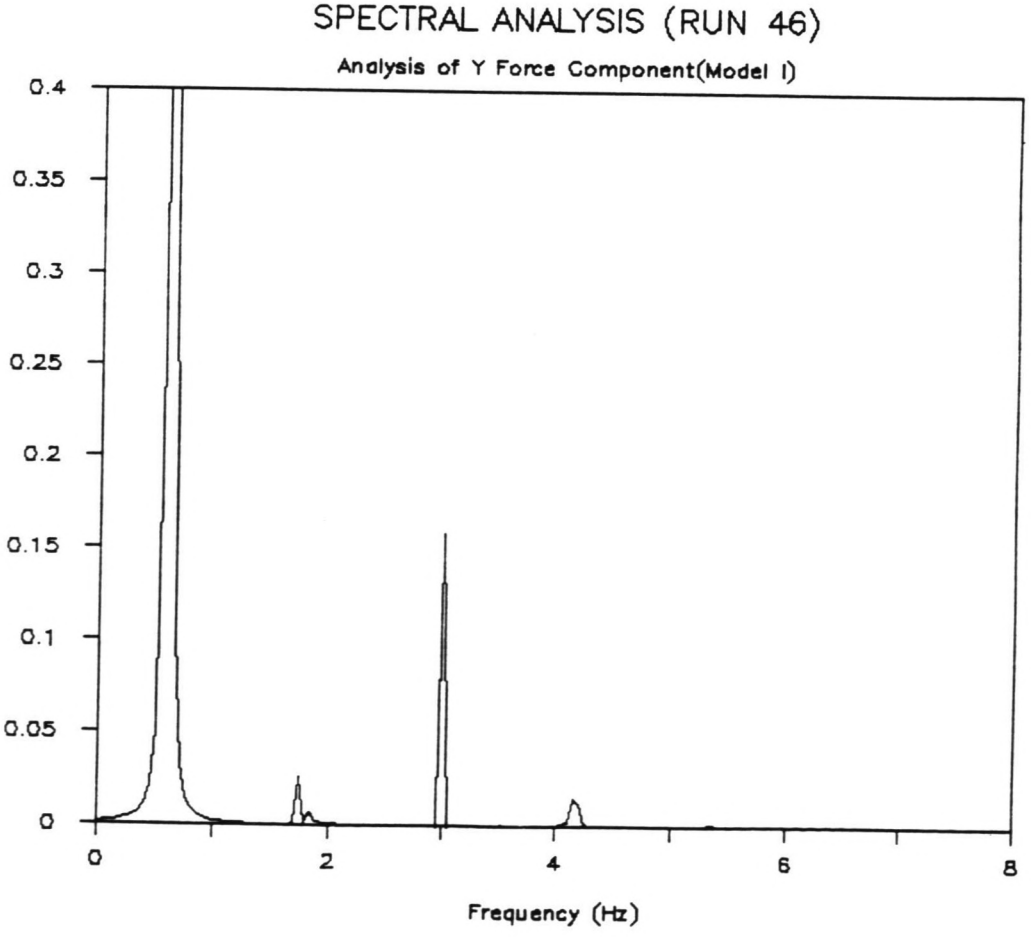

FIGURE G10.1.2

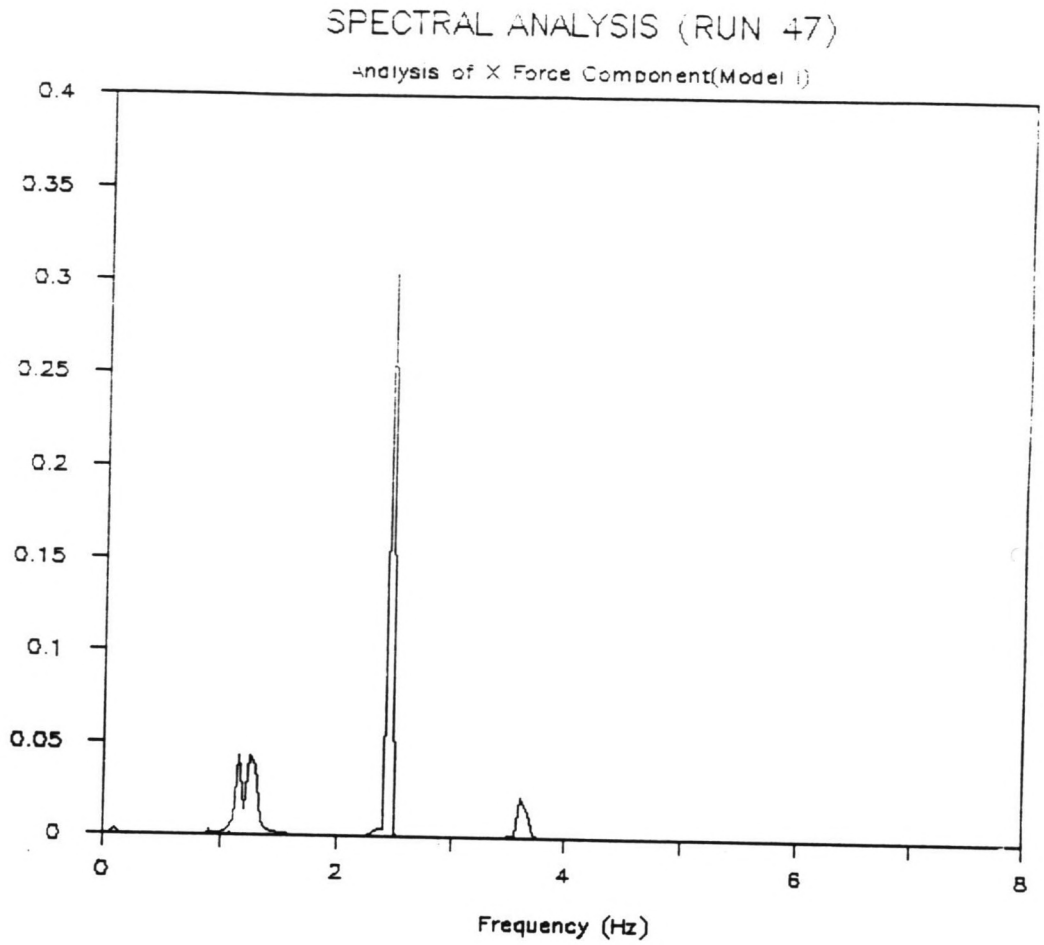

FIGURE G10.2.1

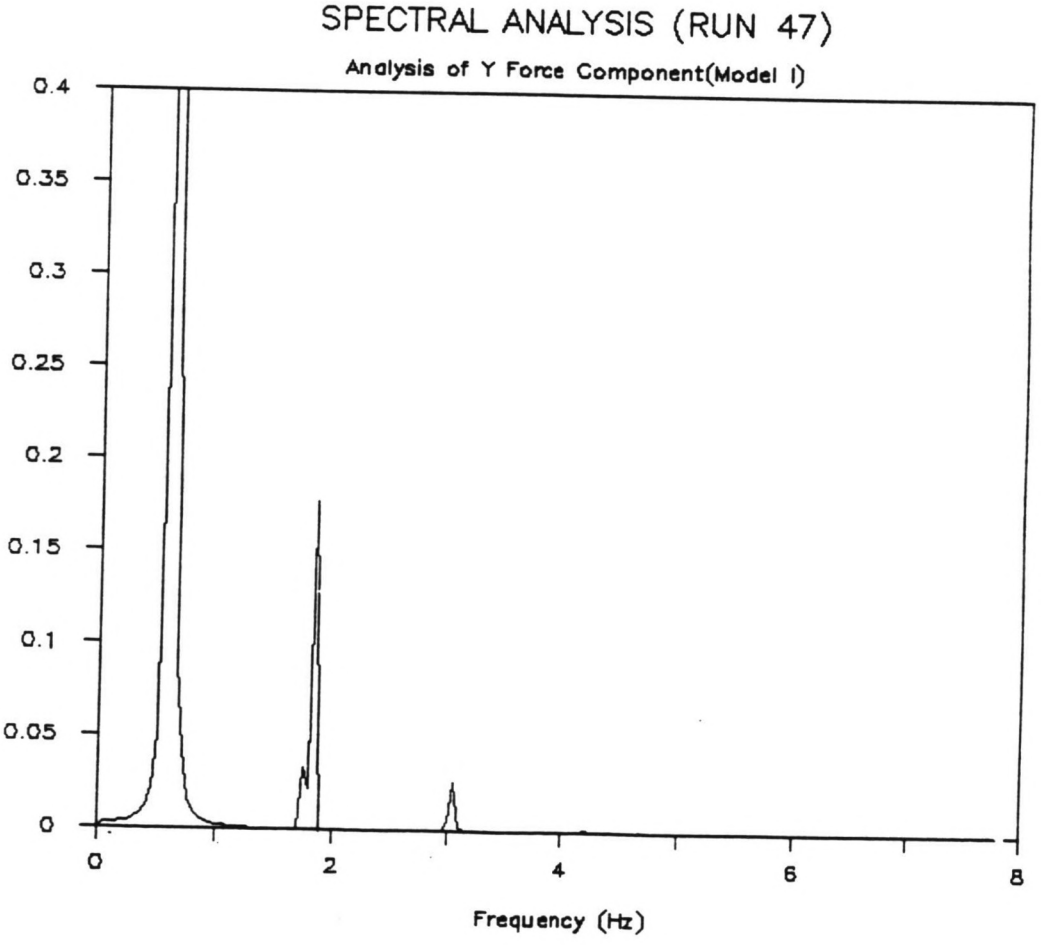

FIGURE G10.2.2

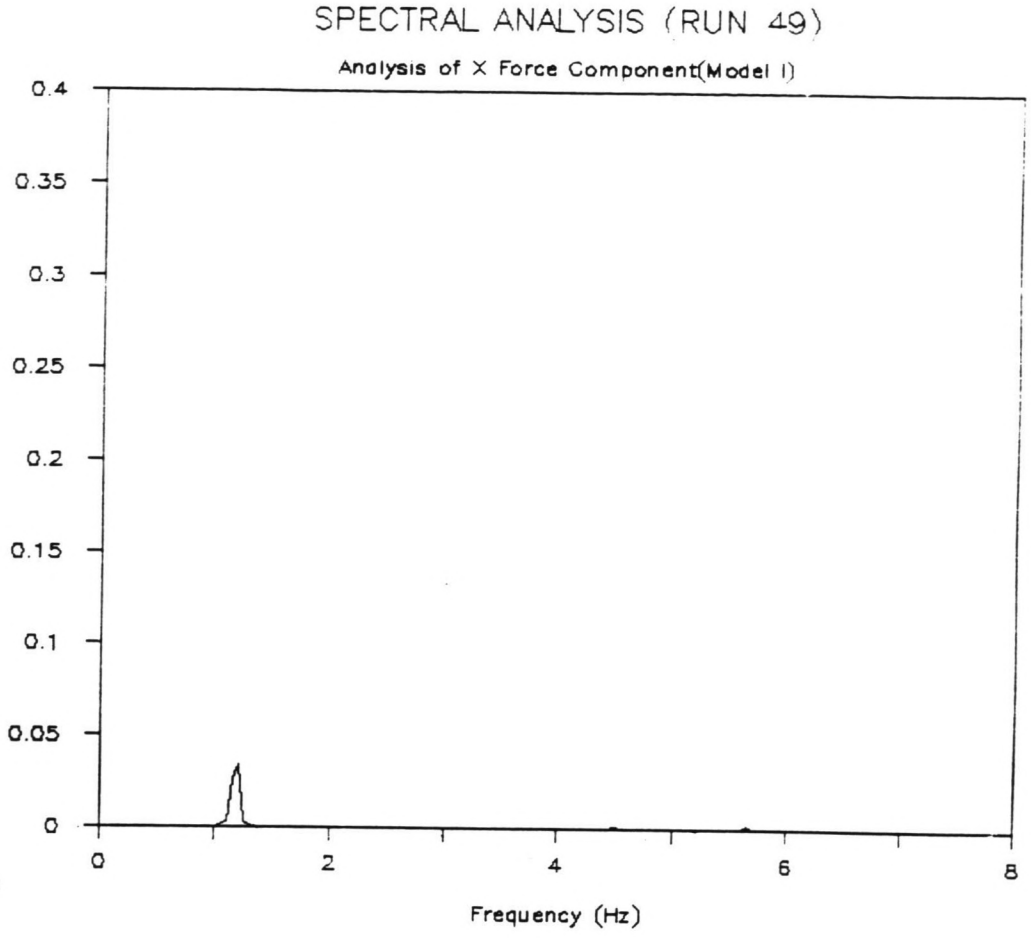

FIGURE G10.3.1

FIGURE G10.3.2

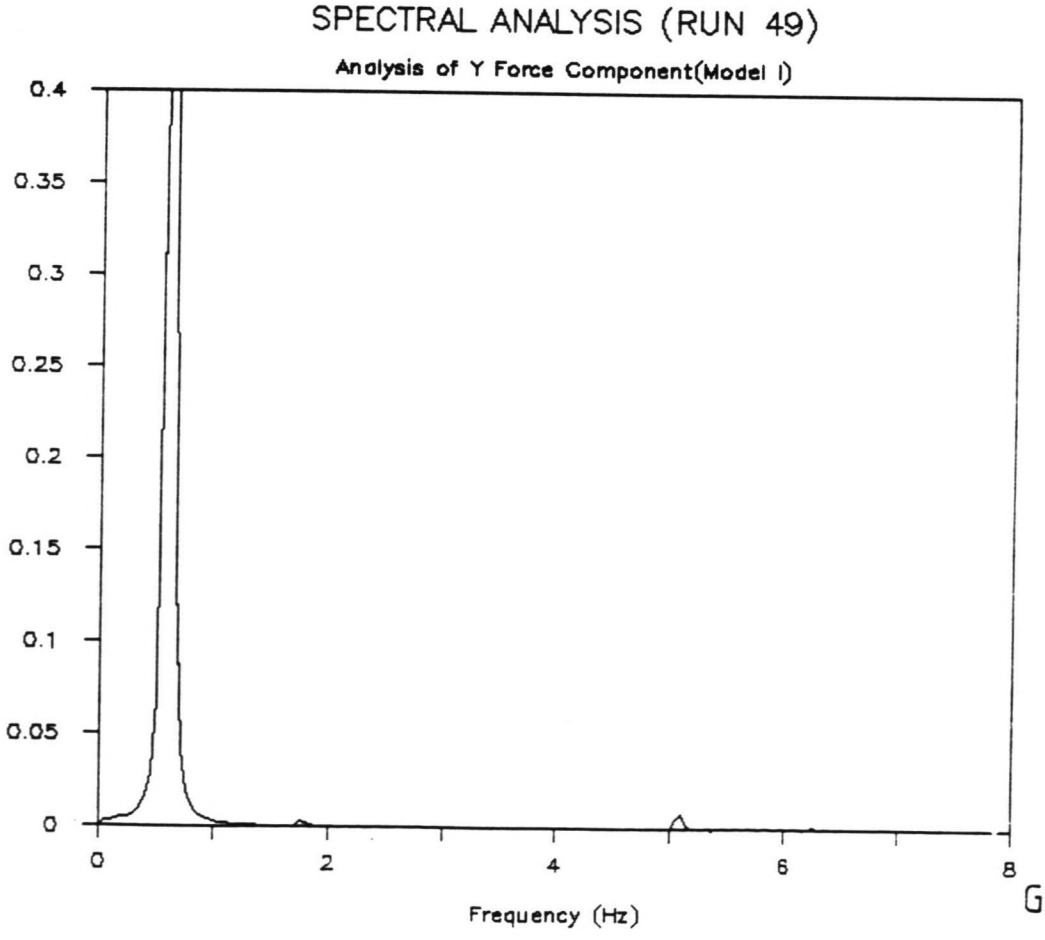

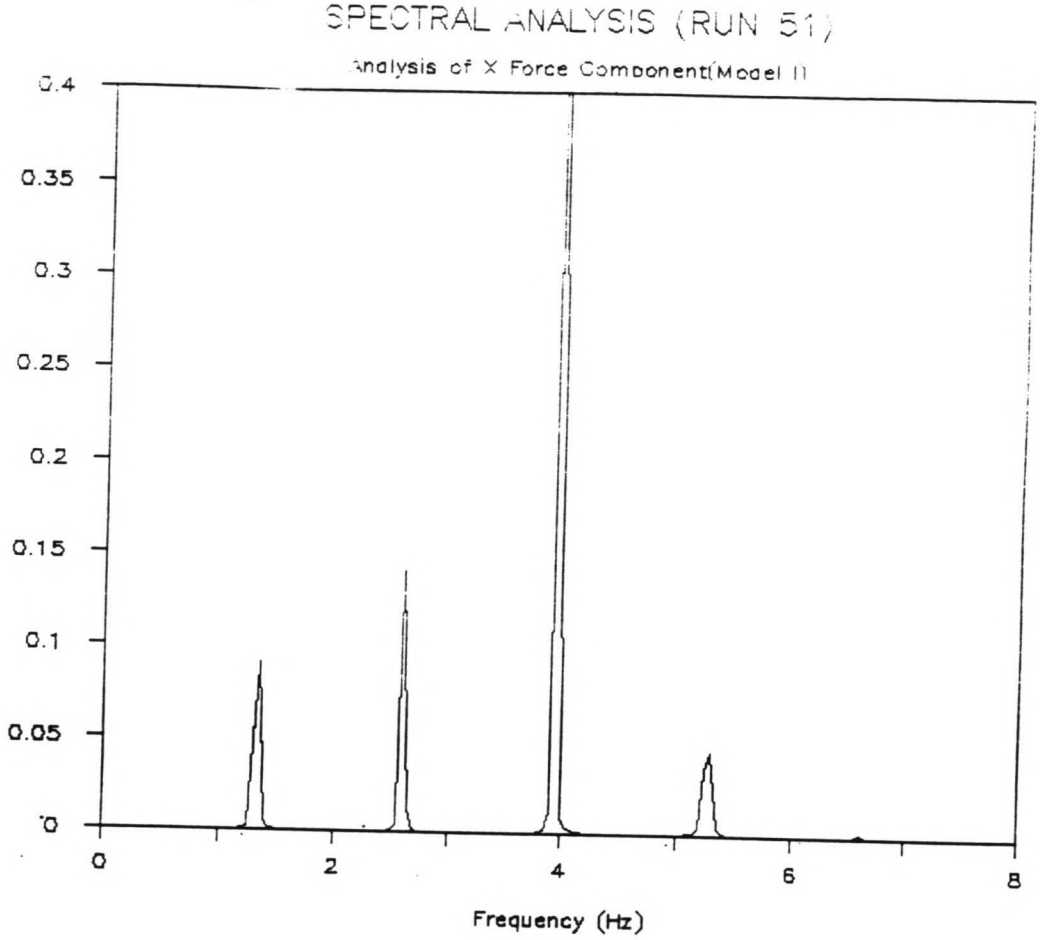

FIGURE G10.4.1

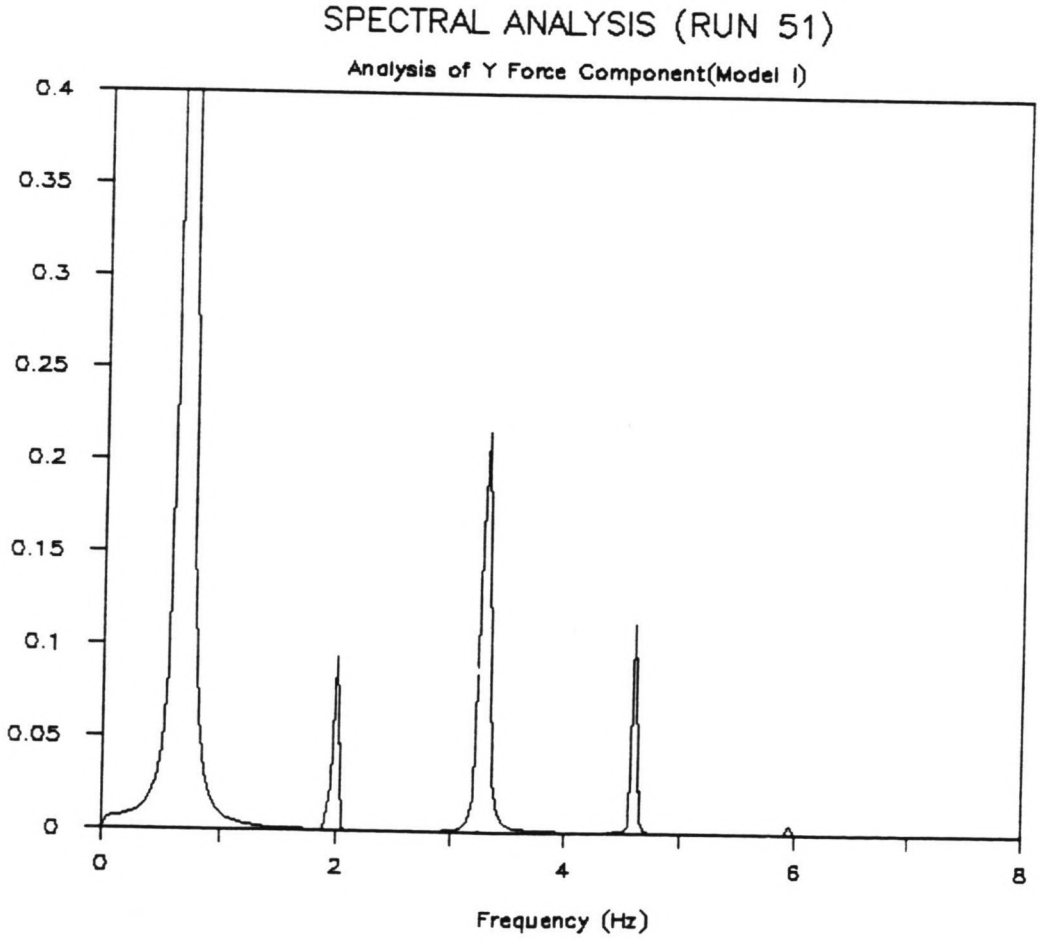

FIGURE G10.4.2

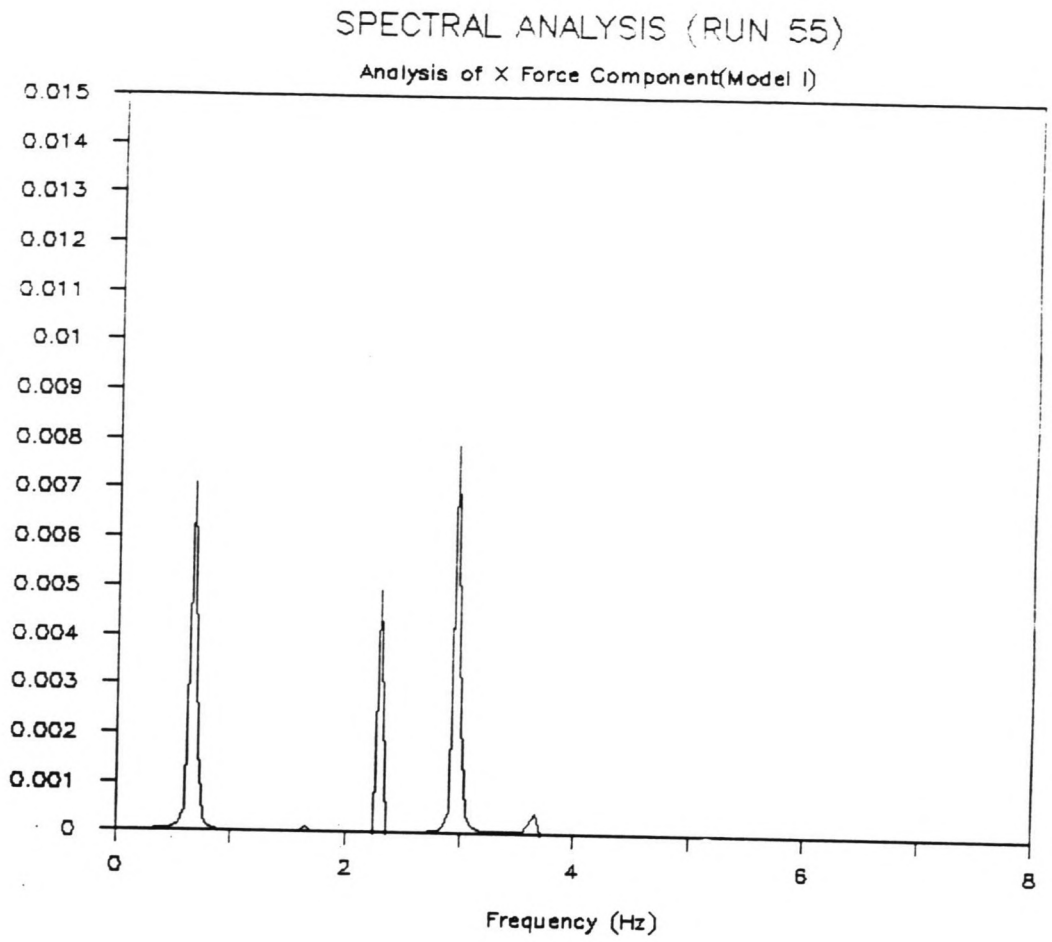

FIGURE G10.5.1

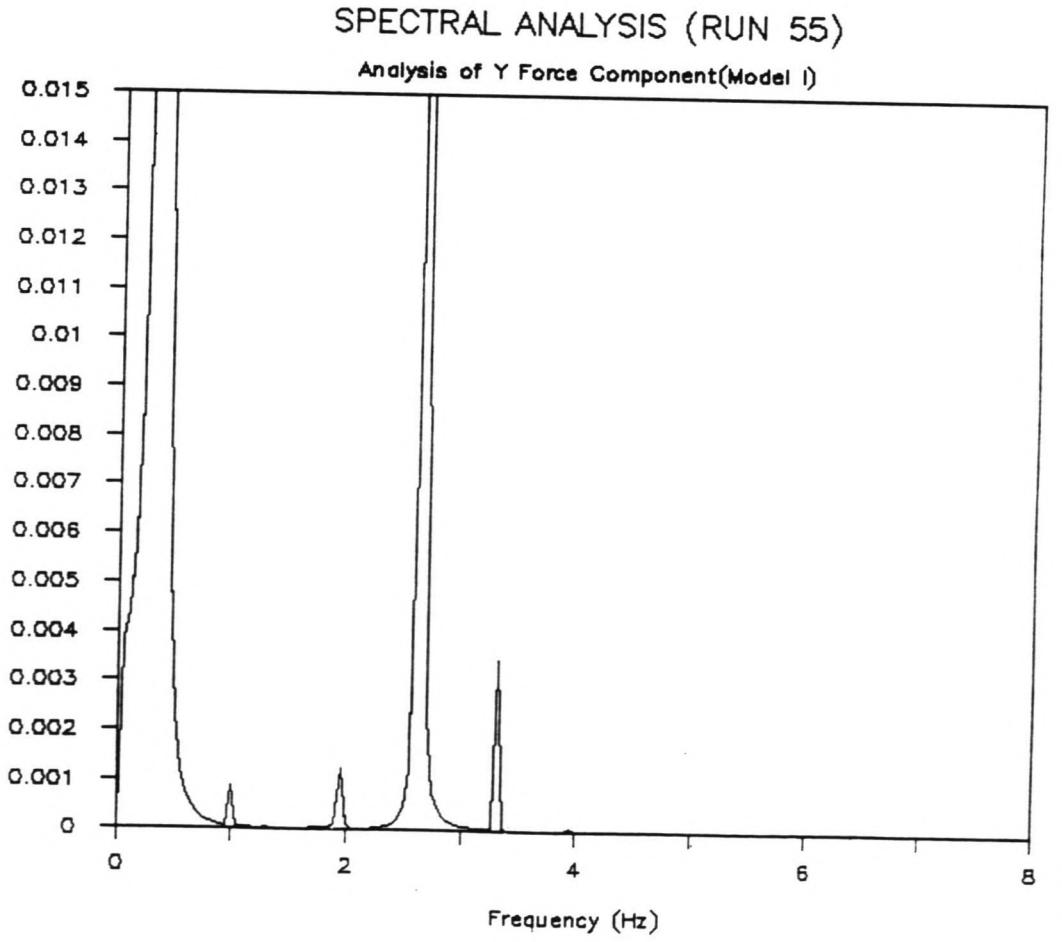

FIGURE G10.5.2

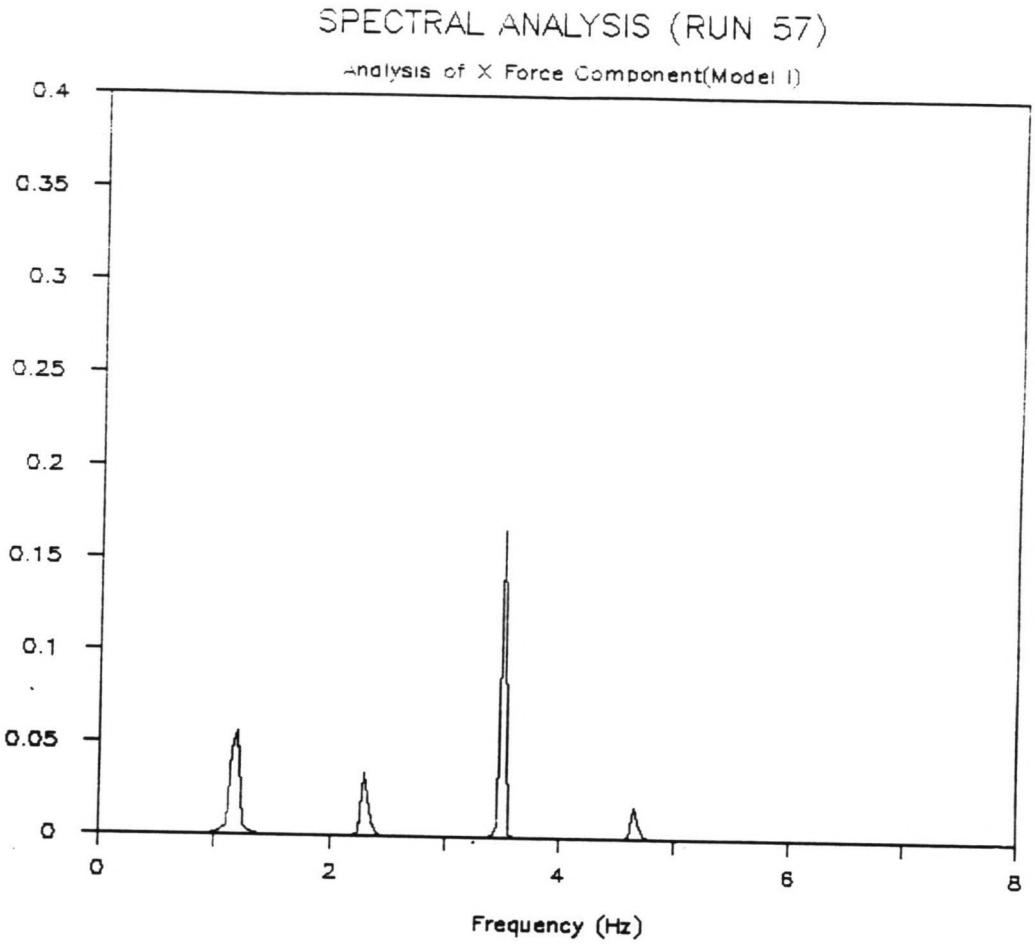

FIGURE G10.6.1

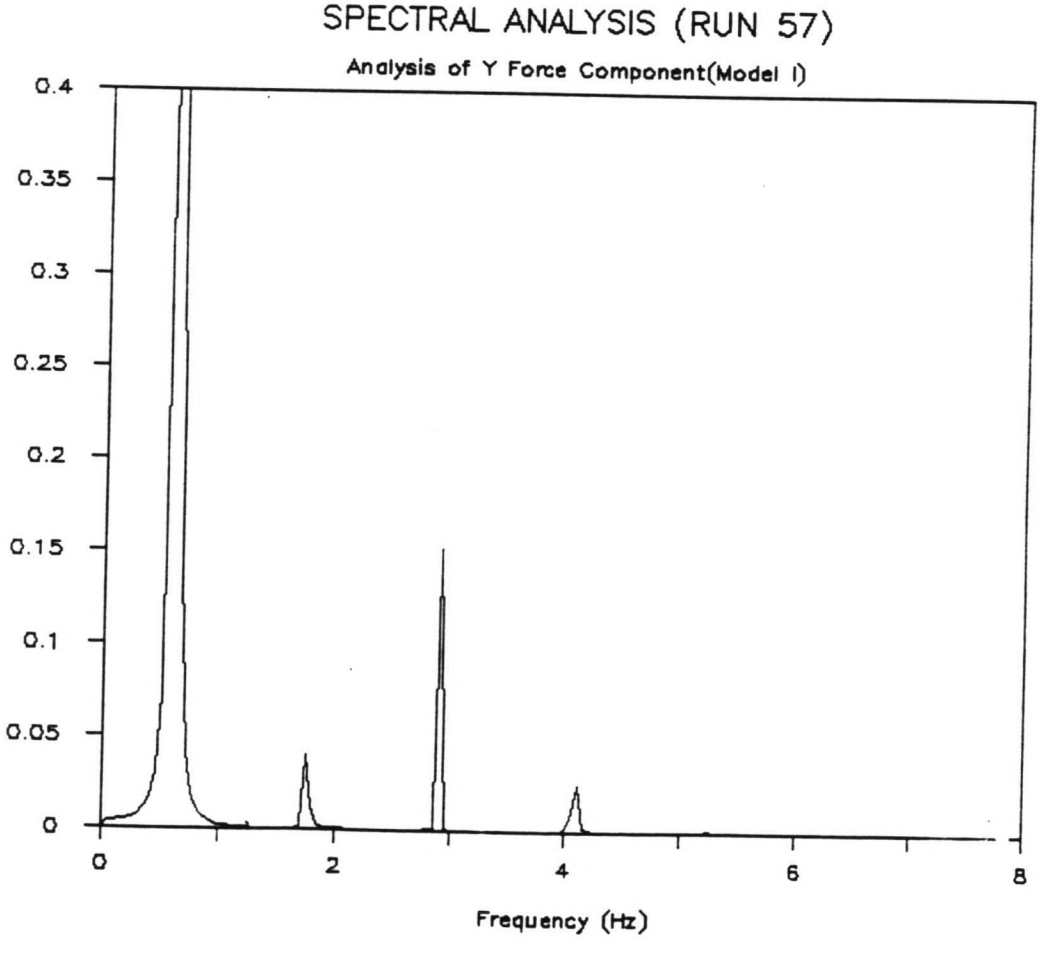

FIGURE G10.6.2

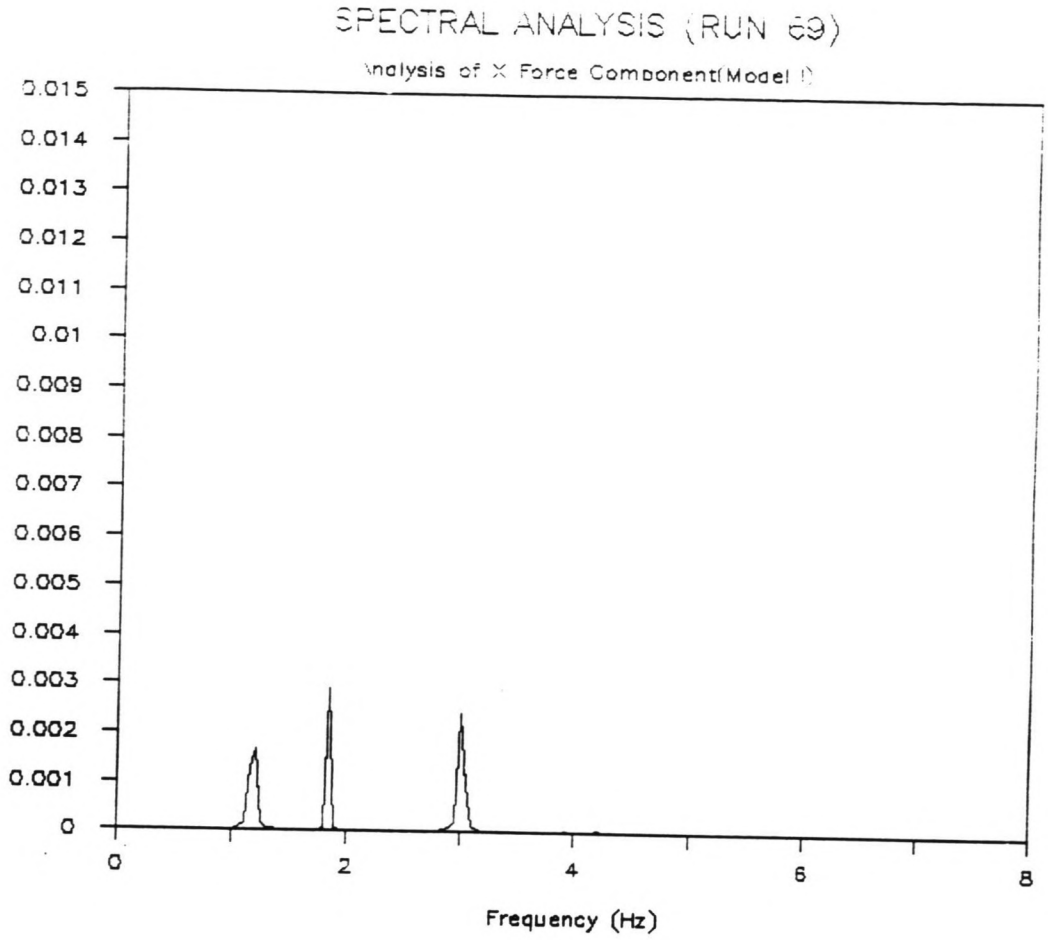

FIGURE G10.7.1

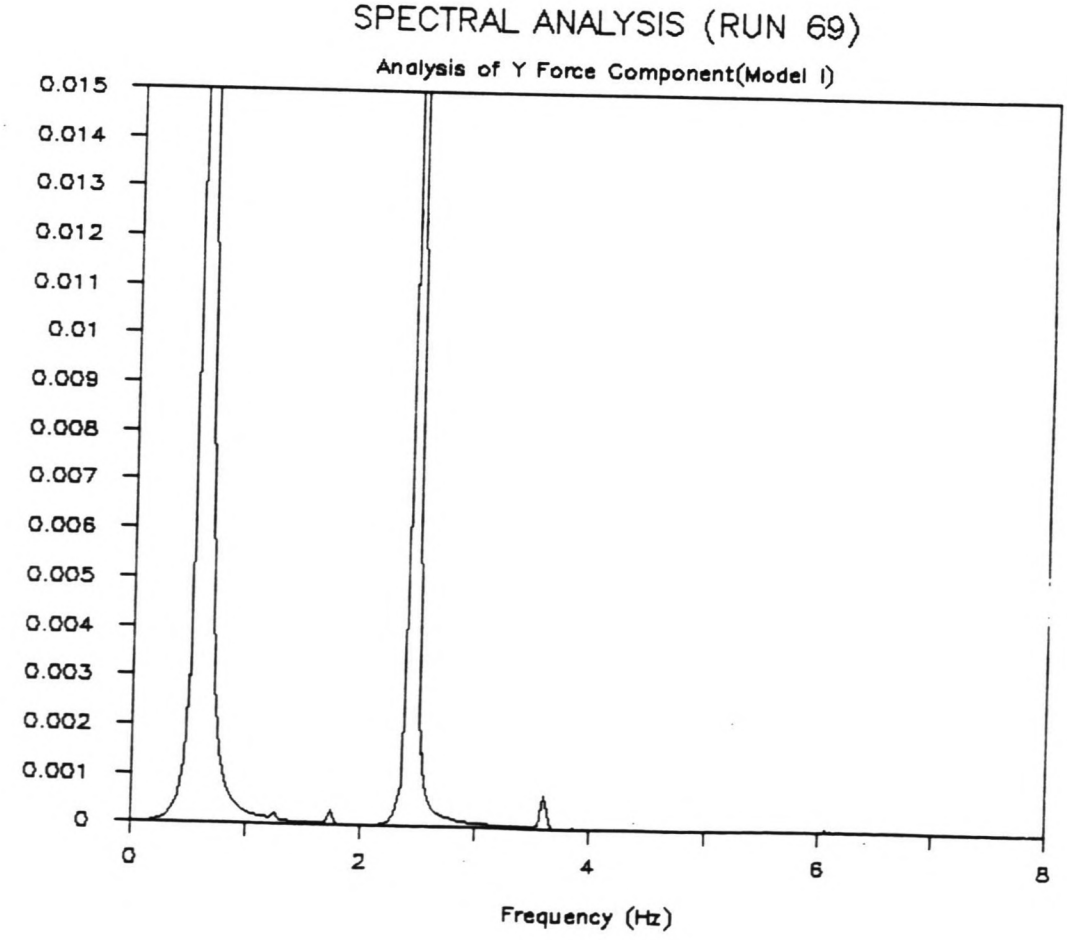

FIGURE G10.7.2

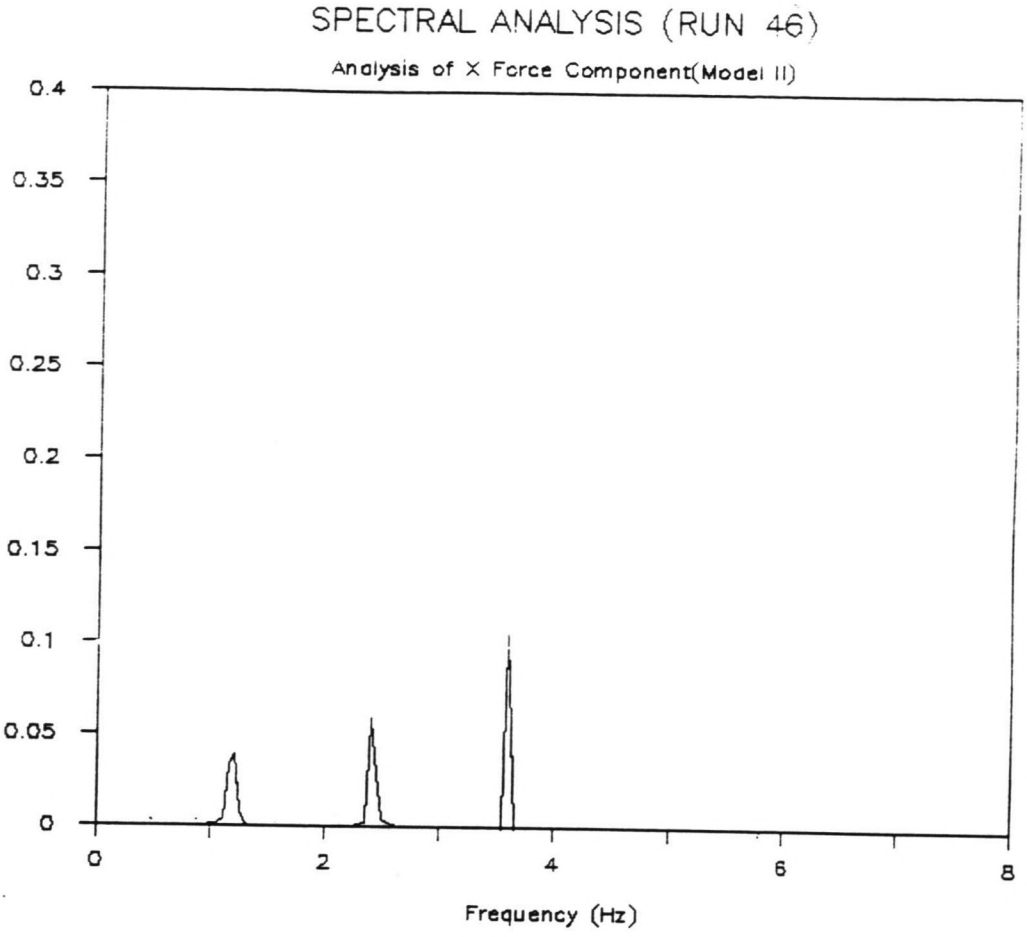

FIGURE G11.1.1

FIGURE G11.1.2

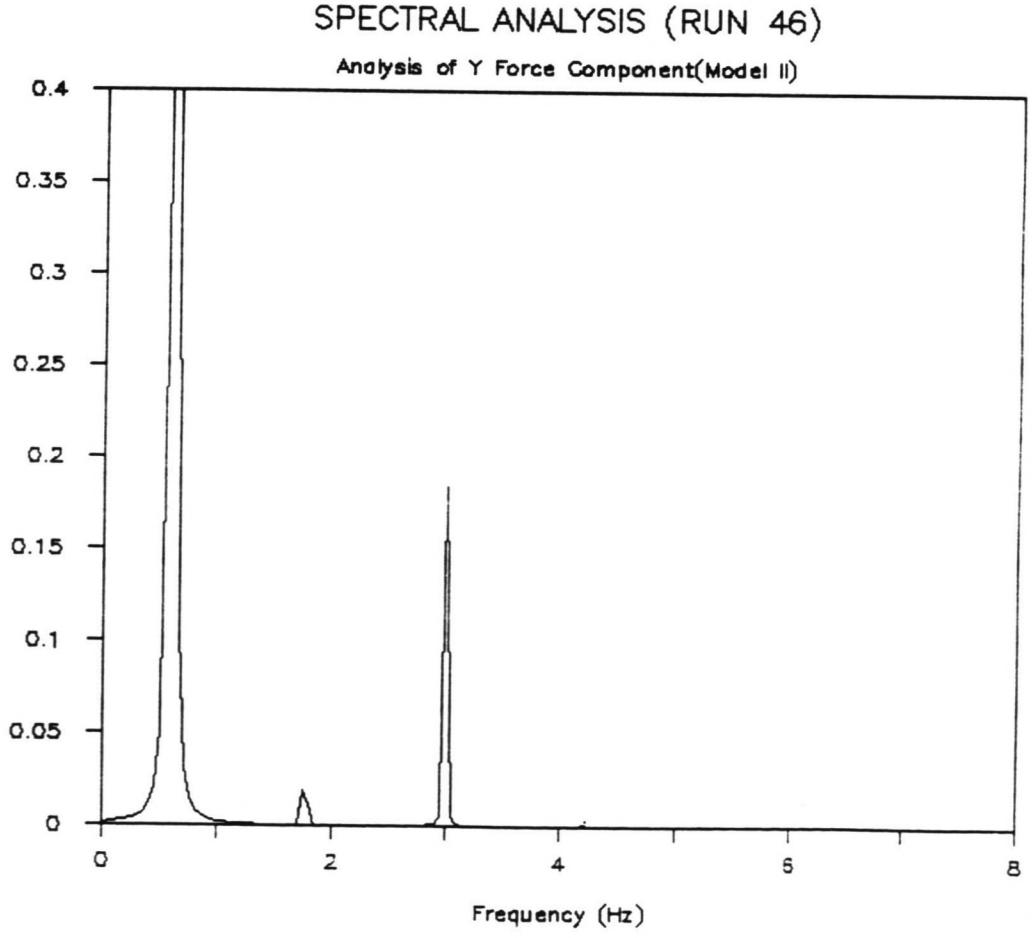

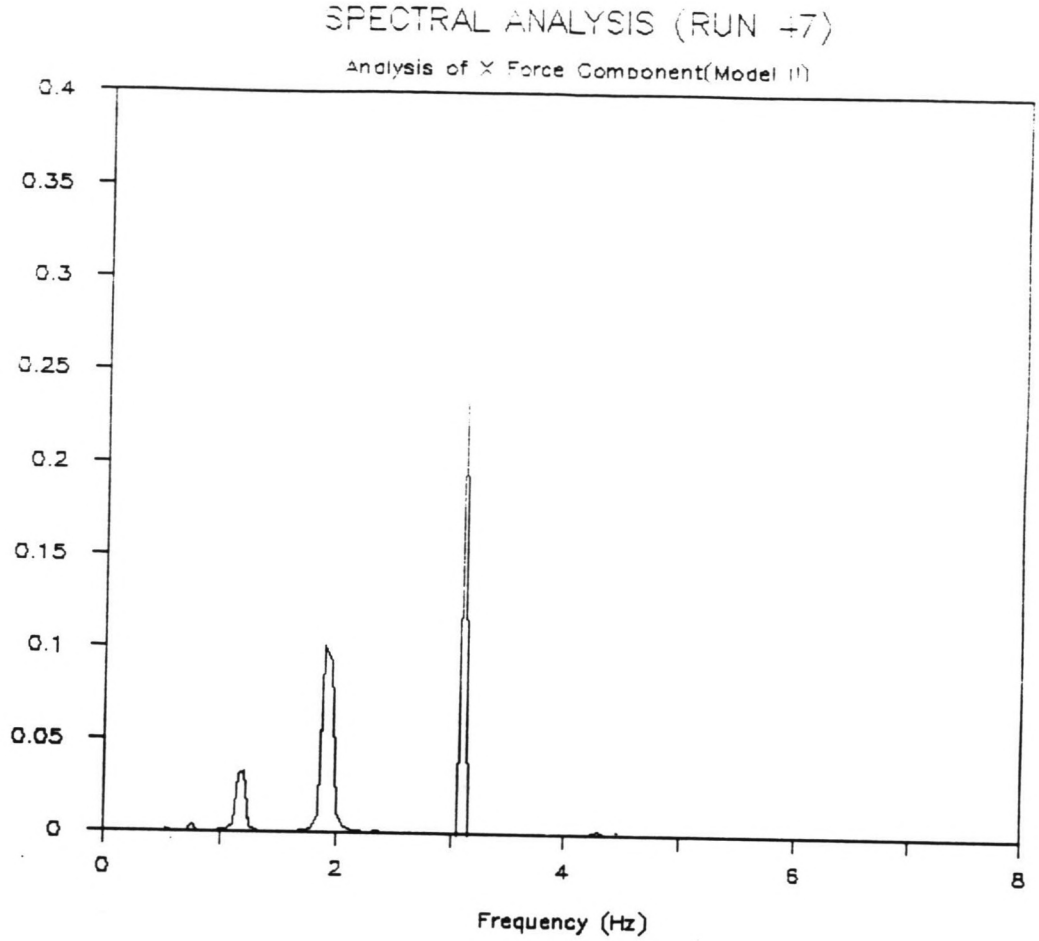

FIGURE G11.2.1

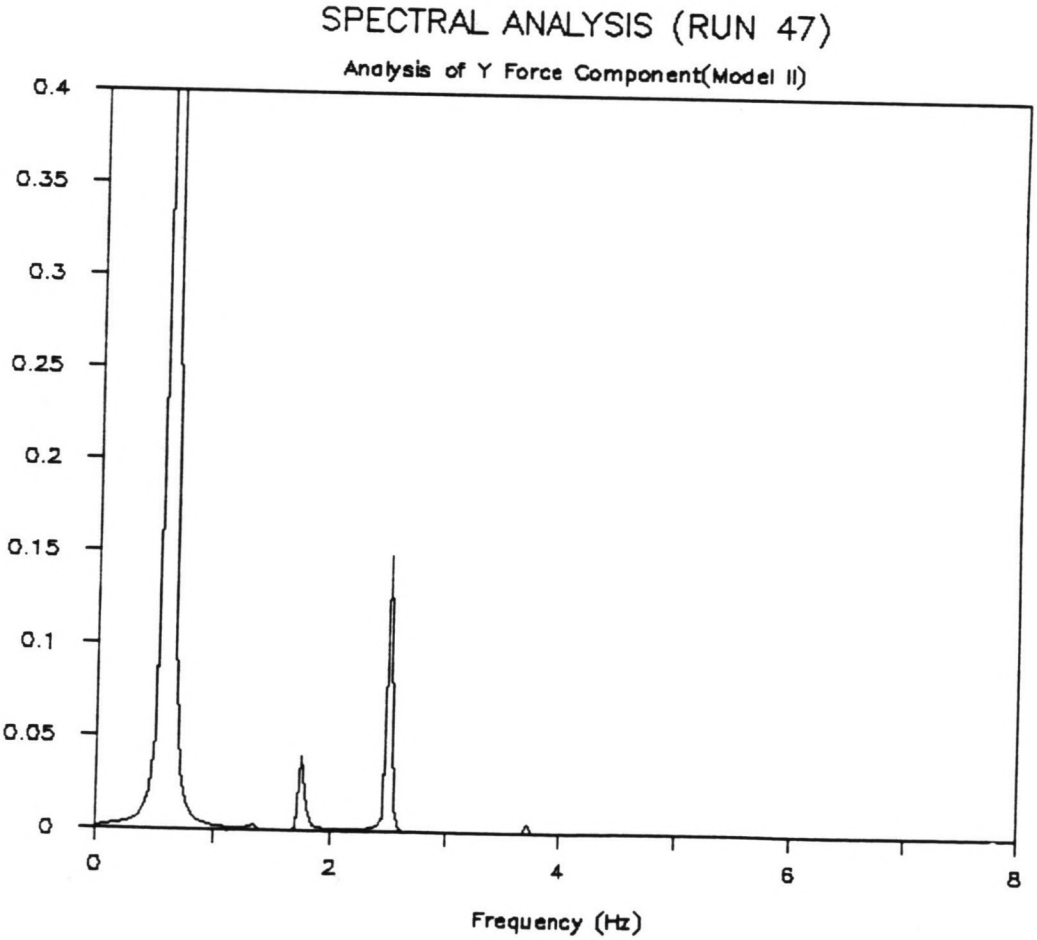

FIGURE G11.2.2

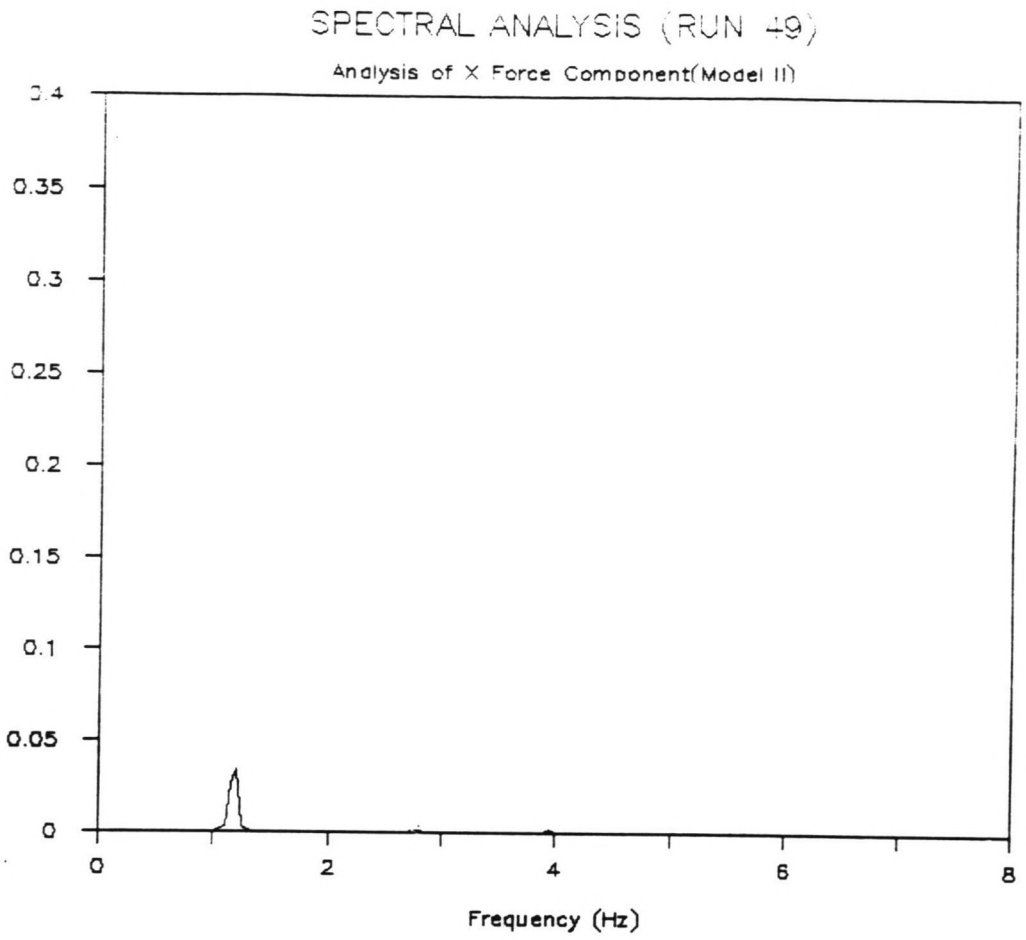

FIGURE G11.3.1

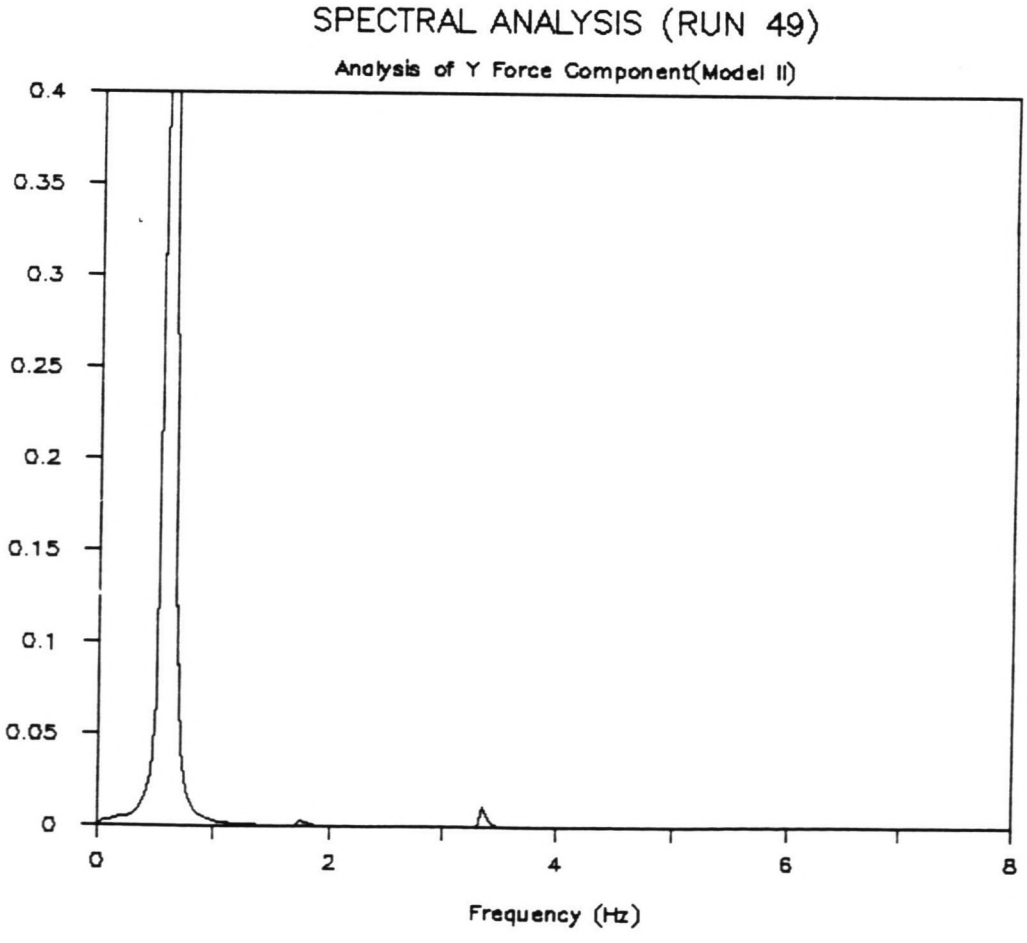

FIGURE G11.3.2

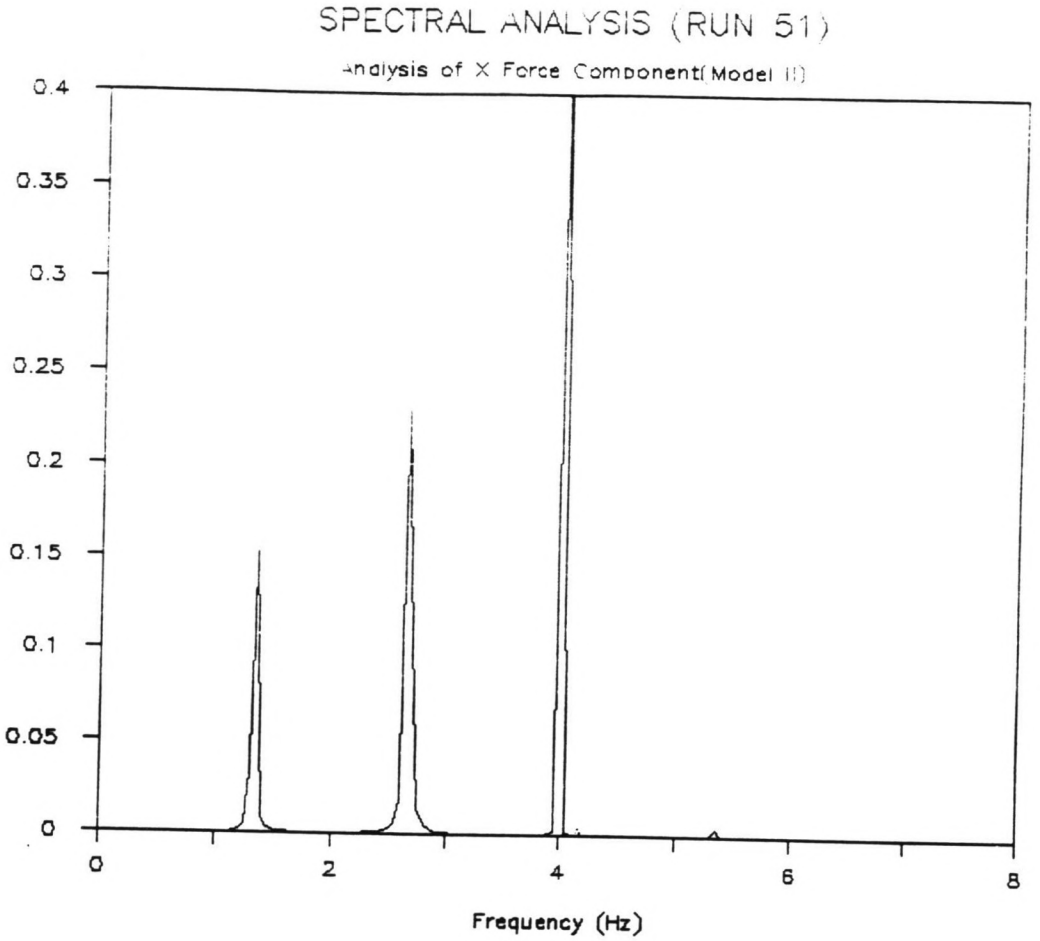

FIGURE G11.4.1

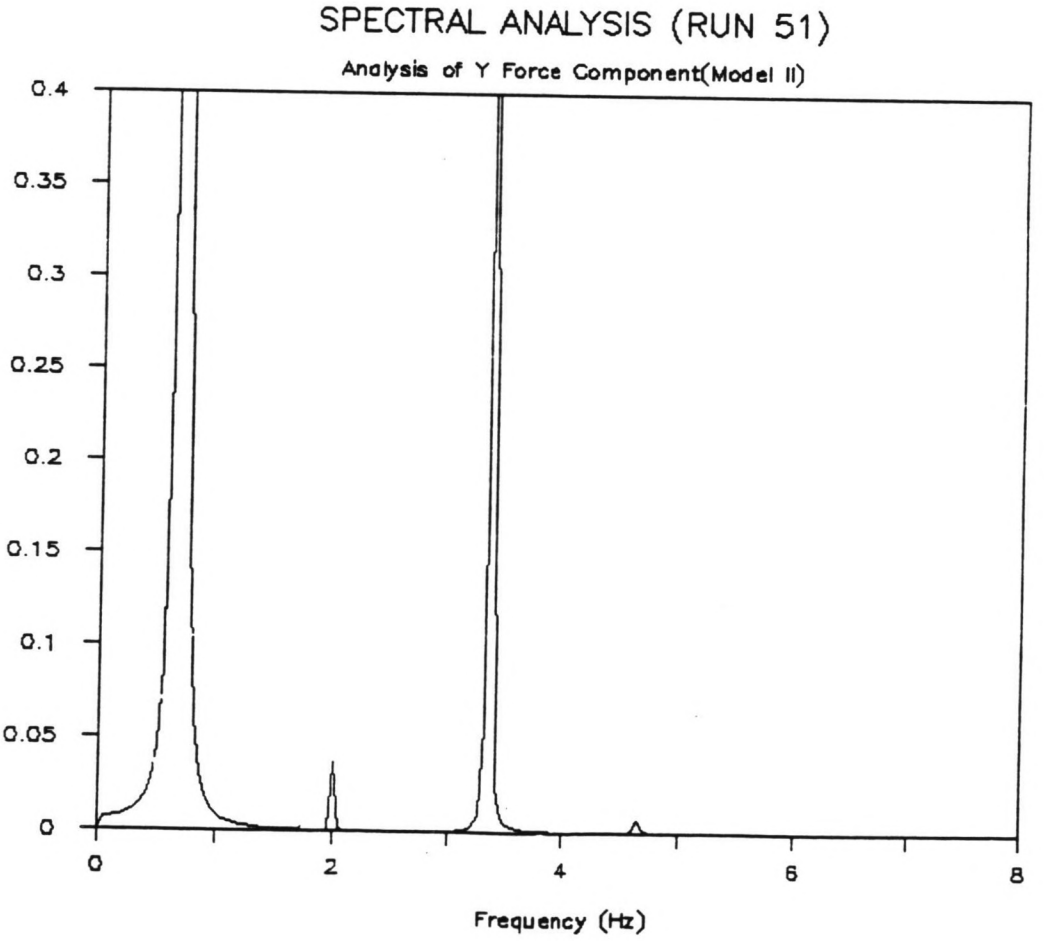

FIGURE G11.4.2

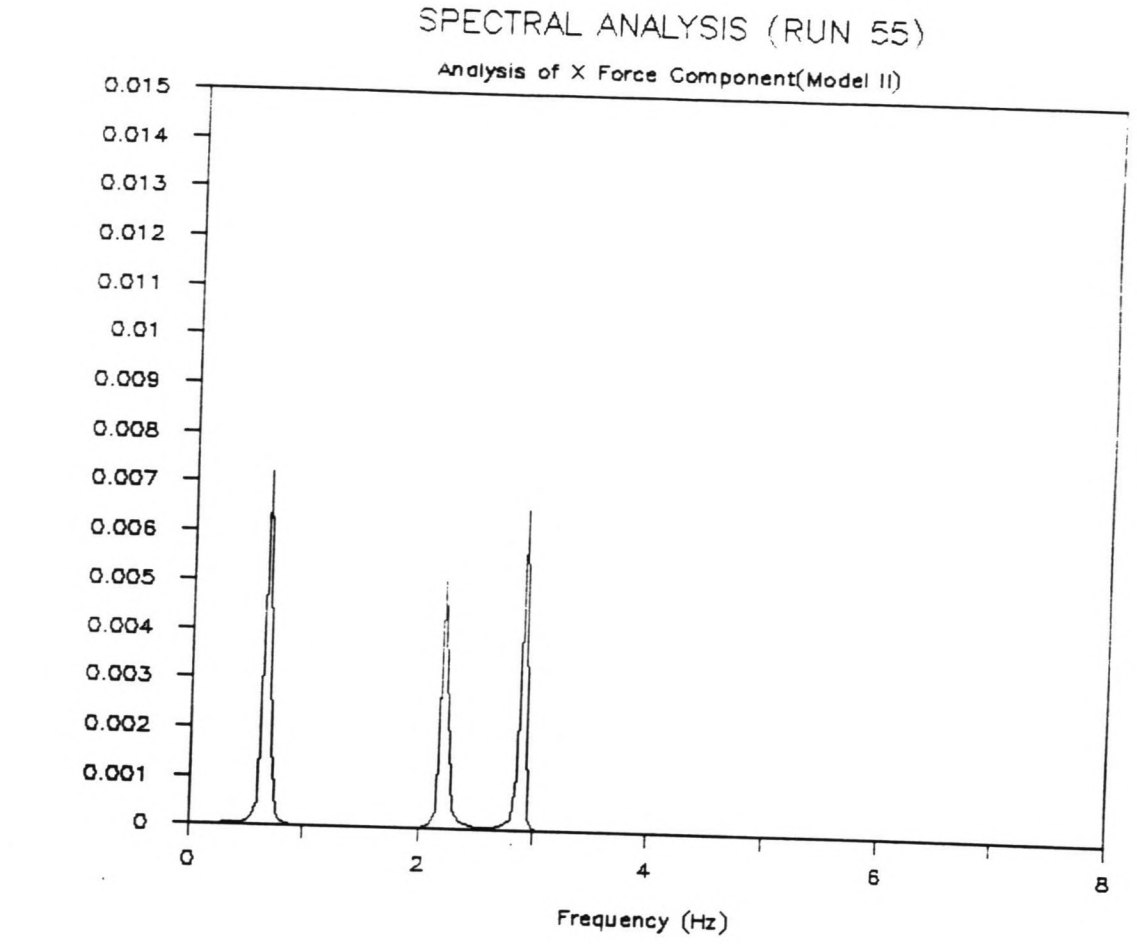

FIGURE G11.5.1

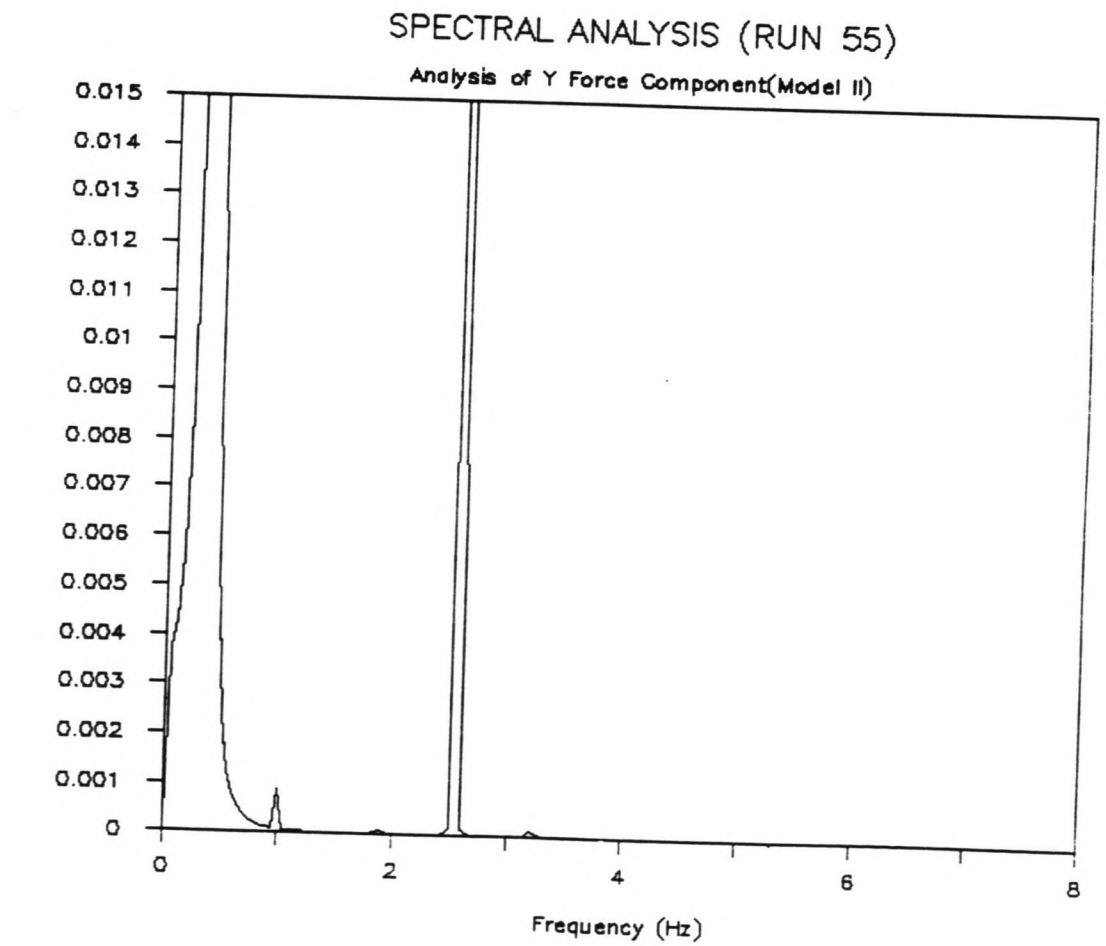

FIGURE G11.5.2

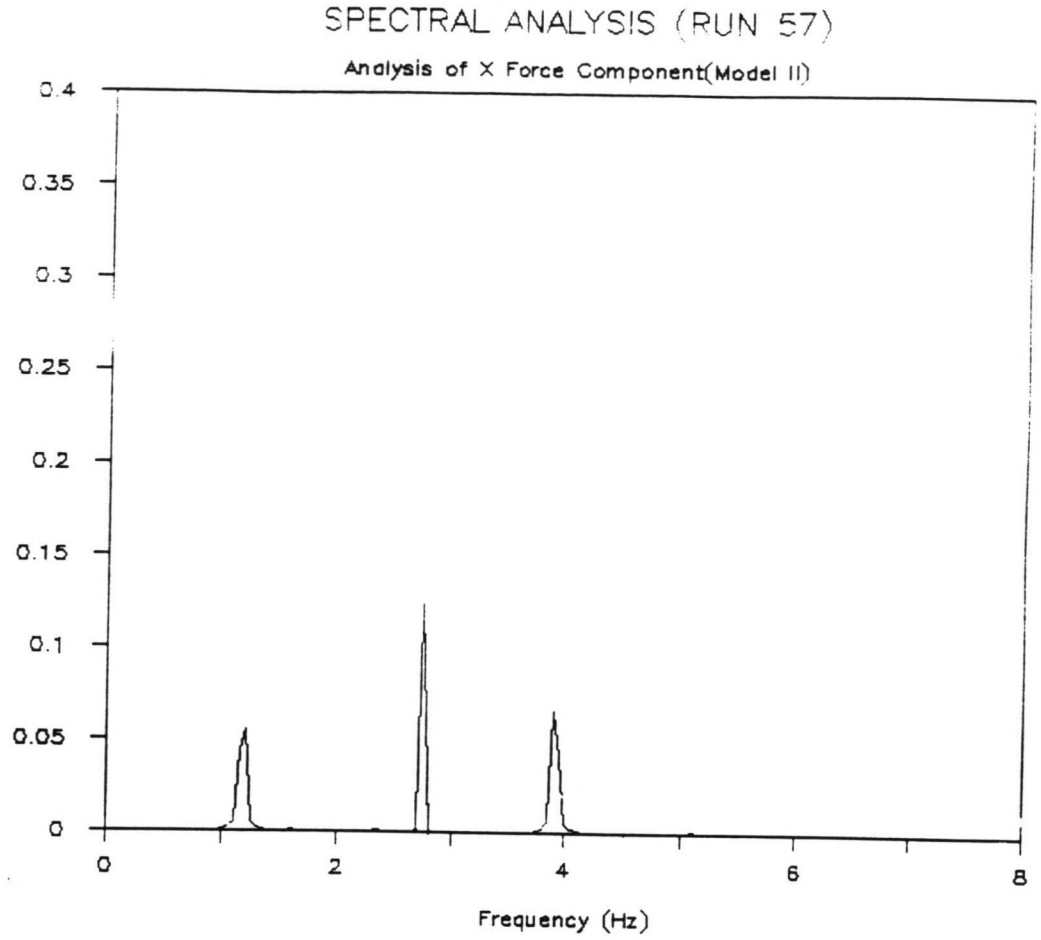

FIGURE G11.6.1

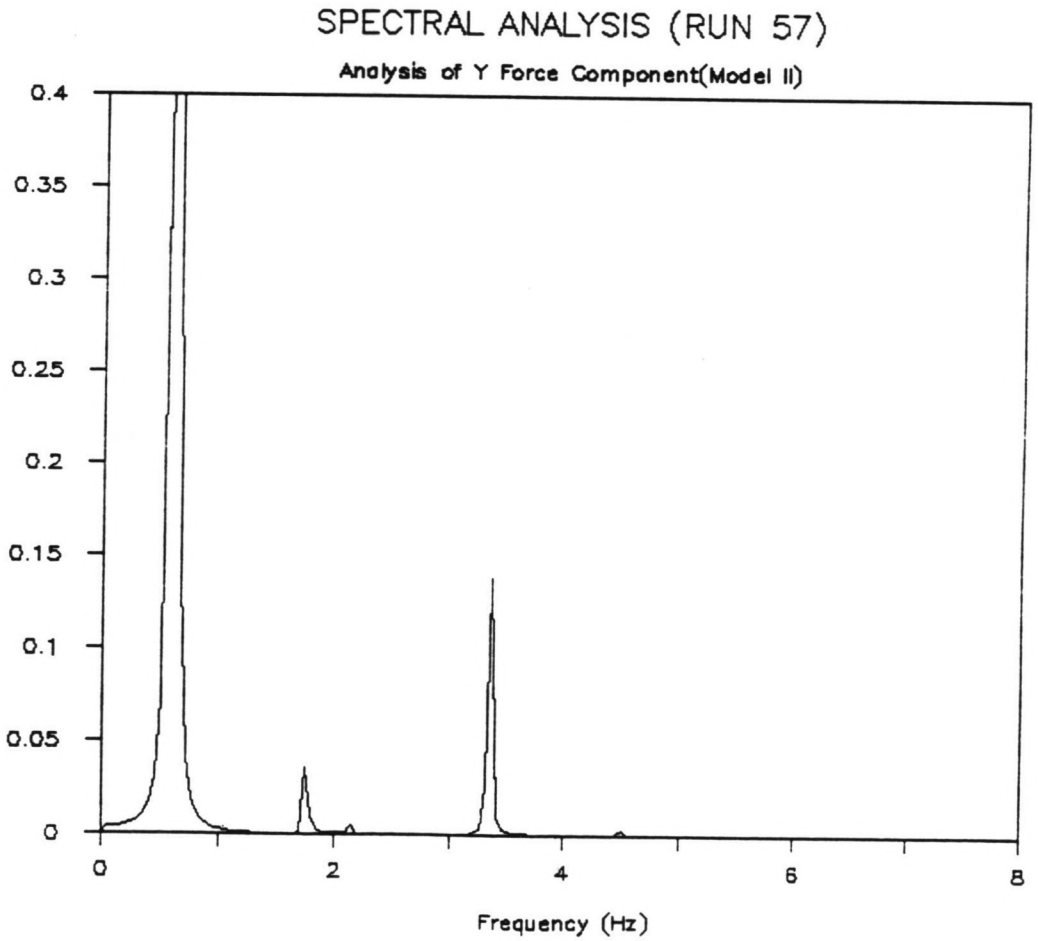

FIGURE G11.6.2

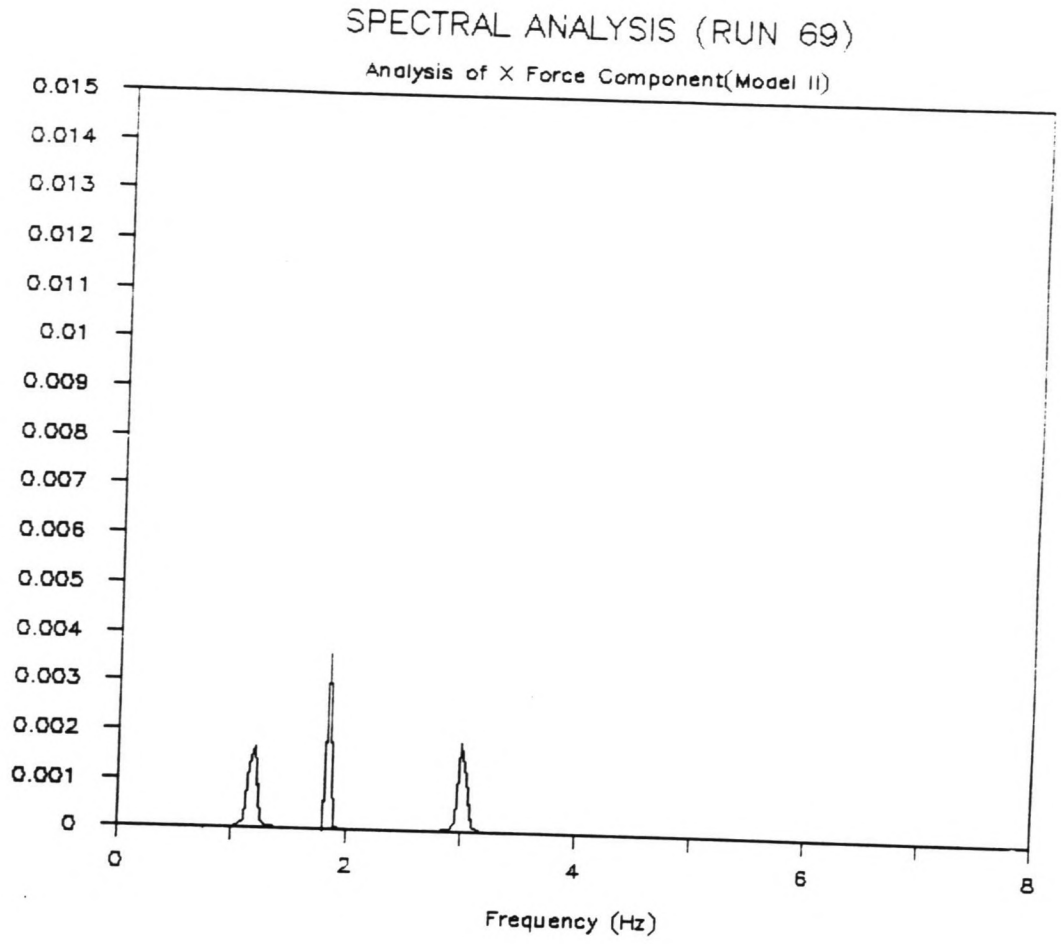

FIGURE G11.7.1

FIGURE G11.7.2